

Kinetic evaluation of the production of *Bacillus* lipopeptides effective against Tuberculosis

by

Emile Johannes

Thesis presented in partial fulfilment
of the requirements for the Degree

of

MASTER OF ENGINEERING
(CHEMICAL ENGINEERING)



The financial assistance of the National Research Foundation (NRF) towards this research is hereby acknowledged. Opinions expressed and conclusions arrived at, are those of the author and are not necessarily attributed to the NRF.

Supervisor:
Prof K.G. Clarke

Co-Supervisor
Dr. R. Pott

April 2019

DECLARATION

By submitting this thesis electronically, I declare that the entirety of the work contained therein is my own, original work, that I am the sole author thereof (save to the extent explicitly otherwise stated), that reproduction and publication thereof by Stellenbosch University will not infringe any third party rights and that I have not previously in its entirety or in part submitted it for obtaining any qualification.

Date: April 2019

Copyright © 2019 Stellenbosch University

All rights reserved

PLAGIARISM DECLARATION

1. Plagiarism is the use of ideas, material and other intellectual property of another's work and to present is as my own.
2. I agree that plagiarism is a punishable offence because it constitutes theft.
3. I also understand that direct translations are plagiarism.
4. Accordingly all quotations and contributions from any source whatsoever (including the internet) have been cited fully. I understand that the reproduction of text without quotation marks (even when the source is cited) is plagiarism.
5. I declare that the work contained in this assignment, except where otherwise stated, is my original work and that I have not previously (in its entirety or in part) submitted it for grading in this module/assignment or another module/assignment.

Initials and surname:

Date:

ABSTRACT

Tuberculosis (TB), caused by *Mycobacterium Tuberculosis*, is the second largest cause of death resulting from a single infectious agent globally. South Africa has one of the highest number of active TB cases globally and it was estimated that approximately 1% of South Africans develops active TB each year. Multi-drug resistant TB (MDR-TB) is of even greater concern due its low cure rate of only 50% for treated MDR-TB patients.

The lipopeptide biosurfactant, surfactin, produced by various *Bacillus* species, offers a promising alternative antimicrobial agent against TB causing organisms due to its ability to lyse cell membranes and alter membrane permeability. The haemolytic activity of surfactin, however, limits its use as a medical drug to be ingested by humans, but does not limit its use in other applications such as detergents and disinfectants in the fight against TB.

The large-scale production of surfactin is limited by low yields and high purification costs, hence economically attractive approaches needs to be developed to realise the commercial production of surfactin as an antimicrobial agent to be used in the fight against TB. Lipopeptide production greatly relies on factors such as medium composition, process conditions and environmental factors, thus by optimising these conditions the cost of both upstream processing, and downstream purification, can be reduced significantly.

The overall aim of this study was to investigate the effect of medium composition and process conditions on the growth and lipopeptide production kinetics of *B. subtilis* in batch culture and advise on the conditions that will improve the upstream production of surfactin, for possible use as an antimicrobial agent against *M. tuberculosis*.

Shake flasks were used to study the effect of distinct nitrogen sources (NH_4^+ and NO_3^-) on the process kinetics by supplying ammonium and nitrate at discrete nitrogen ratios ($\text{NH}_4\text{-N}:\text{NO}_3\text{-N}$). A rigorous kinetic analysis yielded the optimum nitrogen source ratio for surfactin production by *B. subtilis* to be 0.5:0.5. An $\text{NH}_4\text{-N}:\text{NO}_3\text{-N}$ ratio of 0.5:0.5 yielded the highest surfactin concentration (1084 mg/L), the highest surfactin productivity (36.1 mg/L/h), the second highest specific surfactin production ($Y_{p/x} = 0.078$), the highest surfactin yield on glucose ($Y_{p/s} = 0.031$) and the third highest surfactin selectivity ($5.11 \text{ g}_{\text{surfactin}} / \text{g}_{\text{fengycin}}$).

The effect of manganese concentration on the process kinetics were also studied in shake flasks and rigorous kinetic evaluation yielded the optimal manganese concentration for surfactin production to be 0.1 mM, however increasing the manganese concentration from 0.05 to 0.1 mM did not significantly improve the surfactin production kinetics. 0.1 mM manganese yielded the highest surfactin concentration (884 mg/L), the highest surfactin yield on glucose ($Y_{p/s} = 0.022$), the highest surfactin productivity (46.5 mg/L/h), and the second highest the highest specific surfactin productivity ($Y_{p/x} = 0.089$) and surfactin selectivity (5.9 g surfactin / g fengycin).

The optimal nitrogen source ratio and manganese concentration from the shake flask studies were used to evaluate the process kinetics under controlled conditions in a batch bioreactor and were compared to the process kinetics obtained in the shake flasks. All bioreactor kinetic parameters (surfactin concentration – 891 mg/L; $Y_{p/x} = 0.113$; $Y_{p/s} = 0.021$) were almost identical to those in shake flasks (surfactin concentration – 854 mg/L; $Y_{p/x} = 0.087$; $Y_{p/s} = 0.022$), except for μ_{max} (0.39 h⁻¹ in the bioreactor and 0.5 h⁻¹ in the shake flask culture) and surfactin productivity (18.56 mg/L/h in the bioreactor culture and 44.95 mg/L/h the shake flask culture). The differences were attributed to interference caused by antifoam addition in the bioreactor culture due to vigorous foaming, however further investigation is required. It was also recommended that alternative methods to handle foaming, such as foam fractionation, should be investigated in future work.

A response surface methodology (CCD) design of shake flask experiments yielded a nitrogen source ratio (NH₄-N:NO₃-N) of 0.35:075, manganese concentration of 0.06 mM, and a relative filling volume (RFV) of 0.5 as optimal to achieve maximum surfactin production by *B. subtilis*. NH₄-N:NO₃-N ratio and oxygen availability (relative filling volume) were significant parameters ($\alpha = 0.05$) affecting surfactin concentration, $Y_{p/x}$, and surfactin selectivity, whilst manganese concentration did not have a significant effect on any of the responses. It was recommended that nitrogen source ratio and oxygen availability should be optimised under controlled conditions in a batch bioreactor as shake flasks offer limited control over oxygen availability

Finally, the cell-free supernatant was used to test for antimicrobial activity against *Mycobacterium aurum*. The antimicrobial cell-free supernatant did not show any antimicrobial activity against *M. aurum*. It was recommended that the supernatant undergo further processing such as acid precipitation, solvent extraction and/or adsorption followed by antimicrobial testing against *M. aurum* after each purification step. Different methods for antimicrobial testing should also be investigated.

SAMEVATTING

Tuberkulose (TB), veroorsaak deur *Mycobacterium Tuberculosis*, is die tweede grootste oorsaak van sterftes wat resulteer uit 'n enkel aansteeklike agent wêreldwyd. Suid-Afrika het een van die hoogste aantal aktiewe TB-gevalle wêreldwyd en dit is beraam dat omtrent 1% van Suid-Afrikanners aktiewe TB elke jaar ontwikkel. Multimiddelweerstandige-TB (MDR-TB) is van groter kommer as gevolg van die lae genesingstempo van slegs 50% vir behandelde MDR-TB pasiënte.

Die lipopeptiede biosurfaktant, surfactin, vervaardig deur verskeie *Bacillus*-spesies, lyk na 'n belowende alternatiewe antimikrobiale agent teen organismes wat TB veroorsaak as gevolg van sy vermoë om selmembrane te liseer en membraan deurlatentheid te verander. Die hemolitiese aktiwiteit van surfactin beperk egter die gebruik daarvan as 'n mediese geneesmiddel wat deur mense ingeneem kan word, maar beperk nie sy gebruik in ander toepassings, soos in waspoeiers en ontsmettingsmiddels, in die stryd teen TB nie.

Die groot-skaal produksie van surfactin word beperk deur lae opbrengste en hoë suiweringskoste, daarom die behoefte om ekonomies aanloklike benaderings te ontwikkel om die kommersiële produksie van surfactin as 'n antimikrobiale agent te realiseer vir die gebruik in die stryd teen TB. Lipopeptiede produksie steun grootliks op faktore soos medium samestelling, proses toestande en omgewingsfaktore. Deur hierdie toestande te optimeer sal die kostes vir beide stroomop-prosessering en stroomaf-suiwering, beduidend verminder word.

Die algehele doel van hierdie studie was om die effek van medium samestelling en proses toestande op die groei en lipopeptiede produksie kinetika van *B. subtilis* in lotkultuur te ondersoek, en aanbevelings te maak oor die toestande wat die stroomop-produksie van surfactin, vir moontlike gebruik as 'n antimikrobiale agent teen *M. tuberculosis*, te verbeter.

Skudflesse is gebruik om die effek van onderskeie stikstofbronne (NH_4^+ en NO_3^-) op die proses kinetika te bestudeer deur ammonium en nitraat by diskrete stikstofverhoudings ($\text{NH}_4\text{-N}:\text{NO}_3\text{-N}$) te verskaf. 'n Streng kinetiese analise het die optimale stikstofbronverhouding vir surfactin produksie deur *B. subtilis* gelewer, naamlik 0.5:0.5. 'n $\text{NH}_4\text{-N}:\text{NO}_3\text{-N}$ verhouding van 0.5:0.5 het die hoogste surfactin konsentrasie (1084 mg/L), die hoogste surfactin produktiwiteit (36.1 mg/L/h), die tweede hoogste spesifieke surfactin produksie ($Y_{p/x} = 0.078$), die hoogste surfactin opbrengs op glukose ($Y_{p/s} = 0.031$) en die derde hoogste surfactin-selektiwiteit (5.11 g-surfactin / g-fengycin), gelewer.

Die effek van mangaankonsentrasie op die proses kinetika is ook bestudeer in skudflesse. Streng kinetiese evaluasie het die optimale mangaankonsentrasie vir surfactin produksie gelewer, naamlik 0.1 mM, alhoewel die verhoging van mangaankonsentrasie van 0.05 mM tot 0.1 mM nie die surfactin produksie kinetika beduidend verbeter het nie. 0.1 mM mangaan het die hoogste surfactinkonsentrasie (884 mg/L), die hoogste surfactin opbrengs op glukose ($Y_{p/s} = 0.022$), hoogste surfactin produktiwiteit (46.5 mg/L/h), die tweede hoogste spesifieke surfactin produktiwiteit ($Y_{p/x} = 0.089$) en surfactin-selektiwiteit (5.9 g-surfactin / g-fengycin), verskaf.

Die optimale stikstofbronverhouding en mangaankonsentrasie van die skudflesstudie is gebruik om die proses kinetika onder beheerde toestande in 'n lotbioreaktor te evalueer en is vergelyk met die proses kinetika verkry in die skudflesse. Alle bioreaktor kinetiese parameters (surfactinkonsentrasie – 891 mg/L; $Y_{p/x} = 0.113$; $Y_{p/s} = 0.021$) is amper identies aan dié in die skudflesse (surfactinkonsentrasie – 854 mg/L; $Y_{p/x} = 0.087$; $Y_{p/s} = 0.022$), behalwe vir μ_{max} (0.39 h^{-1} in die bioreaktor en 0.5 h^{-1} in die skudfleskultuur) en surfactin produktiwiteit (18.56 mg/L/h in die bioreaktorkultuur en 30.63 mg/L/h in die skudfleskultuur). Die verskille word toegeskryf aan steuring veroorsaak deur die byvoeging van skuimweerder in die bioreaktorkultuur as gevolg van kragtige skuiming, maar verdere ondersoek word benodig. Dit was ook voorgestel dat alternatiewe metodes in die toekoms ondersoek moet word om die skuiming te hanteer, soos skuim fraksionering. 'n Respons oppervlak metodologie (CCD) ontwerp van die skudfleseksperimente het 'n stikstofbronverhouding ($\text{NH}_4\text{-N}:\text{NO}_3\text{-N}$) van 0.35:0.75, mangaankonsentrasie van 0.06 mM, en 'n relatiewe vulvolume (RFV) van 0.5 as optimaal gelewer om maksimum surfactin produksie by *B. subtilis* te bereik. $\text{NH}_4\text{-N}:\text{NO}_3\text{-N}$ -verhouding en suurstof beskikbaarheid (RVF) was beduidende parameters ($\alpha = 0.05$) wat surfactinkonsentrasie, $Y_{p/x}$, en surfactin-selektiwiteit, affekteer, terwyl mangaankonsentrasie nie 'n beduidende effek op enige van die response gehad het nie. Dit was aanbeveel dat stikstofbronverhouding en suurstof beskikbaarheid geoptimeer moet word onder beheerde toestande in 'n lotreaktor, aangesien skudflesse beperkte beheer oor suurstof beskikbaarheid het.

Laastens, die selvrye bo-drywende stof is gebruik vir toetse vir antimikrobiese aktiwiteit teen *Mycobacterium aurum*. Die antimikrobiese selvrye bo-drywende stof het nie enige aktiwiteit teen *M. aurum* gewys nie. Dit was aanbeveel dat die bo-drywende stof verdere prosessering soos suurpresipitasie, oplossing ekstraksie en/of adsorpsie ondergaan, gevolg deur antimikrobiese toetse teen *M. aurum* na elke suiweringsstadium. Verskillende metodes vir antimikrobiese toetse moet ook ondersoek word.

ACKNOWLEDGEMENTS

I would like to express my sincere gratitude to the following people and organisations without whom this project would not have been possible:

- My supervisor, Prof K.G. Clarke, and my co-supervisor Dr R.W. Pott, for their continuous guidance, support and motivation throughout the course of this project
- Dr V. Rangarajan for his guidance during the initial stages of the project
- Mr J. van Rooyen and Mrs L. Simmers for the punctual completion of HPLC analysis
- Mr J. van Rooyen who provided the lipopeptide standard curves
- Prof J Gorgens and Mr A. Arendse for allowing me to make use of their fermenter systems.
- The National Research Foundation (NRF) of South Africa and Stellenbosch University for providing me with the financial support needed to complete this project.
- My friends and family, especially my mother, Fabiola, and my fiancé, Carlo, for their never-ending support and motivation and for always believing in me and never doubting my ability to complete this project.

TABLE OF CONTENTS

Introduction	1
Chapter 1 Literature Review	3
1.1 The <i>Bacillus</i> genus	3
Overview.....	3
<i>Bacillus</i> screening for lipopeptide production	4
1.1.2 Biosurfactants	6
1.1.2 Overview, classification, and structure	6
1.2.1.1 Glycolipids.....	7
1.2.1.1.1 Rhamnolipids.....	7
1.2.1.1.2 Trehalolipids and sophorolipids	8
1.2.1.2 Lipopeptides	8
1.2.1.2.1 Surfactin	8
1.2.1.2.2 Iturin	9
1.2.1.2.3 Fengycin.....	10
1.2.1.3 Phospholipids and polymeric biosurfactants	11
Biosurfactant properties	11
1.2.2.1 Surface tension	12
1.2.2.2 Foaming activity.....	12
1.2.2.3 Emulsification activity.....	13
1.2.2.4 Antimicrobial- and antiviral biosurfactants	13
1.2.2.4.1 Mechanism of antimicrobial and antiviral action.....	16
1.2.2.4.2 Resistance to antimicrobial action	18
Biosurfactant applications	19
1.2.3.1 Bioremediation	19
1.2.3.2 Biomedical	19
1.2.3.2.1 Antimicrobial applications.....	19

1.2.3.2.2	Anticancer applications	20
1.2.3.3	Agriculture	20
1.3	Process conditions.....	21
	Nutrient medium	21
1.3.1.1	Carbon source.....	21
1.3.1.2	Nitrogen source	21
1.3.1	1.3.1.3 Metal ions.....	25
1.3.1.4	Amino acids	27
	Physiological conditions.....	27
1.3.2.1	Oxygen availability.....	27
1.3.2	1.3.2.1.1 Aeration.....	27
	1.3.2.1.2 Agitation	28
1.3.2.2	Temperature.....	29
1.3.2.3	pH.....	30
1.3.3	Operational strategy	30
1.3.3.1	Batch culture	30
	1.3.3.1.1 Shake flask batch cultures	31
	1.3.3.1.2 Bioreactor batch cultures	31
1.3.3.2	Fed-batch culture	32
1.3.3.3	Continuous culture	32
Chapter 2	Hypotheses and Objectives	34
2.1	Hypotheses.....	34
2.2	Objectives.....	36
Chapter 3	Materials and Methods	37
3.2.1	3.2.1 Micro-organisms and culture maintenance.....	37
3.2.2	3.2.2 Culture media	38
	Media preparation.....	38
	Liquid medium containing ammonium nitrate as sole nitrogen source.....	38

	Liquid medium containing ammonium and nitrate as nitrogen sources	39
3.3	Experimental procedures	41
	Inoculum Development	41
	Shake flask experiments.....	41
3.2.3	Bioreactor experiments	41
3.3.4	Analytical Methods.....	42
3.3.2	Cell Concentration	42
3.3.3	3.4.1.1 Cell dry weight	42
3.4.1	3.4.1.2 Absorbance.....	42
	Glucose concentration	43
3.4.2	Nitrogen utilisation	44
3.4.3	3.4.3.1 Nitrate concentration	44
	3.4.3.2 Ammonium concentration	45
3.4.4	Lipopeptide concentration.....	46
	3.4.4.1 Surfactin concentration.....	46
	3.4.4.2 Antifungal concentration.....	47
	3.4.4.2.1 Fengycin concentration	47
3.4.5	3.4.4.2.2 Iturin concentration	48
	Antimicrobial activity	49
3.5	Experimental design	50
Chapter 4 Results and Discussion		52
4.1.1	4.1 The effect of nitrogen source on the growth and lipopeptide production kinetics of <i>B. subtilis</i> in	
4.1.2	shake flasks	52
4.1.3	Growth, substrate utilisation and lipopeptide production patterns of <i>B. subtilis</i> in cultures	
	containing NH_4^+ and NO_3^- as a nitrogen sources at discrete $\text{NH}_4\text{-N}:\text{NO}_3\text{-N}$ ratios	53
	Comparison of growth and substrate utilisation patterns of <i>B. subtilis</i> in cultures containing	
	NH_4^+ and NO_3^- as nitrogen sources at discrete $\text{NH}_4\text{-N}:\text{NO}_3\text{-N}$ ratios.....	63
	Comparison of lipopeptide production patterns of <i>B. subtilis</i> in cultures containing NH_4^+	
	and NO_3^- as nitrogen sources at discrete $\text{NH}_4\text{-N}:\text{NO}_3\text{-N}$ ratios	67

Comparison of growth and lipopeptide associated kinetic parameters of <i>B. subtilis</i> in cultures containing NH_4^+ and NO_3^- as nitrogen sources at discrete $\text{NH}_4\text{-N}:\text{NO}_3\text{-N}$ ratios	71
4.2 The effect of manganese concentration on growth and lipopeptide production kinetics of <i>B. subtilis</i> in shake flasks	75
4.1.4 Growth, substrate utilisation and lipopeptide production patterns of <i>B. subtilis</i> for cultures with different manganese concentrations	75
Comparison of growth and substrate utilisation patterns of <i>B. subtilis</i> cultures containing	
4.2.1 different manganese concentrations	77
4.2.2 Comparison of lipopeptide production patterns of <i>B. subtilis</i> in cultures with different manganese concentrations	81
4.2.3 Comparison of growth and lipopeptide associated kinetic parameters of <i>B. subtilis</i> in cultures with different manganese concentrations.....	83
4.2.4	
4.3 The effect of $\text{NH}_4\text{-N}:\text{NO}_3\text{-N}$ ratio, manganese concentration and oxygen availability on the growth and surfactin production kinetics of <i>B. subtilis</i>	88
4.3.1 The effect of $\text{NH}_4\text{-N}:\text{NO}_3\text{-N}$ ratio, manganese concentration and oxygen availability on surfactin concentration.....	88
4.3.2 The effect of $\text{NH}_4\text{-N}:\text{NO}_3\text{-N}$ ratio, manganese concentration and oxygen availability on $Y_{p/x}$ (surfactin)	93
4.3.3 The effect of $\text{NH}_4\text{-N}:\text{NO}_3\text{-N}$ ratio, manganese concentration and surface oxygen on surfactin selectivity.....	96
4.4 Growth and production kinetics of <i>B. subtilis</i> under controlled conditions in an instrumented	
4.4.1 bioreactor	99
4.4.2 Growth, substrate utilisation and lipopeptide production patterns in a culture containing 0.01 mM Mn^{2+} and 4g/L NH_4NO_3 as a nitrogen source	99
4.4.3 Growth, substrate utilisation and lipopeptide production patterns using the optimum $\text{NH}_4\text{-N}:\text{NO}_3\text{-N}$ ratio and manganese concentration from shake flask studies.....	102
4.4.4	
4.4.5 Comparison of growth and substrate utilisation patterns of batch bioreactor cultures and shake flasks cultures.....	104
Comparison of lipopeptide production patterns of batch bioreactor cultures and shake flask cultures	107
Comparison of normalised cell and lipopeptide concentrations associated kinetic parameters of batch bioreactor and shake flask cultures	110

4.5 Antimicrobial activity of lipopeptide-containing culture supernatant from <i>B. subtilis</i> against <i>Mycobacterium aurum</i>	112
Chapter 5 Conclusions.....	113
Recommendations.....	119
References	121
Appendices.....	131
Appendix A: Growth, substrate utilisation and lipopeptide production patterns for different manganese concentrations	132
Appendix B: Equations and sample calculations	134
Appendix C: HPLC Chromatograms	136

LIST OF FIGURES

Figure 1-1: Overview of metabolic pathways employed by <i>Bacillus</i> spp. to produce biosurfactants	4
Figure 1-2: Example of a surfactin molecule. <i>Redrawn from Ongena and Jacques (2008) using ChemDraw 15.0.</i>	9
Figure 1-3: Example of an iturin molecule. <i>Redrawn from Ongena and Jacques (2008) using ChemDraw 15.0.</i>	10
Figure 1-4: Example of a fengycin molecule. <i>Redrawn from Ongena and Jacques (2008) using ChemDraw 15.0.</i>	11
Figure 1-5: Assimilatory nitrate reduction pathway. Enzymes: 1 - nitrate reductase; 2 - nitrite reductase (Redrawn from White (2000))	22
Figure 3-1: Standard curve relating absorbance at 620 nm to <i>B. subtilis</i> CDW. <i>The data points represent the mean between duplicates and error bars represent the standard deviation of the mean.</i>	43
Figure 3-2: Standard curve relating absorbance at 540 nm to glucose concentration using the DNS glucose detection method. <i>The data points represent the mean between duplicates and error bars represent the standard deviation of the mean.</i>	44
Figure 3-3: Standard curve for phenol-hypochlorite ammonia detection method relating ammonium concentration to absorbance at 600 nm.	45
Figure 3-4: Surfactin standard curve relating the combined peak areas to the concentration	47
Figure 3-5: Fengycin standard curve relating the peak area to concentration	48
Figure 3-6: Iturin standard curve relating the combined peak areas to concentration	48
Figure 3-7: Schematic representation of antimicrobial inhibition zone redrawn from Ballot (2009)	49
Figure 4-1: Graph illustrating the growth (open circles, left hand axis, in $\log(\text{CDW}/\text{CDW}_0)$) of <i>B. subtilis</i> and substrate concentrations of nitrate (open triangles, left hand axis, in g/L), ammonium (crosses, left hand axis, in g/L) glucose (closed diamonds, right hand axis, in g/L) over time in a culture containing nitrate as the sole nitrogen source in shake flasks at 150 rpm and 30 °C.	54
Figure 4-2: Graph illustrating the growth (open circles, left-hand axis, $\log(\text{CDW}/\text{CDW}_0)$) and lipopeptide production (surfactin – closed diamonds, right hand axis, in mg/L; fengycin – open triangles, right hand axis, in mg/L) of <i>B. subtilis</i> over time in a culture containing nitrate as the sole nitrogen source in shake flasks at 150 rpm and 30 °C.	55
Figure 4-3: Graph illustrating the growth (open circles, left hand axis, in $\log(\text{CDW}/\text{CDW}_0)$) of <i>B. subtilis</i> and substrate concentrations of nitrate (open triangles, left hand axis, in g/L), ammonium (crosses, left hand axis, in g/L) glucose (closed diamonds, right hand axis, in g/L) over time in a culture containing NH_4^+ and NO_3^- in a ratio $\text{NH}_4\text{-N}:\text{NO}_3\text{-N} = 0.25:0.75$ as nitrogen sources in shake flasks at 150 rpm and 30 °C.	56

Figure 4-4: Graph illustrating the growth (open circles, left hand axis, in $\log(CDW/CDW_0)$) of *B. subtilis* and substrate concentrations of nitrate (open triangles, left hand axis, in g/L), ammonium (crosses, left hand axis, in g/L) glucose (closed diamonds, right hand axis, in g/L) over time in a culture containing NH_4^+ and NO_3^- in a ratio $NH_4-N:NO_3-N = 0.25:0.75$ as nitrogen sources in shake flasks at 150 rpm and 30 °C. 57

Figure 4-5 Graph illustrating the growth (open circles, left hand axis, in $\log(CDW/CDW_0)$) of *B. subtilis* and substrate concentrations of nitrate (open triangles, left hand axis, in g/L), ammonium (crosses, left hand axis, in g/L) glucose (closed diamonds, right hand axis, in g/L) over time in a culture containing NH_4^+ and NO_3^- in a ratio $NH_4-N:NO_3-N = 0.5:0.5$ as nitrogen sources in shake flasks at 150 rpm and 30 °C. 58

Figure 4-6: Graph showing growth (open circles, left hand axis, $\log(CDW/CDW_0)$) and lipopeptide production (surfactin – closed diamonds, right hand axis, in mg/L; fengycin – open triangles, right hand axis, in mg/L) of *B. subtilis* over time in a culture containing NH_4^+ and NO_3^- in a ratio $NH_4-N:NO_3-N = 0.5:0.5$ as nitrogen sources in shake flasks at 150 rpm and 30 °C. 59

Figure 4-7: Graph illustrating the growth (open circles, left hand axis, in $\log(CDW/CDW_0)$) of *B. subtilis* and substrate concentrations of nitrate (open triangles, left hand axis, in g/L), ammonium (crosses, left hand axis, in g/L) glucose (closed diamonds, right hand axis, in g/L) over time in a culture containing NH_4^+ and NO_3^- in a ratio $NH_4-N:NO_3-N = 0.75:0.25$ as nitrogen sources in shake flasks at 150 rpm and 30 °C. 60

Figure 4-8: Graph illustrating the growth (open circles, left hand axis, $\log(CDW/CDW_0)$) and lipopeptide production (surfactin – closed diamonds, right hand axis, in mg/L; fengycin – open triangles, right hand axis, in mg/L) of *B. subtilis* over time in a culture containing NH_4^+ and NO_3^- in a ratio $NH_4-N:NO_3-N = 0.75:0.25$ as nitrogen sources in shake flasks at 150 rpm and 30 °C. 61

Figure 4-9: Graph illustrating the growth (open circles, left hand axis, in $\log(CDW/CDW_0)$) of *B. subtilis* and substrate concentrations of nitrate (open triangles, left hand axis, in g/L), ammonium (crosses, left hand axis, in g/L) glucose (closed diamonds, right hand axis, in g/L) over time in a culture containing ammonium as the sole nitrogen source in shake flasks at 150 rpm and 30 °C. 62

Figure 4-10: Graph illustrating the growth (open circles, left hand axis, $\log(CDW/CDW_0)$) and lipopeptide production (surfactin – closed diamonds, right hand axis, in mg/L; fengycin – open triangles, right hand axis, in mg/L) of *B. subtilis* over time in a culture containing ammonium as the sole nitrogen source in shake flasks at 150 rpm and 30 °C. 63

Figure 4-11: Comparison of the growth in $\log(CDW/CDW_0)$ of *B. subtilis* over time in cultures containing NH_4^+ and NO_3^- at discrete $NH_4-N:NO_3-N$ ratios as nitrogen sources in shake flasks at 150 rpm and 30 °C. 64

Figure 4-12: Comparison of the maximum CDW (in g/L) of *B. subtilis* in cultures containing NH_4^+ and NO_3^- at discrete $NH_4-N:NO_3-N$ ratios as nitrogen sources in shake flasks at 150 rpm and 30 °C. 65

- Figure 4-13: Comparison of glucose utilisation by *B. subtilis* in cultures containing NH_4^+ and NO_3^- at discrete $\text{NH}_4\text{-N}:\text{NO}_3\text{-N}$ ratios as nitrogen sources in shake flasks at 150 rpm and 30 °C. 65
- Figure 4-14: Comparison of nitrate utilisation by *B. subtilis* in cultures containing NH_4^+ and NO_3^- at discrete $\text{NH}_4\text{-N}:\text{NO}_3\text{-N}$ ratios as nitrogen sources in shake flasks at 150 rpm and 30 °C. 66
- Figure 4-15: Comparison of ammonium utilisation by *B. subtilis* in cultures containing NH_4^+ and NO_3^- at discrete $\text{NH}_4\text{-N}:\text{NO}_3\text{-N}$ ratios as nitrogen sources in shake flasks at 150 rpm and 30 °C. 67
- Figure 4-16: Comparison of surfactin production by *B. subtilis* in cultures containing NH_4^+ and NO_3^- at discrete $\text{NH}_4\text{-N}:\text{NO}_3\text{-N}$ ratios as nitrogen sources in shake flasks at 150 rpm and 30 °C. 69
- Figure 4-17: Comparison of the homologue distribution of surfactin produced by *B. subtilis* in cultures containing NH_4^+ and NO_3^- at discrete $\text{NH}_4\text{-N}:\text{NO}_3\text{-N}$ ratios as nitrogen sources in shake flasks at 150 rpm and 30 °C. 70
- Figure 4-18: Comparison of fengycin production by *B. subtilis* in cultures containing NH_4^+ and NO_3^- at discrete $\text{NH}_4\text{-N}:\text{NO}_3\text{-N}$ ratios as nitrogen sources in shake flasks at 150 rpm and 30 °C. 71
- Figure 4-19: Comparison of normalised growth and lipopeptide related kinetic parameters of *B. subtilis* at maximum surfactin concentration in cultures containing NH_4^+ and NO_3^- at discrete $\text{NH}_4\text{-N}:\text{NO}_3\text{-N}$ ratios as nitrogen sources in shake flasks at 150 rpm and 30 °C. 74
- Figure 4-20: Graph illustrating the growth (open circles, left hand axis, in $\log(\text{CDW}/\text{CDW}_0)$) of *B. subtilis* and substrate concentrations of nitrate (open triangles, left hand axis, in g/L), ammonium (crosses, left hand axis, in g/L) glucose (closed diamonds, right hand axis, in g/L) for a culture containing 0.1 mM Mn^{2+} and 4 g/L NH_4NO_3 as a nitrogen source in shake flasks at 150 rpm and 30 °C. 76
- Figure 4-21: : Graph illustrating the growth (open circles, left hand axis, in $\log(\text{CDW}/\text{CDW}_0)$) and lipopeptide production (surfactin – closed diamonds, right hand axis, in mg/L; fengycin – open triangles, right hand axis, in mg/L) of *B. subtilis* over time in a culture containing 0.1 mM Mn^{2+} and 4 g/L NH_4NO_3 in shake flasks at 150 rpm and 30 °C. 77
- Figure 4-22: Comparison of the growth (in $\log(\text{CDW}/\text{CDW}_0)$) of *B. subtilis* in cultures containing different Mn^{2+} concentrations and 4 g/L NH_4NO_3 in shake flasks at 150 rpm and 30 °C. 77
- Figure 4-23: Comparison of glucose utilisation by *B. subtilis* in cultures containing different Mn^{2+} concentrations and 4 g/L NH_4NO_3 in shake flasks at 150 rpm and 30 °C. 78
- Figure 4-24: Comparison of ammonium utilisation of *B. subtilis* in cultures containing different Mn^{2+} concentrations and 4 g/L NH_4NO_3 in shake flasks at 150 rpm and 30 °C. 79
- Figure 4-25: Nitrate utilisation comparison of *B. subtilis* for different Mn^{2+} concentrations in shake flasks 80
- Figure 4-26: Comparison of normalised growth related kinetic parameters at maximum cell concentration for different Mn^{2+} concentrations 81
- Figure 4-27: Comparison of surfactin production by *B. subtilis* for different Mn^{2+} concentrations and 4 g/L NH_4NO_3 in shake flasks at 150 rpm and 30 °C. 82

- Figure 4-28: Comparison of homologue distribution of surfactin produced by *B. subtilis* in cultures containing different Mn^{2+} concentrations and 4 g/L NH_4NO_3 in shake flasks at 150 rpm and 30 °C. 82
- Figure 4-29: Comparison of fengycin production by *B. subtilis* in cultures containing different Mn^{2+} concentrations and 4 g/L NH_4NO_3 in shake flasks at 150 rpm and 30 °C. 83
- Figure 4-30: Comparison of normalised growth and lipopeptide related kinetic parameters of *B. subtilis* at maximum surfactin concentration for different Mn^{2+} concentrations in shake flasks 150 rpm and 30 °C. 86
- Figure 4-31: Normalised fengycin related kinetic parameters for different manganese concentrations at maximum fengycin concentration in shake flasks 150 rpm and 30 °C. 87
- Figure 4-32: Degree of variable contribution on the concentration of surfactin produced by *B. subtilis* in shake flasks at 150 rpm and 30°C. *Q and L refers to the quadratic and linear terms of the model, respectively. The Pareto chart was generated using STATISTICA 13.2.* 89
- Figure 4-33: The effect of nitrogen source ratio and Mn^{2+} concentration on the surfactin concentration produced by *B. subtilis* after 29 hours in shake flasks at 150 rpm and 30 °C shown as (A) a 3D surface plot and (B) a contour surface plot. *NH₄-N refers to fraction of nitrogen supplied as NH_4^+ . The surface plots were generated using STATISTICA 13.2.* 90
- Figure 4-34: The effect of nitrogen source ratio and oxygen availability on the surfactin concentration produced by *B. subtilis* after 29 hours in shake flasks at 150 rpm and 30 °C shown as (A) a 3D surface plot and (B) a contour surface plot. *RFV refers to relative filling volume of the flask which relates surface oxygen. The surface plots were generated using STATISTICA 13.2.* 91
- Figure 4-35: The effect of Mn^{2+} concentration and surface oxygen on the surfactin concentration produced by *B. subtilis* after 29 h in shake flasks at 150 rpm and 30 °C shown as (A) a 3D surface plot and (B) a contour surface plot. *RFV refers to relative filling volume of the flask which relates surface oxygen. The surface plots were generated using STATISTICA 13.2.* 92
- Figure 4-36: Degree of variable contribution on $Y_{p/x}$ (surfactin) of *B. subtilis* in shake flasks after 29 h at 150 rpm and 30°C. *Q and L refers to the quadratic and linear terms of the model, respectively. The Pareto chart was generated using STATISTICA 13.2.* 94
- Figure 4-37: Graphs showing the lack of fit of the data to the model describing the effects of NH_4 -N: NO_3 -N ratio, Mn^{2+} concentration, and oxygen availability on $Y_{p/x}$ (surfactin) for *B. subtilis* in shake flasks after 29 h at 150 rpm and 30 °C. 95
- Figure 4-38: Degree of variable contribution on the selectivity of surfactin over fengycin (S/F) produced by *B. subtilis* in shake flasks after 29 h at 150 rpm and 30°C. *Q and L refers to the quadratic and linear terms of the model, respectively. The Pareto chart was generated using STATISTICA 13.2.* 96
- Figure 4-39: : Graphs showing the lack of fit of the data to the model describing the effects of NH_4 -N: NO_3 -N ratio, Mn^{2+} concentration, and oxygen availability on the selectivity of surfactin over fengycin (S/F) for *B. subtilis* in shake flasks after 29 h at 150 rpm and 30 °C. 98

- Figure 4-40: Graph illustrating the growth (open circles, left hand axis, in $\log(\text{CDW}/\text{CDW}_0)$) of *B. subtilis* and substrate concentration of nitrate (open triangles, left hand axis, in g/L), glucose (closed diamonds, right hand axis, in g/L), ammonium (crosses, right hand axis, in g/L scaled up by a factor of X100 for clarity) and dissolved oxygen (open diamonds, right hand axis) for a culture containing 4 g/L NH_4NO_3 and 0.01 mM Mn^{2+} in a 1 L controlled bioreactor (0.5 L working volume). 100
- Figure 4-41: Graph illustrating the growth (open circles, left hand axis, in $\log(\text{CDW}/\text{CDW}_0)$) and lipopeptide production (surfactin – closed diamonds, right hand axis, in mg/L; fengycin – open triangles, right hand axis, in mg/L) of *B. subtilis* over time in a culture containing 4 g/L NH_4NO_3 and 0.01 mM Mn^{2+} in a 1 L controlled bioreactor (0.5 L working volume). 101
- Figure 4-42: Graph illustrating the growth (open circles, left hand axis, in $\log(\text{CDW}/\text{CDW}_0)$) of *B. subtilis* and substrate concentration of nitrate (open triangles, left hand axis, in g/L), glucose (closed diamonds, right hand axis, in g/L), ammonium (crosses, right hand axis, in g/L scaled up by a factor of X100 for clarity) and dissolved oxygen (open diamonds, right hand axis) at the optimal nitrogen source ratio ($\text{NH}_4\text{-N}:\text{NO}_3\text{-N}$ ratio = 0.5) and Mn^{2+} concentration (0.05 mM) from shake flask studies in a 1 L controlled bioreactor (0.5 L working volume). 103
- Figure 4-43: Graph illustrating the growth (open circles, left hand axis, in $\log(\text{CDW}/\text{CDW}_0)$) and lipopeptide production (surfactin – closed diamonds, right hand axis, in mg/L; fengycin – open triangles, right hand axis, in mg/L) of *B. subtilis* over time at the optimal nitrogen source ratio ($\text{NH}_4\text{-N}:\text{NO}_3\text{-N}$ ratio = 0.5) and Mn^{2+} concentration (0.05 mM) from shake flask studies in a 1 L controlled bioreactor (0.5 L working volume). 103
- Figure 4-44: Comparison of *B. subtilis* growth in shake flask and batch bioreactor cultures containing 0.01 and 0.05 mM Mn^{2+} and 4 g/L NH_4NO_3 104
- Figure 4-45: Comparison of *B. subtilis* glucose utilisation in shake flask and batch bioreactor cultures containing 0.01 and 0.05 mM Mn^{2+} and 4 g/L NH_4NO_3 105
- Figure 4-46: Comparison of *B. subtilis* ammonium utilisation in shake flask and batch bioreactor cultures containing 0.01 and 0.05 mM Mn^{2+} and 4 g/L NH_4NO_3 106
- Figure 4-47: Comparison of *B. subtilis* nitrate utilisation in shake flask and batch bioreactor cultures containing 0.01 and 0.05 mM Mn^{2+} and 4 g/L NH_4NO_3 106
- Figure 4-48: Comparison of surfactin production by *B. subtilis* in shake flask and batch bioreactor cultures containing 0.01 and 0.05 mM Mn^{2+} and 4 g/L NH_4NO_3 107
- Figure 4-49: Comparison of fengycin production by *B. subtilis* in shake flask and batch bioreactor cultures containing 0.01 and 0.05 mM Mn^{2+} and 4 g/L NH_4NO_3 109
- Figure 4-50: Comparison of normalised growth and lipopeptide production kinetics of *B. subtilis* in shake flask and batch bioreactor cultures containing 0.01 and 0.05 mM Mn^{2+} and 4 g/L NH_4NO_3 evaluated at the time of maximum surfactin concentration 111
- Figure 4-51: *B. subtilis* cell-free supernatant antimicrobial activity against *M. aurum* 112

LIST OF TABLES

Table 1-1: Bacillus screening growth and production kinetics comparison in controlled batch bioreactor cultures (Pretorius <i>et al.</i> , 2015)	5
Table 1-2: Well-known biosurfactants and their most common producers	6
Table 1-3: Organisms susceptible to the antimicrobial action of <i>B. subtilis</i> biosurfactants	15
Table 1-4: Antiviral activity of surfactin produced by <i>B. subtilis</i>	16
Table 3-1: Basal growth medium containing 4 g/L ammonium nitrate as the sole nitrogen source (Pretorius <i>et al.</i> , 2015)	39
Table 3-2: Stock solution concentrations and dilutions used to prepare the basal medium in Table 3-1	39
Table 3-3: Stock solution concentrations and dilutions used to prepare the liquid medium for nitrogen source experiments.....	40
Table 3-4: Final concentrations of NH ₄ Cl and NaNO ₃ used in nitrogen source experiments.....	40
Table 3-5: Stock solution dilutions (24 mL stock solution / 100 mL solution) for nitrogen source ratio experiments	40
Table 3-6: HPLC specifications for surfactin analyses.....	46
Table 3-7: Factor levels for independent variables	50
Table 3-8: Running order and factor levels.....	51
Table 4-1: Summary of <i>B. subtilis</i> growth and lipopeptide related kinetic parameters in cultures containing NH ₄ ⁺ and NO ₃ ⁻ at discrete NH ₄ -N:NO ₃ -N ratios as nitrogen sources in shake flasks at 150 rpm and 30 °C.....	72
Table 4-2: Growth related kinetic parameters at maximum cell concentration for different Mn ²⁺ concentrations	80
Table 4-3: Summary of <i>B. subtilis</i> growth and lipopeptide related kinetic parameters at maximum surfactin concentration in cultures containing different Mn ²⁺ concentrations and 4 g/L NH ₄ NO ₃ in shake flasks at 150 rpm and 30 °C.....	84
Table 4-4: Fengycin related kinetic parameters for different manganese concentrations at maximum fengycin concentration in shake flasks 150 rpm and 30 °C.	86
Table 4-5: Comparison of <i>B. subtilis</i> maximum specific growth rate and maximum CDW in shake flask and batch bioreactor cultures containing 0.01 and 0.05 mM Mn ²⁺ and 4 g/L NH ₄ NO ₃	104
Table 4-6: Summary of <i>B. subtilis</i> growth and lipopeptide related kinetic parameters at maximum surfactin concentration shake flask and bioreactor cultures containing 0.01 and 0.05 mM Mn ²⁺ and 4 g/L NH ₄ NO ₃	110

NOMENCLATURE

μ	Specific growth rate
μL	Microliter
μ_{max}	Maximum specific growth rate
ATCC 21332	Strain of <i>Bacillus subtilis</i>
aq	Aqueous
$\text{CaCl}_2 \cdot 2\text{H}_2\text{O}$	Calcium chloride dihydrate
CDW	Cell dry weight
$\text{FeSO}_4 \cdot 7\text{H}_2\text{O}$	Ferrous sulphate heptahydrate
g	Gram
g/L	Gram per litre
h	Hour
HPLC	High Pressure Liquid Chromatography
KH_2PO_4	Dihydrogen potassium phosphate
L	Litre
mAU*min / g cells/ L	milli-Absorbance Units
mg/L	Milligram per litre
$\text{MgSO}_4 \cdot 7\text{H}_2\text{O}$	Magnesium sulphate heptahydrate
min	Minute
mL	Millilitre
mM	Millimolar
mN/m	Milli-Newton per metre
$\text{MnSO}_4 \cdot \text{H}_2\text{O}$	Hydrous manganese sulphate
mV	Millivolt
Na_2HPO_4	Disodium hydrogen phosphate
NaCl	Sodium chloride
NH_4NO_3	Ammonium nitrate
$\text{NH}_4\text{-N}$	Fraction nitrogen supplied as ammonium
$\text{NO}_3\text{-N}$	Fraction nitrogen supplied as nitrate
P	Product
P_0	Product concentration at time 0
P_i	Product concentration at time i
rpm	Revolutions per minute
S	Substrate

S_0	Substrate concentration at time 0
S_i	Substrate concentration at time i
S/F	Surfactin to fengycin ratio
t	Time
TB	Tuberculosis
UV	Ultraviolet
v/v	Volume per volume
X	Cell concentration
X_0	Cell concentration at time 0
X_i	Cell concentration at time i
$Y_{p/s}$	Product yield on substrate
$Y_{p/x}$	Product yield on biomass
$Y_{x/s}$	Cell yield on substrate

INTRODUCTION

Tuberculosis (TB), second to HIV/AIDS, is one of the major causes of death worldwide resulting from a single infectious agent, according to the World Health Organisation (WHO) 2013 data. The number of TB cases in South Africa is one of the highest globally and it is estimated that approximately 1% of the population develops active TB each year. Of even greater concern is multi-drug resistant TB (MDR-TB) which has a cure rate of only 50% for treated MDR-TB patients (World Health Organization, 2015). WHO estimated 480 000 cases of MDR-TB globally in 2014, with an estimated 190 000 deaths resulting from MDR-TB.

The use of biosurfactants as safe and effective alternatives to synthetic medicines and antimicrobial agents are becoming increasingly popular, especially in a time where the number of drug-resistant pathogenic bacteria are on a rise, thus necessitating the need for alternative therapy methods (Seydlová and Svobodová, 2008). It should be noted that not all biosurfactants are safe for human consumption; surfactin and iturin are strongly haemolytic (Ongena and Jacques, 2008) thus they are not safe for ingestion by humans but would more suitable for use as detergents or disinfectants for example. One example of an antimicrobial biosurfactant that is produced commercially, is the lipopeptide biosurfactant, dectomycin, produced by *Streptomyces roseosporus*, that has shown a high activity against multidrug-resistant bacteria such as methicillin-resistant *Staphylococcus aureus*, and has been approved for treatment of complex skin- and skin-structure infections (Seydlová and Svobodová, 2008).

Surfactin, produced by *Bacillus subtilis* is a lipopeptide biosurfactant that has shown antimicrobial activity against a number of gram-positive and gram-negative bacteria (Benincasa *et al.*, 2004) making it a promising antimicrobial agent to use as a disinfectant and/or diagnostic tool in the fight against TB. Surfactin is an amphipathic cyclic lipopeptide characterised by a heptapeptide interlinked with a β -hydroxy fatty acid chain consisting of 12 to 16 carbon atoms, which may be branched, that forms a cyclic lactone ring structure (Ongena and Jacques, 2008; Seydlová and Svobodová, 2008). Heerklotz, Wieprecht and Seelig (2004) proposed a detergent-like mechanism for the antimicrobial activity of surfactin due to its ability to lyse cell membranes and alter membrane permeability.

Large scale production of biosurfactants such as surfactin are generally coupled with low yields and high purification costs (Mukherjee *et al.*, 2006), which necessitates the development of economically attractive approaches to realise the commercial production of surfactin as an antimicrobial agent against TB. The production of lipopeptides largely depends on the process conditions, medium composition, and environmental factors (Rangarajan and Clarke, 2015), hence by optimising these conditions the cost of both upstream processing, and downstream separation, can be reduced significantly.

B. subtilis has been identified as the most promising surfactin producer amongst other *Bacillus* candidates screened for lipopeptide production (Pretorius *et al.*, 2015). *B. subtilis* produces three lipopeptide families namely surfactin, fengycin and iturin, however this study focused on the production of surfactin. The effect of process parameters, which include nitrogen source, manganese concentration, and dissolved oxygen availability, were investigated through a rigorous kinetic evaluation of growth and lipopeptide production in shake flasks. A central composite design was used to account for the interactive effects between these parameters in an attempt to optimise the conditions for surfactin production. The optimum conditions were then cultured under controlled conditions in an instrumented bioreactor. The cell free supernatant was also tested for antimicrobial activity against *Mycobacterium aurum* which acted as a non-pathogenic surrogate for *M. tuberculosis*.

This thesis will present the background on the *Bacillus* genus, biosurfactants and process conditions in an extensive literature review focused on surfactin (Chapter 1), discuss the hypotheses and objectives resulting from the literature review (Chapter 2), describe the materials and methods employed (Chapter 3), and document and evaluate the obtained results (Chapter 4). Lastly, conclusions based on the results will be made to evaluate the importance and implications of this study (Chapter 5), followed by recommendations for future work.

Chapter 1

LITERATURE REVIEW

1.1 THE *BACILLUS* GENUS

1.1.1 Overview

The *Bacillus* genus consists of a large and diverse group of gram-positive bacteria belonging to the family *Bacillaceae*. Members of the *Bacillus* genus exhibit great diversity in terms of physiology and morphology, however there are a number of characteristics that are shared among members of the genus (Todar, 2002). These characteristics include: ubiquitous occurrence, safe, excellent colonisation ability, versatility in effectively protecting plants from phytopathogens, antibiotic production, and sporulation ability (Baruzzi *et al.*, 2011; Romero *et al.*, 2007; Todar, 2002; Xu *et al.*, 2013) which ensures their survival as their endospores are able to resist desiccation, UV irradiation, heat, and organic solvents (Yáñez-Mendizábal *et al.*, 2011).

The *Bacillus* genus, like many other gram-positive bacteria, has complex cell structure that consists of a capsule, a protein surface layer (S-layer), several layers of peptidoglycan sheeting, and proteins present in the outer surface of the plasma membrane (Todar, 2002). *Bacillus* spp. are chemoheterotrophs (Todar, 2002) and some species such as *B. subtilis* are capable of both aerobic and anaerobic respiration, thus they are facultative anaerobes (Willenbacher *et al.*, 2015). During anaerobic respiration *B. subtilis* utilises nitrate as an alternative electron acceptor as opposed to oxygen (refer to section 1.3.1.2 for a more detailed account of this). Furthermore, *B. subtilis* is also capable fermentative growth in the absence of external electron acceptors (Nakano *et al.*, 1997).

Microorganisms employ different metabolic pathways for substrate conversion and the production of primary and secondary metabolites, enzymes, and amino acids. Figure 1-1 gives a broad overview of the metabolic pathways employed by *Bacillus* spp. to produce biosurfactants.

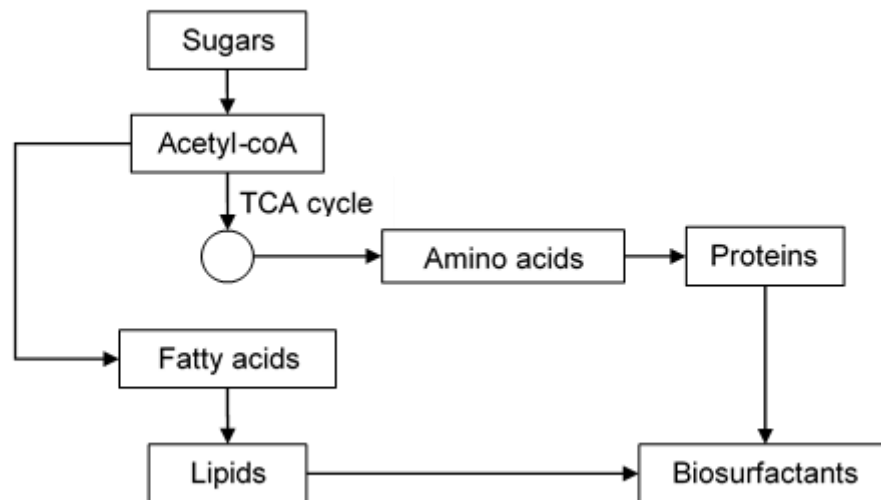


Figure 1-1: Overview of metabolic pathways employed by *Bacillus* spp. to produce biosurfactants

Figure 1-1 shows that sugars are converted to acetyl-coA which is used to produce the building blocks for biosurfactants, namely proteins and lipids via two distinct pathways. Acetyl-coA is either used to produce intermediates for amino acids via the tricarboxylic acid (TCA) cycle or is alternatively converted to fatty acids via the fatty acid biosynthesis pathway (Clarke, 2013)

1.1.2 *Bacillus* screening for lipopeptide production

As discussed in Section 1.1.1 the *Bacillus* genus is a large and diverse group of bacteria. Thus, identifying the optimum *Bacillus* candidate would be the first step when studying and optimising the production kinetics for a specific application. This study focuses on the production kinetics of the lipopeptide biosurfactant, surfactin, as a possible antimicrobial agent against *Mycobacterium Tuberculosis* (refer to section 1.2.2.4 and 1.2.3.2.1).

Pretorius *et al.* (2015) identified four *Bacillus* species as the most promising lipopeptide producers: *B. subtilis* ATCC 21332, *B. subtilis subsp. spizizenii* DSM 347, *B. amyloliquefaciens* DSM 23117 and *B. licheniformis* DSM 13. These *Bacillus* spp. were screened for their lipopeptide production potential by comparing their growth and production kinetics under the same set of conditions in controlled batch bioreactor cultures. The results are shown in Table 1-1.

Table 1-1: Bacillus screening growth and production kinetics comparison in controlled batch bioreactor cultures (Pretorius *et al.*, 2015)

Kinetic parameters	<i>B. amyloliquefaciens</i>	<i>B. licheniformis</i>	<i>B. subtilis</i>	<i>B. spizizenii</i>
<u>Growth</u>				
μ_{\max} (h^{-1})	0.43	0.30	0.45	0.39
CDW (g/L)	4.61	5.00	5.15	8.44
<u>Surfactin</u>				
Max. concentration (mg/l)	68.00	0.00	882.00	36.50
Max yield. ($Y_{p/x}$) (g/g)	0.03	0.00	0.28	0.01
Max productivity (mg/L/h)	3.69	0.00	35.50	2.39
<u>Antifungal lipopeptides</u>				
Max. concentration (mAU*min)	114.60	55.78	35.22	25.21
Max. yield ($Y_{p/x}$) (mAU*min/g cells/L)	21.25	10.97	12.69	5.50
Max. productivity (mAU*min/h)	3.69	0.00	35.50	2.39

The growth kinetics in Table 1-1 show that *B. subtilis* had highest maximum specific growth rate (0.45 h^{-1}) and *B. licheniformis* had the lowest (0.3 h^{-1}). Furthermore, *B. spizizenii* had the highest maximum CDW (8.44 g/L) which was almost double compared to that of *B. amyloliquefaciens* which had the lowest maximum CDW (4.61 g/L). When comparing the lipopeptide production kinetics (maximum concentration, specific production, and productivity) in Table 1-1, *B. subtilis* outperformed the other three *Bacillus* spp. with regards to the surfactin kinetic parameters, while the same observation was made for *B. amyloliquefaciens* in terms of antifungal kinetic parameters.

It can thus be concluded that *B. subtilis* is the optimal candidate for surfactin production which justifies its use in this study.

1.2 BIOSURFACTANTS

1.2.1 Overview, classification, and structure

Biosurfactants are primarily classified according to their chemical composition and microbial origin as outlined in Table 1-2. Generally, the structure of biosurfactants consist of hydrophilic and hydrophobic moieties. The hydrophilic moiety comprises of either amino acids, peptides, cations or anions, or mono-, di-, or polysaccharides, whereas the hydrophobic moiety comprises of either saturated- or unsaturated- fatty acids (Desai and Banat, 1997). Biosurfactants can be classified as follows: glycolipids, lipopeptides and lipoproteins, and polymeric biosurfactants (Desai and Banat, 1997).

Table 1-2: Well-known biosurfactants and their most common producers

Biosurfactants	Organism	Reference
<u>Glycolipids</u>		
Rhamnolipid	<i>Pseudomonas aeruginosa</i>	(Banat <i>et al.</i> , 2010; Haba <i>et al.</i> , 2003; Mulligan, 2005)
	<i>Pseudomonas spp.</i>	(Banat <i>et al.</i> , 2010; Mulligan, 2005)
	<i>Serratia rubidea</i>	(Mulligan, 2005)
Trehalolipids	<i>Rhodococcus erythropolis</i>	(Banat <i>et al.</i> , 2010; Mulligan, 2005)
	<i>Nocardia spp.</i>	(Banat <i>et al.</i> , 2010; Mulligan, 2005)
	<i>N. erythropolis</i>	
	<i>Mycobacterium spp.</i>	(Banat <i>et al.</i> , 2010; Mulligan, 2005)
	<i>Corynebacterium spp.</i>	(Banat <i>et al.</i> , 2010; Mulligan, 2005)
	<i>Arthrobacter paraffineus</i>	(Mulligan, 2005)
Sophorolipids	<i>Torulopsis bombicola</i>	(Banat <i>et al.</i> , 2010; Mulligan, 2005)
	<i>T. apicola</i>	(Banat <i>et al.</i> , 2010; Mulligan, 2005)
	<i>T. pertophilum</i>	(Banat <i>et al.</i> , 2010)
<u>Lipopeptides and Lipoproteins</u>		
Surfactin	<i>Bacillus subtilis</i>	(Banat <i>et al.</i> , 2010; Mulligan, 2005; Stein, 2005)
	<i>B. amyloliquefaciens</i>	(Deleu <i>et al.</i> , 2008; Pretorius <i>et al.</i> , 2015; Stein, 2005)
	<i>B. pumilus</i>	(Banat <i>et al.</i> , 2000; Mulligan, 2005)
Fengycin	<i>Bacillus subtilis</i>	(Deleu <i>et al.</i> , 2008; Gond <i>et al.</i> , 2015; Pretorius <i>et al.</i> , 2015; Stein, 2005)

Biosurfactants	Organism	Reference
	<i>B. amyloliquefaciens</i>	(Chen <i>et al.</i> , 2010; Lee <i>et al.</i> , 2010; Pretorius <i>et al.</i> , 2015)
Iturin A	<i>Bacillus subtilis</i>	(Pretorius <i>et al.</i> , 2015; Romero <i>et al.</i> , 2007; Zohora <i>et al.</i> , 2009)
	<i>B. amyloliquefaciens</i>	(Lin <i>et al.</i> , 2007; Pretorius <i>et al.</i> , 2015)
Subtilisin	<i>B. subtilis</i>	(Desai and Banat, 1997; Seok Oh <i>et al.</i> , 2002; Stein, 2005)
Peptide-lipid	<i>B. licheniformis</i>	(Desai and Banat, 1997)
Gramicidins	<i>B. brevis</i>	(Desai and Banat, 1997)
<u>Polymeric surfactants</u>		
Emulsan	<i>Acinetobacter calcoaceticus</i>	(Banat <i>et al.</i> , 2010; Rahman and Gakpe, 2008)
Biodispersan	<i>A. calcoaceticus</i>	(Desai and Banat, 1997)
Liposan	<i>Candida lipolytica</i>	(Salihu <i>et al.</i> , 2009)
Carbohydrate-protein-lipid	<i>P. fluorescens</i>	(Desai and Banat, 1997)
<u>Phospholipids</u>		
	<i>Thiobacillus thiooxidans</i>	(Rahman and Gakpe, 2008)
	<i>Acinetobacter spp.</i>	(Mulligan, 2005)

1.2.1.1 Glycolipids

Glycolipids are one of the most well-known biosurfactants. Glycolipids are carbohydrates that are bound to either long-chain aliphatic acids, or hydroxyl fatty acids (Desai and Banat, 1997; Shoeb *et al.*, 2013) that are either linked to an ether or ester group (Shoeb *et al.*, 2013). Among the most well-known glycolipids are rhamnolipids produced by *Pseudomonas* sp., trehalose lipids produced by *Mycobacterium* and sophorolipids produced by yeasts (Desai and Banat, 1997; Cameotra and Makkar, 2004; Shoeb *et al.*, 2013).

1.2.1.1.1 Rhamnolipids

Rhamnolipids are one of the best-studied glycolipids and are most commonly produced by *Pseudomonas aeruginosa* (Desai and Banat, 1997; Cameotra and Makkar, 2004). Rhamnolipids are made up of two rhamnose molecules that are linked to one or two β -hydroxydecanoic acid molecules. *Pseudomonas aeruginosa* has been reported to produce various structural homologs of rhamnolipids depending on the bacterial strain, carbon source and process strategy (Haba *et al.*, 2003).

1.2.1.1.2 Trehalolipids and sophorolipids

Trehalolipids and sophorolipids have a similar structure to rhamnolipids (Cooper and Zajic, 1980). Trehalolipids consist of a disaccharide trehalose linked at C₆ to two β -hydroxy- α -branched fatty acids and have been isolated from several strains of *Arthrobacter*, *Mycobacterium*, *Corynebacterium*, *Brevibacterium*, and *Nocardia* spp. (Desai and Banat, 1997). These organisms produce trehalolipids that differ in structure of the fatty acids and degree of unsaturation (Desai and Banat, 1997).

Sophorolipids are made up of a dimeric sophorose molecule linked to a long hydroxyl fatty acid chain and are mainly produced by the yeasts *Torulopsis bombicola* and *T. petrophilum* (Desai and Banat, 1997).

1.2.1.2 Lipopeptides

Lipopeptide biosurfactants are generally produced by *Bacillus* spp. which includes *B. subtilis*, *B. amyloliquefaciens*, *B. licheniformis*, and *B. brevis* (Ben Abdallah *et al.*, 2015; Besson and Michel, 1992; Deleu *et al.*, 2008; Desai and Banat, 1997; Pretorius, 2014). From this family of organisms, the rhizobacterium, *B. subtilis*, is one of the most well-studied lipopeptide producers (Ongena and Jacques, 2008). *B. subtilis* offers many advantages, including the fact that it has GRAS (generally regarded as safe) status as well as its spore forming capabilities which allows it to withstand harsh environments, thus making *B. subtilis* an excellent candidate for biotechnical applications (Ongena and Jacques, 2008).

Lipopeptides generally consist of a hydrophilic amino acid (peptide) chain linked to a hydrophobic fatty acid chain. The hydrophilic peptide can be either linear or cyclic, as is the case for the three lipopeptide families surfactin, fengycin and iturin, produced by *B. subtilis* (Besson and Michel, 1992; Deleu *et al.*, 2008; Ongena and Jacques, 2008; Rahman and Gakpe, 2008).

1.2.1.2.1 Surfactin

Surfactin, produced by various strains of *B. subtilis*, is a cyclic lipopeptide, and is regarded as one of the most powerful biosurfactants yet studied (Hommel, 1990; Wei and Chu, 1998). Surfactin is an amphipathic cyclic lipopeptide characterised by a heptapeptide interlinked with a β -hydroxy fatty acid chain consisting of 12 to 16 carbon atoms, which may be branched, that forms a cyclic lactone ring structure (Ongena and Jacques, 2008; Seydlová and Svobodová, 2008). The peptide ring comprises of seven amino acids, of which the sequence may differ, but is always comprised of five lipophilic and two negatively charged hydrophilic amino acids (Buchoux *et al.*, 2008; Singh and Cameotra, 2004). Furthermore, variations in the fatty acid chain length also exists, resulting in several surfactin homologues (see section 1.3.1.4). One representative member of the surfactin family of lipopeptides is shown in Figure 1-2.

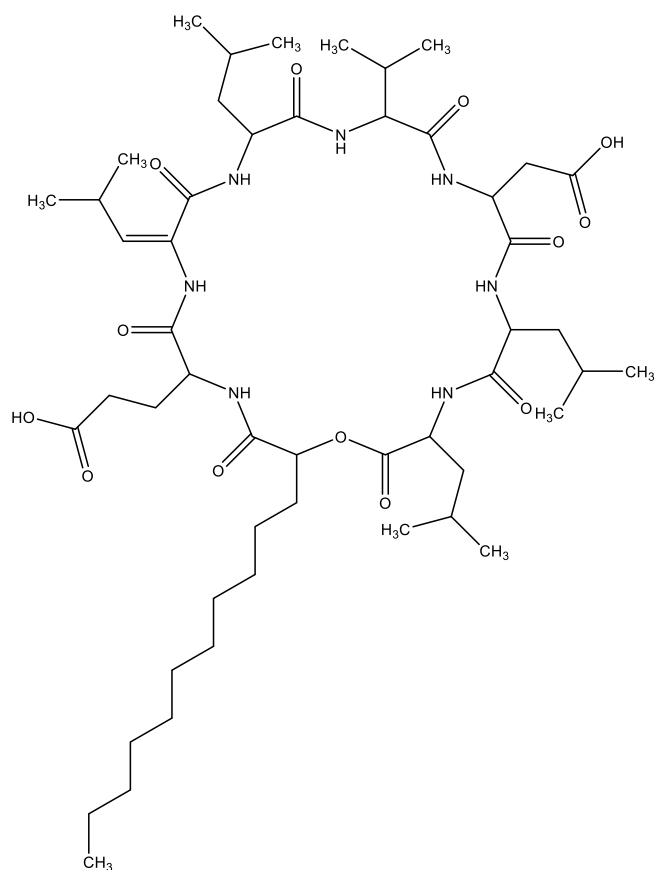


Figure 1-2: Example of a surfactin molecule. Redrawn from Ongena and Jacques (2008) using ChemDraw 15.0.

1.2.1.2.2 Iturin

Iturin is another lipopeptide family produced by all *Bacillus* spp. (Besson and Michel, 1992; Chenikher *et al.*, 2010; Meena and Kanwar, 2015). The iturin family is generally comprised of heptapeptides linked with a β -hydroxy fatty acid chain consisting of 12 to 15 carbon atoms (Ongena and Jacques, 2008). Similar to surfactin, iturin also has a number of structural homologs. One representative of the iturin family is shown in Figure 1-3.

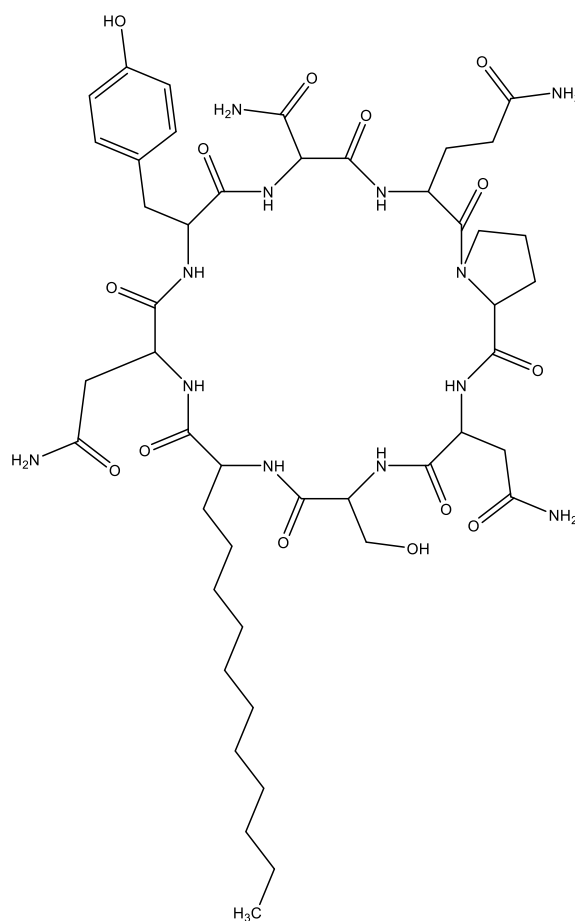


Figure 1-3: Example of an iturin molecule. *Redrawn from Ongena and Jacques (2008) using ChemDraw 15.0.*

1.2.1.2.3 Fengycin

Fengycin is another noteworthy lipopeptide biosurfactant produced by *Bacillus* spp. and generally consists of a lipodecapeptide, with a lactone ring located within the peptidic moiety, and a β -hydroxy fatty acid chain consisting of 14 to 17 carbon atoms that are either saturated or unsaturated giving rise to a number of fengycin homologues and isomers (Ongena and Jacques, 2008; Meena and Kanwar, 2015). The structure of one representative of the fengycin family is shown in Figure 1-4.

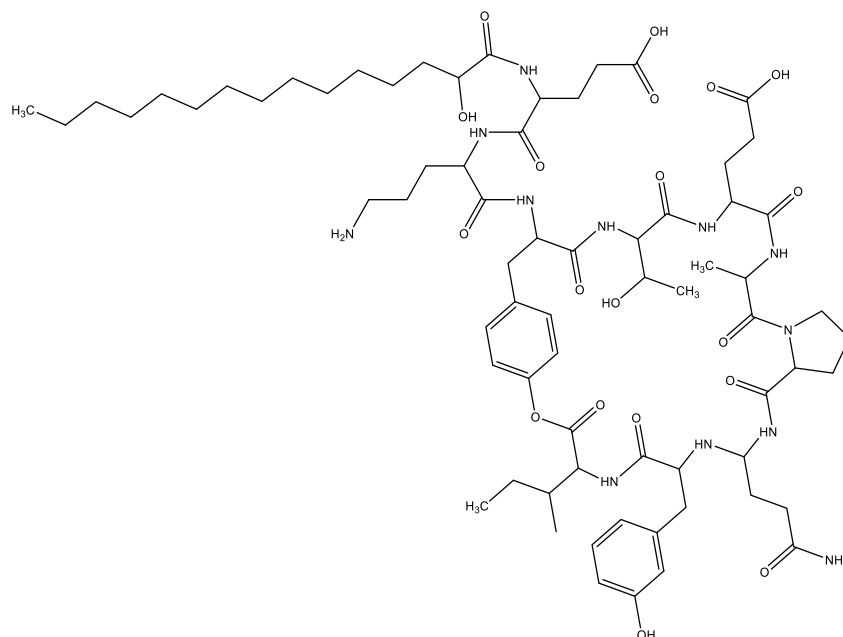


Figure 1-4: Example of a fengycin molecule. Redrawn from Ongena and Jacques (2008) using ChemDraw 15.0.

1.2.1.3 Phospholipids and polymeric biosurfactants

Phospholipids are well known as a major constituent of all cell membranes. Phospholipids consists of fatty acid molecule linked to a cationic phosphate group. *Thiobacillus thiooxidans* is one of the best known producers of phospholipids (Beebe and Umbreit, 1971), whilst it is also produced by *Acinetobacter* spp. and *Aspergillus* spp. (Desai and Banat, 1997).

Polymeric biosurfactants are biological polymers made up of a polysaccharide backbone, linked with fatty acid side chains (Desai and Banat, 1997). Emulsan, liposan, and mannoprotein are among the most well-known polymeric biosurfactants and are produced by *Acinetobacter calcoaceticus*, *Candida lipolytica*, and *Saccharomyces cerevisiae*, respectively (Desai and Banat, 1997).

1.2.2 Biosurfactant properties

Biosurfactants have many properties which make them attractive for use in commercial applications. These properties offer many advantages over chemically synthesised surfactants such as higher biodegradability, lower toxicity, higher foaming, and high specific activity and selectivity at extreme pH, temperature, and ionic strength conditions. Biosurfactants are also environmentally friendly, making them even more attractive in current times where environmental compatibility is an increasingly important factor when selecting industrial chemicals (Desai and Banat, 1997; Katsuragi and Tani, 1997; Muthusamy *et al.*, 2008).

Apart from the excellent physio-chemical properties exhibited by biosurfactants, biosurfactants also exhibits useful biological activities. Biosurfactants have been reported to show antimicrobial, antiviral, and anti-cancer activities (Gudiña *et al.*, 2013; Peypoux *et al.*, 1999; Seydlová and Svobodová, 2008) suggesting that these molecules may be useful in future medical applications such as combatting multi-drug resistant pathogens such as tuberculosis.

1.2.2.1 Surface tension

The amphiphathic nature of biosurfactants allows them to preferentially partition at the interface between fluid phases such as oil/water or air/water interfaces (Desai and Banat, 1997; Katsuragi and Tani, 1997). As a result, biosurfactants are able to reduce interfacial and surface tension in both aqueous solutions and hydrocarbon mixtures (Desai and Banat, 1997). Lipopeptides, glycolipids, fatty acids and polymeric biosurfactants have all been reported to exhibit surface activity (Kim *et al.*, 1997).

One measure of surfactant efficacy is determined by its ability to reduce surface tension, which is a measure of the required surface free energy per unit area to transfer a molecule from the bulk phase to the surface (Mulligan, 2009). The critical micelle concentration (CMC) is defined as the critical level where further surfactant addition does not reduce surface tension. Surfactant addition above this critical level results in the formation of supramolecular structures such as micelles, bilayers and vesicles. CMC is defined by the solubility of a surfactant in the aqueous phase and is often used to measure the efficiency of a surfactant (Desai and Banat, 1997).

1.2.2.2 Foaming activity

Foaming is another property that arises from the amphiphilic structure of biosurfactants and is of particular interest for product development in the detergent, cosmetic and pharmaceutical industries (Thonart *et al.*, 1996). Surfactin has been reported to have excellent foaming properties at concentrations as low as 0.05 g/L compared to commercial surfactants such as sodium dodecyl sulphate (SDS) and bovine serum albumin (BSA) (Thonart *et al.*, 1996). At the same concentration SDS and BSA forms unstable foams that cannot produce the required foam volume (35 mL). Surfactin had a foaming capacity (maximum foam volume/volume of gas injected) of 0.98 at a concentration of 0.05 g/L compared to 0.8 for SDS and 0.94 for BSA at concentrations of 0.1 and 0.2 g/L, respectively. Furthermore, the residual foam volume after 20 mins for surfactin was 88% at a concentration of 0.1 g/L compared to the 0% exhibited by SDS at the same concentration and 65% exhibited by BSA at a concentration of 0.2 g/L. Thonart *et al.* (1996) reported that the excellent foaming capacity and stability of surfactin can be ascribed to its strong surface activity, and may also be a result of the good mechanical and rheological properties of its surface-adsorbed film.

1.2.2.3 Emulsification activity

Emulsions are formed when one liquid phase disperses into another as microscopic droplets. Some biosurfactants can act either as emulsifiers, which stabilise emulsions, whilst others may act as de-emulsifiers, which destabilise emulsions (Desai and Banat, 1997; Muthusamy *et al.*, 2008). High molecular weight biosurfactants have been reported to generally be better emulsifiers compared to low molecular weight biosurfactants. Sophorolipids from *T. bombicola*, for example, have been shown to lower surface and interfacial tension, however are not good emulsifiers. This is in contrast with liposan that does not lower surface tension but have been shown to successfully emulsify edible oils. Polymeric biosurfactants form stable emulsions by coating oil droplets, and are therefore particularly useful for creating oil/water emulsions that can be used in the food and cosmetic industries (Muthusamy *et al.*, 2008).

1.2.2.4 Antimicrobial- and antiviral biosurfactants

With the number of drug resistant bacteria increasing, new research is necessary to develop new antibiotics. Numerous biosurfactants have shown antimicrobial activity against numerous bacteria, fungi and viruses (see Table 1-3 for microorganisms susceptible to *B. subtilis* biosurfactants) and thus presents an opportunity for the development of novel antibiotics.

Bacillus sp. are arguably the largest producers of antimicrobial biosurfactants. *B. subtilis*, *B. licheniformis*, *B. amyloliquefaciens*, *B. brevis*, and *B. pumilus* are only some of the species from the *Bacillus* genus that have been reported to produce antimicrobial biosurfactants (Cameotra and Makkar, 2004; Rodrigues and Teixeira, 2010). Other antimicrobial biosurfactant producing organisms include *C. antarctica* (Arutchelvi *et al.*, 2008), *P. aeruginosa* (Benincasa *et al.*, 2004), *Lactococcus lactis* and *Streptococcus thermophiles* (Rodrigues *et al.*, 2004; L. R. Rodrigues *et al.*, 2006). It has been proposed that microorganisms produce antimicrobial biosurfactants to act as antagonistic agents and to gain a competitive advantage in microbial communities (Van Hamme *et al.*, 2006).

The antimicrobial activities of lipopeptide biosurfactants (surfactin, fengycin, and iturin) produced by *B. subtilis* and rhamnolipids produced by *P. aeruginosa* have been studied intensively and are well documented in the literature. These biosurfactants have been reported to exhibit antimicrobial activity against various Gram-positive and Gram-negative bacteria, as well as fungi (Benincasa *et al.*, 2004; Haba *et al.*, 2003). Table 1-3 gives an overview of the organism susceptible to biosurfactants produced by *B. subtilis*

It has been reported that surfactin exhibits greater antimicrobial activity against Gram-positive bacteria than Gram-negative bacteria (Bechard *et al.*, 1998; Singh and Cameotra, 2004), whilst rhamnolipids exhibited similar antimicrobial activities against both Gram-positive and Gram-negative bacteria (Benincasa *et al.*, 2004; Haba *et al.*, 2003).

No activity was observed for rhamnolipids against yeasts (Benincasa *et al.*, 2004; Haba *et al.*, 2003), whilst no information was found on the activity of surfactin against yeasts. *M. tuberculosis* has characteristics of both Gram-positive and Gram-negative bacteria which further suggests that it may be susceptible to the antimicrobial activity of surfactin produced by *B. subtilis*.

Although structurally related, surfactin exhibits a larger antibacterial spectrum compared to the lipopeptide biosurfactants, fengycin and iturin, also produced by *B. subtilis*. Fengycin and iturin, on the other hand, exhibits greater activity against fungi than against bacteria, whilst it does not exhibit significant antiviral activity (Akpa *et al.*, 2001; Ongena and Jacques, 2008).. The difference in activity of structurally related biosurfactants against different target organisms suggests that the antimicrobial potency of antimicrobial biosurfactants are influenced by the cell structure of the target organism (see section 1.2.2.4.1. for further discussion of this concept).

To establish a comparison between different biosurfactants as antimicrobial agents, a direct comparison of their antimicrobial activities is required. However, different authors have employed different methods to evaluate the antimicrobial activities of biosurfactants, thus making a direct comparison on the basis of reported literature difficult. Since this study focuses on the lipopeptides produced by *B. subtilis*, the organisms susceptible to the antimicrobial action of *B. subtilis* biosurfactants are shown in Table 1-3. Table 1-3 does not include all the organisms susceptible to *B. subtilis*, however it emphasises the broad spectrum of organisms susceptible to *B. subtilis* biosurfactants.

Table 1-3: Organisms susceptible to the antimicrobial action of *B. subtilis* biosurfactants

Micro-organism	Reference
<u>Gram-positive Bacteria</u>	
<i>Enterococcus faecalis</i>	(Fernandes <i>et al.</i> 2007; Singh and Cameotra 2004)
<i>Staphylococcus aureus</i>	(Fernandes <i>et al.</i> , 2007; Singh and Cameotra, 2004; Yakimov <i>et al.</i> , 1995)
<i>Staphylococcus epidermidis</i>	(Singh and Cameotra, 2004)
<i>Bacillus cereus</i>	(Sumi <i>et al.</i> , 2015; Yakimov <i>et al.</i> , 1995)
<i>Bacillus coagulans</i>	(Singh and Cameotra, 2004)
<i>Bacillus subtilis</i>	(Singh and Cameotra, 2004)
<i>Bacillus licheniformis</i>	(Yakimov <i>et al.</i> , 1995)
<i>Mycobacterium smegmatis</i>	(Singh and Cameotra, 2004)
<i>Streptococcus mutans</i>	(Singh and Cameotra, 2004)
<i>Lactococcus lactis subsp. Lactis</i>	(Singh and Cameotra, 2004)
<i>Enterobacter sp. strain 306</i>	(Yakimov <i>et al.</i> , 1995)
<u>Gram-negative bacteria</u>	
<i>Pseudomonas aeruginosa</i>	(Fernandes <i>et al.</i> 2007; Singh and Cameotra 2004)
<i>Pseudomonas acidovorans</i>	(Singh and Cameotra 2004)
<i>Pseudomonas syringae</i>	(Meena and Kanwar 2015)
<i>Pseudomonas fluorescens</i>	(Yakimov <i>et al.</i> , 1995)
<i>Pseudomonas proteofaciens</i>	(Yakimov <i>et al.</i> , 1995)
<i>Pseudomonas acidovorans</i>	(Singh and Cameotra 2004)
<i>Rhodococcus globerulus</i>	(Yakimov <i>et al.</i> , 1995)
<i>Salmonella sp.</i>	(Sumi <i>et al.</i> , 2015)
<i>Acinetobacter calcoaceticus</i>	(Yakimov <i>et al.</i> , 1995)
<i>Alcaligenes eutrophus</i>	(Yakimov <i>et al.</i> , 1995)
<u>Fungi</u>	
<i>Aspergillus flavus</i>	(Ongena <i>et al.</i> , 2004; L. Rodrigues <i>et al.</i> , 2006)
<i>Colletotrichum gloeosporioides</i>	(Sumi <i>et al.</i> , 2015)
<i>Pythium ultimum</i>	(Meena and Kanwar 2015)
<i>Botrytis cinerea</i>	(Meena and Kanwar 2015; Ongena <i>et al.</i> 2004)
<i>Podosphaera fusca</i>	(Meena and Kanwar 2015)
<i>Ascospaera apis</i>	(Sabate, 2009)
<i>Rhizoctonia bataticola</i>	(Joshi <i>et al.</i> , 2008)
<i>Rhizoctonia solani</i>	(Ongena <i>et al.</i> , 2004)

<i>Fusarium udum</i>	(Joshi <i>et al.</i> , 2008)
<i>Fusarium graminearum</i>	(Ongena <i>et al.</i> , 2004)
<i>Trichoderma herzanium</i>	(Joshi <i>et al.</i> , 2008)
<i>Alternaria burnsii</i>	(Joshi <i>et al.</i> , 2008)
<i>Chrysosporium indicum</i>	(Joshi <i>et al.</i> , 2008)
<i>Rhizopus sp.</i>	(Ongena <i>et al.</i> , 2004)
<i>Gaeumannomyces sp</i>	(Ongena <i>et al.</i> , 2004)
<i>Mucor sp.</i>	(Ongena <i>et al.</i> , 2004)

Biosurfactant antiviral action is not as well documented compared to its antibacterial and antifungal properties. Surfactin has been reported to show antiviral activity against various viruses as shown in Table 1-4. The antiviral activity of surfactin has been reported to be strongly linked to the length of the fatty acid chain as well as the charge of the peptide moiety (Kracht *et al.*, 2009) (the mechanism of antiviral action is discussed in more detail in section 1.2.2.4.1).

Table 1-4: Antiviral activity of surfactin produced by *B. subtilis*

Viral Target	Reference
Human immunodeficiency virus 1 (HIV-1)	(L. Rodrigues <i>et al.</i> , 2006)
Herpes simplex virus (1and2)	(L. Rodrigues <i>et al.</i> , 2006; Vollenbroich <i>et al.</i> , 1997)
Suid herpes virus	(Kracht <i>et al.</i> , 2009; L. Rodrigues <i>et al.</i> , 2006)
Simian immunodeficiency virus	(L. Rodrigues <i>et al.</i> , 2006; Vollenbroich <i>et al.</i> , 1997)
Vesicular stomatitis virus	(Kracht <i>et al.</i> , 2009; L. Rodrigues <i>et al.</i> , 2006)
Murine encephalomyocarditis virus	(L. Rodrigues <i>et al.</i> , 2006)
Feline calicivirus	(L. Rodrigues <i>et al.</i> , 2006)
Semliki Forest virus	(Kracht <i>et al.</i> , 2009; L. Rodrigues <i>et al.</i> , 2006)

1.2.2.4.1 Mechanism of antimicrobial and antiviral action

The antimicrobial activity and potency of a substance is dependent on the mode of action it uses to inhibit or kill target organisms as well as the cell structure of the target organism (Walsh, 2003). Antibiotics can generally be classified into four categories according to their mode of action in bacterial cells: (1) cell wall synthesis inhibitors; (2) cell membrane inhibitors; (3) protein synthesis inhibitors; (4) antibiotics that interfere with DNA and RNA synthesis (Todar, 2002; Walsh, 2003). The mode of action of an antibiotic is one of the most important factors to consider when evaluating the potential of a new antibiotic.

Lipopeptides readily bind to the surface bilayer of bacterial cells and change the arrangement of local lipid linkages on negatively charged fatty acids. This ultimately restructures the lipid bilayer and consequently prevents cellular processes from occurring (Sumi *et al.*, 2015). Surfactin has been reported to show a detergent-like action on cell-membranes by inducing curvature in the membranes. This causes disruption of the acyl chains and decreases membrane thickness and lateral packing density resulting in the loss of membrane stability (Carrillo *et al.*, 2003; Shaligram and Singhal, 2010). It has been reported that surfactin interferes with membrane integrity in a dose-dependent manner (Ongena and Jacques, 2008). At low concentrations (surfactin-to-lipid mole ratio (R_b) < 0.04), surfactin induces limited perturbation by inserting exclusively in the outer leaflet of the membrane. Transient permeabilizations and membrane reannealing occurs at intermediate concentrations (R_b 0.05-0.01). High concentrations (R_b 0.1-0.2) causes irreversible pore formation due to surfactin-rich clusters being inserted into the membrane. Further addition of surfactin, above the critical micelle concentration (CMC) results in complete disruption and solubilisation of the lipid bilayer (Carrillo *et al.*, 2003; Ongena and Jacques, 2008). Furthermore, it has been suggested that the antimicrobial potency of lipopeptides is also dependent on the chain length of the lipid as well as the charge of the hydrophilic headgroup (Maget-Dana and Ptak, 1995). Further reports have been made that the antimicrobial potency of surfactin is increased in the presence of Ca^{2+} ions through the formation of surfactin- Ca^{2+} complexes which are believed to insert themselves even deeper into phospholipid bilayers (Grau *et al.*, 1999).

The cellular interaction of iturin, a lipopeptide also produced by *B. subtilis* differs from that of surfactin since it is unable to disrupt and solubilise cell membranes. Instead, iturin diffuses into the membrane through osmotic perturbation as a result of the formation of ion conducting pores (Ongena and Jacques, 2008). As a result, iturin interacts with nuclear and cytoplasmic organelle membranes. The ion conducting pores and membrane interactions facilitate the release of cytoplasmic components resulting in cell death (Pathak, 2011; Rodrigues and Teixeira, 2010).

The mechanism of action of fengycin, also produced by *B. subtilis*, is less well known compared to other lipopeptides. Fengycin readily interacts with lipid layers and is able to retain its potential to change cell-membrane structure and permeability in a dose dependent manner (Ongena and Jacques, 2008). At low concentrations (fengycin/phospholipid mole ratios (X_f) = 0.002), fengycin only inserts into the bilayer, increasing its surface tension without permeabilizing it. Intermediate fengycin concentrations (X_f = 0.026) causes fengycin to agglomerate resulting in the leakage of cellular contents. Micelles are formed at high fengycin concentrations (X_f = 0.5) suggesting that the bi-layer is solubilized into the extracellular medium (Deleu *et al.*, 2008).

A mechanism analogous to the antimicrobial action of surfactin against bacteria has been proposed for the antiviral action of surfactin. It has been suggested that the physiochemical interactions between surfactin and the virus lipid membrane is responsible for its antiviral action due to permeability changes. At high concentrations surfactin causes the mycoplasma membrane system to disintegrate by a detergent-like effect (Vollenbroich *et al.*, 1997).

1.2.2.4.2 Resistance to antimicrobial action

Many microorganisms have developed resistance to common antibiotics such as penicillin, vancomycin, streptomycin, and methicillin, as a result over-use and misuse of these antibiotics (Walsh, 2003). The resistance of bacteria to antibiotics may be an inherent trait of the organism which makes it naturally resistant, or resistance may be acquired through mutation of its own DNA or it may acquire resistance-conferring DNA from another source (Todar, 2008). The resistance mechanisms of target organisms greatly influence the antimicrobial activity of a substance (Walsh, 2003).

As discussed in section 1.2.2.4.1 antibiotics have different modes of antimicrobial action that are influenced by the cell structure of the target organism. Antimicrobial resistance resulting from differences in the cell wall structure of different organisms is an example natural resistance to antibiotics (Todar, 2008). Some common antibiotics, e.g. vancomycin, only exhibit antimicrobial activity against Gram-positive bacteria and show no activity against Gram-negative bacteria as a direct result of the difference in cell-wall structure between these organisms (Walsh, 2003). The cell wall of Gram-positive bacteria consists of an inner bilayer membrane as well as a peptidoglycan layer, however it lacks an outer phospholipid bilayer membrane that is present in Gram-negative bacteria although the peptidoglycan layer in the cell wall of Gram-negative bacteria is much thinner compared to Gram-positive bacteria (Walsh, 2003). The resistance of Gram-negative bacteria to some antibiotics that are only active against Gram-positive bacteria can be ascribed to two features of its outer membrane: (1) the presence of lipopolysaccharides attached to the outer membrane and (2) porins present in the outer membrane (Walsh, 2003). Porins are possible targets for antibiotics as it is considered to be passage channels for certain molecules (Walsh, 2003). A great deal of variation exists in the cell-wall structure of different bacteria, and even among bacteria of the same genus (Walsh, 2003). The cell-wall of *P. aeruginosa*, an opportunistic human pathogen, contains porins with very small pores that reduces antibiotic passage into the periplasmic space and thus reducing its vulnerability to common antibiotics compared to other Gram-negative bacteria.

In addition to natural resistance, bacteria have developed several mechanisms that allow them to resist certain antibiotics, either by chemically modifying the antibiotic, inactivating the antibiotic by physically removing it from the cell, or modifying the target site making it unrecognisable by the antibiotic (Todar, 2008; Walsh, 2003).

1.2.3 Biosurfactant applications

The structure and properties of biosurfactants discussed in section 1.2.1 and 1.2.2 make them useful for a wide range of applications in different industries, which will be unpacked in the following sections. For instance, biosurfactants are used for bioremediation; in medicine as antibiotics or for antiviral and anticancer applications; in the petrochemical industry to promote oil recovery; as well as in agriculture where biosurfactants are used for biocontrol. Furthermore, biosurfactants offer significant advantages over their synthetic counterparts, such as having a lower toxicity; higher biodegradability; better environmental compatibility; as well being able to be synthesised from renewable feedstocks (Desai and Banat, 1997; Banat, Makkar and Cameotra, 2000; Mulligan, 2005).

1.2.3.1 Bioremediation

Bioremediation aims to provide cost-effective, contaminant-specific treatments that reduce individual or environmental contaminant concentrations (Banat *et al.*, 2000). The emulsification properties of biosurfactants allow for the emulsification of hydrocarbon-water mixtures that aids the degradation of hydrocarbons in the environment, making biosurfactants a suitable solution in bioremediation applications such as combatting oil pollution along the shoreline or at sea (Banat *et al.*, 2000). Furthermore, biosurfactants, in comparison with their chemical counter parts provide the advantage of having a lower toxicity and shorter persistence in the environment (Banat *et al.*, 2000). One example where biosurfactants were successfully applied in bioremediation is the Exxon Valdez oil spill in 1989 (Banat *et al.*, 2000).

1.2.3.2 Biomedical

1.2.3.2.1 Antimicrobial applications

Biosurfactants are becoming increasingly popular as safe and effective alternatives to synthetic medicines and antimicrobial agents, especially in a time where the number of drug-resistant pathogenic bacteria are on a rise necessitating the need for alternative therapy lines (Seydlová and Svobodová, 2008). Lipopeptide biosurfactants are of particular interest as a result of their high surface activities and antibiotic potential against a vast number of infectious pathogens (Meena and Kanwar, 2015). One example of an antimicrobial lipopeptide that is produced commercially, is deptomycin, produced by *Streptomyces roseosporus*, that has been shown to have a high activity against multidrug-resistant bacteria such as methicillin-resistant *S. aureus*, and has been approved for treatment of complex skin- and skin-structure infections (Seydlová and Svobodová, 2008).

An unnamed lipopeptide biosurfactant from *B. subtilis* R14 has shown good antimicrobial activity against eight resistant strains of *P. aeruginosa* (Fernandes *et al.*, 2007). The authors reported inhibition zone diameters ranging from 9.8 to 12.1 mm (a larger inhibition diameter is indicative of a stronger antimicrobial activity) against the various drug resistant strains of *P. aeruginosa*. This suggested that antimicrobial biosurfactants offer a promising alternative to synthetic antibiotics which many infectious pathogens have developed a resistance to.

Furthermore, the same biosurfactant also exhibited good antimicrobial activity against different strains of *Enterococcus faecalis*, *Staphylococcus aureus*, and *Escherichia coli*, with mean inhibition zone diameters of 14.6, 14.2, and 28.1 mm, respectively (Fernandes *et al.*, 2007). The biosurfactant, surfactin, from *B. subtilis* has also shown antimicrobial activity against *Mycobacterium aurum*, a surrogate for *M. tuberculosis*, with inhibition zones increasing linearly from 4 mm to 24 mm for surfactin concentrations ranging from 208 mg/L to 1662 mg/L (Bence, 2009) which suggested that the antimicrobial activity is dose-dependent. The inhibition exhibited by surfactin against *M. aurum* suggested that it may be an effective antimicrobial agent for possible use in detergents and disinfectants to combat the spread of TB and possibly MDR-TB.

The antimicrobial activity of biosurfactants against many common infectious pathogens (see section 1.2.2.4) gives rise to possible application as antibiotics to fight against, and possibly prevent the spread of known pathogenic micro-organisms when it is used in detergents or disinfectants. One such organism is *Mycobacterium tuberculosis* which is the causative agent of tuberculosis (TB), one of the leading causes of death in South Africa (World Health Organisation, 2016). One of the aims of this study is to evaluate to antimicrobial activity of the surfactin containing cell-free supernatant from *B. subtilis* against *Mycobacterium aurum*, a non-pathogenic surrogate for *M. tuberculosis*.

1.2.3.2.2 Anticancer applications

Reports of biosurfactants showing specific toxicity against certain cancer cell lines have been made, promising possible application for treatment of various cancers (Gudiña *et al.*, 2013; Seydlová and Svobodová, 2008). Lipopeptides from *Bacillus*, *Pseudomonas*, and *Serratia* spp. have shown antitumoral activity against a number of human cancer cells (Gudiña *et al.*, 2013). The biosurfactant, monoolein, produced by *Exophiala dermatitidis*, exhibited inhibition of leukemia and cervical cancer cell lines. Both of these cell lines showed shrinkage of cells, DNA fragmentation and membrane blebbing (Gudiña *et al.*, 2013). Activity against human breast cancer cells by a glycoprotein produced by *Lactobacillus paracasei* have also been reported (Gudiña *et al.*, 2013). It should be noted that these biosurfactants are in use yet, and that it is still undergoing research to possibly be used in cancer treatments.

1.2.3.3 Agriculture

Pesticide pollution has become a growing concern hence prompting alternative biocontrol strategies (Banat *et al.*, 2000). The antimicrobial and antifungal properties of biosurfactants have made them promising biocontrol agents for use in the agricultural industry (Ben Abdallah *et al.*, 2015; Ongena and Jacques, 2008; Rangarajan and Clarke, 2015). Growth inhibition of *Aspergillus flavus*, *A. niger*, *Penicillium oxalicum*, and *Botryodiplodia teobromae*, which are all microorganisms related to spoilage of intermediate moisture foods (such as fruit), have been exhibited by the supernatant of a *B. subtilis* culture, containing lipopeptides (Okigbo and Emeka, 2010; Zhang *et al.*, 2008).

1.3 PROCESS CONDITIONS

A microorganism's ability to grow and produce metabolites such as biosurfactants is dependent on the environment in which growth and product synthesis takes place. Since this study focuses on the production of surfactin by *B. subtilis*, this section will primarily deal with the process conditions required for growth and enhanced surfactin production. The conditions that influence growth and product formation is the nutrient medium, which include a carbon and nitrogen source and different metal ions, and the physiological conditions which include temperature, pH, and dissolved oxygen (affected by aeration and agitation). Different modes of reactor operation will also be discussed.

1.3.1 Nutrient medium

1.3.1.1 Carbon source

The selection of an appropriate carbon source is essential for biosurfactant production. Conventionally, pure laboratory media have been used for biosurfactant production, however the pure media is very expensive and would significantly increase production cost should the process be commercialised. The use of waste oils from the food industry as well as agro-based raw materials have been demonstrated to provide promising alternatives to laboratory media (Abas *et al.*, 2013; Vedaraman and Venkatesh, 2011). The use of these waste media often have the disadvantage of containing insoluble substances that may result in complications during downstream separation and purifications (Rangarajan and Clarke, 2015). Furthermore, bacterial and fungal spores may also be present in agro- and industrial liquid wastes (Rangarajan and Clarke, 2015).

Carbohydrate substrates such as glucose, sucrose, and starch (Abushady *et al.*, 2005; Kim *et al.*, 1997; Makkar and Cameotra, 1997) are usually associated with high cell- and biosurfactant concentrations (Yeh *et al.*, 2006). Among these substrates glucose is one of the most frequently employed carbon sources for lipopeptide production. Although a wide range of glucose concentrations (2.5 – 60 g/L) (Abdel-Mawgoud *et al.*, 2008; Abushady *et al.*, 2005; Akpa *et al.*, 2001; Atwa *et al.*, 2013; Wei and Chu, 1998; Willenbacher *et al.*, 2015) have been used, it has been established that 40 g/L glucose is the optimum for surfactin production (Abushady *et al.*, 2005; Kim *et al.*, 1997).

1.3.1.2 Nitrogen source

Nitrogen is essential for protein synthesis and nucleic acid production in all biological growth processes (Painter, 1970). A nitrogen source is also required for growth and biosurfactant production by *B. subtilis*, as a medium devoid of a nitrogen source results in poor cell growth and negligible biosurfactant production (Makkar and Cameotra, 1997). *B. subtilis* is known to be a facultative anaerobe meaning that it is able to grow under both aerobic and anaerobic conditions (Nakano *et al.*, 1997). The choice of nitrogen source is especially important during anaerobic growth or growth under oxygen limiting conditions.

In the presence of both ammonium and nitrate, ammonium is utilised in preference to nitrate during the aerobic stages of growth, however, nitrate is utilised by *B. subtilis* when either ammonium or oxygen is depleted (Davis *et al.*, 1999). In the absence of oxygen, nitrate, instead of oxygen, is utilised as the terminal electron acceptor by *B. subtilis* (Hoffmann *et al.*, 1998; Nakano *et al.*, 1997; Nakano and Hulett, 1997). The high midpoint redox potential ($E^0 = 430$ mV) of nitrate, makes it the preferred terminal electron acceptor under oxygen depleted conditions (Nakano *et al.*, 1997). When nitrate is depleted, nitrite, which is the product of nitrate reduction, is utilised as an alternative electron acceptor (Davis *et al.*, 1999).

Two distinct ways exist in which micro-organisms are able to utilise nitrate: either through assimilation or dissimilation (Painter, 1970). Assimilation, illustrated in Figure 1-5, involves reduction of nitrate to ammonia, via nitrite, with subsequent production of nitrogenous cell constituents (Glaser *et al.*, 1995; Painter, 1970). Dissimilation, also known as nitrate respiration, on the other hand, is an oxidative process whereby nitrate instead of oxygen is used as the terminal hydrogen acceptor (Painter, 1970). Nitrogen is not incorporated into the cell constituents with dissimilation and the process yields either nitrate, ammonia, nitrous oxide or nitrogen as end products depending on the organism (Hoffmann *et al.*, 1998; Painter, 1970). Two special cases of dissimilation can be distinguished depending on the end products; in cases where nitrogen or nitrous oxide is produced the process is termed denitrification (Painter, 1970) and in cases where ammonia is produced the process is termed ammonification (Hoffmann *et al.*, 1998). *B. subtilis* does not produce any nitrogen or nitrogen oxide during anaerobic growth and as a result has been suggested to be an ammonifying facultative aerobe (Hoffmann *et al.*, 1998).

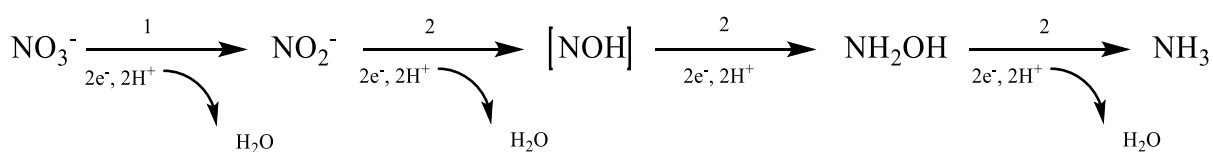


Figure 1-5: Assimilatory nitrate reduction pathway. Enzymes: 1 - nitrate reductase; 2 - nitrite reductase (Redrawn from White (2000))

B. subtilis is able to utilise both organic and inorganic nitrogen sources for biosurfactant production, however higher biosurfactant yields have been reported for inorganic nitrogen sources (Abushady *et al.*, 2005; Makkar and Cameotra, 1997). Biosurfactant concentrations of 731 and 724 mg/L were achieved on KNO₃ and NaNO₃, respectively, whilst peptone and yeast extract only yielded 327 and 458 mg/L of biosurfactant, respectively (Makkar and Cameotra, 1997).

NH_4NO_3 and NaNO_3 were found to yield the highest surfactin concentrations compared to other inorganic nitrogen sources such as NH_4Mo , NH_4HCO_3 , and NH_4Cl (Abushady *et al.*, 2005). Approximately 2100 and 2750 mg/L surfactin was reported for NaNO_3 and NH_4NO_3 , respectively, compared to other inorganic nitrogen sources that only yielded about 1700 mg/L surfactin or lower (Abushady *et al.*, 2005). Another study, however, reported that NH_4HCO_3 resulted in the best biosurfactant yield at a NH_4HCO_3 concentration of 13.5 g/L (Kim *et al.*, 1997). The same study also revealed that the supplementing the medium with 0.5 g/L yeast extract further increased the biosurfactant yield.

Abushady *et al.* (2005) investigated the effect of NH_4NO_3 concentration (1.6 to 9 g/L) on surfactin production and found that 4.6 g/L NH_4NO_3 was optimal for surfactin production. A more recent study (Pretorius *et al.*, 2015) found the optimum NH_4NO_3 concentration for surfactin production to be 8 g/L. One of the main differences between the two studies, besides the composition of the growth medium and the bacterial strain, is the fact that experiments by Abushady *et al.* (2005) were carried out in shake flasks, whereas Pretorius *et al.* (2015) used an instrumented bioreactor controlled at a pH of 6.8 and temperature of 30 °C.

The conditions of nitrogen metabolism have been found to have a significant impact on surfactin production by *B. subtilis* (Davis *et al.*, 1999). When NH_4NO_3 is used as the nitrogen source in a defined medium, enhanced surfactin production can be linked to the onset of nitrate-limited growth (Davis *et al.*, 1999; Rangarajan *et al.*, 2015). Nitrate-limited, oxygen-depleted conditions have been reported to yield the highest product yield per cell ($Y_{p/x} = 0.075$), compared to ammonium-limited oxygen depleted (0.012), carbon-limited oxygen-depleted (0.0069), aerobic carbon-limited (0.0068) and aerobic nitrogen-limited (0.021) conditions (Davis *et al.*, 1999).

Davis *et al.* (1999) investigated the growth of *B. subtilis* in a medium containing nitrate as the sole nitrogen source in the form of sodium nitrate. Poor growth was observed for all tested concentrations of sodium nitrate (1-10 g/L) with biomass concentrations only reaching a maximum of 1.2-1.4 g/L. This suggests that the presence of ammonium plays an important role in the aerobic growth of *B. subtilis* since much higher cell concentrations and consequently higher surfactin production are achieved when ammonium is present in the growth medium (Davis *et al.*, 1999). Nitrate, however, is preferred over ammonium under oxygen depleted conditions (Davis *et al.*, 1999). It can be concluded that ammonium plays an important role in cell growth by *B. subtilis*, while nitrate plays an important role in surfactin production, hence it is possible that some optimum ammonium to nitrate ratio exists that is able to support sufficient growth, whilst maximizing the surfactin yield.

Most studies to date have focused on finding the optimum total nitrogen concentration for biosurfactant production (Abushady *et al.*, 2005; Kim *et al.*, 1997; Pretorius *et al.*, 2015), however little is known about the ammonium-nitrate ratio that yields optimum surfactin production kinetics. The importance of this parameter therefore warrants further investigation.

Microbial production of lipopeptides is often coupled with the co-production of different lipopeptide families or isoforms. One such organism is *B. subtilis*, that has been reported to co-produce three different lipopeptide families, namely surfactin, iturin and fengycin. Another example is *B. megaterium* that has been shown to co-produce surfactin and fengycin. The latter does not produce any iturin. (Fahim *et al.*, 2012; Pretorius *et al.*, 2015; Rangarajan *et al.*, 2015). Since lipopeptide selectivity is strongly influenced by medium composition and environmental process conditions, optimising these parameters and maximising selectivity during the production stages can significantly reduce downstream purification costs and complexity (Rangarajan and Clarke, 2015). Lipopeptide selectivity has previously been linked to nitrogen source limitation (Rangarajan *et al.*, 2015), however the effect of nitrogen source on lipopeptide selectivity was not quantified and hence requires further investigation. The effect of nitrogen source concentration on lipopeptide production has been studied (Pretorius *et al.*, 2015) for NH_4NO_3 concentrations of 4, 8, 10 and 12 g/L. Significant differences in the ratio of surfactin to antifungals (fengycin and iturin) was observed for these concentrations. For 4, 8, 10, and 12 g/L NH_4NO_3 , surfactin to antifungal ratios (gL^{-1} surfactin / $\text{mAu} \cdot \text{min}$ antifungals) were calculated to be 0.59, 1.17, 1.60, 1.44, respectively. From these ratios it is clear that lipopeptide selectivity is coupled with nitrogen source utilisation, however, since NH_4NO_3 is a dual nitrogen source, it is unclear how and which of these nitrogen sources affects lipopeptide selectivity. One way to overcome this, is to vary the ratio of nitrogen supplied by ammonium and nitrate respectively and to quantify its effect on lipopeptide selectivity.

In conclusion, the findings in this section highlighted the importance of nitrogen for cell growth and biosurfactant production by *B. subtilis*. Typically, nitrogen is added to growth medium in the form of an ammonium or nitrate salt, or as the dual nitrogen source ammonium nitrate. In the presence of both ammonium and nitrate, *B. subtilis* utilises ammonium in preference to nitrate during aerobic growth, whilst nitrate is utilised when either oxygen or ammonium is depleted. Lipopeptide selectivity has been reported to be influenced by medium composition and environmental process conditions and has previously been linked to nitrogen limitation. Previous studies have focused on optimising the concentration of ammonium nitrate in the growth medium, however the effect of varying the ratio of nitrogen supplied as ammonium ($\text{NH}_4\text{-N}$) and nitrogen supplied as nitrate ($\text{NO}_3\text{-N}$) on lipopeptide production kinetics is still unexplored.

1.3.1.3 Metal ions

It has been reported that adding certain metal cations, such as iron, manganese, magnesium or potassium, can significantly enhance surfactin production by *B. subtilis*. Whilst others, such as those from salts such as MgSO_4 , CaCl_2 , Na_2HPO_4 , KH_2PO_4 , NaNO_3 , ZrOCl_2 , $\text{UO}_2(\text{C}_2\text{H}_3\text{O}_2)_3$, or VOSO_4 , had little to no effect on either biomass or surfactin concentrations. Whilst ZnSO_4 suppressed the growth of *B. subtilis*, and certain others (CuSO_4 , NiSO_4 , CoSO_4 , and $\text{Al}_2(\text{SO}_4)_3$) completely inhibited growth. (Abdel-Mawgoud *et al.*, 2008; Abushady *et al.*, 2005; Cooper *et al.*, 1981; Kim *et al.*, 1997; Wei and Chu, 1998, 2002). The inhibition of growth was most likely the result of the toxic properties that is coupled with some of these metals. More recent studies (Wei *et al.*, 2007), however, found that surfactin concentration is significantly decreased (to 25% of the concentration of the control) in the absence of Mg^{2+} and K^+ . It has been suggested that Mg^{2+} is essential for growth as a medium devoid of Mg^{2+} results in a significant decrease in microbial growth (Abdel-Mawgoud *et al.*, 2008).

Mn^{2+} was also found to be an important trace metal, since it not only affects lipopeptide production, but also nitrogen utilisation, which in turn also affects lipopeptide production (refer to section 1.3.1.2 for further discussion on the effect of nitrogen on lipopeptide production). Nitrogen utilisation, K^+ uptake, as well as other biochemical functions, are all affected by Mn^{2+} (Wei and Chu, 2002). Mn^{2+} has been shown to influence the nitrogen metabolism of *B. subtilis* and resulted in 6.2-fold increase in surfactin production when the concentration of Mn^{2+} was increased from 0 to 0.01 mM (Huang *et al.*, 2015).

It has been previously reported that when NH_4NO_3 is used as a nitrogen source *B. subtilis* prefers ammonium over nitrate under aerobic conditions (Davis *et al.*, 1999), however when Mn^{2+} is present the usage ratio of ammonium and nitrate changes. At lower Mn^{2+} concentrations (0.001 – 0.005 mM) NH_4^+ acts as the main nitrogen source, however increasing the concentration of Mn^{2+} increases nitrate usage ratio resulting in a shift from NH_4^+ to NO_3^- as the main nitrogen source for 0.05 – 0.1 mM Mn^{2+} (Huang *et al.*, 2015). This phenomenon can be attributed to a significant increase in nitrate reductase activity that corresponds to increased nitrate usage at higher Mn^{2+} concentrations (Huang *et al.*, 2015). Huang *et al.* (2015) reported a 6.2-fold increase in surfactin yield, in the presence of Mn^{2+} , compared to a medium devoid of Mn^{2+} .

The addition of iron salts, such as FeSO_4 , to the mineral salts medium have also been found to be a simple and effective way of overproducing surfactin by *B. subtilis* (Wei and Chu, 1998). Iron addition, however, results in acidification of the broth causing surfactin to go out of solution as result of precipitation when pH levels drop below 5.0 (Wei and Chu, 1998). However, this can be easily overcome by either delaying, avoiding, or reversing (through alkaline addition and keeping the pH above 6.0) the acidification phenomenon, resulting in surfactin concentrations as high as 3500 mg/L (Wei and Chu, 1998).

By controlling the pH of the culture broth at 6.5, it was found that cell concentration increased 8-fold and surfactin yield increased 10-fold, at an optimum Fe^{2+} dosage of 4.0 mM, compared to a medium devoid of iron (Wei *et al.*, 2004). Wei, Wang and Chang (2004) performed their experiments in bioreactors where the pH can easily be controlled. Many studies, such as this one, however uses shake flasks due to their ease of use compared to bioreactors. Shake flasks, however, does not offer pH control and thus it is necessary to add buffers such as KH_2PO_4 and Na_2HPO_4 to maintain a pH above 5.0 in to avoid the precipitation of surfactin during shake flask studies.

Large variations in growth media can be noted between literature sources depending on the specific objectives of the different studies as well as the requirements of the microorganism or bacterial strain being studied. Although these differences may sometimes be small they can have a significant effect on the maximum biosurfactant concentration. For instance, the maximum surfactin concentrations reported by Wei and Chu, (1998) and Wei and Chu, (2002) were 2600 mg/L and 3500 mg/L respectively. These experiments were performed under the same conditions (temperature, agitation speed, flask size, culture time) using the same strain but with slight differences in the mineral salt compositions in an attempt to optimise the medium composition in terms of Mn^{2+} (Wei and Chu, 2002) and Fe^{2+} (Wei and Chu, 1998) concentrations that yields the maximum surfactin concentration. The optimum Mn^{2+} and Fe^{2+} concentrations, that yielded the maximum surfactin concentration, were reported as 0.01 (Wei and Chu, 2002) and 5 mM (Wei and Chu, 1998), respectively. The 5 mM Fe^{2+} concentration was also reported as the maximum allowable concentration that prevented surfactin precipitation from occurring as result of the effect of Fe^{2+} on the pH (Wei and Chu, 1998). Another study by Abdel-Mawgoud *et al.* (2008) found that the optimum mineral salt concentrations that resulted in maximum biosurfactant production in shake flasks were 1 mM for ZnSO_4 , FeCl_2 , MgSO_4 , and 0.1 mM for MnSO_4 .

Most mineral salt optimisation studies were performed by optimising the concentration of one metal ion at a time (Abdel-Mawgoud *et al.*, 2008; Abushady *et al.*, 2005; Cooper *et al.*, 1981; Wei and Chu, 2002, 1998), however it is evident from the different optimum mineral salt concentrations reported by various authors that some degree of interaction exists between the different metal ions. By studying the effect of omitting different metal ions from the growth media in an attempt to optimise the trace element solution for enhanced surfactin production it was found that Mg^{2+} , K^+ , Mn^{2+} , and Fe^{2+} have the most significant effect on surfactin production by *B. subtilis* (Wei *et al.*, 2007). By performing a statistical design, the interactive effects of the significant metal ions on surfactin production was studied and it was found that only the interaction of Mg^{2+} and K^+ reached significant level (Wei *et al.*, 2007). The authors found the optimum concentration of Mg^{2+} , K^+ , Mn^{2+} , Fe^{2+} , and Ca^{2+} to be 2.4, 10, 0.01, 0.008 mM, and 7 μM , respectively, when interaction is considered. The optimum trace element composition resulted in a maximum surfactin concentration of 3340 mg/L.

1.3.1.4 Amino acids

It has been reported that amino acid addition influences both the lipopeptide selectivity, increasing the ratio of surfactin or iturin for instance (Besson and Michel, 1992), as well as which lipopeptide homologues are produced (Akpa *et al.*, 2001; Liu *et al.*, 2012; Youssef *et al.*, 2005). This leads to the possibility of selectively producing certain lipopeptide families and/or homologues for specific applications by supplying the correct amino acid or combination of amino acids. Supplementing the glucose medium with amino acids does not increase the biosurfactant concentration, however amino acid addition to the culture medium has been reported to alter the relative abundance of biosurfactant homologues that are produced (Akpa *et al.*, 2001; Liu *et al.*, 2012).

From the results of Akpa *et al.*, (2001) and Liu *et al.*, (2012) it can be concluded that by adding certain amino acids to the culture medium it is possible to selectively enhance the production of certain surfactin homologues thus providing an easy and economical way to selectively produce certain surfactin homologues.

1.3.2 Physiological conditions

1.3.2.1 Oxygen availability

1.3.2.1.1 Aeration

B. subtilis is a facultative anaerobe, as discussed in section 1.3.1.2, resulting in a number of studies on both anaerobic and aerobic biosurfactant production with the latter being the most common mode of operation. These studies, however, often contradict each other with regards to optimum oxygen conditions that results in maximum biosurfactant yield. Furthermore, studies have shown that oxygen availability plays a significant role in lipopeptide yield and selectivity (Fahim *et al.*, 2012; Pretorius, 2014; Rangarajan *et al.*, 2015).

Generally, aerobic conditions are more favourable for cell growth than anaerobic conditions, as demonstrated by the maximum optical density of 3.0 under aerobic conditions, compared to the 0.12 achieved by *B. subtilis* under anaerobic conditions (Clements *et al.*, 2002). It has also been reported that increasing the volumetric oxygen percentage (decreasing the filling volume of shake flask) has a positive effect on surfactin production (Abushady *et al.*, 2005). The authors reported an increase in surfactin concentration from 1200 to 2100 mg/L when the volumetric oxygen percentage is increased from 30 to 90%. Pretorius, van Rooyen and Clarke (2015) reported increases in both biomass and lipopeptide production by *B. amyloliquefaciens* when utilising enriched air containing 30% O₂.

In contradiction to the findings of Clements *et al.* (2002), biomass concentration for *B. subtilis* C9 increased 3-fold under oxygen limiting conditions (300 rpm, 0.1 vvm) compared to oxygen sufficient conditions (300 rpm, 1 vvm) (Kim *et al.*, 1997).

It should be noted that the two studies used different strains of *B. subtilis* which suggests that the oxygen requirements of the organism may be strain dependent. Surfactin concentration has been reported to increase almost 10-fold from 45.3 mg/L in a system where DO levels were maintained above 80% to 439 mg/L when dissolved oxygen became depleted after 10 hours of cultivation in a batch bioreactor system with an agitation rate of 220 rpm and aeration rate of 0.5 vvm (Davis *et al.*, 1999). Kim *et al.*, (1997) reported that surfactin concentration increased from 1300 mg/L under oxygen sufficient conditions (300 rpm, 1 vvm) to 4500 mg/L under oxygen limiting conditions (300 rpm, 0.1 vvm). Pretorius, van Rooyen and Clarke (2015) suggested that the controversy in literature regarding oxygen limitation exists as a result of lipopeptide production coinciding with oxygen limitation in batch culture.

One advantage of operating under anaerobic conditions is that it eliminates the vigorous foaming that is experienced during the aerobic fermentation of *B. subtilis* (Willenbacher *et al.*, 2015). Willenbacher *et al.* (2015) reported that the specific product yields achieved under strict anaerobic conditions exceeded those of the conventional aerobic fermentations with foam fractionation. However, this may be due to lower cell concentrations achieved under anaerobic conditions.'

As mentioned in Section 1.3.1.2 medium formulation and environmental parameters affect the selective production of different lipopeptide families or isoforms. The oxygen transfer condition is also one such parameter that plays a significant role on the selective production of different lipopeptide families (Fahim *et al.*, 2012). Surfactin and fengycin are coproduced by *B. subtilis* BBG21 and by varying the oxygen transfer conditions (through adjusting flask size, filling volume, and agitation frequency). Fahim *et al.* (2012) have demonstrated that lipopeptide production can be directed towards either mixed-production or surfactin mono-production. The authors have demonstrated that the volumetric oxygen transfer coefficient ($K_L a$) is a key parameter in controlling lipopeptide productivity and selectivity. Maximum surfactin concentration (2 g/L) and maximum surfactin fraction towards total lipopeptide production was achieved when increasing $K_L a$ to values between 0.04 and 0.08 s⁻¹. Maximum fengycin concentration (0.3 g/L), on the other hand, was achieved at moderate oxygen supply ($K_L a = 0.01$ s⁻¹) which agrees with a study by Rangarajan, Dhanarajan and Sen (2015). Since the conditions of oxygen availability and nitrogen utilisation are so closely related it is imperative that the effect of oxygen availability on lipopeptide selectivity also be investigated.

1.3.2.1.2 Agitation

Agitation rate is known to affect the volumetric oxygen transfer coefficient ($K_L a$), where an increase in agitation rate causes the $K_L a$ to increase and as a result also affects biosurfactant production (Abushady *et al.*, 2005; Fahim *et al.*, 2012; Rangarajan *et al.*, 2015; Yeh *et al.*, 2006). The effect of agitation rate have been studied between 0 – 200 rpm in shake flasks (Abushady *et al.*, 2005) and 200 – 350 rpm in a batch bioreactor culture (Yeh *et al.*, 2006).

Abushady *et al.* (2005) reported a linear increase in surfactin concentration (from 1000 to 1600 mg/L) when agitation rate was increased up to 150 rpm in shake flasks. The authors only observed a small increase in surfactin concentration (to 1700 mg/L) when the agitation rate was increased above 150 rpm and proposed that this may have been the result of an increase shear on the organisms at higher agitation rates. Yeh, Wei and Chang (2006) made a similar observation in an instrumented batch bioreactor where surfactin concentration increased to 6450 mg/L for agitation speeds up to 300 rpm. The authors found that increasing the agitation speed to 350 rpm caused surfactin concentration to decrease to 1010 mg/L. This observation may be the result of excessive foaming at high agitation rates (Pretorius *et al.*, 2015).

Agitation rate, by affecting oxygen transfer, has the ability to significantly increase lipopeptide production and selectivity, however its effect is limited by the increased shear on the organisms as well as excessive foaming caused by high agitation rates. Care should thus be exercised when selecting the agitation speed for surfactin production to avoid the detrimental effects of excessive shear or loss of surfactin due to excessive foaming.

1.3.2.2 Temperature

Temperature is an important environmental factor as it affects both cell growth and biosurfactant production. Unfortunately, it is unclear from the literature what the optimum temperature is that will result in the best kinetics for biosurfactant production, as attempted optimisation studies are somewhat contradictory. Most authors (Akpa *et al.*, 2001; Chen *et al.*, 2006; Chenikher *et al.*, 2010; Davis *et al.*, 1999; Fernandes *et al.*, 2007; Kim *et al.*, 1997; Makkar and Cameotra, 1997; Seok Oh *et al.*, 2002; Wei and Chu, 1998) have carried out experiments between 30 and 37 °C with 30 °C being the most common.

Temperature optimisation studies, with temperatures ranging from 25 – 60 °C, for *B. subtilis* BBk1 and strain BS5, have found that both cell and surfactin reaches its maximum at 30 °C (Abdel-Mawgoud *et al.*, 2008; Abushady *et al.*, 2005). Another temperature optimisation study for *B. subtilis* RB14 was carried out between 23 and 48 °C in solid state fermentation and it was found that the optimum temperatures for surfactin and iturin production was 37 and 25 °C, respectively (Ohno *et al.*, 1995). In an attempt to statistically optimise the environmental conditions (pH, temperature, and agitation and aeration rates), the optimum temperature for surfactin production was reported as 37.4 °C (Sen and Swaminathan, 1997).

1.3.2.3 pH

The pH of the culture medium plays a significant role on the maximum biosurfactant concentration attainable as pH levels below 5.0 causes a significant decrease in supernatant surfactin concentration as a result of precipitation (Makkar and Cameotra, 1997; Wei *et al.*, 2003) as discussed in section 1.3.1.3. As a result, pH is kept above 6 in most studies. Precipitation of surfactin at pH levels below 5.0 further suggests that it could be used as a process parameter that would assist in product recovery in the downstream purification steps.

The effect of pH on cell and biosurfactant concentration has been studied (Makkar and Cameotra, 1997) and it has been found that a pH of 7 corresponds to the maximum cell and biosurfactant concentration. Biosurfactant concentration increased from 108 to 840 mg/L and cell concentration increased from 200 mg/L to 2190 mg/L when the pH is increased from 4.5 to 7.0 (Makkar and Cameotra, 1997). Both cell and biosurfactant concentration decreased when the pH is increased above 7.0 (Makkar and Cameotra, 1997). Similar results were reported by other studies (Abdel-Mawgoud *et al.*, 2008; Abushady *et al.*, 2005; Sen and Swaminathan, 2005) who reported optimum pH values of 6.5, 6.8, and 6.8, respectively.

1.3.3 Operational strategy

In addition to the nutrient and physiological requirements of microorganisms, development of an appropriate process strategy is essential for optimal product formation. The three most extensively used process strategies are batch, fed-batch, and continuous cultures. Batch culture is the most commonly used strategy, however fed-batch and continuous cultures are preferred in some instances (Clarke, 2013). The mode of operation employed is often dependent on the phase in which the product is produced. Batch conditions may be more suitable for the production of secondary metabolites that are produced towards the stationary phase (Jacques *et al.*, 1999; Ongena *et al.*, 2004) whereas fed-batch and continuous operations might be more suitable for growth associated products (Ohno *et al.*, 1995; Peypoux *et al.*, 1999). Pretorius, van Rooyen and Clarke (2015) reported lipopeptides to be secondary metabolites that are produced towards the stationary phase rather than growth associated products which suggests that batch conditions may be more suitable for surfactin production.

1.3.3.1 Batch culture

Lab-scale batch culture experiments are commonly used due to their relatively easy setup and the fact that they do not require additional considerations in terms of feeding rates (as required by fed-batch and continuous cultures). Furthermore, batch cultures have also proven to be very useful when conducting preliminary tests for investigating the possibility of fed-batch or continuous cultures. Batch culture is the preferred mode of operation for high cost products where the product is highly specialised and/or produced in low yields and thus the objective is to maximise product concentration rather than productivity (Clarke, 2013)

Batch cultures provide an unsteady environment where nutrient and product concentrations vary over time and as a result often become nutrient-limited during the cell growth and biosurfactant production phases. The interaction of microorganisms with their environment gives rise to the familiar growth cycle (lag, exponential, stationary and death phases). Changes in the environment, nutrient depletion, and the increase of toxic by-products facilitates the transitions between growth phases (Hoskisson and Hobbs, 2005) and as such the growth cycle is almost exclusively observed for batch cultures.

Batch experiments can be conducted in shake flasks or bioreactors.

1.3.3.1.1 Shake flask batch cultures

Due to their ease of use shake flasks are widely used as preliminary tests for further bioreactor testing, or when a bioreactor is not available. However, shake flasks have the disadvantage of offering less control over operating conditions such as pH and aeration and as a result often have lower product yields compared to bioreactors operating at the same conditions. This has been demonstrated by the results of Chen, Baker and Darton (2006) who showed surfactin concentrations of 92 and 136 mg/L in a shake flask and bioreactor, respectively. Higher biosurfactant concentrations have however been reported for experiments conducted in shake flasks through optimisation of process conditions as seen by the 2000 mg/L reported by Fernandes *et al.* (2007) and the 3500 mg/L by Wei *et al.* (2003).

1.3.3.1.2 Bioreactor batch cultures

Bioreactors offer better control over operating conditions such as pH and temperatures that allow for higher yields compared to shake flasks as demonstrated by the comparative study performed by Chen, Baker and Darton (2006). 136 mg/L of surfactin was obtained in a bioreactor whilst a shake flask only yielded 92 mg/L surfactin. The potential for maximum biosurfactant production can be further increased by optimising the nutrient medium and process conditions as demonstrated by Kim *et al.* (1997) who reported a concentration of 4500 mg/L for surfactin-like lipopeptide biosurfactant using a batch reactor configuration.

1.3.3.2 Fed-batch culture

Fed-batch culture involves the gradual, aseptic addition of nutrients to without any removal of the culture during operation thus increasing the culture volume in the bioreactor over time until the maximum volume is reached and the cultivation process is stopped (Clarke, 2013). Fed-batch culture overcomes the detrimental effect on yield and production resulting from changes in nutrient concentrations and reduces the effect of inhibitory substrates on growth and product formation (Lee *et al.*, 1999; Clarke, 2013).

Fed-batch cultures are usually employed in cases that requires a constant specific growth rate, to prevent the accumulation of toxic compounds in the culture broth, or to achieve high cell densities (Guez *et al.*, 2007; Lee *et al.*, 1999; Seok Oh *et al.*, 2002), especially when the product of interest is growth-associated. The disadvantage of using fed-batch culture, however, is that it can be quite complex in terms of feeding strategy as both overfeeding and underfeeding may have detrimental effects.

Despite the added complexity, fed-batch culture has been successfully employed for both primary and secondary metabolite production (Lee *et al.*, 1999). Chenikher *et al.* (2010) and Lee *et al.* (1999) have reported an optimum specific growth rate of 0.05-0.07 h⁻¹ for *B. subtilis* BBG100. The optimum specific growth rate has been related to the maximum yield of mycosubtilin (1.27 mg/g dry biomass) by Guez *et al.* (2007).

1.3.3.3 Continuous culture

Continuous culture is characterised by the addition of nutrients and removal of the culture broth at a constant dilution rate (residence time) to maintain a constant culture volume with a homogeneous distribution that is facilitated by constant mixing. Continuous culture conditions provide stability in terms of biomass, substrate, and biosurfactant concentrations. Under these conditions, a steady-state metabolism can be achieved and the process conditions can be altered to achieve optimal production of the desired product. Continuous culture is employed for large volume products where high productivities significantly reduce the production costs (Clarke, 2013). Furthermore, continuous culture has the potential for high productivity, relatively unsophisticated process control, and reliability in terms of product quality (Chen *et al.*, 2006). It also prevents masking of physiological changes due to secondary growth and bacterial stress effects and thus allows for a single parameter to be studied whilst all other parameters are kept constant (Hoskisson and Hobbs, 2005). However, continuous culture has two major drawbacks when operated on large scale: (1) increased risk of contamination during nutrient addition and waste removal and (2) the production of desired metabolites over extended periods of time can lead to genetic mutation of the microorganism (Paulová *et al.*, 2013)

Chen, Baker and Darton (2006) investigated the effect of dilution rate (D) on growth and surfactin production by *B. subtilis* BBK 006. The authors reported that the dilution rate should be maintained between $0.2 - 0.4 \text{ h}^{-1}$ to prevent growth limitation due to maintenance metabolism ($D < 0.2 \text{ h}^{-1}$) or cell washout ($D > 0.4 \text{ h}^{-1}$). The authors concluded that surfactin production is optimised at lower dilution rates ($0.1 - 0.2 \text{ h}^{-1}$).

The same authors conducted a comparative study between batch and continuous culture by performing the batch and continuous experiments under the same conditions. Both cell (520 mg/L) and surfactin concentration (136 mg/L) was higher in batch culture compared to the concentrations achieved in continuous culture (290 and 12.2 mg/L). Lin *et al.* (1994) reported similar results for biosurfactant production by *B. licheniformis* JF-2 in batch culture (33 mg/L) and continuous culture (5.3 mg/L).

Chapter 2

HYPOTHESES AND OBJECTIVES

2.1 HYPOTHESES

The following hypotheses were proposed based on the conclusions drawn from the literature review in Chapter 1:

- 1) The ratio of nitrogen supplied by ammonium ($\text{NH}_4^+\text{-N}$)¹ and nitrate ($\text{NO}_3^-\text{-N}$)² will affect the process kinetics in terms of growth and lipopeptide production, as well as the selectivity of surfactin relative to the co-produced antifungal lipopeptides (fengycin and iturin). An optimum $\text{NH}_4\text{-N}:\text{NO}_3\text{-N}$ ratio exists which will maximise the process kinetics for surfactin production by *B. subtilis*.**

Nitrogen is essential for protein synthesis and nucleic acid production in all biological growth processes and is required for cell growth biosurfactant production by *B. subtilis*. Typically, nitrogen is added to growth medium in the form of an ammonium or nitrate salt, or as the dual nitrogen source ammonium nitrate. In the presence of both ammonium and nitrate, *B. subtilis* utilises ammonium in preference to nitrate during aerobic growth, whilst nitrate is utilised when either oxygen or ammonium is depleted. Lipopeptide selectivity is influenced by medium composition and environmental process conditions and has previously been linked to nitrogen limitation. Previous studies have focused on optimising the concentration of ammonium nitrate in the growth medium, however the effect of varying the ratio of nitrogen supplied by ammonium ($\text{NH}_4\text{-N}$) and nitrogen supplied by nitrate ($\text{NO}_3\text{-N}$) on lipopeptide production is still unexplored.

¹ $\text{NH}_4^+\text{-N}$ denotes the fraction of nitrogen supplied by ammonium

² $\text{NO}_3^-\text{-N}$ denotes the fraction of nitrogen supplied by nitrate

- 2) **The concentration of manganese in the growth medium will affect the nitrogen metabolism of *B. subtilis* which will consequently affect the process kinetics in terms growth and lipopeptide production, as well as the selectivity of surfactin relative to the co-produced antifungal lipopeptides (fengycin and iturin). An optimum Mn^{2+} concentration exists which will maximise the process kinetics for surfactin production by *B. subtilis*.**

The addition of certain metal cations, such as iron, manganese, magnesium, and potassium has been shown to have a positive effect on biosurfactant production by *B. subtilis*. Previous studies show that nitrogen utilisation, K^+ uptake, as well as other biochemical functions, are all affected by Mn^{2+} . It has been reported that Mn^{2+} affects the usage ratio of ammonium and nitrate, when both are present in the nutrient medium. At low Mn^{2+} concentrations *B. subtilis* utilises NH_4^+ in preference to NO_3^- , however increasing the Mn^{2+} concentration, increases nitrate utilisation resulting in a shift from NH_4^+ to NO_3^- as the main nitrogen source. However, based on the literature, the effect of Mn^{2+} concentration on the growth and lipopeptide production kinetics, and the selectivity of surfactin relative to the coproduced antifungal lipopeptides, by *B. subtilis* remains unclear.

- 3) **The nitrogen source ratio ($NH_4-N:NO_3-N$), manganese concentration, and conditions of oxygen availability that optimises surfactin concentration, specific surfactin yield ($Y_{p/x}$), and surfactin selectivity relative to the co-produced antifungal lipopeptides can be determined.**

B. subtilis is a facultative aerobe meaning that it is able to grow both in the presence and absence of oxygen. High oxygen availability has been shown to promote surfactin production and selectivity. It has been well established that *B. subtilis* utilises NO_3^- as an alternative electron acceptor under oxygen-depleted conditions thus sustaining cellular metabolism towards growth and lipopeptide production. As previously mentioned, Mn^{2+} affects the nitrogen utilisation by *B. subtilis*. The conditions of nitrogen source, Mn^{2+} concentration and oxygen availability appear to be interlinked, however no reports have been made on the interactive effect on the growth and lipopeptide production kinetics.

- 4) **The optimum nitrogen source ratio and manganese concentration from shake flask studies will yield similar kinetics when performed under controlled conditions in a batch bioreactor.**

5) ***B. subtilis* produces a culture supernatant that exhibits antimicrobial activity against *Mycobacterium aurum*.**

Surfactin has shown antimicrobial activity against various multi-drug resistant phytopathogens and has also exhibited antimicrobial activity against *M. aurum* which acts as a surrogate for *M. tuberculosis*.

2.2 OBJECTIVES

Surfactin production is generally associated with low yields and high purification costs. To overcome the high costs associated with surfactin production, economically attractive approaches need to be developed in order to commercialise the production of surfactin as an antimicrobial agent against TB. Lipopeptide production is largely dependent on the composition of the culture medium, process conditions, and environmental factors, hence optimising these parameters will reduce the cost of both upstream processing and downstream separation.

The overall aim of this study was to investigate the effect of medium composition and process conditions on the growth and lipopeptide production kinetics of *B. subtilis* in batch culture, for possible use as an antimicrobial agent against *M. tuberculosis*. In order to achieve this aim the following objectives, necessary to prove or disprove the hypotheses made in Section 2.1, were identified:

- 1) Evaluate and quantify the effect of nitrogen supplied as ammonium ($\text{NH}_4\text{-N}$) and nitrate ($\text{NO}_3\text{-N}$) at discrete $\text{NH}_4\text{-N}:\text{NO}_3\text{-N}$ ratios on biomass concentration, maximum growth rates, lipopeptide production (specifically surfactin production), and other kinetic parameters ($Y_{p/x}$, $Y_{p/s}$, $Y_{x/s}$, productivity, and selectivity) of *B. subtilis* in shake flasks.
- 2) Evaluate and quantify the effect of Mn^{2+} concentration on biomass concentration, maximum growth rates, lipopeptide production (specifically surfactin production), and other kinetic parameters ($Y_{p/x}$, $Y_{p/s}$, $Y_{x/s}$, productivity, and selectivity) of *B. subtilis* in shake flasks.
- 3) Evaluate and quantify the individual and interactive effects of discrete $\text{NH}_4\text{-N}:\text{NO}_3\text{-N}$ ratios, manganese concentrations, and oxygen availability on lipopeptide production (specifically surfactin production), by *B. subtilis* in shake flasks. Determine the $\text{NH}_4\text{-N}:\text{NO}_3\text{-N}$ ratio, manganese concentration, and conditions of oxygen availability that will optimise surfactin production and selectivity.
- 4) Evaluate and quantify the growth and production kinetics of the optimum nitrogen source ratio ($\text{NH}_4\text{-N}:\text{NO}_3\text{-N}$) and manganese concentration from shake flask studies under controlled conditions in batch culture in an instrumented bioreactor and compare it to the kinetics from shake flask studies.
- 5) Evaluate the antimicrobial activity of surfactin in the cell-free supernatant against *Mycobacterium aurum*.

Chapter 3

MATERIALS AND METHODS

3.1 MICRO-ORGANISMS AND CULTURE MAINTENANCE

B. subtilis ATCC 21332 was used to perform lipopeptide production experiments. Freeze-dried cultures were obtained from the American Type Culture Collection (ATCC).

Cultures were recovered from frozen stocks stored in 30% (v/v) glycerol at -20 °C by aseptically adding 1 mL of nutrient broth to the culture and followed by incubation at 30 °C for 30 minutes. 100 µL of the subculture was then aseptically spread onto a nutrient agar plate and incubated at 30 °C for 24 hours. Cultures were maintained by aseptically streaking onto nutrient agar plates followed by incubation (Labcon) at 30 °C for 24 hours and storing it in the refrigerator at 4 °C for a maximum period of 4 weeks.

Mycobacterium aurum DSM 43999 was used to perform lipopeptide efficacy tests. Freeze-dried cultures were obtained from the Leibniz Institute DSMZ-German Collection of Microorganisms and Cell Cultures.

M. aurum was recovered from the freeze-dried culture by aseptically transferring a small piece of the freeze-dried culture into a sterile 2 mL Eppendorf tube containing 1 mL of Middlebrook 7H9 broth base enriched with OADC growth supplement (10% v/v). The bacterial pellet was gently mixed by hand and allowed to rehydrate for 30 min at room temperature after which it was streaked onto Middlebrook 7H10 agar plates enriched with OADC growth supplement (10% v/v). The plates were incubated at 37 °C for 48 hours. Subcultures were then made by aseptically streaking from the Middlebrook agar plates onto nutrient agar plates followed by incubation at 37 °C for 24 hours. The plates were stored in a refrigerator at 4 °C for a maximum period of 4 weeks.

Furthermore, 450 µL aliquots of the remaining rehydrated bacterial pellet was aseptically transferred to 100 mL baffled Erlenmeyer flasks containing 9.5 mL sterile Middlebrook 7H9 broth enriched with OADC growth supplement to prepare frozen glycerol culture stocks. The culture was incubated for 24 hours in a shaker incubator (Labcon) at 37 °C and 150 rpm. In 2 mL Eppendorf tubes, 600 µl of the culture broth was added to 600 µl of 80% glycerol to yield a final glycerol concentration of 40%. The culture-glycerol mixture was left to stand for 30 minutes, to allow the bacterial cells to incorporate the glycerol into the cell membrane, after which it was dipped in liquid nitrogen and stored at -18 °C.

3.2 CULTURE MEDIA

3.2.1 Media preparation

The liquid medium was sterilised using an autoclave (Speedy Autoclave) operated at 121 °C and 100 kPa for 15 minutes. However, due to the Milliard reaction that occurs between glucose and nitrogen at elevated temperatures, these components had to be prepared and autoclaved separately. Furthermore, it was observed that iron precipitates from the solution when exposed to elevated temperatures in the autoclave. As a result, trace elements were prepared separately, and filter sterilised using a Bucher vacuum filter lined with a 0.22 µm filter paper disk.

In cases where the nitrogen concentration remained constant, nitrogen and phosphate sources were combined to form one solution. The different solutions (glucose, nitrogen/phosphate, and trace elements) were combined aseptically to make up the final medium compositions. Where the concentration of one or more medium components were varied, these components were prepared separately, and aseptically combined with the rest of the liquid medium solution. The calculations used to determine the required concentrations of NH_4Cl and NaNO_3 for a given nitrogen source ratio is illustrated in Appendix B.

It was assumed that all nutrients were depleted at the end of inoculation period and the concentration of nutrients in the inoculum was negligible. Consequently, the test media were prepared to have a concentration that is 10% higher than the final concentration required, to account for 10% volume addition of the inoculum.

3.2.2 Liquid medium containing ammonium nitrate as sole nitrogen source

A liquid medium containing ammonium nitrate as the sole nitrogen source was obtained from literature (Pretorius *et al.*, 2015) and used as the basal medium for all experiments. This medium was also used to prepare the first and second stage inoculums for all experiments. Variations from the basal medium will be described in the following sections.

The final composition of the basal growth medium is given in Table 3-1.

Table 3-1: Basal growth medium containing 4 g/L ammonium nitrate as the sole nitrogen source (Pretorius *et al.*, 2015)

Source	Component	Concentration (g/L)	Concentration (mM)
Carbon	Glucose	40	
Nitrogen	NH ₄ NO ₃	4	50
	Yeast extract	0.5	
Phosphate	Na ₂ HPO ₄ (buffer)	7.098	50
	KH ₂ PO ₄ (buffer)	6.805	50
Trace elements	MgSO ₄ ·7H ₂ O	0.592	2.4
	MnSO ₄ ·H ₂ O	0.0017	0.01
	FeSO ₄ ·7H ₂ O	0.002	0.008
	CaCl ₂ ·2H ₂ O	0.001	0.007

Three stock solutions (carbon, nitrogen/phosphate, and trace elements) were prepared and diluted according to Table 3-2 to obtain the desired concentrations specified in Table 3-1.

Table 3-2: Stock solution concentrations and dilutions used to prepare the basal medium in Table 3-1

Source	Component	Concentration (g/L)	Solution (mL/100 mL)
Carbon	Glucose monohydrate	91.7	48
Nitrogen	NH ₄ NO ₃	8.0	50
	Yeast extract	1.0	
Phosphate	Na ₂ HPO ₄	14.2	50
	KH ₂ PO ₄ (buffer)	13.6	
Trace element solution	MgSO ₄ ·7H ₂ O	16.6	2
	MnSO ₄ ·H ₂ O	0.85	
	CaCl ₂ ·2H ₂ O	0.05	
	FeSO ₄ ·7H ₂ O	0.11	

3.2.3 Liquid medium containing ammonium and nitrate as nitrogen sources

The ratio of nitrogen supplied by ammonium and nitrate was varied to determine its effect on growth and production kinetics. Individual ammonium and nitrate sources, namely NH₄Cl and NaNO₃, replaced ammonium nitrate from the Basal media outlined in Table 3-1. The total nitrogen concentration was kept constant at 1.4 g/L (equimolar to the nitrogen content of 4 g/L NH₄NO₃ as given in Table 3-1) whilst varying the ratio of nitrogen supplied by ammonium and nitrate respectively. All other concentrations were kept the same as in Table 3-1.

Four stock solutions (carbon, nitrogen, phosphate, and trace elements) were prepared and diluted according to Table 3-3 to obtain the desired concentrations used for nitrogen source experiments.

Table 3-3: Stock solution concentrations and dilutions used to prepare the liquid medium for nitrogen source experiments

Source	Component	Concentration (g/L)	Solution (mL/100 mL)
Carbon	Glucose	101.85	48
Nitrogen	Total nitrogen	6.48	24
	Yeast extract	2.14	26
Phosphate	Na ₂ HPO ₄ (buffer)	30.33	
	KH ₂ PO ₄ (buffer)	29.08	
Trace element solution	MgSO ₄ .7H ₂ O	18.44	2
	MnSO ₄ .H ₂ O	0.0944	
	FeSO ₄ .7H ₂ O	0.1222	
	CaCl ₂ .2H ₂ O	0.0556	

The final concentrations for NH₄Cl and NaNO₃ for the different ratio experiments are given in Table 3-4.

Table 3-4: Final concentrations of NH₄Cl and NaNO₃ used in nitrogen source experiments

Nitrogen ratio (NH ₄ -N:NO ₃ -N)	NH ₄ Cl concentration (g/L)	NaNO ₃ concentration (g/L)
0:1	0	8.4939
0.25:0.75	1.3364	6.3705
0.5:0.5	2.6728	4.2470
0.75:0.25	4.0092	2.1235
1:0	5.3456	0

Stock solutions of NH₄Cl (30 g/L) and NaNO₃ (80 g/L) were used for nitrogen source experiments. The stock solutions were diluted with an appropriate volume of demineralised water to a total of 24 mL / 100 mL liquid medium to yield the final concentrations (Table 3-4) as shown in Table 3-5.

Table 3-5: Stock solution dilutions (24 mL stock solution / 100 mL solution) for nitrogen source ratio experiments

Nitrogen ratio (NH ₄ :NO ₃)	Volume NH ₄ Cl stock solution (mL)	Volume NaNO ₃ stock solution (mL)	Volume water (mL)
0	0	11.80	12.20
0.25	4.95	8.85	10.20
0.5	9.90	5.90	8.20
0.75	14.85	2.95	6.20
1	19.80	0	4.20

3.3 EXPERIMENTAL PROCEDURES

3.3.1 Inoculum Development

Inoculum development was performed in two stages to ensure a more consistent final inoculum culture. Inoculation times were chosen as such to ensure minimal lag time in the test flask and bioreactor experiments.

A single colony of the *B. subtilis* culture was transferred aseptically to 100 mL of sterile Basal liquid medium (described in Table 3-1) and incubated in rotary shaker incubator (Labcon®) at 30 °C and 150 rpm for 18 hours in 500 mL baffled Erlenmeyer flasks. The second inoculum was prepared by transferring 10 mL of the first inoculum to 90 mL of sterile liquid medium and incubating for 5 hours under the same conditions as the first inoculum. Test flasks were prepared by transferring 15 mL (equivalent to 10 % (v/v)) of the second inoculum to 135 mL sterile liquid medium (unless otherwise stated).

3.3.2 Shake flask experiments

Shake flask experiments were conducted in duplicate in 500 mL baffled Erlenmeyer flasks prior to bioreactor experiments. Each shake flask contained 150 mL liquid medium (including inoculum) (unless otherwise stated). Incubation of shake flasks was carried out at 30 °C in a rotary shaker incubator (Labcon®) at 150 rpm. Samples were taken at time defined intervals and analysed using the analytical methods described in the section 3.4.

3.3.3 Bioreactor experiments

Bioreactor experiments were performed in a 1.3 L instrumented modular benchtop reactor (New Brunswick Scientific) with a maximum working volume of 1 L. Temperature was controlled at 30 °C (unless otherwise stated) using a heating-jacket and cooling water flowing through an internal unit. The initial pH was set to a value of 7 and allowed to decrease no lower than 6.8 through controlled addition of sterile 2 M NaOH_(aq) using an automatic peristaltic pump. The dissolved oxygen (DO) concentration was monitored throughout and an aeration rate of 0.8 vvm and agitation rate of 300 rpm was applied. Temperature, pH and DO probes (Mettler Toledo) were used to monitor each of these variables, respectively. A 10% (v/v) solution of Antifoam A (30% aqueous polymer emulsion, Fluka) was added to bioreactor as required to regulate excessive foaming.

3.4 ANALYTICAL METHODS

3.4.1 Cell Concentration

Cell concentration was determined *via* two methods namely cell dry weight (CDW) (direct method) and absorbance measurements (indirect method). Each of these methods are discussed in the subsequent sections.

3.4.1.1 Cell dry weight

Shake flasks were prepared using the methods discussed in section 3.3.1 with the exception that the second stage inoculum was incubated for 24 hours to ensure that the culture cell density is high enough to allow for a dilution series with a minimum of five data points. 15 mL samples were taken from each dilution and filtered through a Bucher vacuum filter (Millipore) lined with 0.22 µm filter paper disks (Anatech®) to separate the cells from the supernatant. The cells were rinsed with 5 mL demineralised water to ensure that any salts have been removed. The filter paper disks were dried in an oven (Mettler) at 60 °C for 24 hours, before filtration, and cooled in a desiccator after which it was weighed to 4 decimal places. After filtration, the wet filter paper disks were dried again (24 h, 60 °C), followed by cooling in a desiccator, and weighed as before. The weight difference (prior to and after filtration) represents the CDW.

3.4.1.2 Absorbance

Absorbance was measured using a UV-visible spectrophotometer (AE-560-40 UV VIS) at 620 nm (visible light region) and calibrated against the CDW data to construct a standard curve (Figure 3-1) that allows cell concentration to easily be determined *via* the indirect method of OD determination.

To determine the OD versus CDW curve duplicate 1 mL samples were withdrawn from each of the dilutions as prepared in 3.4.1.1 and pipetted into micro-centrifuge tubes and then centrifuged (Eppendorf® Minispin Plus) at 14500 rpm for 5 minutes to separate the cells from the supernatant. The resulting cell pellet was separated from the supernatant and re-suspended in 1 mL demineralised water by vortexing it until the cell pellet was completely re-suspended. Absorbance of the resuspended cells were measured using a spectrophotometer (AE-560-40 UV VIS) at 620 nm against a demineralised water blank. The linear region of CDW versus absorbance standard curve is limited to an absorbance reading below 0.80, hence samples were diluted to ensure that the measurements remain within the linear region of the standard curve.

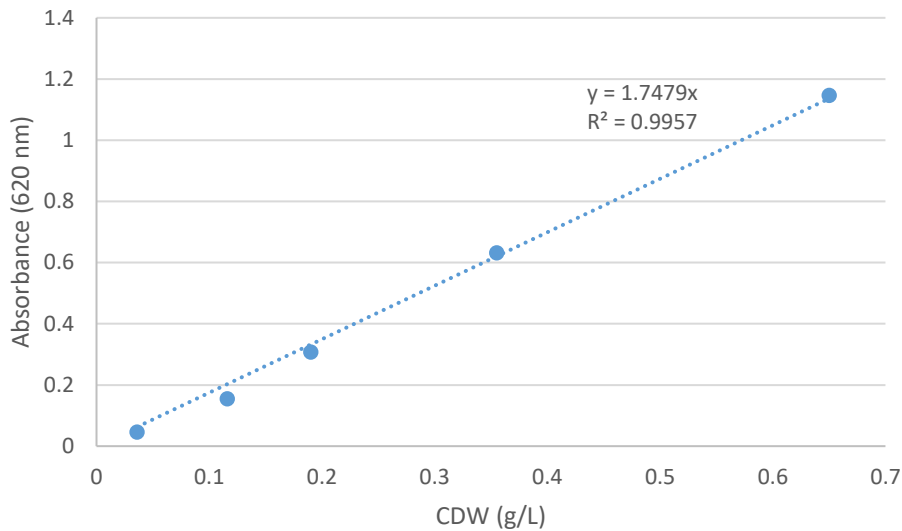


Figure 3-1: Standard curve relating absorbance at 620 nm to *B. subtilis* CDW. The data points represent the mean between duplicates and error bars represent the standard deviation of the mean.

3.4.2 Glucose concentration

Glucose concentration was determined using the dinitrosalicylic acid (DNS) method.

The DNS reagent was prepared as follows:

100 mL of a 1% (w/v) NaOH solution was prepared in a foil wrapped Schott bottle using demineralised water and placed on a magnetic stirrer. 1 g 3,5 dinitrosalicylic acid, 200 mg phenol, and 50 mg $\text{Na}_2\text{S}_2\text{O}_5$ were then added to the NaOH solution and stirred continuously for a minimum of 20 minutes to ensure that a homogenous mixture was obtained.

A pure D-Glucose (Sigma-Aldrich®) standard curve was constructed for glucose standard concentrations ranging from 150 to 500 mg/L (Figure 3-2).

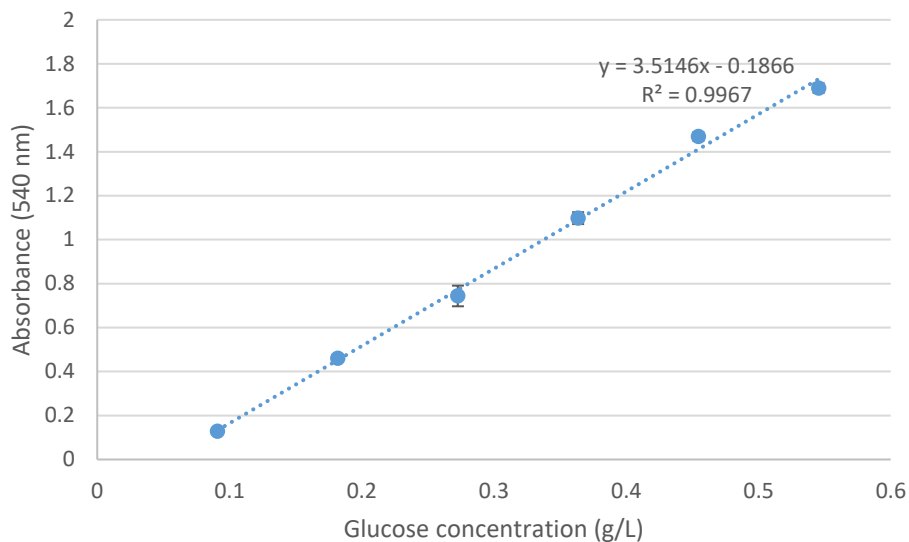


Figure 3-2: Standard curve relating absorbance at 540 nm to glucose concentration using the DNS glucose detection method. The data points represent the mean between duplicates and error bars represent the standard deviation of the mean.

Samples for glucose analysis by DNS were prepared by transferring 1 mL samples from the culture broth into an Eppendorf micro-centrifuge tube. The samples were then centrifuged (14500 rpm, 5 min) to separate the cells from the supernatant. The supernatant was then diluted with demineralised water to ensure that absorbance measurements falls within the linear region of the glucose DNS standard curve. 1 mL of DNS reagent was added to 1 mL of the diluted supernatant in a test tube (du Preez *et al.*, 2015; Sharma *et al.*, 2014), vortexed, and placed in water at 100 °C for 5 minutes. 330 µL of a 40 % (w/v) $\text{KNaC}_4\text{H}_4\text{O}_6 \cdot 4\text{H}_2\text{O}$ solution was then added the test tube, vortexed, and allowed to cool in ice water for 2 minutes. Absorbance was then measured at 540 nm using a spectrophotometer (AE-560-40 UV VIS) against a blank consisting of 1 mL demineralised water.

3.4.3 Nitrogen utilisation

Nitrogen utilisation was quantified by measuring the ammonium and nitrate concentrations of culture broth at time defined intervals.

3.4.3.1 Nitrate concentration

Nitrate colorimetric test strips (MQuant) were used to measure nitrate concentration. Samples from the culture broth were centrifuged (14500 rpm, 5 min) to separate the cells from the supernatant. The supernatant was then diluted to be in the measurement range (10 – 500 mg/L NO_3^-) of the colorimetric test strips making up a final volume of at least 500 µL in a 1.5 mL Eppendorf tube. The strips were then inserted into the diluted supernatant for 1 second and left for 1 minute before the nitrate concentration was read from the colour chart.

3.4.3.2 Ammonium concentration

The modified phenol-hypochlorite ammonia detection method (du Preez *et al.*, 2015; Pereira, 1998) was used to determine the ammonia concentration in the culture broth.

The reagents for the phenol-hypochlorite ammonia detection method were prepared as follows:

For Reagent A, 5 g phenol and 25 mg nitroprusside were added to 500 mL of demineralised water in a foil covered Schott bottle and stored at 4°C. Reagent B was prepared by adding 2.5 g of sodium hydroxide and 6 mL of 3.5% (v/v) solution of sodium hypochlorite to 500 mL demineralised water in a foil covered Schott bottle and stored at 4°C.

Standard ammonium concentrations ranging from 0.25 to 2 mM were prepared using NH₄Cl and used to construct a standard curve relating ammonium concentration to absorbance at 600 nm (Figure 3-2).

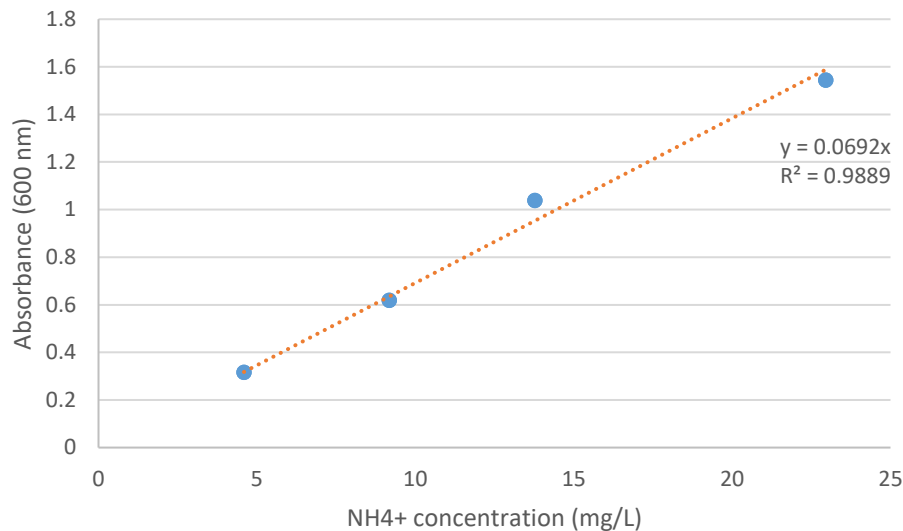


Figure 3-3: Standard curve for phenol-hypochlorite ammonia detection method relating ammonium concentration to absorbance at 600 nm.

1 mL samples from the culture broth were pipetted into 1 mL Eppendorf® centrifuge tubes and centrifuged (14500 rpm, 5 min) to separate the cells from the supernatant. The supernatant was then diluted with demineralised water to obtain ammonium concentrations in the range 0.25 to 2 mM. 1400 µL of Reagent A was then added to 350 µL of the diluted supernatant, followed by 1400 µL of Reagent B. The samples were then vortexed and kept in water bath at 25 °C before the absorbance was measured. The method from du Preez *et al.* (2015) was slightly adapted by keeping the samples in ice water after 15 minutes to slow down the reaction while measuring the absorbance. Absorbance was measured at 600 nm against a demineralised water blank following the same preparation procedure.

3.4.4 Lipopeptide concentration

3.4.4.1 Surfactin concentration

HPLC was used to measure surfactin concentration. The HPLC specifications for surfactin concentration are given in Table 3-6.

Table 3-6: HPLC specifications for surfactin analyses

Column	Phenomenex Luna μ m C18 column (250 x 4.6 mm)
Detector	Dionex Ultimate 3000 Diode-array detector
Mobile phase A	0.05% (v/v) Trifluoroacetic acid (Fluka®) in water
Mobile phase B	0.05% (v/v) Trifluoroacetic acid in acetonitrile (High purity UV grade, Burdick and Jackson)
Mobile phase gradient	Start at 35% B, increase to 40% B during the next 2 minutes, isocratic at 40% B for the next 5 minutes, increase to 63% B during the next 43 minutes, increase to 80% B during the next 10 minutes, increase to 87% B during the next 35 minutes, return to 35% B during the next 10 minutes and isocratic stabilization at 35% B for the next 5 minutes.
Flow rate	0.9 mL/min
Absorbance	210 nm

Pure surfactin (Sigma-Aldrich®) was used to prepare standard concentrations ranging from 0.15 to 2.5 g/L to construct a standard concentration curve (Figure 3-4). Six major peaks, corresponding to different surfactin homologues at their respective retention times, can be observed from the standard surfactin chromatograms (see example of surfactin chromatogram in Appendix C). It should be noted that peaks 5 and 6 were grouped together for analyses.

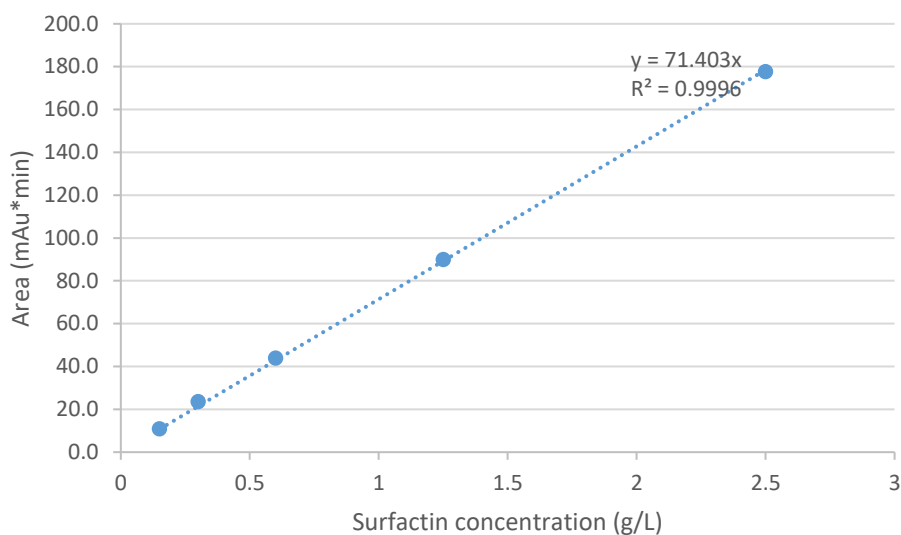


Figure 3-4: Surfactin standard curve relating the combined peak areas to the concentration

The following sample preparation procedure was used for surfactin HPLC analyses:

1 mL samples from the culture broth were pipetted into 1 mL Eppendorf centrifuge tubes and centrifuged (14500 rpm, 5 min) to separate the cells from the supernatant. 500 μ L of the supernatant was added to 500 μ L acetonitrile mixture (99.95% acetonitrile, 0.05% trifluoroacetic acid) to allow precipitation (the precipitate is unknown; however, it was found not to effect the concentration of surfactin). The acetonitrile/supernatant mixture was stored at 4 °C until it was sent for HPLC analysis. Prior to being sent for HPLC analysis, the supernatant/ acetonitrile mixture was filtered using a 0.22 μ m syringe filter to remove any precipitate that might obstruct the flow through the HPLC column. 50 μ L of the supernatant/acetonitrile mixture was injected onto the column and the eluent absorbance was monitored at 210 nm. Sample absorption peaks was then compared to those of the pure surfactin standard to determine the surfactin concentration.

3.4.4.2 Antifungal concentration

The same sample preparation procedure and HPLC method used for surfactin quantification was used to quantify antifungal concentrations.

3.4.4.2.1 Fengycin concentration

Pure fengycin (Sigma-Aldrich®) was used to prepare standard concentrations ranging from 100 to 500 mg/L to construct a standard concentration curve (Figure 3-5). All peaks between 26 and 47 minutes were grouped together for fengycin analyses (Appendix D).

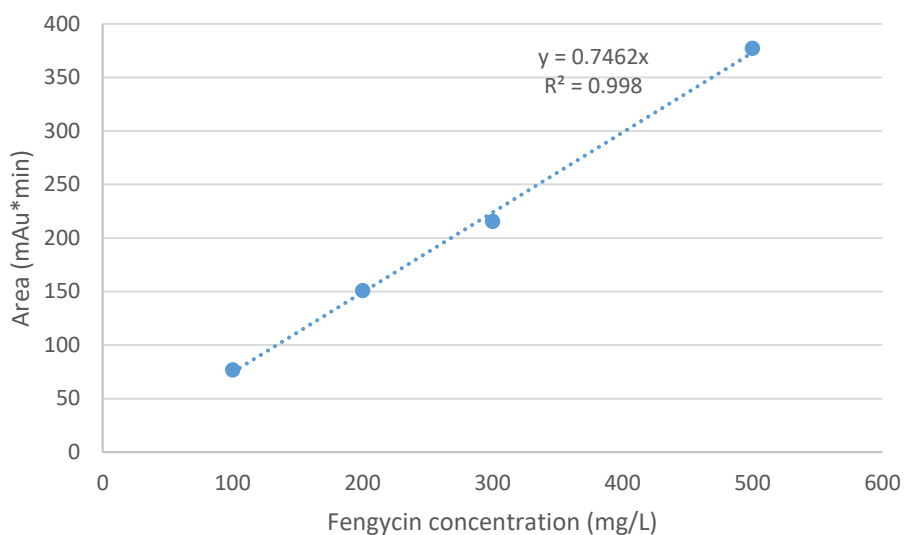


Figure 3-5: Fengycin standard curve relating the peak area to concentration

3.4.4.2.2 Iturin concentration

Pure iturin (Sigma-Aldrich®) was used to prepare standard concentrations ranging from 50 to 200 mg/L to construct a standard concentration curve (Figure 3-6). All peaks between 26 and 47 minutes were grouped together for fengycin analyses (Appendix D shows details of these analyses).

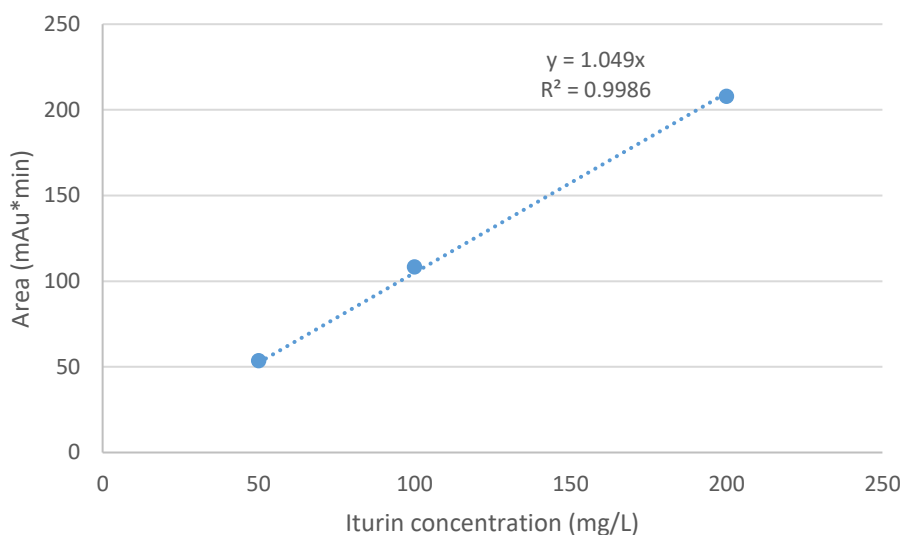


Figure 3-6: Iturin standard curve relating the combined peak areas to concentration

3.4.5 Antimicrobial activity

The antimicrobial activity of surfactin was determined using the modified soft agar overlay method (Ballot, 2009). The modified soft agar overlay method that was used to determine the antimicrobial activity of surfactin is as follows:

Mycobacterium aurum, grown on nutrient agar plates at an incubation temperature of 37°C for 48 hours, was used to test the antimicrobial activity of crude surfactin. *M. aurum* colonies were aseptically suspended in sterile physiological saline (0.85% w/v NaCl) to obtain an optical density of 0.3 measured with a spectrophotometer (UV-VIS AE-560-40) at 620 nm. 2 mL of the saline suspension of *M. aurum* was then added to 10 mL of a soft nutrient agar solution (nutrient broth containing 7.5% agar) and vortexed for approximately 30 seconds.

The back ends of sterile 1 mL pipette tips were cut off and placed in Petri-dishes (3 per plate, evenly spaced). The vortexed solution of *M. aurum* was then aseptically poured into the Petri-dish and allowed to settle around the cut-off back ends of the pipette tips. The cut-off back ends of the pipette tips were then removed from the agar using sterile forceps, leaving three wells in the agar.

Test samples (biosurfactant supernatant) were filter sterilized using a 0.22 µm syringe filter (Anatech®) to ensure that all the cells had been separated from the supernatant. 40 µL of the filtered solution was then aseptically pipetted into two of the wells and 40 µL of sterile physiological saline (0.85% w/v NaCl) was aseptically pipetted into the remaining well to serve as a control. The plates were then incubated in duplicate at 37°C for 48 hours after which the inhibition zone diameters (defined as the difference between the inhibition zone diameter and well diameter) were measured Figure 3-7.

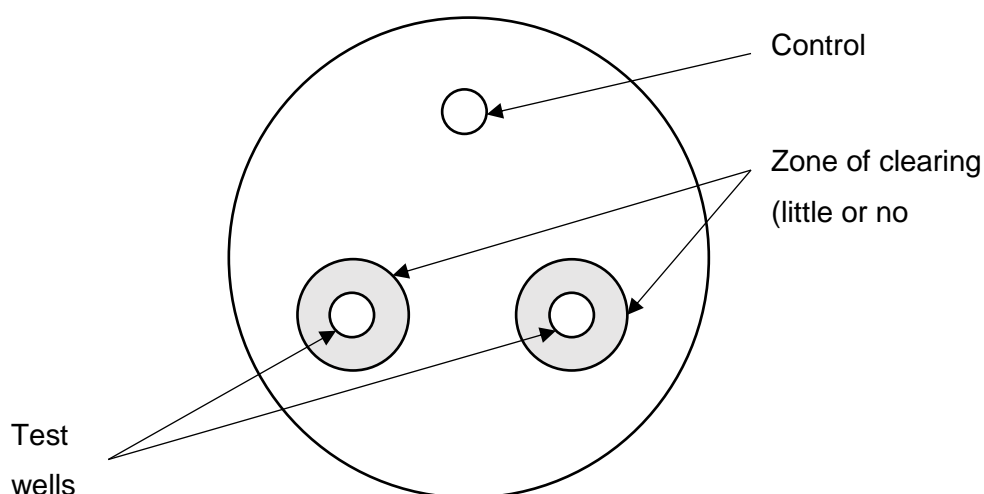


Figure 3-7: Schematic representation of antimicrobial inhibition zone redrawn from Ballot (2009)

3.5 EXPERIMENTAL DESIGN

The experiments needed to investigate the effect of nitrogen source, manganese concentration and oxygen availability on lipopeptide production were completed using a central composite design (CCD) in which a conventional 2-level 3-factor (2^3) full factorial design was augmented with central and axial points.

The CCD is a highly rotatable design, meaning that the variance of any value of the dependent variable predicted by the model is only dependent on its distance from the central point, irrespective of the direction. This means that the variance of an estimated point is constant and equal to all the other points that are the same distance from the central point. The rotatability of the design is calculated using Equation 5.1:

$$\alpha = \sqrt[4]{2^k} \quad (5.1)$$

When $\alpha > 1$, each factor was assessed at 5 levels ($-\alpha$, -1 , 0 , 1 and α) In this case $\alpha = 1.68$. These values were used to determine the factor levels for each independent variable. Experimental data was used to fit a response surface model describing the dependent variable as a continuous surface within the experimental boundaries.

This method offers the advantage of extracting the maximum amount of data from the minimum number of experiments which also reduces the cost and time needed to perform the experiments. Furthermore, it allows the examination of the interactive effect of the independent variables (nitrogen source ratio, manganese concentration and oxygen availability) on the dependent variables ($Y_{p/x}$, maximum surfactin concentration and selectivity) as well as their combined effects.

The effect of nitrogen source (at constant total N), manganese concentration and oxygen availability on $Y_{p/x}$ and maximum surfactin concentration were investigated using a CCD approach with the factor levels as shown in Table 3-7. The factor levels were chosen based on typical ranges used in literature.

Table 3-7: Factor levels for independent variables

Variables	Units	Extra Low	Low	Mid	High	Extra High
Factor level		-1.68	-1.00	0.00	1.00	1.68
NH4-N:NH4-N		0.08:0.92	0.25:0.75	0.50:0.50	0.75:0.25	0.92:0.08
Manganese concentration	mM	0.00	0.02	0.05	0.08	0.10
Relative filling volume (RFV)	(mL/mL)	0.20	0.24	0.30	0.36	0.40

The standard order of experiments is given in Table 3-8.

Table 3-8: Running order and factor levels

Standard Run	NH ₄ -N:NO ₃ -N	Mn ²⁺ concentration	Relative filling volume (RFV)
1	-1.00	-1.00	-1.00
2	-1.00	-1.00	1.00
3	-1.00	1.00	-1.00
4	-1.00	1.00	1.00
5	1.00	-1.00	-1.00
6	1.00	-1.00	1.00
7	1.00	1.00	-1.00
8	1.00	1.00	1.00
9	-1.68	0.00	0.00
10	1.68	0.00	0.00
11	0.00	-1.68	0.00
12	0.00	1.68	0.00
13	0.00	0.00	-1.68
14	0.00	0.00	1.68
15 (C)	0.00	0.00	0.00
16 (C)	0.00	0.00	0.00

Chapter 4

RESULTS AND DISCUSSION

4.1 THE EFFECT OF NITROGEN SOURCE ON THE GROWTH AND LIPOPEPTIDE PRODUCTION KINETICS OF *B. SUBTILIS* IN SHAKE FLASKS

B. subtilis can utilise both organic and inorganic nitrogen sources for growth and lipopeptide production, however higher biosurfactant yields have been reported for inorganic nitrogen sources (this is discussed in section 1.3.1.2). Ammonium and nitrate are by far the most common nitrogen sources used for lipopeptide production and are generally added to the culture medium in the form of the dual nitrogen source, ammonium nitrate (NH_4NO_3). Ammonium is generally utilised by the organism during the aerobic stages of cell growth whilst nitrate serves a dual purpose as it can be converted to ammonium to be utilised as a nitrogen source or it can act as an electron acceptor under oxygen limiting conditions.

Different authors (Abushady *et al.*, 2005; Pretorius *et al.*, 2015) have investigated the effect of NH_4NO_3 concentration on growth and lipopeptide production to find the optimum NH_4NO_3 concentration for growth and lipopeptide production, however this method masks the individual effects of ammonium and nitrate concentrations on the growth and lipopeptide production kinetics. To overcome this, ammonium and nitrate were supplied separately as the salts ammonium chloride (NH_4Cl) and sodium nitrate (NaNO_3) in this study.

Discrete ratios ($\text{NH}_4\text{-N}:\text{NO}_3\text{-N}$) of nitrogen from ammonium ($\text{NH}_4\text{-N}$) and nitrogen from nitrate ($\text{NO}_3\text{-N}$) at a constant total nitrogen concentration of 1.46 g/L (equivalent to 4 g/L NH_4NO_3) were used to study the effect of ammonium and nitrate concentrations on the growth and lipopeptide kinetics of *B. subtilis* in batch culture. The $\text{NH}_4\text{-N}:\text{NO}_3\text{-N}$ ratios considered were: 0:1, 0.25:0.75, 0.5:0.5, 0.75:0.25 and 1:0. All experiments were conducted in duplicate shake flasks and the results presented in this section are based on the averages from the duplicate experiments. Error bars are used to show the standard deviation between duplicate runs.

The growth, substrate utilisation, and lipopeptide production patterns, for each of the ratios used, is discussed in section 4.1.1 followed by a comparison of the growth and substrate utilisation patterns in section 4.2.2, lipopeptide production patterns in section 4.1.3, and finally the normalised kinetic parameters in section 4.1.4 for the different ratios. Although *B. subtilis* produces all three lipopeptide families, iturin is not included in the discussion as its concentration was negligible compared to that of surfactin and fengycin.

4.1.1 Growth, substrate utilisation and lipopeptide production patterns of *B. subtilis* in cultures containing NH_4^+ and NO_3^- as a nitrogen sources at discrete $\text{NH}_4\text{-N}:\text{NO}_3\text{-N}$ ratios

A semi-log plot of CDW scaled to the initial CDW against time was used to illustrate cell growth in Figure 4-1 as it allows easy distinction of the different cell growth phases. This convention will be used throughout the rest of the text. No lag phase was observed for the culture that contained nitrate as the sole nitrogen source, as can be seen in Figure 4-1. The culture entered the exponential growth phase immediately after inoculation, with a maximum specific growth rate (μ_{max}) of 0.42 h^{-1} . The specific growth rate (μ) decreased after 4 h, however the cells continued to grow exponentially until it reached the stationary phase at 43 h. The decrease in growth rate is likely due to the depletion of the residual ammonium from the inoculum and nitrate being utilised as the nitrogen source. Nitrate is a less accessible source of nitrogen compared to ammonium because it first needs to be converted to ammonium to be utilised by the cells (these concepts are discussed in detail in section 1.3.1.2) hence resulting in a decrease in the growth rate.

A maximum cell concentration of 13.2 g/L was achieved after 43 h of cultivation. At this point both glucose and nitrate was essentially depleted (less than 10% of the initial concentration) suggesting growth was limited by these two nutrients. Glucose consumption started immediately after inoculation and continued at a nearly constant rate until it was depleted at 52 h.

It was assumed that the residual ammonium present in the culture broth after inoculation has no significant effect on the results since the concentration (0.08 g/L) was insignificant compared to the maximum ammonium concentration used in this set of experiments. Figure 4-1 shows that nitrate was consumed at a nearly constant rate immediately after inoculation until it was depleted at 43 h. The immediate consumption of nitrate validated the assumption that the residual ammonium from the inoculum was insignificant since ammonium is the preferred nitrogen source for *B. subtilis* under oxygen sufficient conditions (Davis *et al.*, 1999).

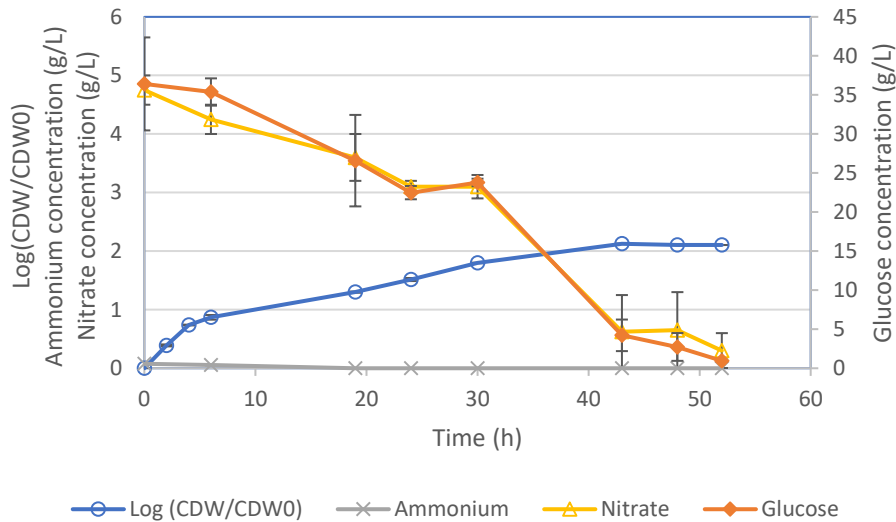


Figure 4-1: Graph illustrating the growth (open circles, left hand axis, in log (CDW/CDW₀)) of *B. subtilis* and substrate concentrations of nitrate (open triangles, left hand axis, in g/L), ammonium (crosses, left hand axis, in g/L) glucose (closed diamonds, right hand axis, in g/L) over time in a culture containing nitrate as the sole nitrogen source in shake flasks at 150 rpm and 30 °C.

Figure 4-2 shows the growth and lipopeptide production profiles for the culture that contained nitrate as the sole nitrogen source. Surfactin production was slow during the first 19 h of growth with only 101 mg/L surfactin produced during this period. The surfactin production rate increased after 19 h and was essentially constant until 43 h when glucose and nitrate were less than 10% of the initial concentrations. Surfactin production continued at a slower rate after 43 h, reaching a maximum concentration of 716 mg/L at 52 h when both glucose and nitrate was depleted. Surfactin accounted for approximately 58% of the total lipopeptides (surfactin and fengycin, with negligible iturin) produced after 52 h of cultivation.

Fengycin production started later than surfactin production. There was essentially no fengycin produced during the first 30 hours of cultivation. Fengycin production started as growth approached the stationary phase, after 30 h, and continued at a constant rate until it reached a maximum concentration of 514 mg/L at the end of the stationary phase at 52 h (although it is not depicted in Figure 4-2, fengycin concentration only increased by 68 mg/L between 52 and 72h, hence the maximum fengycin concentration was taken at 52 h). Fengycin production ceased due to glucose and nitrate being depleted at 52 h.

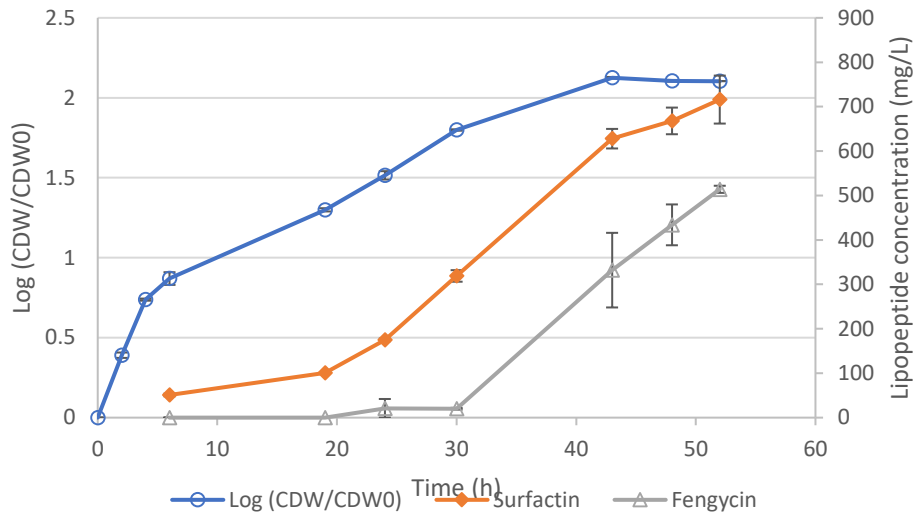


Figure 4-2: Graph illustrating the growth (open circles, left-hand axis, $\log(\text{CDW}/\text{CDW}_0)$) and lipopeptide production (surfactin – closed diamonds, right hand axis, in mg/L; fengycin – open triangles, right hand axis, in mg/L) of *B. subtilis* over time in a culture containing nitrate as the sole nitrogen source in shake flasks at 150 rpm and 30 °C.

Figure 4-3 shows the growth and substrate utilisation patterns for $\text{NH}_4\text{-N}:\text{NO}_3\text{-N} = 0.25:0.75$. The culture entered the exponential phase immediately after inoculation, with a maximum specific growth rate (μ_{max}) of 0.43 h^{-1} for the first 4 h of growth. Exponential growth continued at a lower specific growth rate between 4 and 19 h. The specific growth rate further decreased at 19 h when ammonium became depleted, and the culture entered the stationary phase at 30 h, yielding a maximum CDW of 10.6 g/L. The cell concentration remained constant for a further 13 h after which it decreased due to glucose and nitrate depletion at 43 h.

Glucose consumption started immediately after inoculation and continued at a nearly constant rate until it was depleted at 43 h. Ammonium consumption also started immediately after inoculation and was consumed at a constant rate until it was depleted at 19 h. A slight increase in ammonium concentration was observed between 19 and 24 h, however the error bars indicate that ammonium was in fact depleted at 19 h and the increase in concentration was most likely the result of uncertainty in the colorimetric method used to determine ammonium concentration

Nitrate concentration remained constant during the first 19 h of growth when ammonium was still in excess. Nitrate was consumed at a nearly constant rate following ammonium depletion at 19 h, until it was depleted at 43 h. The nearly constant nitrate concentration during the first 19 h of cultivation suggests that oxygen was still in excess during this period, as nitrate was not utilised as an electron acceptor, nor was it used as nitrogen source as ammonium, which is the preferred nitrogen source, was still in excess.

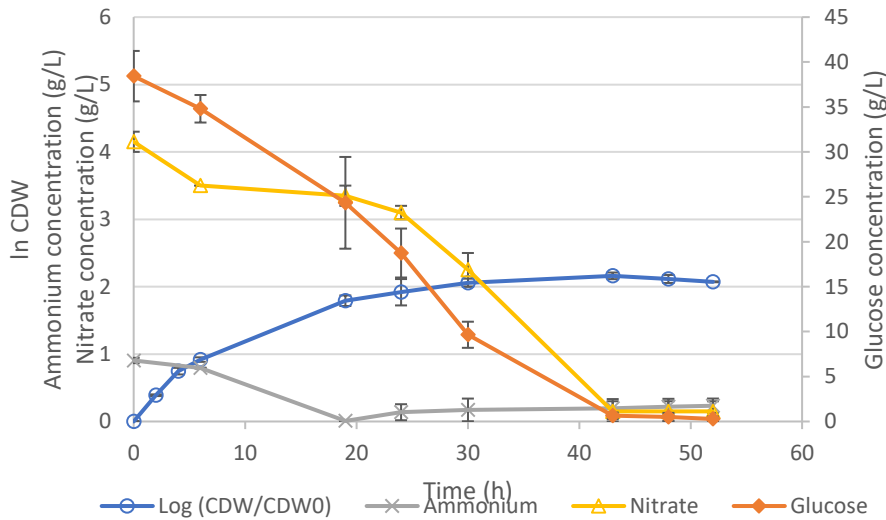


Figure 4-3: Graph illustrating the growth (open circles, left hand axis, in log (CDW/CDW₀)) of *B. subtilis* and substrate concentrations of nitrate (open triangles, left hand axis, in g/L), ammonium (crosses, left hand axis, in g/L) glucose (closed diamonds, right hand axis, in g/L) over time in a culture containing NH₄⁺ and NO₃⁻ in a ratio NH₄-N:NO₃-N = 0.25:0.75 as nitrogen sources in shake flasks at 150 rpm and 30 °C.

The growth and lipopeptide production patterns for NH₄-N:NO₃-N = 0.25:0.75 is shown in Figure 4-4. Surfactin was produced at a constant rate between 6 and 30 h. A maximum surfactin concentration of 637 mg/L was observed at 30 h and the concentration remained constant for the remainder of the experimental run. The period of surfactin production coincided with the active growth phase and ceased at the start of the stationary phase at 30 h. Surfactin accounted for approximately 91% of the total lipopeptides produced after 30 h of cultivation. Since surfactin production remained constant after 30 h, whilst fengycin production continued to increase until 43 h, harvesting after 30 h will result in a crude product with a lower surfactin percentage which will adversely affect the downstream processing costs. Harvesting at 43 h instead of 30 h will cause the percentage surfactin to decrease from 91 to 71%.

Figure 4-4 shows that fengycin production started later than surfactin. No fengycin was produced during the first 19 h of cultivation. Fengycin was produced at a nearly constant rate between 19 and 43 h at which point it reached its maximum concentration of 249 mg/L and remained constant for the duration of the experimental run. Fengycin production ceased due to glucose and nitrate depletion at 43 h.

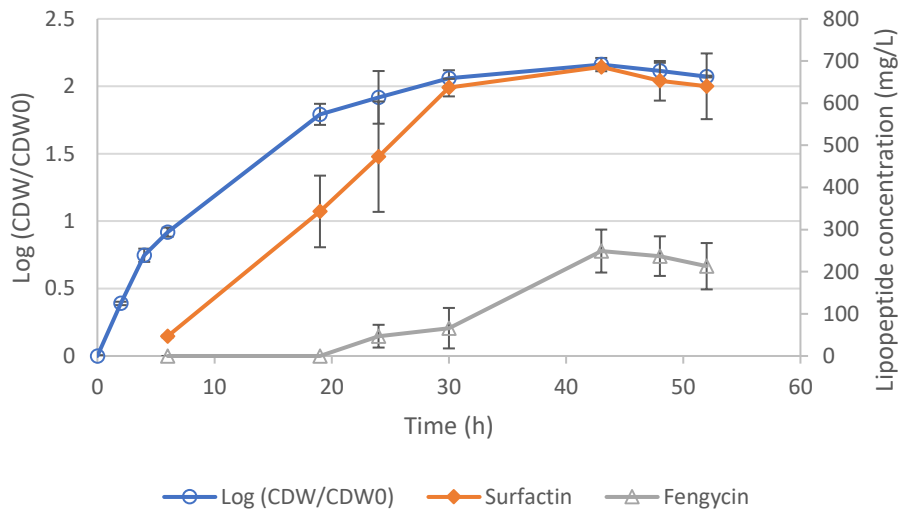


Figure 4-4: Graph illustrating the growth (open circles, left hand axis, in log (CDW/CDW₀)) of *B. subtilis* and substrate concentrations of nitrate (open triangles, left hand axis, in g/L), ammonium (crosses, left hand axis, in g/L) glucose (closed diamonds, right hand axis, in g/L) over time in a culture containing NH₄⁺ and NO₃⁻ in a ratio NH₄-N:NO₃-N = 0.25:0.75 as nitrogen sources in shake flasks at 150 rpm and 30 °C.

The growth and substrate utilisation patterns for the NH₄-N:NO₃-N = 0.5:0.5 is shown in Figure 4-5. A slight lag was observed during the first 2 hours of growth after which the culture entered the exponential phase, with a maximum specific growth rate (μ_{max}) of 0.44 h⁻¹ between 2 and 6 h. Exponential growth continued at a lower specific growth rate between 6 and 19 h. A deceleration phase was observed between 19 and 30 h after which the culture entered the stationary growth phase. The onset of the stationary phase at 30 h coincided with the time both glucose and nitrate were depleted. Cell concentration reached a maximum concentration of 14.6 g/L after 30 h of growth and remained constant for the remainder of the experimental run.

Figure 4-5 shows that glucose was consumed at a nearly constant rate immediately after inoculation until it was completely consumed at 30 h. Similarly, ammonium was also consumed at a nearly constant rate immediately after inoculation, however consumption ceased at 30 h when both glucose and nitrate were depleted.

Nitrate consumption was slow during the first 19 h of growth when ammonium was still in excess. A rapid increase in nitrate consumption was observed after 19 h. *B. subtilis* utilises nitrate as nitrogen source in the absence of ammonium or as an electron acceptor when oxygen becomes limiting (Davis *et al.*, 1999). Since ammonium was still in excess at 19 h the increase in nitrate consumption suggests that oxygen became limiting. Both nitrate and glucose was depleted at 30 h which coincided with the start of the stationary phase suggesting that growth was glucose and nitrate limited.

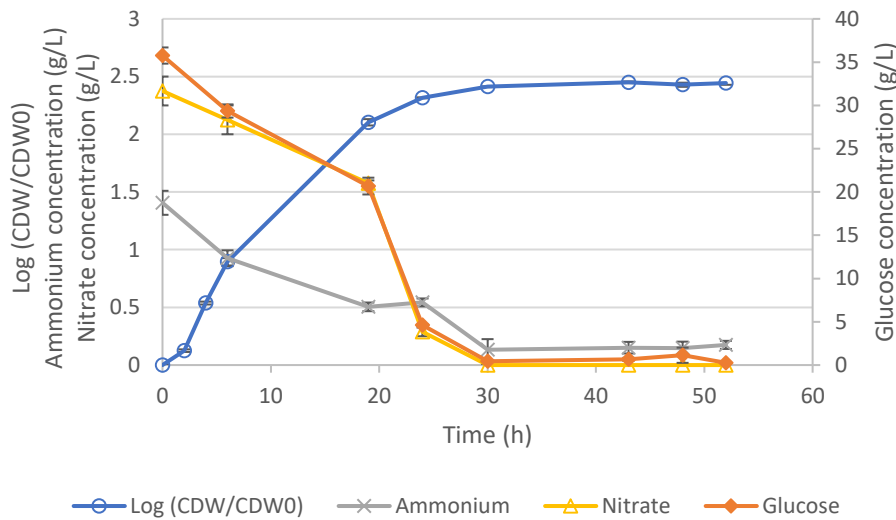


Figure 4-5 Graph illustrating the growth (open circles, left hand axis, in log (CDW/CDW₀)) of *B. subtilis* and substrate concentrations of nitrate (open triangles, left hand axis, in g/L), ammonium (crosses, left hand axis, in g/L) glucose (closed diamonds, right hand axis, in g/L) over time in a culture containing NH₄⁺ and NO₃⁻ in a ratio NH₄-N:NO₃-N = 0.5:0.5 as nitrogen sources in shake flasks at 150 rpm and 30 °C.

Figure 4-6 shows the growth and lipopeptide production patterns for NH₄-N:NO₃-N = 0.5:0.5. Surfactin was produced at a nearly constant rate between 6 and 30 h and then plummeted rapidly after 30 h. The decrease in surfactin concentration coincided with glucose and nitrate depletion at 30 h. Cell concentration remained constant following glucose and nitrate depletion whilst surfactin concentration plummeted. The rapid decrease in surfactin concentration was most likely caused by nitrate depletion causing the pH to drop below 5, which resulted in surfactin precipitating from solution (see section 1.3.2.3). Surfactin reached a maximum concentration of 1084 mg/L and accounted for approximately 84% of the total lipopeptides produced after 30 h of cultivation. Since surfactin concentration plummeted after 30 h, whilst the concentration of fengycin essentially remained constant, harvesting after 30 h will not only result in a supernatant with a lower surfactin concentration, but will also yield a product with a lower surfactin percentage. Harvesting at 24 h instead of 30 h slightly increases the percentage surfactin from 84 to 88 % at the expense of having a supernatant with a lower surfactin concentration (888 mg/L).

Fengycin was produced at nearly constant rate between 6 and 30 h. A maximum fengycin concentration of 212 mg/L was observed at 30 h when glucose and nitrate were depleted. Unlike surfactin, fengycin concentration did not decrease after 30 h when glucose and nitrate were depleted, but instead remained constant between 30 and 43 h. A slight decrease in fengycin concentration was observed after 43 h.

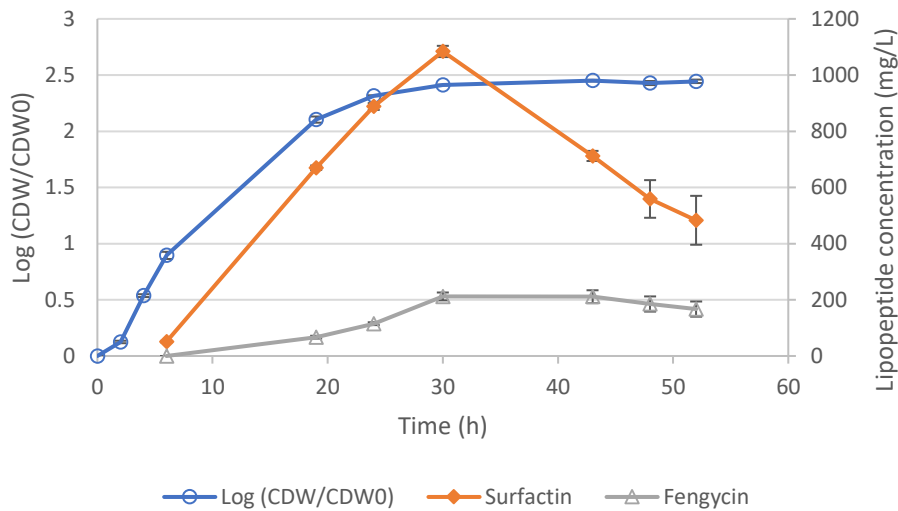


Figure 4-6: Graph showing growth (open circles, left hand axis, $\log(\text{CDW}/\text{CDW}_0)$) and lipopeptide production (surfactin – closed diamonds, right hand axis, in mg/L; fengycin – open triangles, right hand axis, in mg/L) of *B. subtilis* over time in a culture containing NH_4^+ and NO_3^- in a ratio $\text{NH}_4\text{-N}:\text{NO}_3\text{-N} = 0.5:0.5$ as nitrogen sources in shake flasks at 150 rpm and 30 °C.

Figure 4-7 shows the growth and substrate utilisation patterns for $\text{NH}_4\text{-N}:\text{NO}_3\text{-N} = 0.75:0.25$. A slight lag was observed during the first 2 hours of growth after which the culture entered the exponential phase, with a maximum specific growth rate (μ_{max}) of 0.46 h^{-1} between 2 and 6 h. Exponential growth continued at a lower specific growth rate between 6 and 24 h. A deceleration phase was observed between 24 and 43 h after which the culture entered the stationary growth phase. A maximum CDW of 19.5 g/L was observed at 43 h, after which cell concentration remained constant for the duration of the experimental run.

Glucose was consumed at a nearly constant rate immediately after inoculation until consumption ceased at 30 h. At 30 h, 3.2 g/L glucose was still present in the culture broth thus glucose was not the growth-limiting nutrient. Ammonium consumption was slow during the first 6 h of growth, after which it was consumed at a nearly constant rate until consumption ceased at 30 h. At 30 h, 0.37 g/L ammonium was still present in the culture broth.

Nitrate concentration remained constant during the first 6 h of growth after which it was consumed at a constant rate until depletion at 24 h. Since ammonium, which is the preferred nitrogen source, was still in excess during this period, the rapid consumption of nitrate suggest that oxygen became limiting after 6 h. Growth ceased shortly after nitrate was depleted thus nitrate, and since no alternative electron acceptor was available following nitrate depletion, nitrate became the growth-limiting nutrient.

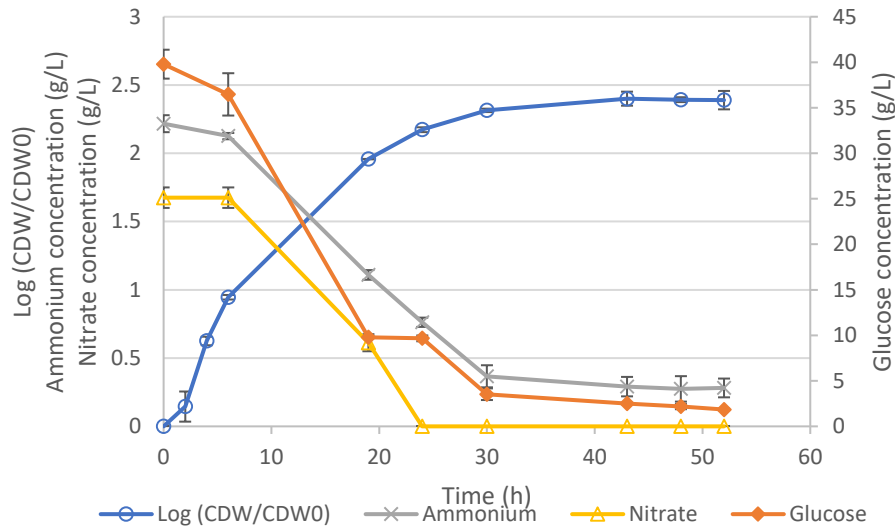


Figure 4-7: Graph illustrating the growth (open circles, left hand axis, in log (CDW/CDW₀)) of *B. subtilis* and substrate concentrations of nitrate (open triangles, left hand axis, in g/L), ammonium (crosses, left hand axis, in g/L) glucose (closed diamonds, right hand axis, in g/L) over time in a culture containing NH₄⁺ and NO₃⁻ in a ratio NH₄-N:NO₃-N = 0.75:0.25 as nitrogen sources in shake flasks at 150 rpm and 30 °C.

Figure 4-8 shows the growth and lipopeptide production patterns for NH₄-N:NO₃-N = 0.75:0.25. Surfactin production was rapid between 6 and 19 h and then decreased at a nearly constant rate until it was almost completely consumed at 43 h. Glucose, ammonium, and nitrate was still in excess at the time surfactin concentration started decreasing, however nitrate became depleted shortly after at 24 h (Figure 4-7) suggesting that nitrate limited growth and surfactin production since there was no alternative electron acceptor following nitrate depletion. A maximum surfactin concentration of 604 mg/L was observed at 19 h. Surfactin accounted for approximately 91% of the total lipopeptides produced after 19 h of cultivation. Again, a rapid decrease in surfactin concentration was observed after nitrate was depleted. Since surfactin concentration plummeted after 19 h whilst the concentration of fengycin continued to increase, harvesting after 19 h will not only result in a supernatant with a lower surfactin concentration, but will also yield a supernatant with a lower surfactin percentage.

Fengycin was produced at a nearly constant rate between 6 and 30 h. Fengycin concentration plummeted at a nearly constant rate after 30 h and was almost completely consumed at 43 h. Glucose and ammonium was still in excess at the time fengycin concentration started decreasing, but nitrate was already depleted (Figure 4-7) suggesting that nitrate limited fengycin production. A maximum fengycin concentration of 105 mg/L was observed at 30 h.

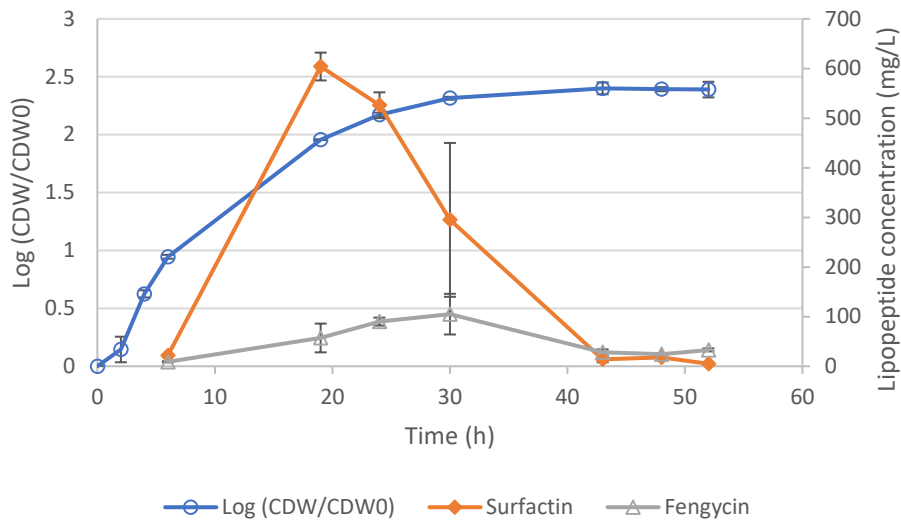


Figure 4-8: Graph illustrating the growth (open circles, left hand axis, $\log(\text{CDW}/\text{CDW}_0)$) and lipopeptide production (surfactin – closed diamonds, right hand axis, in mg/L; fengycin – open triangles, right hand axis, in mg/L) of *B. subtilis* over time in a culture containing NH_4^+ and NO_3^- in a ratio $\text{NH}_4\text{-N}:\text{NO}_3\text{-N} = 0.75:0.25$ as nitrogen sources in shake flasks at 150 rpm and 30 °C.

Figure 4-9 shows the growth and substrate utilisation patterns for the culture that contained ammonium as the sole nitrogen source. A slight lag was observed during the first 2 h of growth after which the culture entered the exponential growth phase, with a maximum specific growth rate (μ_{max}) of 0.45 h^{-1} between 2 and 6 h. Exponential growth continued at a lower specific growth rate between 6 and 19 h. A deceleration phase was observed between 19 and 30 h after which the culture entered the stationary growth phase. A maximum cell concentration of 12.7 g/L was observed at 30 h after which cell concentration remained constant for the remainder of the experimental run.

Figure 4-9 shows that 0.26 g/L of nitrate was present in the culture broth immediately after inoculation. The nitrate observed at 0 h was transferred from the inoculum since no nitrate was added to test flask medium. The concentration of nitrate remained constant during the first 6 h of growth, after which it was completely consumed between 6 and 19 h. Ammonium, which is the preferred nitrogen source was still in excess during this period, suggesting that oxygen became limiting and nitrate was used as electron acceptor rather than a nitrogen source. If no ammonium was present in the culture broth, nitrate would have acted as a nitrogen source as well as an electron acceptor. Growth ceased shortly after the residual nitrate was consumed, thus it can be concluded that growth was oxygen limited since only surface oxygen was available in the system. Nitrate acts as an alternative electron acceptor under oxygen-depleted conditions and since the culture essentially contained no nitrate, this resulted in growth ceasing when oxygen became limiting.

Glucose was consumed at constant rate immediately after inoculation until consumption ceased at 19 h. Glucose consumption ceased at the same time the residual nitrate became depleted. Approximately 12 g/L glucose remained in the culture broth following the depletion of the residual nitrate.

Similar to glucose, ammonium was consumed at a nearly constant rate immediately after inoculation until consumption ceased at 19 h when the residual nitrate was depleted. Approximately 1.2 g/L ammonium remained in the culture broth following the depletion of the residual nitrate.

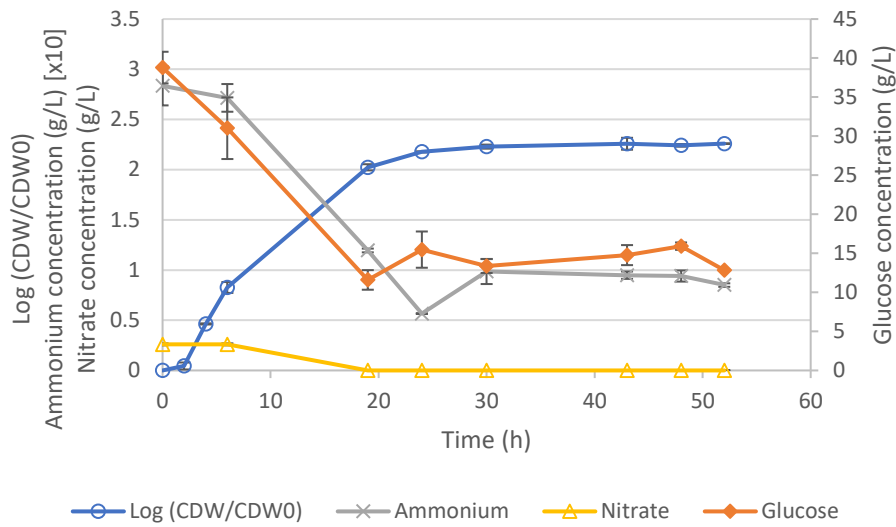


Figure 4-9: Graph illustrating the growth (open circles, left hand axis, in log (CDW/CDW₀)) of *B. subtilis* and substrate concentrations of nitrate (open triangles, left hand axis, in g/L), ammonium (crosses, left hand axis, in g/L), glucose (closed diamonds, right hand axis, in g/L) over time in a culture containing ammonium as the sole nitrogen source in shake flasks at 150 rpm and 30 °C.

Figure 4-10 shows the growth and lipopeptide production patterns for a culture that contained ammonium as the sole nitrogen source. Surfactin concentration increased to 130 mg/L between 6 and 19 h after which a rapid decrease in surfactin concentration was observed. Almost all the surfactin produced was consumed between 19 and 24 h. Again, the rapid decrease in surfactin concentration was most likely due to precipitation when pH dropped below 5 following the depletion of the residual nitrate. The decrease in surfactin concentration was observed at the same time the residual nitrate became depleted (Figure 4-9). This suggests that surfactin production was limited by oxygen since the culture essentially contained no nitrate to act as an alternative electron acceptor following oxygen depletion. Surfactin made up approximately 87% of the total lipopeptides produced after 19 h of cultivation.

Fengycin concentration increased to 34 mg/L between 6 and 19 h after which a slow decrease in the fengycin concentration was observed. Similar to surfactin, the decrease in fengycin concentration was observed at the same time the residual nitrate became depleted (Figure 4-9).

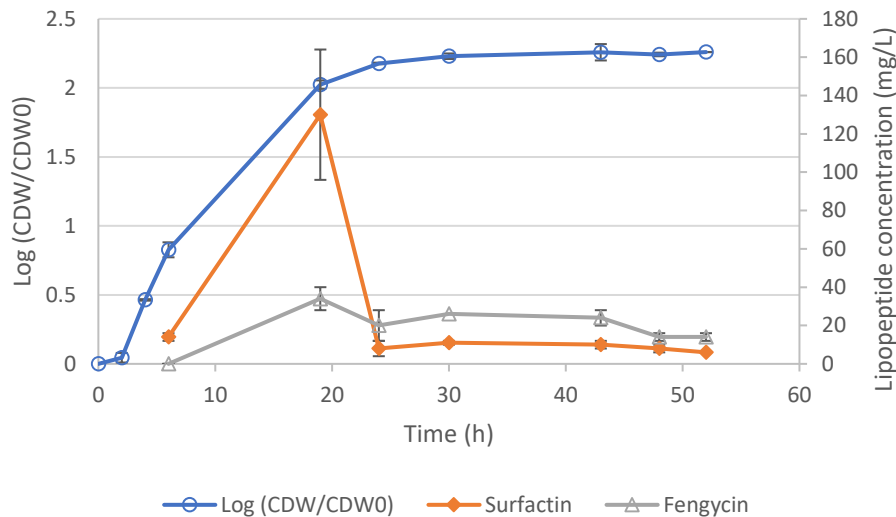


Figure 4-10: Graph illustrating the growth (open circles, left hand axis, log (CDW/CDW₀)) and lipopeptide production (surfactin – closed diamonds, right hand axis, in mg/L; fengycin – open triangles, right hand axis, in mg/L) of *B. subtilis* over time in a culture containing ammonium as the sole nitrogen source in shake flasks at 150 rpm and 30 °C.

4.1.2 Comparison of growth and substrate utilisation patterns of *B. subtilis* in cultures containing NH₄⁺ and NO₃⁻ as nitrogen sources at discrete NH₄-N:NO₃-N ratios

Figure 4-11 compares the growth profiles of *B. subtilis* associated with each of the nitrogen source ratios investigated. A similar basic trend was observed for all the growth curves; however, these curves differ from each other with respect to the slope of the exponential phase and the point where the cultures entered the stationary phase. Figure 4-11 shows that the nitrogen source ratio also affected the duration of exponential growth, which is especially evident from the culture that only contained nitrate as a nitrogen source where exponential growth only ceased after 43 h compared to 19 h for the culture that only contained ammonium as a nitrogen source. In nitrate-rich cultures, nitrate acts as an electron acceptor when oxygen becomes limiting thus extending the period of active growth. When nitrate was absent, growth ceased when oxygen became limiting as no nitrate was available to act as an alternative electron acceptor.

It can be seen in Figure 4-11 that after 6 h, the culture that contained nitrate as the sole nitrogen source, grew slower compared to the other nitrogen source ratios and took longer to reach the stationary phase. This was not surprising since nitrate is a less accessible nitrogen source compared to ammonium because it first needs to be converted to ammonia to be metabolised as a nitrogen source by *B. subtilis* (see section 1.3.1.2). Furthermore, since this culture contained no ammonium, nitrate served a dual purpose; it acted as a nitrogen source and acted as an alternative electron acceptor when oxygen became limiting, which consequently reduced the available nitrogen for growth and biosurfactant production.

Furthermore Figure 4-11 shows that it takes longer for the cultures to reach the stationary phase as the fraction of nitrogen from nitrate is increased. This is because nitrate acts as an alternative electron acceptor under oxygen-limiting conditions. The nitrate utilisation curves (Figure 4-14) indicates that oxygen became limiting between 6 and 19 h as nitrate utilisation was either constant or very slow during the first 6 h growth and then increased between 6 and 19 h, whilst ammonium was still in excess (Figure 4-15). Thus, by having a higher nitrate concentration it possible to extend the active growth phase even if oxygen-limitation occurs, given that all other nutrients are still in excess.

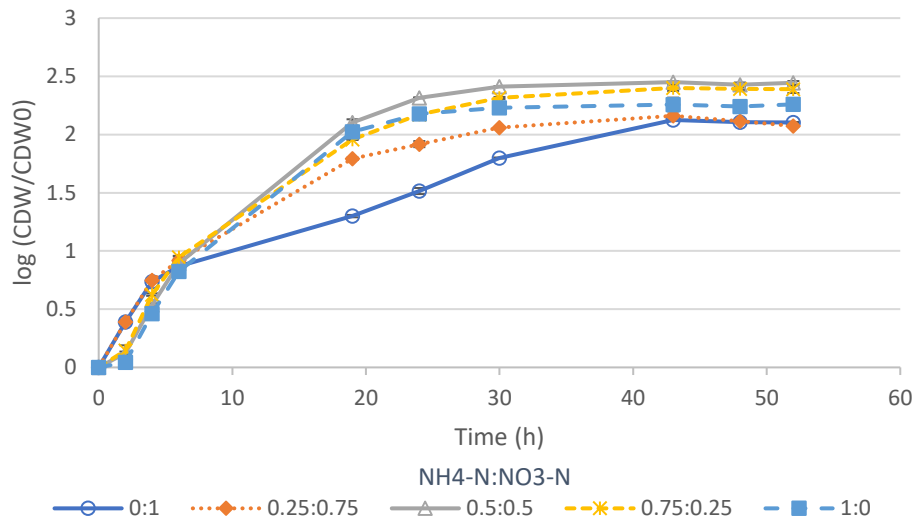


Figure 4-11: Comparison of the growth in $\log(\text{CDW}/\text{CDW}_0)$ of *B. subtilis* over time in cultures containing NH_4^+ and NO_3^- at discrete $\text{NH}_4\text{-N}:\text{NO}_3\text{-N}$ ratios as nitrogen sources in shake flasks at 150 rpm and 30 °C.

μ_{max} increased from 0.425 to 0.461 h^{-1} as the fraction of nitrogen from ammonium was increased from 0 to 0.75 and decreased to 0.45 h^{-1} for the culture that only contained ammonium as a nitrogen source. The small differences in μ_{max} for the different nitrogen source ratios indicated that nitrogen source ratio did not have a significant effect on μ_{max} as shown in Table 4-1.

The effect of the nitrogen source ratio on CDW (Figure 4-12) was similar to its effect on μ_{max} , however the effect on CDW was much more significant as shown in Figure 4-12. CDW increased from 13.2 to 19.5 g/L as the fraction of nitrogen from ammonium was increased from 0 to 0.75 and then decreased to 13.4 g/L for the culture that only contained ammonium as a nitrogen source. The increase in CDW with an increasing fraction nitrogen from ammonium was expected since ammonium is the preferred nitrogen source during aerobic growth. The low CDW of the culture that only contained ammonium as a nitrogen source resulted from oxygen-limited growth because no nitrate was present to act as an alternative electron acceptor when oxygen was depleted.

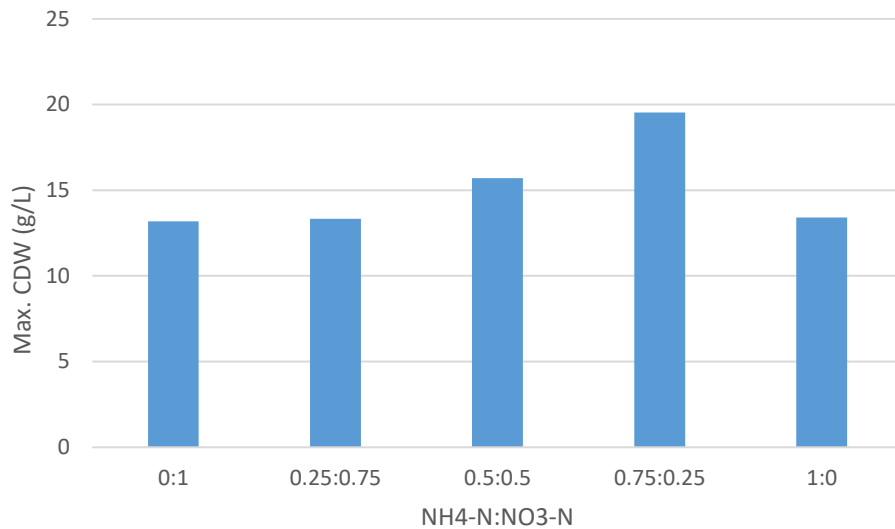


Figure 4-12: Comparison of the maximum CDW (in g/L) of *B. subtilis* in cultures containing NH₄⁺ and NO₃⁻ at discrete NH₄-N:NO₃-N ratios as nitrogen sources in shake flasks at 150 rpm and 30 °C.

The glucose utilisation patterns for the different nitrogen source ratios are compared in Figure 4-13. Glucose utilisation started immediately after inoculation for all the nitrogen source ratios and was consumed at a nearly constant rate until it was either depleted or utilisation ceased due to limitations caused by other nutrients. Glucose was depleted for all the nitrogen source ratios, except for the 0.75:0.25 nitrogen source ratio and the culture that contained only ammonium as a nitrogen source. Glucose utilisation for these ratios ceased due to nitrate being depleted or being absent in the respective cultures. Figure 4-13 shows that the glucose consumption rate increased as the fraction of nitrogen from ammonium increased. This was expected since cell concentration increased with an increasing fraction of nitrogen from ammonium resulting in higher glucose consumption.

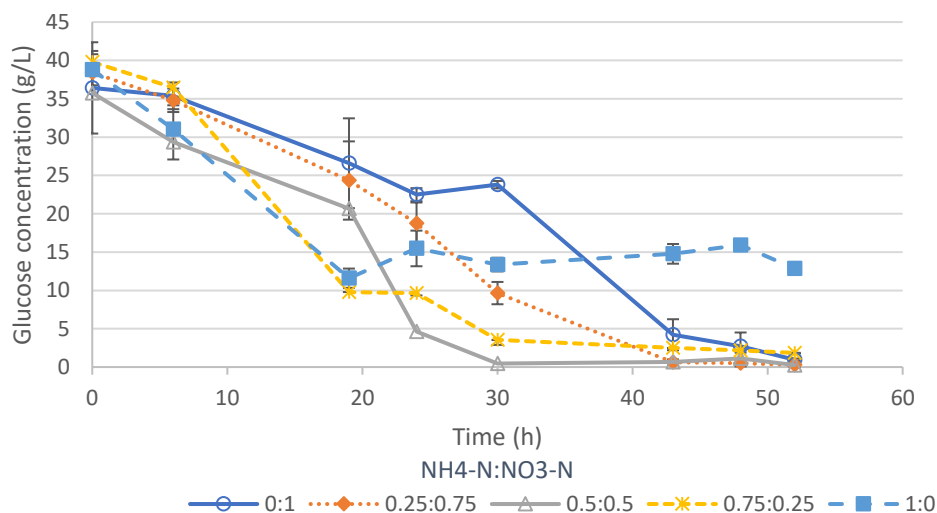


Figure 4-13: Comparison of glucose utilisation by *B. subtilis* in cultures containing NH₄⁺ and NO₃⁻ at discrete NH₄-N:NO₃-N ratios as nitrogen sources in shake flasks at 150 rpm and 30 °C.

The nitrate utilisation patterns for the different nitrogen source ratios are compared in Figure 4-14. In the culture that only contained nitrate as a nitrogen source nitrate utilisation started immediately after inoculation and was consumed at a nearly constant rate until utilisation ceased at 43 h. The immediate consumption of nitrate was expected since nitrate was the only nitrogen source present in the culture medium. For the rest of the nitrogen source ratios, nitrate utilisation only started between 6 and 19 h when oxygen became limiting and nitrate was consumed as an alternative electron acceptor. In the cases where there was no ammonium or where ammonium was depleted, nitrate acted as both a nitrogen source, by first being converted to ammonia, as well as an electron acceptor when oxygen limitation occurred (Figure 1-5). Nitrate was not completely consumed in the cultures containing a higher fraction of nitrogen from nitrate ($\text{NH}_4\text{-N}:\text{NO}_3\text{-N} = 0:25:0.75$ and $0:1$). Figure 4-13 and 4-15 shows that nitrate utilisation ceased when glucose was depleted or reached very low concentrations. Nitrate was completely consumed for all other nitrogen source ratios.

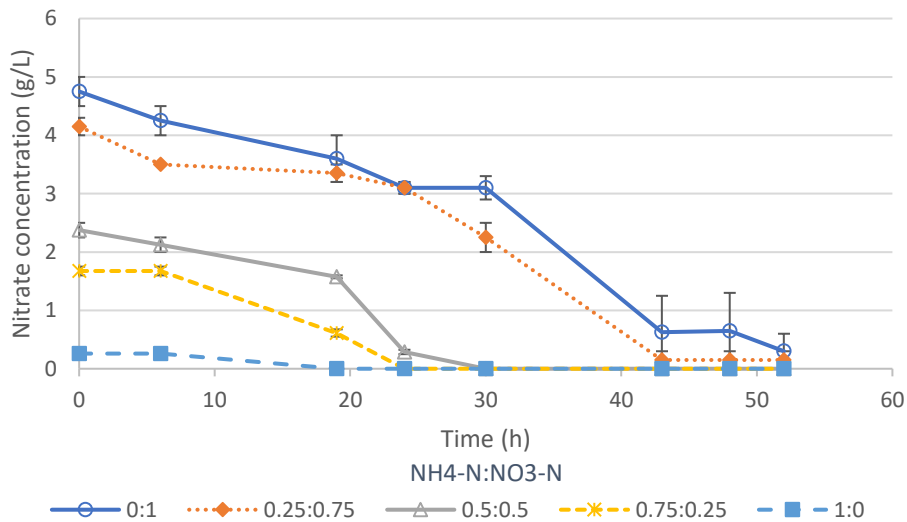


Figure 4-14: Comparison of nitrate utilisation by *B. subtilis* in cultures containing NH_4^+ and NO_3^- at discrete $\text{NH}_4\text{-N}:\text{NO}_3\text{-N}$ ratios as nitrogen sources in shake flasks at 150 rpm and 30 °C.

The ammonium utilisation patterns for the different nitrogen source ratios are compared in Figure 4-15. Ammonium consumption started immediately after inoculation for all the nitrogen source ratios. A similar ammonium utilisation trend was observed for all the nitrogen source ratios; ammonium was consumed at a nearly constant rate until it either became depleted or consumption ceased due to another nutrient being depleted. Ammonium was in excess for all the nitrogen source ratios that contained ammonium, except for the 0.25:0.75 ratio where ammonium was depleted after 19 h of growth. Ammonium consumption ceased when either glucose, oxygen, nitrate, or a combination of these nutrients were limiting.

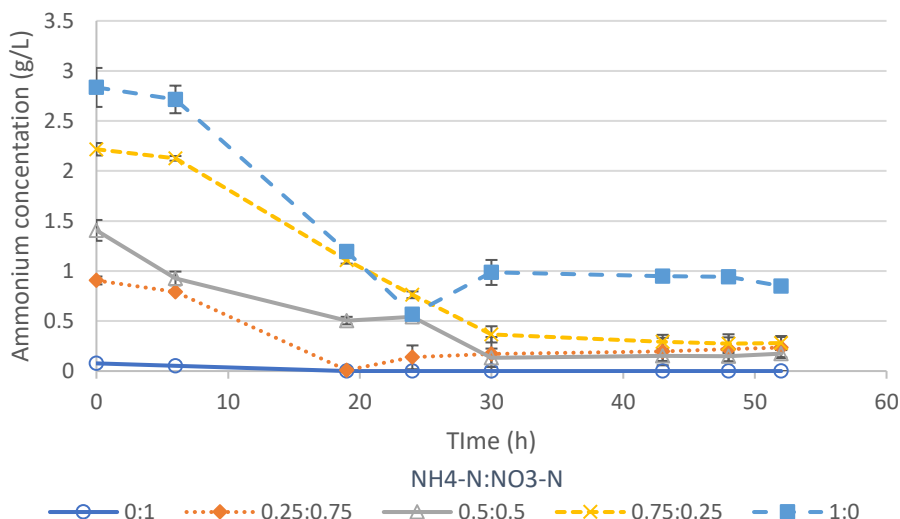


Figure 4-15: Comparison of ammonium utilisation by *B. subtilis* in cultures containing NH_4^+ and NO_3^- at discrete $\text{NH}_4\text{-N}:\text{NO}_3\text{-N}$ ratios as nitrogen sources in shake flasks at 150 rpm and 30 °C.

4.1.3 Comparison of lipopeptide production patterns of *B. subtilis* in cultures containing NH_4^+ and NO_3^- as nitrogen sources at discrete $\text{NH}_4\text{-N}:\text{NO}_3\text{-N}$ ratios

The surfactin production patterns for the different nitrogen source ratios are compared in Figure 4-16. The concentration of surfactin at the start of the experimental runs were assumed to be 0 since no samples were taken for surfactin analysis immediately after inoculation. This is a reasonable assumption given the low concentrations (< 51 mg/L) of surfactin at 6 h for the different nitrogen source ratios. Surfactin production was slow during the first 6 h of cultivation. The surfactin production rate then rapidly increased after 6 h for all nitrogen source ratios except the culture that only contained nitrate as a nitrogen source. The nitrate-only culture only reached its maximum production rate after 19 h of cultivation.

Depending on the nitrogen source ratio, the concentration of surfactin then either plateaued or plummeted at the point of maximum surfactin concentration. The decrease in surfactin concentration was only observed for cultures where the fraction of nitrogen from ammonium was above 0.5. The decrease in surfactin concentration observed for these cultures can be ascribed to the pH dropping below 5.0, which causes surfactin to precipitate from solution. The consumption of ammonium causes a decrease in pH which is counteracted by the simultaneous consumption of nitrate, however when the fraction of nitrogen from ammonium was above 0.5, the concentration of nitrate was too low to maintain a pH above 5.0, hence causing surfactin to precipitate. The secretion of organic acids, induced by nutrient limitation, may also have contributed to rapid decrease in pH and consequent precipitation of surfactin.

Surfactin production (Figure 4-16) was most rapid during the period of active growth (Figure 4-11) which also coincided with the period of rapid ammonium utilisation (Figure 4-15) and oxygen limitation (implicit from Figure 4-14 and Figure 4-15). Surfactin production was promoted by oxygen limitation due to the competitive nature of *B. subtilis* under nutrient limiting conditions. *B. subtilis* produces surfactin, which has antimicrobial properties (as discussed in section 1.2.2.4), as a secondary metabolite in order to eliminate competition to secure its survival under oxygen limiting conditions.

Surfactin production ceased when the cultures entered the stationary phase for all nitrogen ratios. The fraction of nitrogen from ammonium had a significant effect on the rate at which surfactin was produced. Surfactin production rate increased as the fraction of nitrogen from ammonium increased from 0 to 0.5 and decreased for higher fractions of nitrogen from ammonium. The decrease in surfactin production rate of the cultures with a lower fraction nitrogen from ammonium ($\text{NH}_4\text{-N}:\text{NO}_3\text{-N} = 0.25:0.75$ and $0:1$) resulted from ammonium being depleted in these cultures and nitrate being utilised as a nitrogen source following ammonium depletion. Nitrate is a less accessible nitrogen source compared to ammonium because it first needs to be converted to ammonia before it is utilised by the cells, hence reducing both the growth and surfactin production rates. This was especially evident in the culture that contained no ammonium, where surfactin only reached its maximum production rate after 19 h compared to 6 h for the cultures that contained ammonium.

The culture that contained only ammonium as a nitrogen source had the poorest performance in terms of surfactin production, only reaching a maximum concentration of 130 mg/L. The poor performance of this culture most likely resulted from oxygen limitation during the early growth stages since the culture contained no nitrate to act as an alternative electron acceptor under oxygen-limiting conditions. The culture that contained equal fractions of nitrogen from ammonium and nitrate (0.5:0.5) achieved the highest surfactin concentration (1084 mg/L). The maximum concentration was reached after 30 h of cultivation which coincided with the time glucose and nitrate became depleted (Figure 4-13 and Figure 4-14). The 0:1, 0.25:0.75 and 0.75:0.25 nitrogen ratios reached similar surfactin concentrations: 716, 637, and 604 mg/L respectively; however, each had significantly different productivities as shown in Table 4-1. Productivity increased with an increased fraction of nitrogen from ammonium.

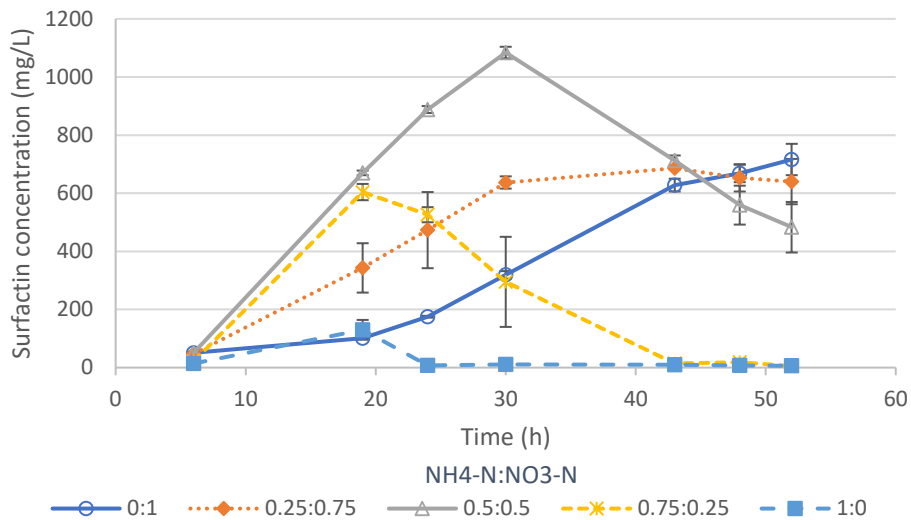


Figure 4-16: Comparison of surfactin production by *B. subtilis* in cultures containing NH_4^+ and NO_3^- at discrete $\text{NH}_4\text{-N}:\text{NO}_3\text{-N}$ ratios as nitrogen sources in shake flasks at 150 rpm and 30 °C.

B. subtilis is known to produce several homologues of surfactin. Six peaks, corresponding to different surfactin homologues were identified from the HPLC chromatograms. These peaks were named Surfactin 1-6 with peaks 5 and 6 grouped together for analysis as these peaks were too close together to be analysed separately. The homologue distributions (homologue concentration/total surfactin concentration) for the different nitrogen source ratios are shown in Figure 4-17, and as can be seen from the figure, the nitrogen source ratio did not have a significant effect on the homologue distribution. Surfactin 3 was the most abundant homologue, followed by Surfactin 5 and 6 which had a concentration that was approximately equal to that of Surfactin 3. Surfactin 2 and 4 were produced in approximately equal proportions with Surfactin 2 being slightly more than Surfactin 4. Surfactin 1 was the least abundant homologue. Further analysis of the homologues and their relative antimicrobial efficacies is recommended.

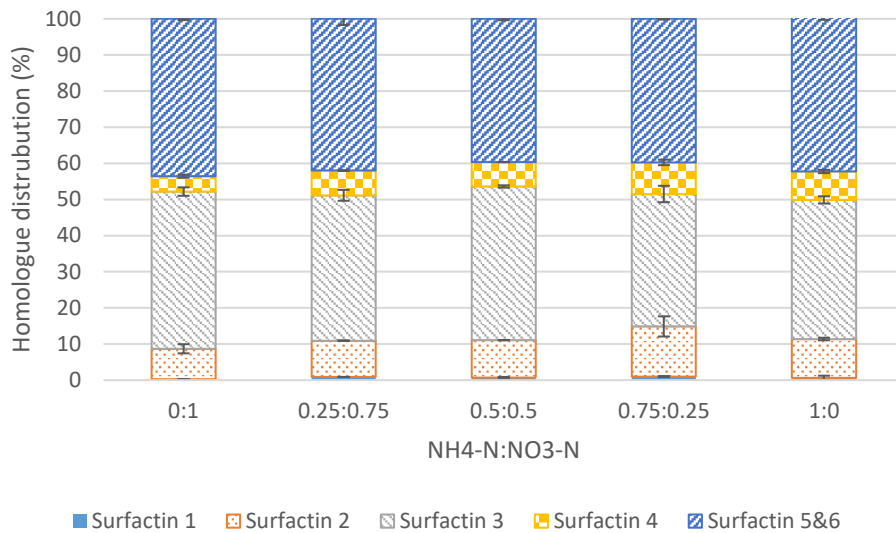


Figure 4-17: Comparison of the homologous distribution of surfactin produced by *B. subtilis* in cultures containing NH_4^+ and NO_3^- at discrete $\text{NH}_4\text{-N}:\text{NO}_3\text{-N}$ ratios as nitrogen sources in shake flasks at 150 rpm and 30 °C.

The fengycin production patterns for the different nitrogen source ratios are presented in Figure 4-18. Generally, fengycin production started towards the end of the exponential growth phase which coincided with the period of rapid nitrate utilisation. Fengycin production for the nitrate-only culture (1:0) and the 0.25:0.75 nitrogen source ratio started much later than the rest of the nitrogen ratios where fengycin production started after 6 h of cultivation. This can be attributed to ammonium being depleted during the early stages of growth and nitrate being utilised as a nitrogen source following ammonium depletion. Nitrate is a less accessible source of nitrogen as it first needs to be converted to ammonia for it to be utilised by the cells, hence delaying the production of fengycin. Fengycin production started after 19 h for the 0.25:0.75 nitrogen source ratio and 30 h for the nitrate-only culture.

The maximum fengycin concentration increased as the fraction nitrogen from nitrate was increased from 0 to 1. The ammonium-only culture (1:0) had the lowest maximum fengycin concentration (34 mg/L) due to oxygen-limited growth in the absence of nitrate. Unlike surfactin, the nitrate-only culture had the highest fengycin concentration (582 mg/L). It can thus be concluded that fengycin production is favoured by oxygen limitation and high nitrate concentrations. Having ammonium present in the medium reduces the time it takes for fengycin production to start, hence increasing fengycin productivity.

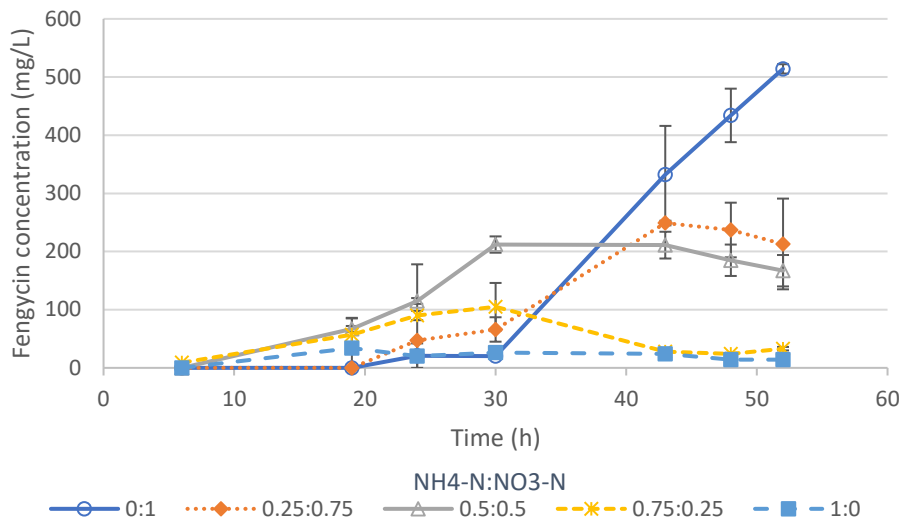


Figure 4-18: Comparison of fengycin production by *B. subtilis* in cultures containing NH_4^+ and NO_3^- at discrete $\text{NH}_4\text{-N:NO}_3\text{-N}$ ratios as nitrogen sources in shake flasks at 150 rpm and 30 °C.

4.1.4 Comparison of growth and lipopeptide associated kinetic parameters of *B. subtilis* in cultures containing NH_4^+ and NO_3^- as nitrogen sources at discrete $\text{NH}_4\text{-N:NO}_3\text{-N}$ ratios

Various kinetic parameters were used to evaluate the performance of the different nitrogen source ratios in terms of growth and lipopeptide production. These parameters are summarised in Table 4-1. The equations used to calculate the kinetic parameters are given in Appendix B. Since this study was focused on surfactin production, all kinetic parameters were evaluated at the time where surfactin concentration reached a maximum (Table 4-1). The kinetic parameters were normalised relative to the parameter with the maximum value for ease of comparison and the results are presented graphically in Figure 4-19.

Table 4-1: Summary of *B. subtilis* growth and lipopeptide related kinetic parameters in cultures containing NH_4^+ and NO_3^- at discrete $\text{NH}_4\text{-N}:\text{NO}_3\text{-N}$ ratios as nitrogen sources in shake flasks at 150 rpm and 30 °C.

Kinetic Parameters	NH ₄ -N:NO ₃ -N				
	0:1	0.25:0.75	0.5:0.5	0.75:0.25	1:0
Time at max surfactin conc. (h)	52	30	30	19	19
μ_{max} (h^{-1})	0.425	0.430	0.443	0.461	0.450
CDW (g/L)	12.564	10.565	14.377	7.036	7.721
$Y_{x/s}$ (g/g)	0.352	0.364	0.406	0.232	0.281
<u>Surfactin</u>					
Surfactin concentration (mg/L)	716	637	1084	604	130
$Y_{p/s}$ (g/g)	0.020	0.022	0.031	0.020	0.005
$Y_{p/x}$ (g/g)	0.057	0.061	0.076	0.087	0.017
Productivity (mg/L/h)	13.769	21.233	36.133	31.789	6.842
<u>Fengycin</u>					
Fengycin concentration (mg/L)	514	66	212	57	34
$Y_{p/s}$ (g/g)	0.014	0.002	0.006	0.002	0.001
$Y_{p/x}$ (g/g)	0.041	0.006	0.015	0.008	0.004
Productivity (mg/L/h)	9.885	2.200	7.067	3.000	1.789
Selectivity (S/F) [g/g]	1.393	9.652	5.113	10.596	3.824

The cell and lipopeptide yields per unit substrate (glucose) consumed are expressed as the kinetic parameters $Y_{x/s}$ and $Y_{p/s}$ (p is either surfactin or fengycin) in Figure 4-19. These parameters are an indication of how effectively the substrate was utilised for cell and lipopeptide production respectively. The specific lipopeptide production (lipopeptide yield per gram cells) is expressed as the kinetic parameter $Y_{p/x}$ (p is either surfactin or fengycin) in Figure 4-19. $Y_{p/x}$ is a representation of the cells capacity to produce lipopeptides and is an important parameter to consider when evaluating the optimum conditions for lipopeptide production. A high value of $Y_{p/x}$ indicates that the cells had a high capacity for lipopeptide production under those conditions. Productivity in Figure 4-19 is an indication of the rate at which the lipopeptide was produced. Since *B. subtilis* produces more than one lipopeptide family, selectivity also becomes an important parameter to consider when evaluating the optimum conditions for surfactin production. Selectivity is expressed as the ratio of surfactin to fengycin (S/F) (since iturin concentration was disregarded because of low concentrations) in Figure 4-19.

The culture that contained equal fractions of nitrogen from ammonium and nitrate exhibited the most efficient use of substrate for cellular production expressed by the highest $Y_{x/s}$ value in Figure 4-19. $Y_{x/s}$ increased as the fraction of nitrogen from ammonium increased from 0 to 0.5 and decreased for higher fractions of nitrogen from ammonium. $Y_{x/s}$ for the culture that contained ammonium as the sole nitrogen source was higher than that of the 0.75:0.25 nitrogen source ratio. This was due to the high residual glucose concentration in the ammonium-only culture that resulted from oxygen-limited growth (Figure 4-9).

The highest surfactin concentration was achieved in the culture that had equal fractions of nitrogen from ammonium and nitrate ($\text{NH}_4\text{-N}:\text{NO}_3\text{-N} = 0.5:0.5$) followed by the culture that only contained nitrate as a nitrogen source. The culture that only contained ammonium as a nitrogen source had the lowest surfactin concentration. In all cases oxygen became depleted and nitrate was utilised as an alternative electron acceptor. Surfactin production ceased when either glucose or nitrate were depleted. In the case of the ammonium-only culture, no nitrate was present to act as an electron acceptor causing oxygen to limit growth and lipopeptide production thus explaining the low surfactin yield.

The same trend was observed for $Y_{p/s, \text{surfactin}}$ and surfactin productivity. The highest values for both these parameters were observed in the culture that contained equal fractions of nitrogen from ammonium and nitrate. $Y_{p/s, \text{surfactin}}$ and surfactin productivity increased as the fraction of nitrogen from ammonium was increased from 0 to 0.5 and decreased for higher fractions of nitrogen from ammonium. The culture that contained equal fractions of nitrogen from ammonium and nitrate thus provided the optimum conditions in terms of surfactin production rate and substrate utilisation for surfactin production.

The 0.75:0.25 nitrogen source ratio had the highest $Y_{p/x, \text{surfactin}}$. $Y_{p/x}$ increased as the fraction of nitrogen from ammonium was increased from 0 to 0.75. The culture that contained ammonium had the lowest $Y_{p/x}$ due to the growth limitation caused by oxygen in the absence of nitrate.

Selectivity is an important parameter to consider when an organism such as *B. subtilis* produces more than one lipopeptide family as it will affect the number of downstream processing steps required and consequently affect the downstream processing costs. By maximising the selectivity upstream, it is possible to reduce the downstream processing costs. Figure 4-19 shows that the nitrogen source ratio had a significant effect on the selectivity of lipopeptides produced by *B. subtilis* as seen by the large differences in selectivity (S/F) exhibited by the different nitrogen source ratios. Selectivity was the lowest in the culture that contained nitrate as the sole nitrogen source where surfactin and fengycin was produced in nearly equal proportions. For all other nitrogen source ratios surfactin accounted for 84-91% of the total lipopeptides produced. The 0.75:0.25 nitrogen source ratio had the highest surfactin selectivity (S/F) followed by the 0.25:0.75 ratio. The culture that contained equal fractions of nitrogen from ammonium and nitrate had a surfactin selectivity that was nearly half of that of the 0.75:0.25 nitrogen source ratio.

The same trend was observed for all the kinetic parameters related to fengycin. All the kinetic parameters were maximised in the culture that only contained nitrate as a nitrogen source. This result is not surprising as fengycin production took place during the period where rapid nitrate utilisation occurred; the high concentration of nitrate extended the period of nitrate utilisation which allowed fengycin to reach a higher concentration. Except for the 0.25:0.75 nitrogen source ratio, all the kinetic parameters related to fengycin increased as the fraction of nitrogen from nitrate was increased.

Ideally the optimum nitrogen source ratio would be the one that maximises all the kinetic parameters related to the lipopeptide of interest, which in this case is surfactin. However, in the case of surfactin the 0.5:0.5 nitrogen source ratio maximised surfactin concentration, $Y_{p/s}$, and productivity but not $Y_{p/x}$ and selectivity. $Y_{p/x}$ and selectivity were maximised by the 0.75:0.25 nitrogen source ratio. The 0.5:0.5 ratio yielded a surfactin concentration that was nearly two times higher than that of the 0.75:0.25 nitrogen source ratio and had a $Y_{p/x}$ similar to that of the 0.75:0.25 ratio. Based on this evaluation, and the fact that surfactin is a low-volume high-value product, the 0.5:0.5 ratio is the most preferable nitrogen source ratio for surfactin production. The culture that contained nitrate as the sole nitrogen source provided the optimum conditions for fengycin production by *B. subtilis* as it maximised all the fengycin related kinetic parameters.

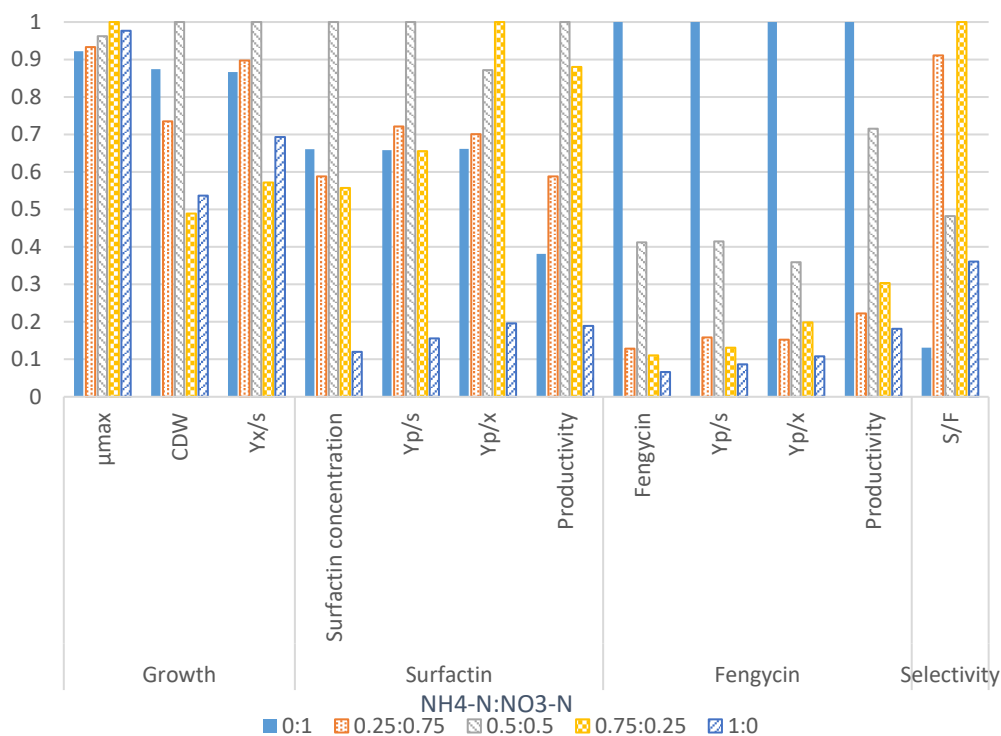


Figure 4-19: Comparison of normalised growth and lipopeptide related kinetic parameters of *B. subtilis* at maximum surfactin concentration in cultures containing NH_4^+ and NO_3^- at discrete $NH_4-N:NO_3-N$ ratios as nitrogen sources in shake flasks at 150 rpm and 30 °C.

4.2 THE EFFECT OF MANGANESE CONCENTRATION ON GROWTH AND LIPOPEPTIDE PRODUCTION KINETICS OF *B. SUBTILIS* IN SHAKE FLASKS

Several studies have reported the positive effect of manganese on surfactin production by *B. subtilis* (this is discussed in depth in section 1.3.1.3). Wei and Chu (2002) investigated the effect of manganese concentration on surfactin production for Mn^{2+} concentrations ranging from 0 to 0.5 mM and the authors reported that an optimum Mn^{2+} concentration of 0.01 mM increased surfactin concentration to 2600 mg/L compared to 330 mg/L surfactin produced in a culture that contained no Mn^{2+} . Huang *et al.* (2015) found that surfactin concentration increased to 1500 mg/L when the manganese concentration was increased from 0.001 to 0.1 mM. The authors also reported that increasing the manganese concentration improved the ammonium nitrate utilisation rates. Although both studies agreed on the positive effect of manganese on surfactin production, there was a 10-fold difference in the optimum Mn^{2+} concentration reported by the two studies.

Due to the discrepancy in the results from two studies, and the apparent importance of the parameter, the effect of manganese concentration on surfactin production and nitrogen utilisation was studied in shake flasks. Manganese concentrations ranging from 0 to 0.1 mM was investigated using the medium as defined in Table 3-1. All experiments were conducted in duplicate shake flasks and the results presented in this section are based on the averages from the duplicate experiments. Error bars are used to show the standard deviation between duplicate runs. The growth, substrate and lipopeptide production patterns are discussed in section 4.2.1 followed by a comparison of the growth and substrate utilisation patterns and related kinetic parameters (section 4.2.2) and lipopeptide production patterns and related kinetic parameters (section 4.2.3) for the different manganese concentrations.

4.2.1 Growth, substrate utilisation and lipopeptide production patterns of *B. subtilis* for cultures with different manganese concentrations

Similar growth and substrate utilisation patterns were observed for all the tested manganese concentrations. To avoid repetition, only the 0.1 mM concentration will be used to discuss the growth, substrate and lipopeptide production patterns. The growth, substrate utilisation and lipopeptide production patterns for the rest of the manganese concentrations were very similar and are shown in Appendix B, following a similar discussion as for 0.1 mM manganese.

The growth and substrate utilisation patterns for 0.1 mM manganese are shown in Figure 4-20. No lag phase was observed as the culture entered the exponential phase immediately after inoculation at a maximum specific growth rate of 0.48 h^{-1} . Exponential growth continued between 6 and 19 h, at a lower specific growth rate. Glucose was consumed at a constant rate immediately after inoculation and was depleted at 19 h.

Growth ceased at 19 h which coincided with glucose depletion, thus glucose was the growth limiting nutrient as both ammonium and nitrate was still in excess at this time. Ammonium was consumed at a nearly constant rate immediately after inoculation and consumption ceased at 19 h when glucose was depleted. Nitrate concentration remained constant during the first 6 h of growth after which it was consumed rapidly whilst ammonium was still in excess, suggesting that oxygen-limitation occurred during this period. The decrease in growth rate between 6 and 19 h was due to oxygen depletion and nitrate being utilised as an alternative electron acceptor. Nitrate consumption decreased after glucose was depleted at 19 h and ceased at 30 h. No stationary phase was observed for 0.1 mM manganese as cell concentration started dying immediately after glucose was depleted at 19 h.

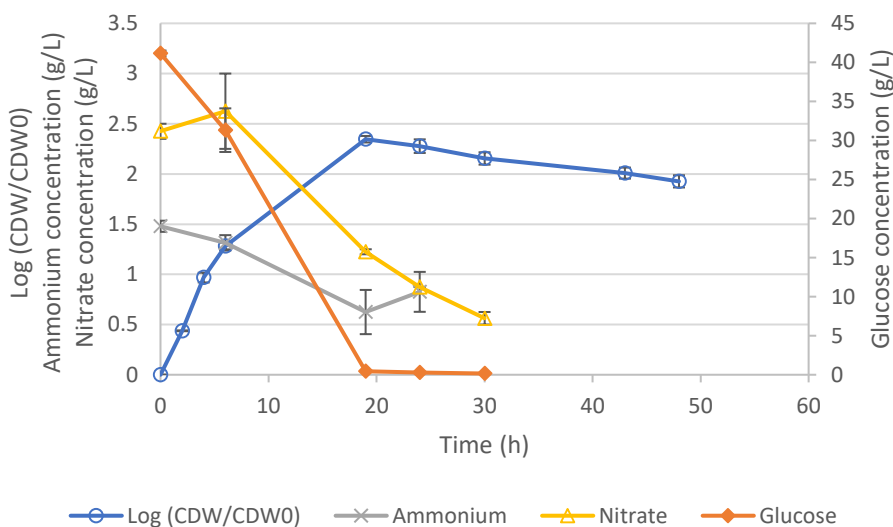


Figure 4-20: Graph illustrating the growth (open circles, left hand axis, in log (CDW/CDW₀)) of *B. subtilis* and substrate concentrations of nitrate (open triangles, left hand axis, in g/L), ammonium (crosses, left hand axis, in g/L) glucose (closed diamonds, right hand axis, in g/L) for a culture containing 0.1 mM Mn²⁺ and 4 g/L NH₄NO₃ as a nitrogen source in shake flasks at 150 rpm and 30 °C.

The growth and lipopeptide production patterns for 0.1 mM manganese are shown in Figure 4-21. Surfactin production was slow during the first 6 h of growth and then increased rapidly between 6 and 19 h, reaching a maximum concentration of 884 mg/L at 19 h when glucose became limiting. Surfactin concentration remained constant between 19 and 43 h after which a decrease in the surfactin concentration was observed. Again, the decrease in surfactin concentration was most likely due to pH dropping below 5.0 causing surfactin to precipitate from the solution. Fengycin production also took place during the first 19 h of growth and reached a maximum concentration of 149 mg/L when glucose became limiting. All other tested Mn²⁺ concentrations exhibited the same key characteristics as shown in Appendix A.

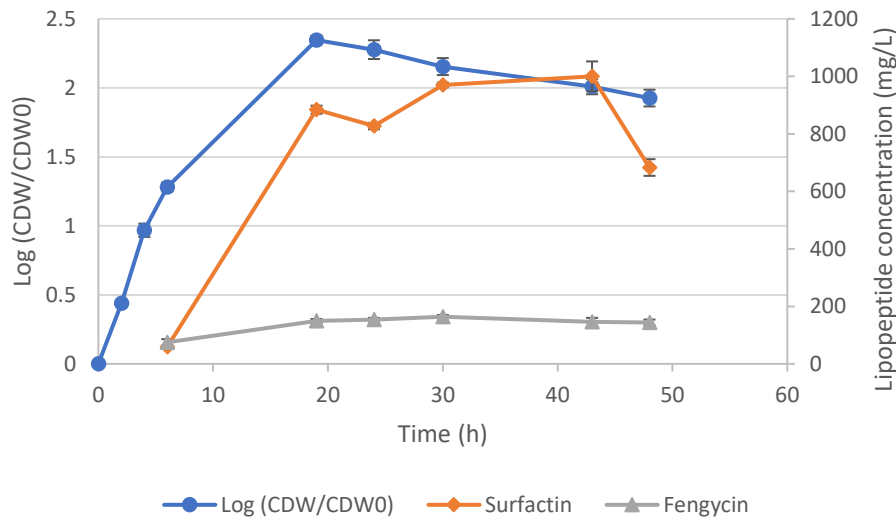


Figure 4-21: : Graph illustrating the growth (open circles, left hand axis, in log (CDW/CDW₀)) and lipopeptide production (surfactin – closed diamonds, right hand axis, in mg/L; fengycin – open triangles, right hand axis, in mg/L) of *B. subtilis* over time in a culture containing 0.1 mM Mn²⁺ and 4 g/L NH₄NO₃ in shake flasks at 150 rpm and 30 °C.

4.2.2 Comparison of growth and substrate utilisation patterns of *B. subtilis* cultures containing different manganese concentrations

Figure 4-22 shows a comparison of the growth profiles associated with different manganese concentrations. No significant difference was observed in the growth profiles for the different manganese concentrations; all the cultures entered the exponential phase immediately after inoculation and growth ceased after 19 h of cultivation which coincided with glucose depletion. A decrease in cell concentration was observed after 19 h for 0.05 and 0.01 mM manganese. Cell concentration remained constant after 19 h for all other manganese concentrations. A similar observation was made by Huang *et al.* (2015) who observed a decrease in cell concentration.

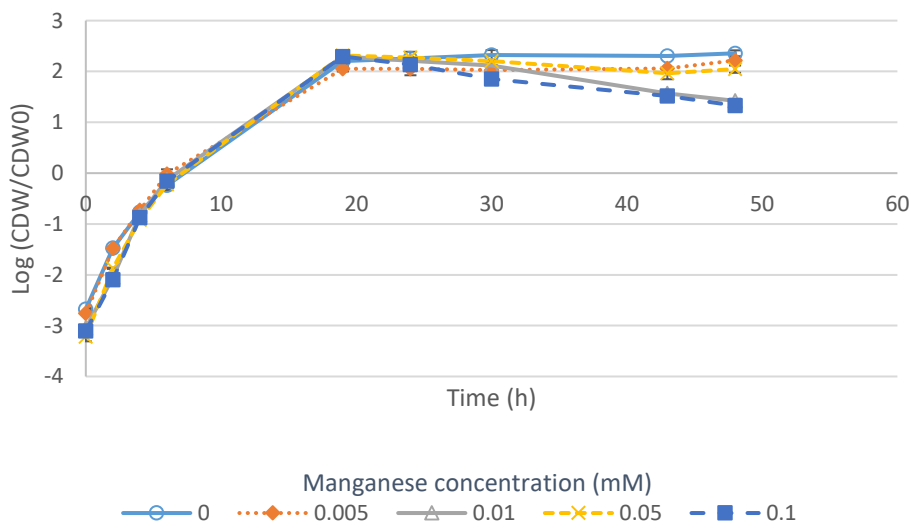


Figure 4-22: Comparison of the growth (in log (CDW/CDW₀)) of *B. subtilis* in cultures containing different Mn²⁺ concentrations and 4 g/L NH₄NO₃ in shake flasks at 150 rpm and 30 °C.

The glucose utilisation profiles for the different manganese concentrations are shown in Figure 4-23. All the manganese concentrations followed the same glucose utilisation pattern; glucose was consumed at a constant rate immediately after inoculation until it was depleted at 19 h. All other nutrients were still in excess at the time glucose became depleted, thus glucose was the growth limiting nutrient as cell growth ceased following glucose depletion.

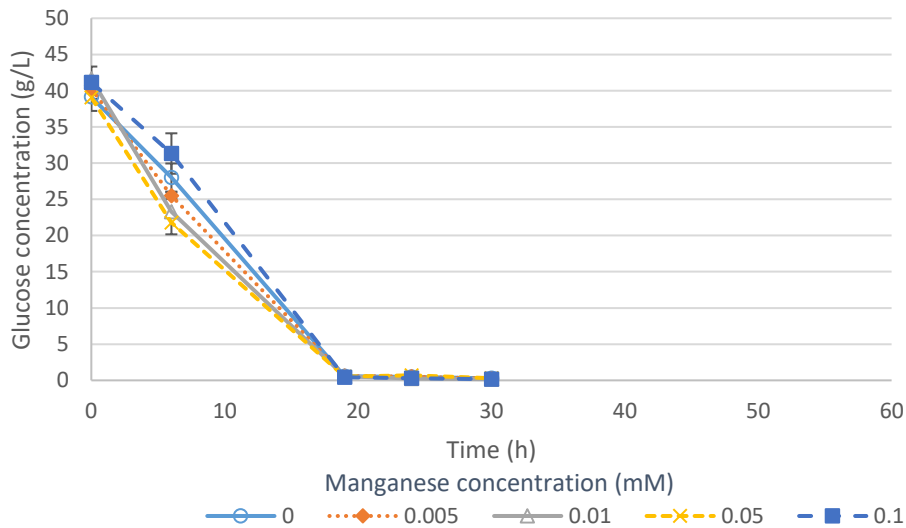


Figure 4-23: Comparison of glucose utilisation by *B. subtilis* in cultures containing different Mn²⁺ concentrations and 4 g/L NH₄NO₃ in shake flasks at 150 rpm and 30 °C.

The same trend was observed for ammonium utilisation for the different manganese concentrations shown in Figure 4-24. Ammonium was consumed at a nearly constant rate immediately after inoculation and consumption ceased after 19 h of cultivation when glucose became depleted. Figure 4-24 shows a slight increase in the ammonium concentration at 24 h for all manganese concentrations except for the culture that contained no manganese. The error bars in Figure 4-24 indicate that the increase in ammonium concentration at 24 h was most likely due to the sensitivity of the method used to measure the ammonium concentration.

Ammonium was in excess for all the tested manganese concentrations. Ammonium consumption was the highest for the culture that contained no manganese with only 0.18 g/L ammonium remaining after 19 h of growth. Ammonium consumption was similar for the cultures that contained manganese with 0.47 – 0.62 g/L ammonium remaining after 19 h of cultivation. The higher ammonium consumption in the culture that contained no manganese is in agreement with the findings of Huang *et al.* (2015) who reported a higher ammonium consumption for low manganese concentrations (< 0.005 mM).

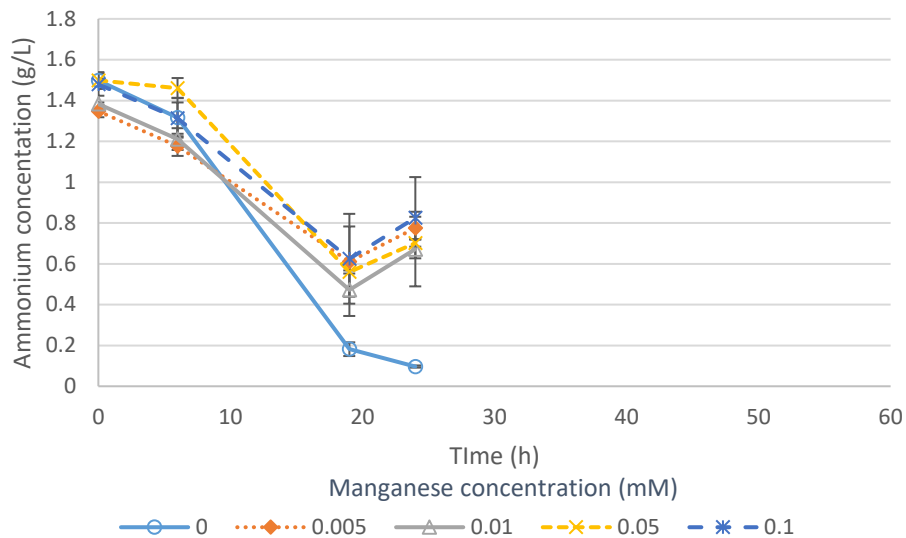


Figure 4-24: Comparison of ammonium utilisation of *B. subtilis* in cultures containing different Mn^{2+} concentrations and 4 g/L NH_4NO_3 in shake flasks at 150 rpm and 30 °C.

The same nitrate utilisation trend was observed for the different manganese concentrations (Figure 4-25). Nitrate concentration remained constant during the first 6 h of growth and was consumed at a nearly constant rate after 6 h until consumption ceased between 19 and 30 h following glucose depletion. Since ammonium was still in excess between 6 and 19 h, the consumption of nitrate during this period suggests that oxygen became depleted as nitrate is only utilised when either ammonium or oxygen is depleted. Nitrate thus acted as an alternative electron acceptor following oxygen depletion.

Nitrate consumption was lower for the cultures that had a low manganese concentration (<0.005 mM) than for those with higher manganese concentrations (>0.01 mM). Nitrate consumption was the same for manganese concentrations above 0.01 mM with approximately 0.56 g/L nitrate remaining after 30 h of cultivation. The culture that contained no manganese had 1.56 g/L nitrate remaining after 30 h whilst 1 g/L nitrate remained in the culture that contained 0.005 mM manganese. The higher nitrate consumption for manganese concentrations above 0.01 mM is in agreement with the findings of Huang *et al.* (2015) who made a similar observation. Huang *et al.* (2015) found that the higher nitrate consumption was due to an increase in nitrate reductase activity associated with an increase in manganese concentration.

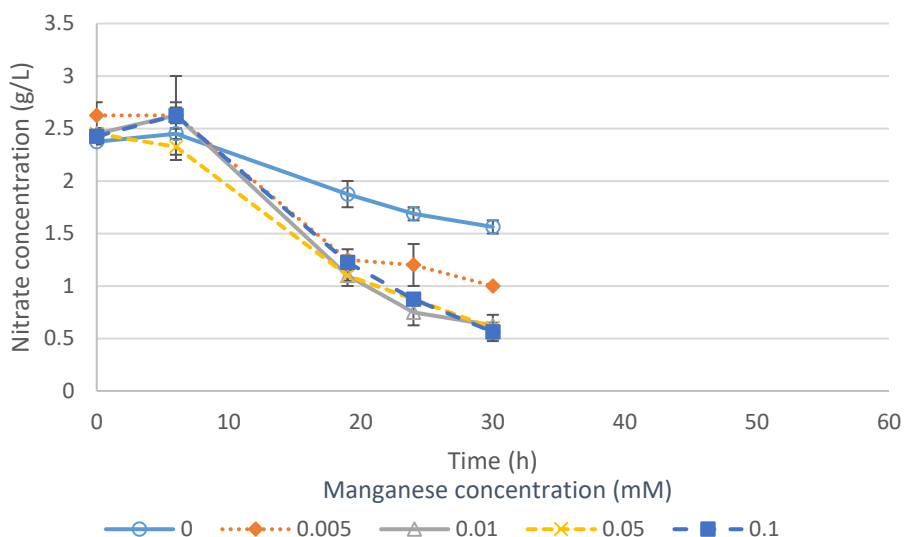


Figure 4-25: Nitrate utilisation comparison of *B. subtilis* for different Mn^{2+} concentrations in shake flasks

The growth-related kinetic parameters calculated at the time of maximum cell concentration for the different manganese concentrations are given in Table 4-2. These parameters were normalised for ease of comparison to evaluate the effect on manganese on cell growth and the results are presented graphically in Figure 4-26.

Table 4-2: Growth related kinetic parameters at maximum cell concentration for different Mn^{2+} concentrations

Kinetic Parameters	Manganese concentration (mM)				
	0	0.005	0.01	0.05	0.1
Time at max. CDW (h)	30	24	19	19	19
μ_{max} (h^{-1})	0.478	0.508	0.574	0.499	0.504
CDW (g/L)	10.237	9.238	10.266	9.909	9.923
$Y_{x/s}$ (g/g)	0.262	0.228	0.249	0.256	0.243

Figure 4-26 shows that the maximum specific growth rate (μ_{max}) increased for manganese concentrations up to 0.01 mM and decreased for higher manganese concentrations. μ_{max} increased from $0.478 h^{-1}$ in a culture that contained no manganese to $0.574 h^{-1}$ for 0.01 mM manganese. Similar growth rates were observed 0.05 and 0.1 mM manganese.

Varying the manganese concentration between 0 and 0.1 mM had no significant effect on the maximum cell concentrations as similar cell concentrations were observed at all the tested manganese concentrations as shown in Figure 4-26. The highest cell concentration (10.27 g/L) was observed in a culture that contained 0.01 mM manganese whilst the lowest cell concentration (9.24 g/L) was observed in the 0.005 mM manganese culture. This is in contrast with the findings of Huang *et al.* (2015) who found that manganese played a significant role in cell growth. The authors reported an 11.4-fold increase in cell concentration when the manganese concentration was increased from 0 to 0.005 mM. Manganese concentration was found to significantly affect μ_{max} .

μ_{\max} increased from 0.48 h^{-1} in a culture devoid of manganese to a maximum of 0.57 h^{-1} in a culture containing 0.01 mM manganese.

Cell yield per gram substrate ($Y_{x/s}$) was the highest in the culture that contained no manganese (0.262) followed by 0.05 mM manganese (0.256) and 0.01 mM manganese (0.249) and the lowest for 0.005 mM manganese (0.228). Based on the results in Figure 4-26, a manganese concentration of 0.01 mM was optimal for cell growth since it had yielded the highest μ_{\max} and cell concentration and had a high yield of cells per gram substrate (>0.95).

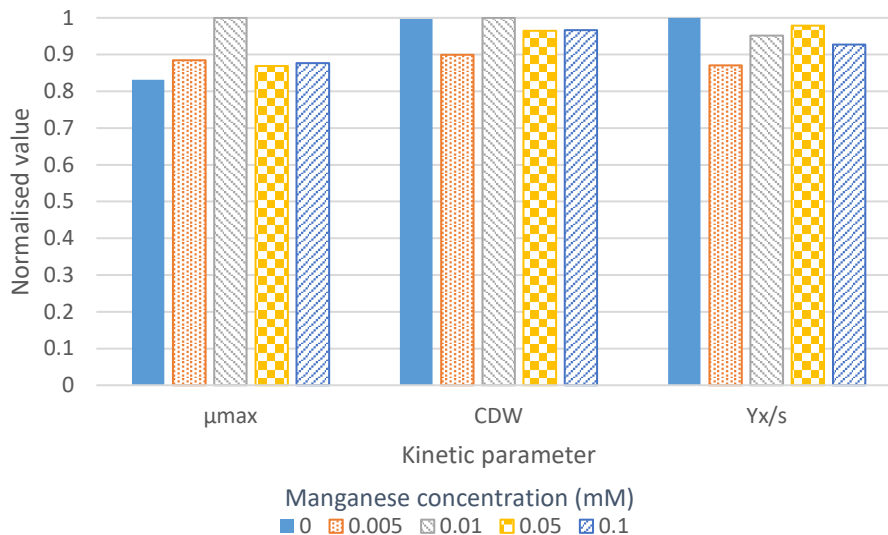


Figure 4-26: Comparison of normalised growth related kinetic parameters at maximum cell concentration for different Mn^{2+} concentrations

4.2.3 Comparison of lipopeptide production patterns of *B. subtilis* in cultures with different manganese concentrations

The surfactin production profiles for the different manganese concentrations are compared in Figure 4-27. Surfactin concentration increased rapidly between 6 and 19 h and reached a maximum concentration at 19 h for all tested manganese concentrations due to glucose limitation. Surfactin concentration was the highest in the culture that contained 0.1 mM reaching a maximum concentration of 884 mg/L . A 2-fold increase was observed in surfactin production when the manganese concentration was increased from 0 to 0.1 mM . The increase in surfactin production was much lower than the 6.2-fold increase reported by Huang *et al.* (2015) for the same manganese concentrations. Nitrogen usage remained the same when the manganese concentration was 0.01 , 0.05 and 0.1 mM whilst surfactin yield gradually increased, suggesting that a bigger amount of the nitrogen assimilated by *B. subtilis* was utilised for surfactin production.

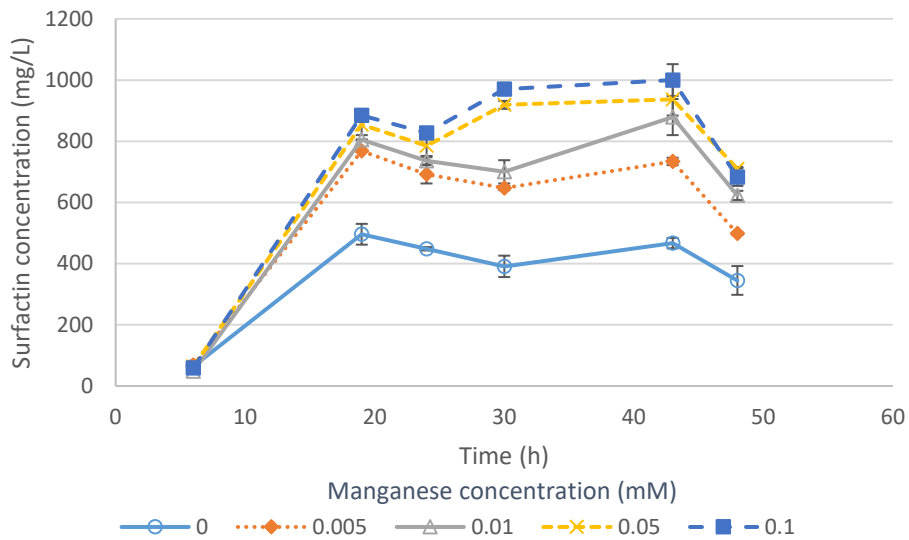


Figure 4-27: Comparison of surfactin production by *B. subtilis* for different Mn^{2+} concentrations and 4 g/L NH_4NO_3 in shake flasks at 150 rpm and 30 °C.

The surfactin homologue distribution for the different manganese concentrations are compared in Figure 4-28. The homologue distribution of Surfactin 1, 2 and 4 was the same for all the manganese concentrations, constituting approximately 1.3, 11 and 11% of the total surfactin concentration respectively. Surfactin 5 and 6 increased from approximately 37% to 42% when the manganese concentration was increased from 0 to 0.01. No change was observed in the Surfactin 5 and 6 percentage for manganese concentrations above 0.01 mM. Surfactin 2 decreased from 40% to 34% when manganese concentration increased from 0 to 0.1 mM. No change was observed in the Surfactin 2 percentage for manganese concentrations above 0.01 mM.

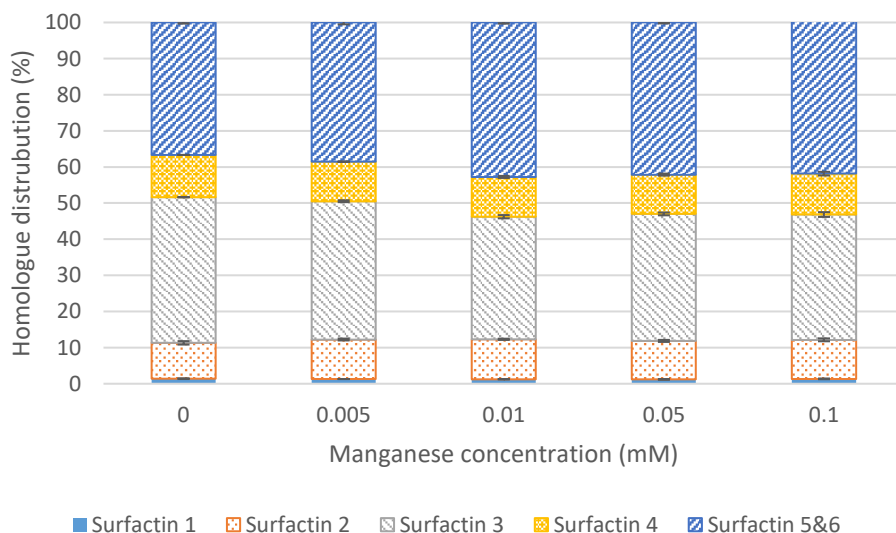


Figure 4-28: Comparison of homologue distribution of surfactin produced by *B. subtilis* in cultures containing different Mn^{2+} concentrations and 4 g/L NH_4NO_3 in shake flasks at 150 rpm and 30 °C.

The fengycin production profiles for the different manganese concentrations are compared in Figure 4-29. The highest fengycin concentration was observed for 0.01 mM manganese where fengycin reached a maximum concentration of 225 mg/L after 24 h of cultivation. The culture that contained no manganese reached a maximum fengycin concentration of 183 mg/L after 30 h of growth. The maximum fengycin concentration for the rest of the manganese concentrations were slightly lower, reaching concentrations of approximately 164 mg/L.

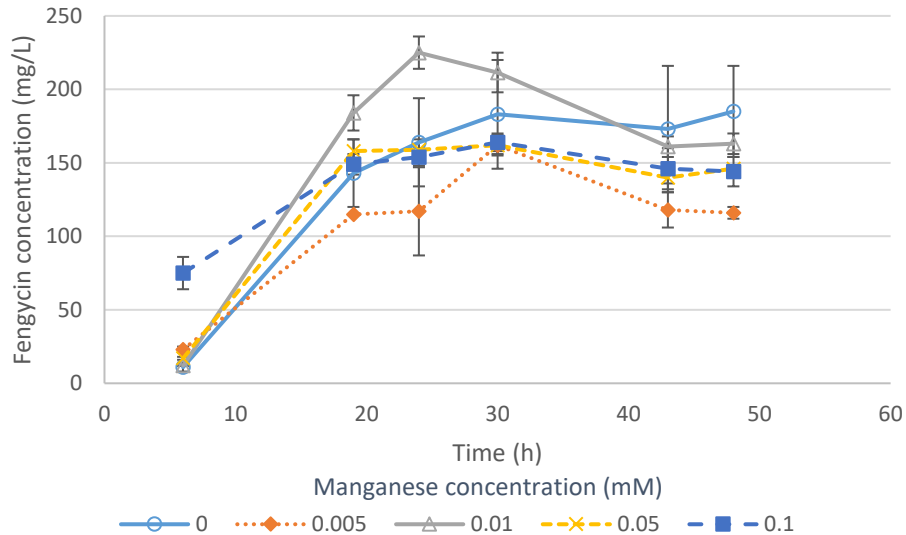


Figure 4-29: Comparison of fengycin production by *B. subtilis* in cultures containing different Mn^{2+} concentrations and 4 g/L NH_4NO_3 in shake flasks at 150 rpm and 30 °C.

4.2.4 Comparison of growth and lipopeptide associated kinetic parameters of *B. subtilis* in cultures with different manganese concentrations

Since this study focused on the effect of manganese concentration on surfactin production, the different kinetic parameters in Table 4-3 were calculated at the time when surfactin concentration reached a maximum. These parameters were normalised relative to their respective maximum values and are presented graphically in Figure 4-30 for ease of comparison.

Table 4-3: Summary of *B. subtilis* growth and lipopeptide related kinetic parameters at maximum surfactin concentration in cultures containing different Mn²⁺ concentrations and 4 g/L NH₄NO₃ in shake flasks at 150 rpm and 30 °C.

Kinetic Parameters	Manganese concentration (mM)				
	0	0.005	0.01	0.05	0.1
Time at max surfactin conc. (h)	19	19	19	19	19
μ_{\max} (h ⁻¹)	0.478	0.508	0.574	0.499	0.504
CDW (g/L)	9.045	7.810	10.116	9.909	9.923
$Y_{x/s}$ (g/g)	0.233	0.195	0.245	0.256	0.243
<u>Surfactin</u>					
Surfactin concentration (mg/L)	496	768	805	854	884
$Y_{p/s}$ (g/g)	0.013	0.019	0.020	0.022	0.022
$Y_{p/x}$ (g/g)	0.055	0.099	0.080	0.087	0.089
Productivity (mg/L/h)	26.105	40.421	42.368	44.947	46.526
<u>Fengycin</u>					
Fengycin concentration (mg/L)	143	115	184	158	149
$Y_{p/s}$ (g/g)	0.004	0.003	0.004	0.004	0.004
$Y_{p/x}$ (g/g)	0.016	0.015	0.018	0.016	0.015
Productivity	7.526	6.053	9.684	8.316	7.842
Selectivity (S/F) [g/g]	4.937	6.678	4.375	5.405	5.933

The growth related kinetic parameters (CDW and $Y_{x/s}$) in Figure 4-30 represent their values at the time surfactin concentration reached a maximum. These parameters were previously discussed in section 4.2.2 where the values were based on the maximum cell concentration and as such it will not be discussed again in this section.

Surfactin concentration increased gradually as the manganese concentration was increased from 0 to 0.1 mM. The increase in surfactin concentration was much lower for higher manganese concentrations (>0.01) where surfactin concentration only increased by 9% compared the nearly 2-fold increase in surfactin concentration when the manganese concentration was increased from 0 to 0.1 mM. The small increase (3%) in surfactin concentration between 0.05 and 0.1 mM manganese suggests that increasing the manganese concentration above 0.1 mM will not significantly increase surfactin concentration and might even result in the concentration decreasing if the manganese concentration reaches a toxic level. A manganese concentration of 0.1 mM thus maximises surfactin production by *B. subtilis*.

$Y_{p/s, \text{ surfactin}}$ also increased as the manganese concentration was increased up to 0.05 mM after which no further increase in $Y_{p/s, \text{ surfactin}}$ was observed. $Y_{p/s, \text{ surfactin}}$ was the same for 0.05 and 0.1 mM manganese. Glucose consumption was the same for all manganese concentrations (Figure 4-25), however surfactin concentration increased with increasing manganese concentration. Thus, by increasing manganese concentration up to 0.05 mM, the amount of glucose utilised for surfactin production was increased.

Nitrate consumption increased as the manganese concentration was increased from 0 to 0.01 mM and remained constant for 0.01, 0.05, and 0.1 mM manganese whilst surfactin concentration increased, thus more nitrate was utilised for surfactin as the concentration of manganese was increased. It can thus be concluded that increasing manganese concentration increases the amount of carbon and nitrogen nutrition assimilated by *B. subtilis* for surfactin production.

$Y_{p/x, \text{ surfactin}}$ increased as the manganese concentration was increased from 0 to 0.1 mM, except for 0.005 mM manganese which was significantly higher than the other tested manganese concentrations due to having a significantly lower cell concentration at the time of maximum surfactin concentration. The reason for this observation requires further investigation, however the general trend was that increasing manganese concentration increases the cells capacity to produce surfactin. Surfactin productivity also increased as the concentration of manganese was increased from 0 to 0.1 mM. Surfactin productivity was the highest for 0.1 mM manganese followed by 0.05 mM manganese and the lowest in the culture that contained no manganese. Similar productivities were observed for 0.05 and 0.1 mM manganese. Surfactin selectivity was the highest for 0.005 mM manganese, followed by 0.1 mM manganese which had a selectivity that was only 8% higher than for 0.05 mM manganese. The high selectivity of 0.005 mM manganese was due to fengycin not having reached its maximum concentration at the time surfactin reached its maximum.

Based on the results in Figure 4-30 a manganese concentration of 0.1 mM was optimal for surfactin production by *B. subtilis* as it maximised surfactin concentration, $Y_{p/s, \text{ surfactin}}$, and productivity and had the second highest $Y_{p/x, \text{ surfactin}}$ and selectivity. The highest $Y_{p/x, \text{ surfactin}}$ and surfactin selectivity was observed for 0.005 mM manganese.

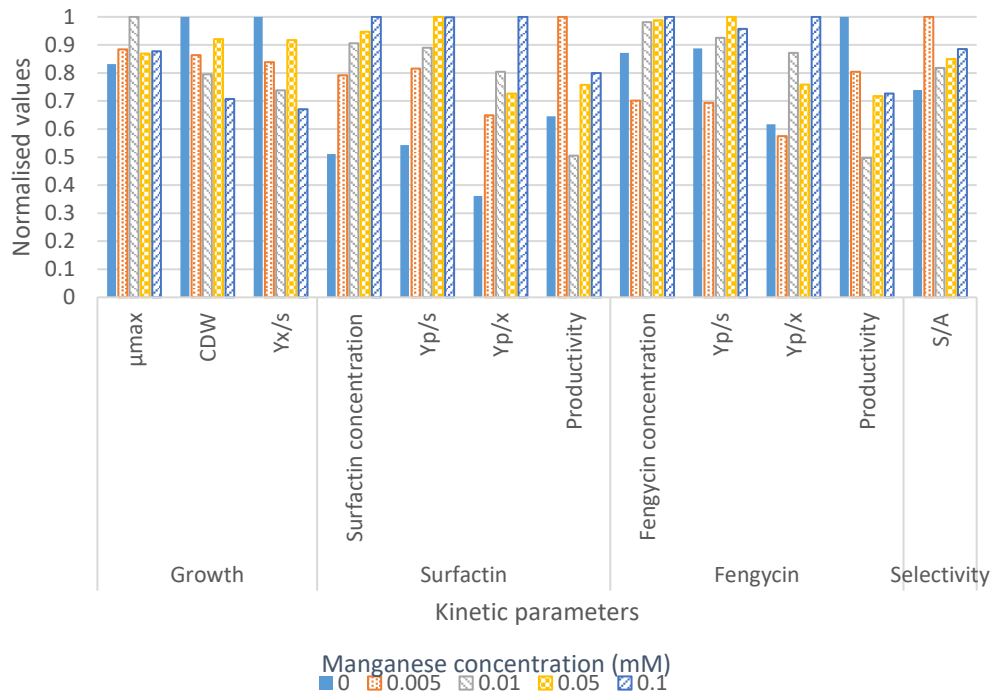


Figure 4-30: Comparison of normalised growth and lipopeptide related kinetic parameters of *B. subtilis* at maximum surfactin concentration for different Mn^{2+} concentrations in shake flasks 150 rpm and 30 °C.

The fengycin related kinetic parameters in Figure 4-30 were calculated at the time of maximum surfactin concentration and are not an accurate reflection of the effect of manganese concentration on fengycin production by *B. subtilis*. To evaluate the effect of manganese concentration on fengycin production the fengycin related kinetic parameters were calculated at the time of maximum fengycin concentration and the results are given in Table 4-4 together with the normalised values in Figure 4-31.

Table 4-4: Fengycin related kinetic parameters for different manganese concentrations at maximum fengycin concentration in shake flasks 150 rpm and 30 °C.

Kinetic parameters	Manganese concentration (mM)				
	0	0.005	0.01	0.05	0.1
Time at maximum fengycin conc. (h)	30	19	24	19	19
Fengycin concentration (mg/L)	183	115	225	158	149
$Y_{p/s}$ (g/g)	0.005	0.003	0.005	0.004	0.004
$Y_{p/x}$ (g/g)	0.018	0.015	0.023	0.016	0.015
Productivity (mg/L/h)	6.100	6.053	9.375	8.316	7.842
Selectivity (F/S) [g/g]	2.137	6.678	3.271	5.405	5.933

A similar trend was observed for fengycin concentration and related kinetic parameters, $Y_{p/s}$ and $Y_{p/x}$, where 0.01 mM manganese resulted in the highest values for these parameters followed by the culture that contained no manganese. 0.05 and 0.1 mM manganese had similar values for all the kinetic parameters in Figure 4-31. The highest fengycin productivity was observed for 0.01 mM followed by 0.05 mM manganese.

Fengycin productivity was the lowest for 0 and 0.005 mM manganese which had almost identical productivities. When 0.005 mM manganese is ignored, fengycin selectivity increased gradually as the manganese concentration was increased from 0 to 0.1 mM.

Based on the results in Figure 4-31, 0.01 mM manganese outperformed all other manganese concentrations for all kinetic parameters except for selectivity and is thus the optimal manganese concentration for fengycin production by *B. subtilis*. It should be noted that the aim of the study is to produce surfactin and not fengycin, hence this optimum will not be used in further experiments.

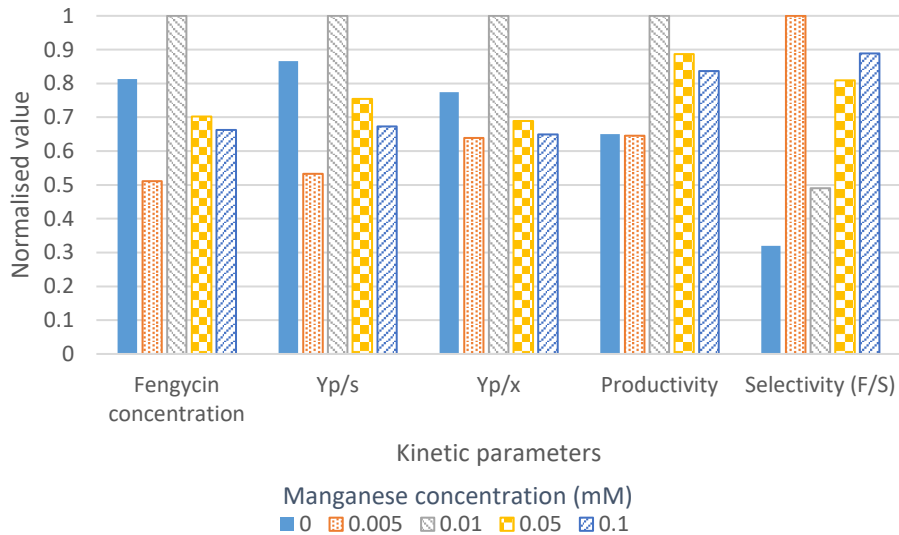


Figure 4-31: Normalised fengycin related kinetic parameters for different manganese concentrations at maximum fengycin concentration in shake flasks 150 rpm and 30 °C.

4.3 THE EFFECT OF NH₄-N:NO₃-N RATIO, MANGANESE CONCENTRATION AND OXYGEN AVAILABILITY ON THE GROWTH AND SURFACTIN PRODUCTION KINETICS OF *B. SUBTILIS*

The factors that affect the growth and surfactin production kinetics of *B. subtilis* were identified to be nitrogen source ratio, Mn²⁺ concentration, and oxygen availability. Response surface methodology (RSM) was used to design shake flask experiments to optimise the growth and surfactin production kinetics, by optimisation of the three main factors: (1) NH₄-N:NO₃-N ratio, (2) Mn²⁺ concentration and (3) oxygen availability. Since no oxygen was supplied, the only available oxygen was surface oxygen which was varied by varying the relative filling volume (RFV) of the shake flasks.

To date, several studies has focused on the individual effects of nitrogen source, Mn²⁺ concentration, and oxygen availability on the production of surfactin by *B. subtilis*. However, there has not been an attempt to find the optimal combination of these variables that optimises the growth and surfactin related kinetic parameters. Furthermore, the interactive effects of the three variables on the growth and surfactin production kinetics of *B. subtilis* have not previously been established.

The three variables were optimised through a rotatable design, with surfactin concentration, Y_{p/x} (surfactin), and the selectivity of surfactin over fengycin (S/F) after 29 hours chosen as response variables. The kinetic parameters were evaluated at 29 hours because at this point all the experiments has reached the stationary growth phase and this is also where most of the experiments reached its maximum surfactin concentration.

4.3.1 The effect of NH₄-N:NO₃-N ratio, manganese concentration and oxygen availability on surfactin concentration.

ANOVA analysis and the standardised effect estimate of each variable revealed that the NH₄-N:NO₃-N ratio and oxygen availability (RFV) were significant factors that affected the concentration of surfactin produced by *B. subtilis* after 29 h. More specifically, the model used to determine the significance of the variables revealed that the both the quadratic and linear terms of the NH₄-N:NO₃-N ratio and linear term of RFV was significant in the concentration of surfactin produced by *B. subtilis* after 29 hours as shown in Figure 4-32.

A quadratic effect serves as an indication that the optimum level of a variable falls within the experimental ranges studied and its effect depends on the interaction(s) with the other variables studied. A linear effect, on the other hand, indicates that the variable itself has a significant effect, whether positive or negative, on the response with no interaction with the other variables that were studied. By implication this means that the NH₄-N:NO₃-N ratio's interaction with oxygen availability was necessary to obtain the optimal surfactin concentration whilst oxygen availability on its own was sufficient in having a significant effect on concentration of surfactin produced by *B. subtilis* after 29 h.

The Pareto chart in Figure 4-32 shows the contribution of each variable, in descending order, for determining the optimal conditions to achieve the maximum surfactin concentration after 29 hours. The $\text{NH}_4\text{-N}:\text{NO}_3\text{-N}$ ratio followed by oxygen availability had a significant effect on the surfactin produced by *B. subtilis* after 29 hours. Figure 4-33 shows that the two extremes i.e. the cultures containing only ammonium and only nitrate were not favourable for surfactin production by *B. subtilis* and that a combination of the two nitrogen sources maximised surfactin production. Furthermore, Figure 4-33 shows that increasing the concentration of manganese up to 0.06 mM, increased surfactin production by *B. subtilis*. No significant increase in surfactin concentration was observed for manganese concentrations above 0.06 mM. Surfactin concentration was favoured by a high RFV i.e. conditions of low oxygen availability as seen in Figure 4-34 where surfactin concentration increased as the RFV was increased. Oxygen-limiting conditions favours surfactin production as a secondary metabolite due to the competitive nature of the micro-organism. The antimicrobial properties of surfactin aids the microorganism's chance of survival under oxygen-limiting conditions du

Figure 4-33 - Figure 4-35 shows the two-way interaction between the different variables and the effect on the concentration of surfactin produced by *B. subtilis* after 29 hours. Figure 4-33 - Figure 4-35 was used to determine the optimum conditions as 0.35 and 0.5 for $\text{NH}_4\text{-N}:\text{NO}_3\text{-N}$ ratio and RFV, respectively. The negative values in these figures are a result from the model artefact and has no meaning. Figure 4-34 and Figure 4-35 shows that the optimum RFV did not fall within the studied range, however the figures show that the optimum RFV is slightly above 0.5, hence 0.5 was assumed to be the optimal RFV. The optimal Mn^{2+} concentration was found to be 0.06 mM.

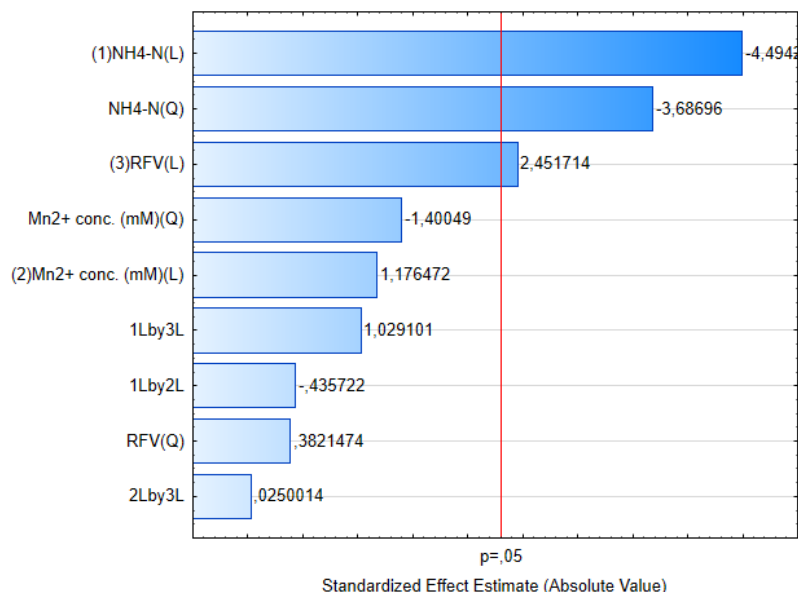


Figure 4-32: Degree of variable contribution on the concentration of surfactin produced by *B. subtilis* in shake flasks at 150 rpm and 30°C. Q and L refers to the quadratic and linear terms of the model, respectively. The Pareto chart was generated using STATISTICA 13.2.

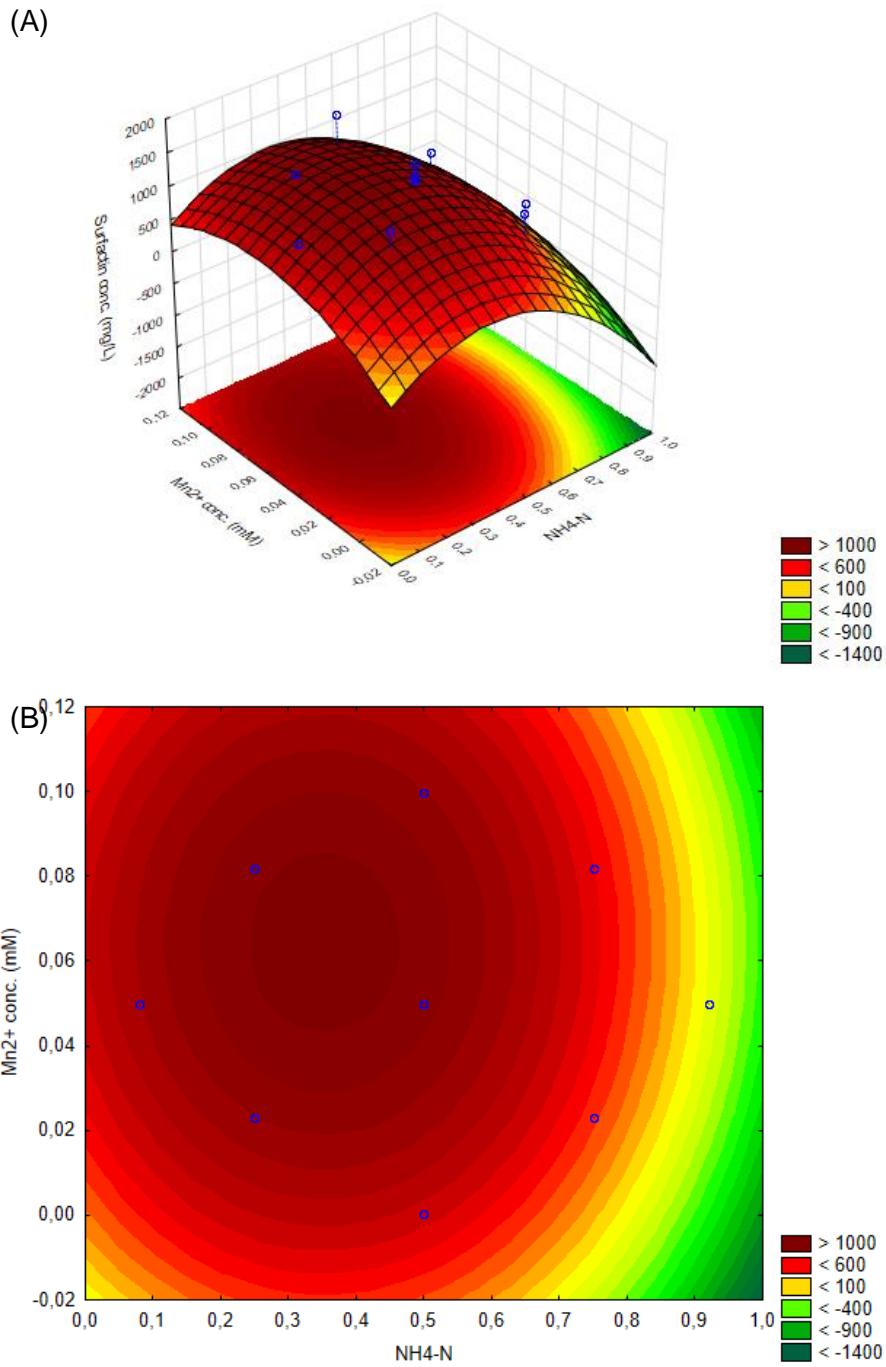


Figure 4-33: The effect of nitrogen source ratio and Mn^{2+} concentration on the surfactin concentration produced by *B. subtilis* after 29 hours in shake flasks at 150 rpm and 30 °C shown as (A) a 3D surface plot and (B) a contour surface plot. NH_4-N refers to fraction of nitrogen supplied as NH_4^+ . The surface plots were generated using STATISTICA 13.2.

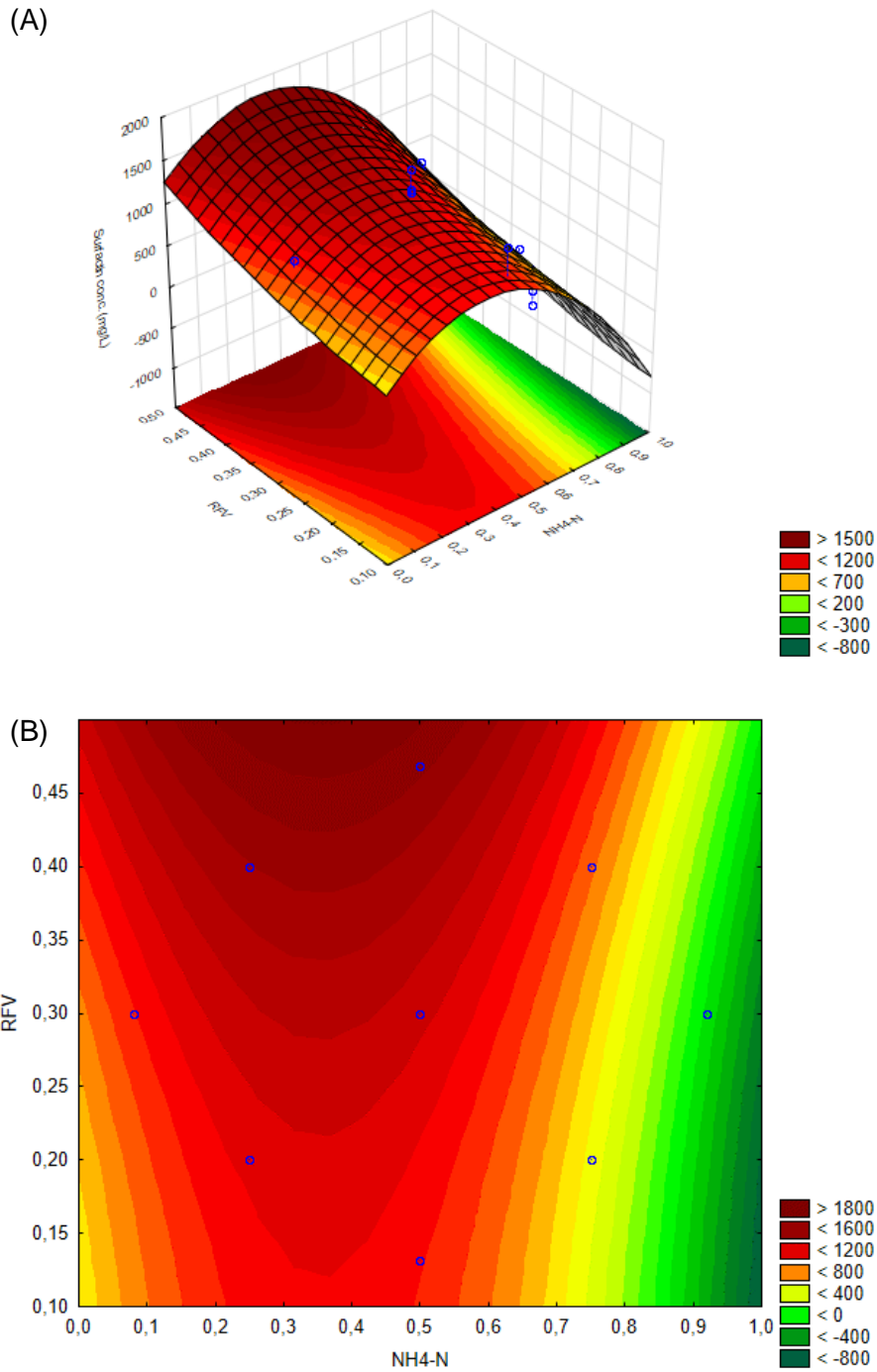


Figure 4-34: The effect of nitrogen source ratio and oxygen availability on the surfactin concentration produced by *B. subtilis* after 29 hours in shake flasks at 150 rpm and 30 °C shown as (A) a 3D surface plot and (B) a contour surface plot. RFV refers to relative filling volume of the flask which relates surface oxygen. The surface plots were generated using STATISTICA 13.2.

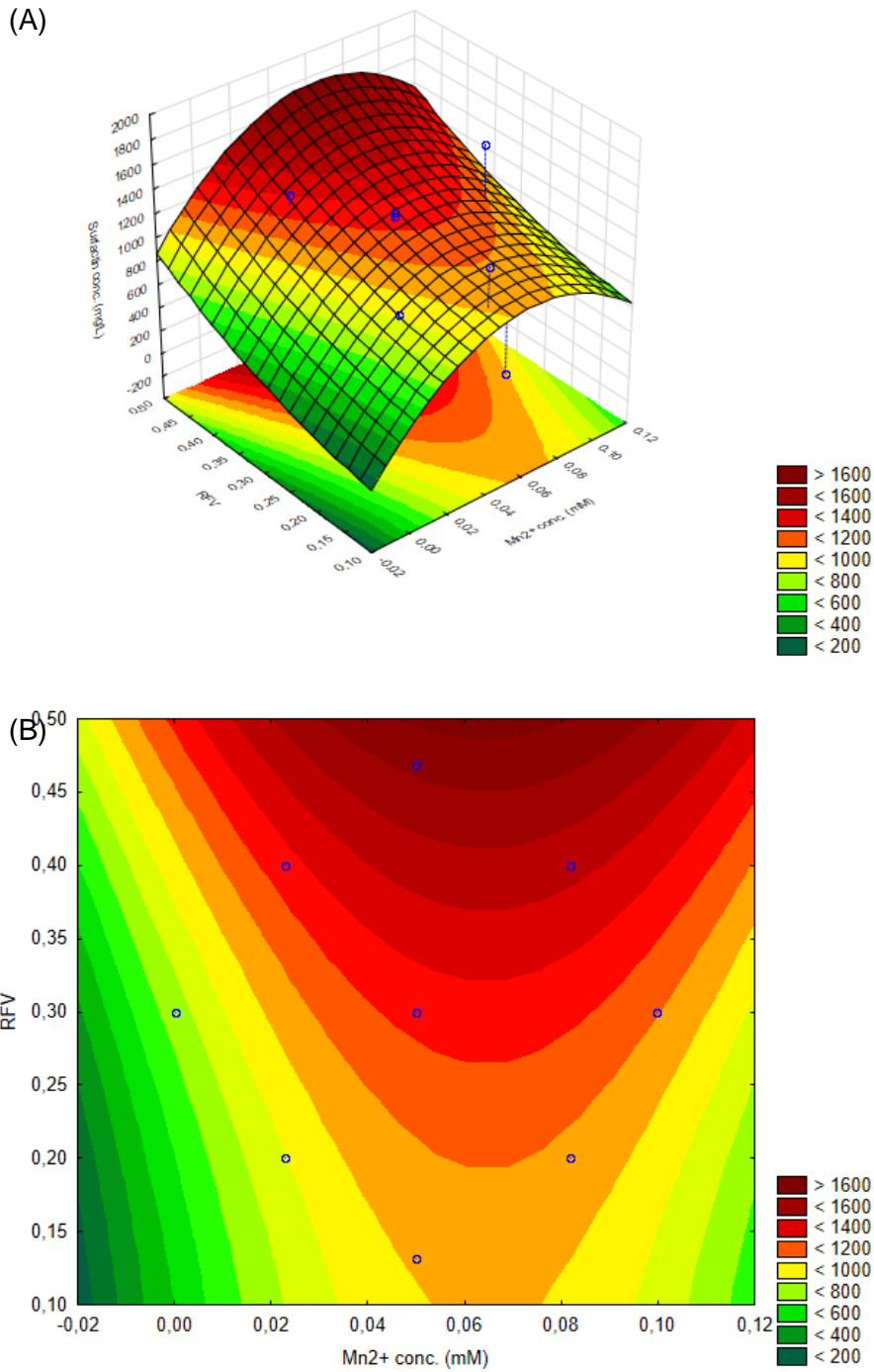


Figure 4-35: The effect of Mn²⁺ concentration and surface oxygen on the surfactin concentration produced by *B. subtilis* after 29 h in shake flasks at 150 rpm and 30 °C shown as (A) a 3D surface plot and (B) a contour surface plot. RFV refers to relative filling volume of the flask which relates surface oxygen. The surface plots were generated using STATISTICA 13.2.

4.3.2 The effect of NH₄-N:NO₃-N ratio, manganese concentration and oxygen availability on

$Y_{p/x}$ (surfactin)

The NH₄-N:NO₃-N ratio was found to be the only significant variable to influence $Y_{p/x}$ (surfactin) of *B. subtilis* after 29 h as shown in Figure 4-36. Both the quadratic and linear terms of NH₄-N:NO₃-N ratio were found to significantly influence $Y_{p/x}$ (surfactin). Figure 4-36 shows that the linear term of RFV falls just outside of the line of significance which indicates that RFV may also have significant influence on $Y_{p/x}$ (surfactin). If this is the case, the same variables that had a significant effect on surfactin concentration, affected the $Y_{p/x}$ (surfactin) in a similar manner.

The optimal conditions for $Y_{p/x}$ (surfactin) could not be determined surface plots could not be fitted to data as shown in Figure 4-37. This implies that the selected model could not adequately describe the effect of the different variables on $Y_{p/x}$ (surfactin). This may have been the result of the sensitivity of $Y_{p/x}$ which is dependent on two variables namely surfactin concentration and cell concentration. Like most biological systems, there exists a large degree of variability even when the experiments are executed under the exact same conditions. The experiments were conducted in shake flasks which may have contributed to lack of fit of the model for $Y_{p/x}$ (surfactin). Shake flasks have the disadvantage of offering less control over operating conditions such as pH and aeration and thus has a higher variability as opposed to experiments conducted in instrumented bioreactors where these conditions are controlled. It is suggested that the experimental design be reviewed and that the experiments are carried out in an instrumented bioreactor, under controlled conditions, to study the effect of the variables on $Y_{p/x}$ and to find to optimal conditions that will maximise $Y_{p/x}$.

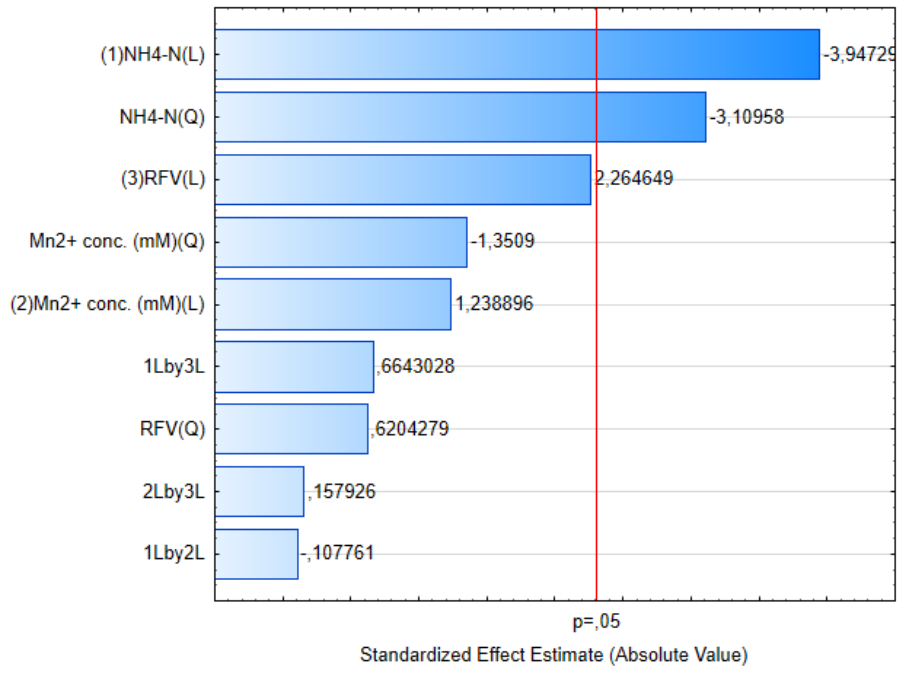
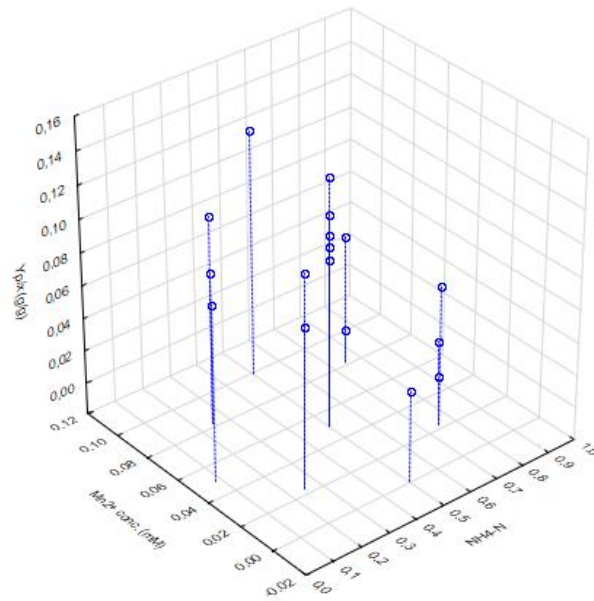


Figure 4-36: Degree of variable contribution on $Y_{p/x}$ (surfactin) of *B. subtilis* in shake flasks after 29 h at 150 rpm and 30°C. Q and L refers to the quadratic and linear terms of the model, respectively. The Pareto chart was generated using STATISTICA 13.2.



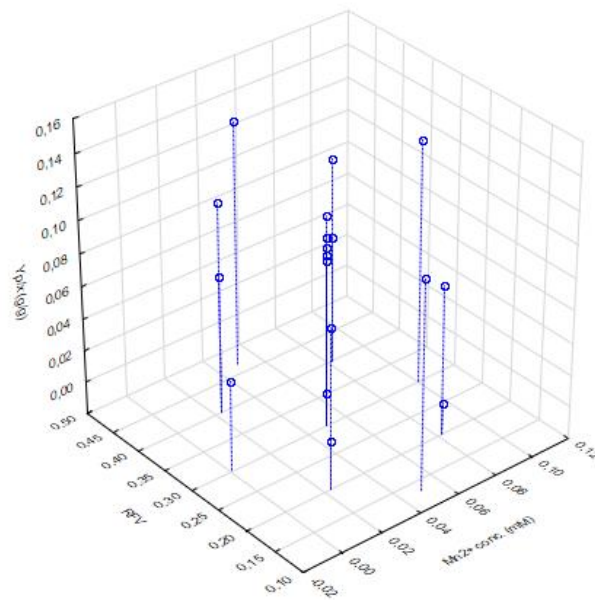
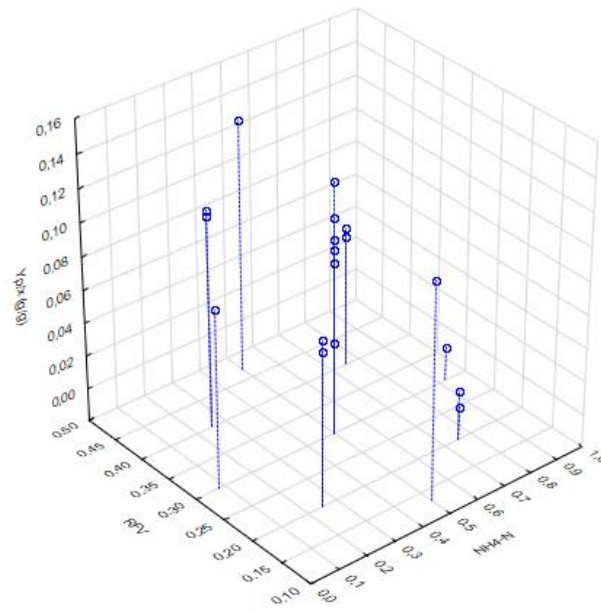


Figure 4-37: Graphs showing the lack of fit of the data to the model describing the effects of $\text{NH}_4\text{-N}:\text{NO}_3\text{-N}$ ratio, Mn^{2+} concentration, and oxygen availability on $Y_{p/x}$ (surfactin) for *B. subtilis* in shake flasks after 29 h at 150 rpm and 30 °C.

4.3.3 The effect of NH₄-N:NO₃-N ratio, manganese concentration and surface oxygen on surfactin selectivity

The NH₄-N:NO₃-N ratio together with its linear interaction with oxygen availability had a significant effect on the selectivity of surfactin over fengycin (S/F) as shown in Figure 4-38. Unlike the case for surfactin concentration and $Y_{p/x}$ (surfactin) in section 4.3.1 and 4.3.2, where the quadratic term for NH₄-N:NO₃-N ratio had a significant effect on the responses, it did not have a significant effect on the selectivity of surfactin over fengycin. Similar to surfactin concentration and $Y_{p/x}$ (surfactin), Mn²⁺ concentration had no effect on surfactin selectivity.

As was the case with $Y_{p/x}$ (surfactin), the optimal conditions that maximises surfactin selectivity could not be determined as the model could not adequately describe the effects of the variables on surfactin selectivity as shown in Figure 4-38. This may be due to the same reasons as discussed in section 4.3.2 and it is thus recommended that the experimental design be reviewed and for the experiments to be conducted under controlled conditions to limit variability in order to study the effects of the variables on surfactin selectivity and to determine the optimal conditions that will maximise surfactin selectivity.

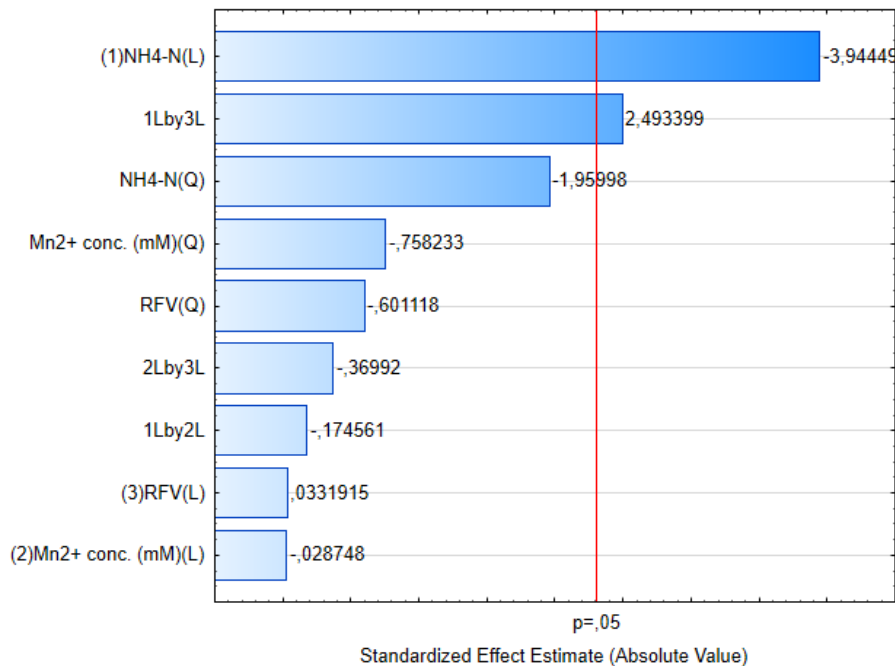
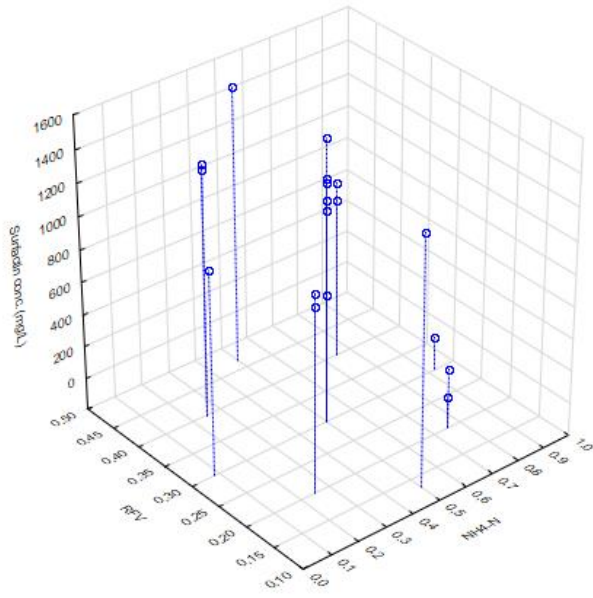
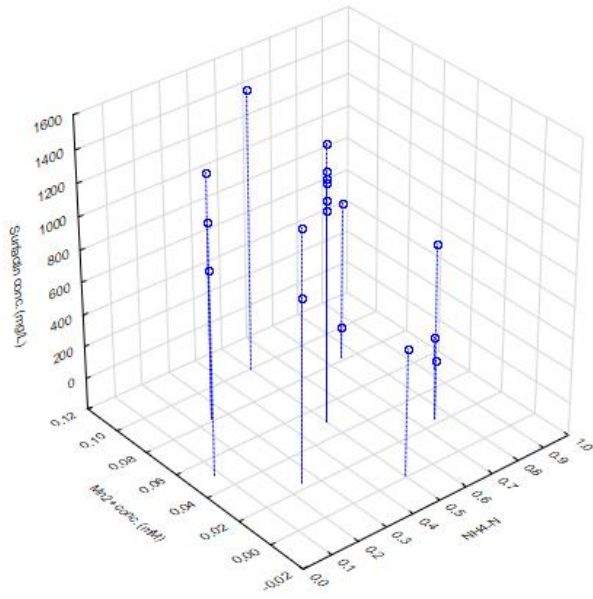


Figure 4-38: Degree of variable contribution on the selectivity of surfactin over fengycin (S/F) produced by *B. subtilis* in shake flasks after 29 h at 150 rpm and 30°C. Q and L refers to the quadratic and linear terms of the model, respectively. The Pareto chart was generated using STATISTICA 13.2.



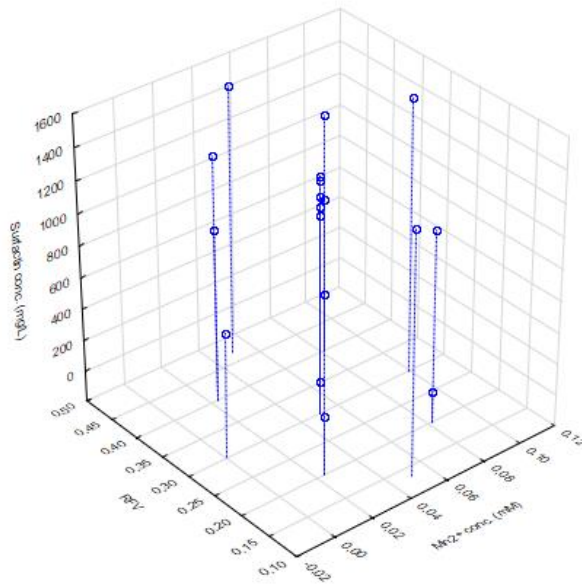


Figure 4-39: : Graphs showing the lack of fit of the data to the model describing the effects of NH₄-N:NO₃-N ratio, Mn²⁺ concentration, and oxygen availability on the selectivity of surfactin over fengycin (S/F) for *B. subtilis* in shake flasks after 29 h at 150 rpm and 30 °C.

4.4 GROWTH AND PRODUCTION KINETICS OF *B. SUBTILIS* UNDER CONTROLLED CONDITIONS IN AN INSTRUMENTED BIOREACTOR

Shake flasks are widely used as preliminary tests for further bioreactor studies due to their ease of use, however shake flasks has the disadvantage of offering less control over conditions such as pH and aeration and often result in lower yields compared to bioreactors operated under the same conditions. Chen, Baker and Darton (2006) reported lower surfactin concentrations in shake flasks than in a bioreactor operated at the same conditions. This is in contrast with Fernandes *et al.* (2007) and Wei *et al.* (2003) who reported higher biosurfactant concentrations in shake flasks.

The shake flask studies in section 4.1 and 4.2 revealed that a $\text{NH}_4\text{-N}:\text{NO}_3\text{-N}$ ratio of 0.5 and a Mn^{2+} concentration of 0.1 mM optimised the kinetics for surfactin production by *B. subtilis*. The results in section 4.2 showed that increasing the Mn^{2+} concentration from 0.05 to 0.1 mM only resulted in a small improvement in the surfactin production kinetics of *B. subtilis* and as a result 0.05 mM Mn^{2+} was used together with the optimal nitrogen source ratio to evaluate the growth and production kinetics of *B. subtilis* under controlled conditions in an instrumented batch bioreactor and was evaluated against the same conditions that was used by Pretorius, van Rooyen and Clarke (2015) who provided the basis for the operating conditions used in this study.

4.4.1 Growth, substrate utilisation and lipopeptide production patterns in a culture containing 0.01 mM Mn^{2+} and 4g/L NH_4NO_3 as a nitrogen source

Figure 4-40 shows the growth and substrate utilisation patterns for a culture containing 4 g/L NH_4NO_3 and 0.01 mM Mn^{2+} in a controlled batch bioreactor. The culture conditions were exactly the same as those employed by Pretorius, van Rooyen and Clarke (2015). The growth curve in Figure 4-40 shows no lag phase. The culture entered the exponential phase immediately after inoculation, with a maximum specific growth rate of 0.39 h^{-1} between 0 and 8 h. The specific growth rate decreased after 8 h, however the cells continued to grow exponentially until 21 h where it entered a deceleration phase. The decrease in the specific growth rate after 8 hours can be attributed to dissolved oxygen levels dropping below 10% as shown in Figure 4-40. A deceleration phase was observed between 21 and 32 h after which the culture entered the stationary phase. The culture reached a maximum CDW of 9.9 g/L at 32 h and cell concentration remained constant until the experiment was terminated at 48 h.

Figure 4-40 shows that glucose was consumed at a constant rate immediately after inoculation until 21 h after which a decrease in the glucose utilisation rate was observed. The decrease in the glucose utilisation rate coincided with the onset of the deceleration phase at 21 h. Glucose was essentially depleted after 32 h with only 1.2 g/L remaining at this time. The depletion of glucose coincided with the onset of the stationary at 32 h. Glucose was thus the growth-limiting nutrient.

Nitrate concentration remained constant during the first 5 hours of growth during which both ammonium and oxygen was still in excess. Nitrate consumption started after 5 hours when the dissolved oxygen levels dropped below 17% and was consumed at a nearly constant rate until it was depleted at 32 h. Ammonium was still in excess during the period of rapid nitrate utilisation whilst oxygen became limiting during this period, suggesting that nitrate was used as an alternative electron acceptor when the dissolved oxygen levels dropped below 17%. The depletion of nitrate coincided with the onset of the stationary growth phase at 32 h whilst ammonium was still in excess at this time.

Figure 4-40 shows that ammonium was consumed at a nearly constant rate immediately after inoculation. Ammonium consumption ceased at 28 h as a result of glucose limitation. At 32 h, 0.17 g/L ammonium was present in the culture broth. Ammonium was consumed alongside nitrate, suggesting that ammonium is was utilised as a nitrogen source for growth and cell maintenance whilst nitrate was utilised as an electron acceptor following oxygen-limitation.

Figure 4-40 shows that oxygen was consumed rapidly during the first 4 h of growth, with dissolved oxygen levels dropping from 100 to 17.4 % during this period and continued to decrease at a slower rate until it became limiting at 12 h. Cell growth continued after oxygen became limiting due to nitrate being present in the culture broth to act as an alternative electron acceptor.

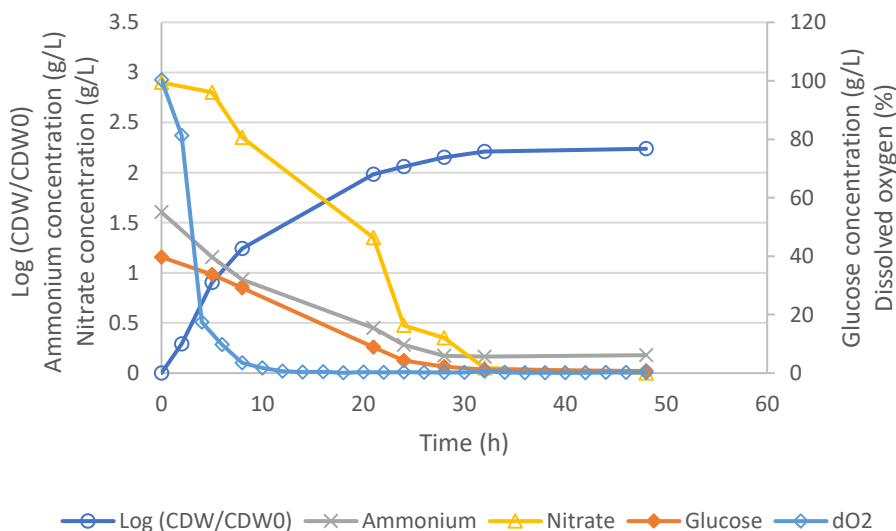


Figure 4-40: Graph illustrating the growth (open circles, left hand axis, in $\log(\text{CDW}/\text{CDW}_0)$) of *B. subtilis* and substrate concentration of nitrate (open triangles, left hand axis, in g/L), glucose (closed diamonds, right hand axis, in g/L), ammonium (crosses, right hand axis, in g/L scaled up by a factor of X100 for clarity) and dissolved oxygen (open diamonds, right hand axis) for a culture containing 4 g/L NH_4NO_3 and 0.01 mM Mn^{2+} in a 1 L controlled bioreactor (0.5 L working volume).

The lipopeptide production profiles for the controlled bioreactor culture containing 4 g/L NH_4NO_3 and 0.01 mM Mn^{2+} is shown in Figure 4-41. Surfactin and fengycin production was slow during the first 8 h of growth, after which an increase in the production rates was observed. Both surfactin and fengycin was produced at a constant rate after 8 h until they reached their respective maximum concentrations of 974 and 236 mg/L at 32 h. Surfactin concentration remained constant following glucose and nitrate depletion, unlike the shake flask experiments with the same medium composition in section 4.1 and 4.2 where a decrease in surfactin was observed. Unlike the shake flask experiments, pH was controlled at 7.0 which explains why the surfactin concentration remained constant in the bioreactor. The maximum surfactin concentration compares well with the 882 mg/L obtained by Pretorius, van Rooyen and Clarke (2015) under the same conditions. Fengycin concentration could not be compared with (Pretorius *et al.*, 2015) as the authors grouped all antifungal lipopeptides together because they did not have standard curves for the antifungal lipopeptides. A slight decrease in the surfactin concentration was observed between 32 and 48 h, whilst fengycin concentration essentially remained constant during this period. The maximum lipopeptide concentrations coincided with the onset of the stationary phase at 32 h when nitrate became limiting.

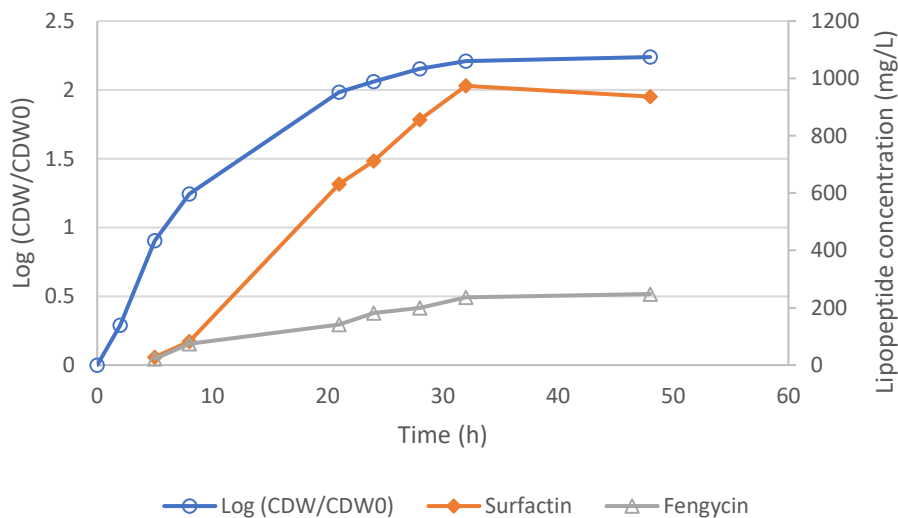


Figure 4-41: Graph illustrating the growth (open circles, left hand axis, in $\log(\text{CDW}/\text{CDW}_0)$) and lipopeptide production (surfactin – closed diamonds, right hand axis, in mg/L; fengycin – open triangles, right hand axis, in mg/L) of *B. subtilis* over time in a culture containing 4 g/L NH_4NO_3 and 0.01 mM Mn^{2+} in a 1 L controlled bioreactor (0.5 L working volume).

4.4.2 Growth, substrate utilisation and lipopeptide production patterns using the optimum $\text{NH}_4\text{-N}:\text{NO}_3\text{-N}$ ratio and manganese concentration from shake flask studies

The shake flask studies in section 4.1 and 4.2 revealed that a $\text{NH}_4\text{-N}:\text{NO}_3\text{-N}$ ratio of 0.5 and Mn^{2+} concentration of 0.05 mM yielded the optimal kinetics for surfactin production by *B. subtilis*. Since NH_4NO_3 contains equal fractions of nitrogen from ammonium and nitrate, it was not necessary to supply ammonium and nitrate separately as NH_4Cl and NaNO_3 ; hence 4 g/L NH_4NO_3 was used instead of using the equivalent combination of NH_4Cl and NaNO_3 . These conditions were used to study the growth and lipopeptide kinetics in a controlled bioreactor. The growth and substrate utilisation patterns are shown in Figure 4-42 and the corresponding lipopeptide production profiles are shown Figure 4-43.

The growth curve in shows that the culture entered the exponential phase immediately after inoculation with a maximum specific growth rate of 0.37 h^{-1} until 8 h, after which the specific growth rate decreased, however the cells continued to grow exponentially until 28 h. The decrease in the specific growth rate after 8 hours can be attributed to dissolved oxygen levels dropping below 10% as shown in Figure 4-42. A maximum CDW of 9.9 g/L was observed at 32 h.

Glucose was consumed at a nearly constant rate immediately after inoculation until 24 h after which it was consumed at a lower rate and was essentially depleted at 32 h. Nitrate concentration was constant during the first 5 h of growth after which it was consumed rapidly at a nearly constant rate between 5 and 24 h. The nitrate consumption rate decreased after 24 h until it was completely consumed at 32 h. The culture entered the stationary phase when glucose became limiting after 28 h.

Ammonium was consumed at a nearly constant rate until 21 h, after which a decrease in the in the ammonium consumption rate was before consumption ceased at 28 h when glucose became limiting. Figure 4-42 shows a rapid decrease in the dissolved oxygen levels in the first 4 hours of growth, from 100 to 12%, after which it continued to decrease at slower rate until it reached 0 at 12 h. Nitrate acted as an alternative electron acceptor after the dissolved oxygen levels dropped below 10%. Both ammonium and nitrate were consumed simultaneously after 5 h suggesting that ammonium as nitrogen source was utilised for growth and cell maintenance and nitrate was utilised as an electron acceptor following oxygen limitation.

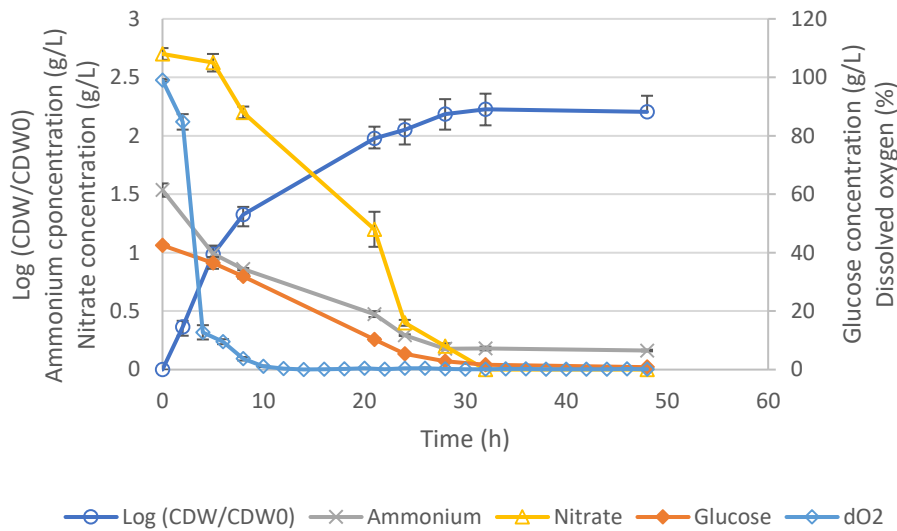


Figure 4-42: Graph illustrating the growth (open circles, left hand axis, in $\log(\text{CDW}/\text{CDW}_0)$) of *B. subtilis* and substrate concentration of nitrate (open triangles, left hand axis, in g/L), glucose (closed diamonds, right hand axis, in g/L), ammonium (crosses, right hand axis, in g/L scaled up by a factor of X100 for clarity) and dissolved oxygen (open diamonds, right hand axis) at the optimal nitrogen source ratio ($\text{NH}_4\text{-N}:\text{NO}_3\text{-N}$ ratio = 0.5) and Mn^{2+} concentration (0.05 mM) from shake flask studies in a 1 L controlled bioreactor (0.5 L working volume).

Figure 4-43 shows that surfactin production was slow during the first 5 h of growth, after which the surfactin concentration increased at a constant rate until 32 h. Surfactin continued to increase at a slower rate after 32 h until the experiment was terminated at 48 h. Surfactin concentration was not expected to increase significantly after 48 h as both glucose and nitrate has already been depleted, hence the concentration of 891 mg/L at 48 h was assumed to be the maximum surfactin concentration. Figure 4-43 shows that fengycin production only started after 28 h. Fengycin was produced at a constant rate after 28 h, reaching a concentration of 285 mg/L at 48 h when the experiment was terminated.

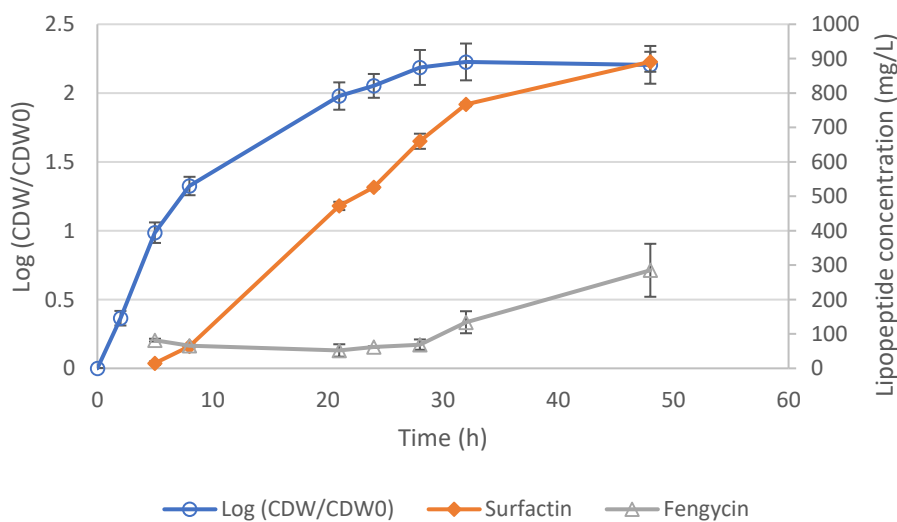


Figure 4-43: Graph illustrating the growth (open circles, left hand axis, in $\log(\text{CDW}/\text{CDW}_0)$) and lipopeptide production (surfactin – closed diamonds, right hand axis, in mg/L; fengycin – open triangles, right hand axis, in mg/L) of *B. subtilis* over time at the optimal nitrogen source ratio ($\text{NH}_4\text{-N}:\text{NO}_3\text{-N}$ ratio = 0.5) and Mn^{2+} concentration (0.05 mM) from shake flask studies in a 1 L controlled bioreactor (0.5 L working volume).

4.4.3 Comparison of growth and substrate utilisation patterns of batch bioreactor cultures and shake flask cultures

Similar growth curves were observed for the 0.01 and 0.05 mM Mn²⁺ bioreactor cultures as shown in Figure 4-44, however the growth curves differed from the corresponding shake flask cultures. The bioreactor cultures took longer (32 h) to reach the stationary phase compared to the shake flask cultures, where the stationary phase was reached after 19 h.

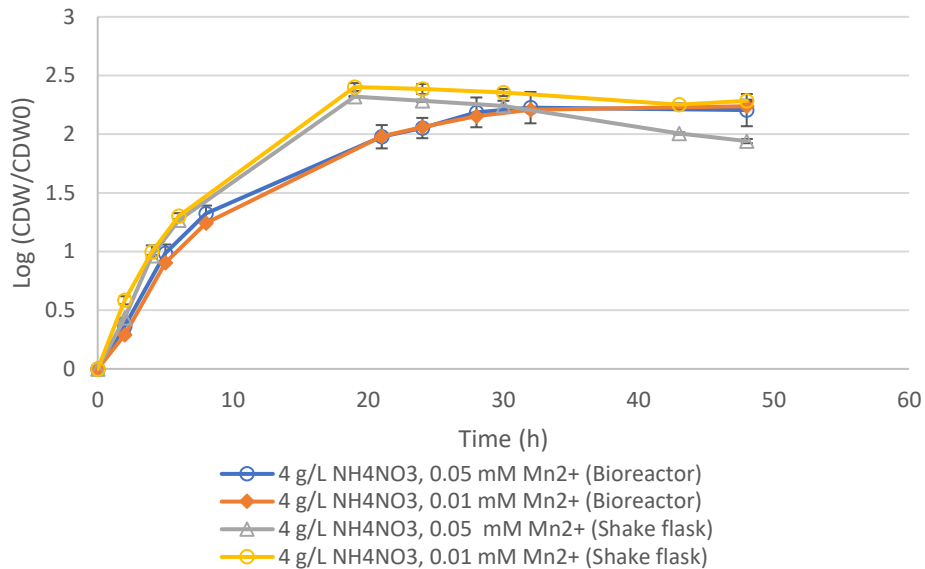


Figure 4-44: Comparison of *B. subtilis* growth in shake flask and batch bioreactor cultures containing 0.01 and 0.05 mM Mn²⁺ and 4 g/L NH₄NO₃

Table 4-5 shows that there was no significant difference in the maximum CDW achieved in the bioreactors compared to that achieved in shake flasks. The Mn²⁺ concentration had no significant impact on the maximum CDW in both shake flasks and bioreactors. This suggests that there was a significant excess of manganese, thus the lipopeptide producing enzymes had more than enough active site substrate. Table 4-5 shows that μ_{\max} was higher in shake flasks compared to that achieved in the bioreactors. The higher Mn²⁺ concentration yielded a lower μ_{\max} in both the shake flasks and bioreactors. μ_{\max} for 0.01 mM Mn²⁺ was slightly lower than the 0.45 h⁻¹ reported by (Pretorius *et al.*, 2015) at the same conditions.

Table 4-5: Comparison of *B. subtilis* maximum specific growth rate and maximum CDW in shake flask and batch bioreactor cultures containing 0.01 and 0.05 mM Mn²⁺ and 4 g/L NH₄NO₃

Culture conditions	Shake flask		Bioreactor	
	0.01 mM Mn ²⁺	0.05 mM Mn ²⁺	0.01 mM Mn ²⁺	0.05 mM Mn ²⁺
Max CDW	9.97	10.02	9.16	9.89
μ_{\max} (h ⁻¹)	0.57	0.50	0.39	0.37

Figure 4-45 shows that Mn^{2+} concentration did not have a significant effect on glucose utilisation in both shake flasks and in the bioreactors as similar trends were observed for 0.01 and 0.05 mM Mn^{2+} . There was however a significant difference in glucose utilisation in the shake flask cultures compared to the bioreactor cultures. Glucose was consumed much more rapidly in the shake flask cultures than in the bioreactor cultures. Glucose was completely consumed after 19 h in shake flasks, whereas in the bioreactor cultures glucose was only depleted after 32 h.

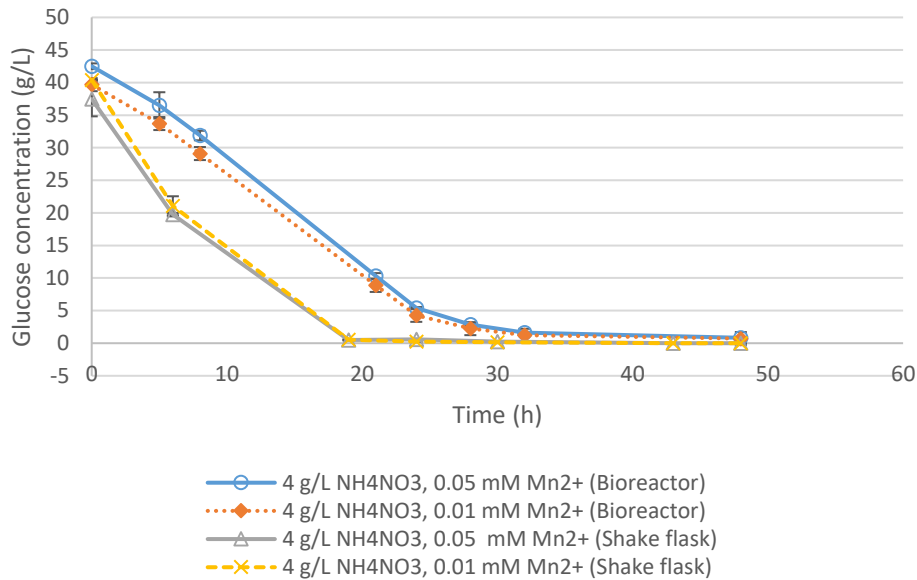


Figure 4-45: Comparison of *B. subtilis* glucose utilisation in shake flask and batch bioreactor cultures containing 0.01 and 0.05 mM Mn^{2+} and 4 g/L NH_4NO_3

Figure 4-46 shows that Mn^{2+} concentration did not have a significant effect on ammonium utilisation in both shake flasks and in the bioreactors as similar trends were observed for 0.01 and 0.05 mM Mn^{2+} . Ammonium was consumed at a constant rate immediately after inoculation and consumption ceased when glucose became limiting in both the bioreactor and shake flasks cultures. The only difference between the shake flask and bioreactor cultures was the time at which ammonium consumption ceased. In shake flasks ammonium consumption stopped after 19 h whereas consumption ceased at 28 h in the bioreactor cultures.

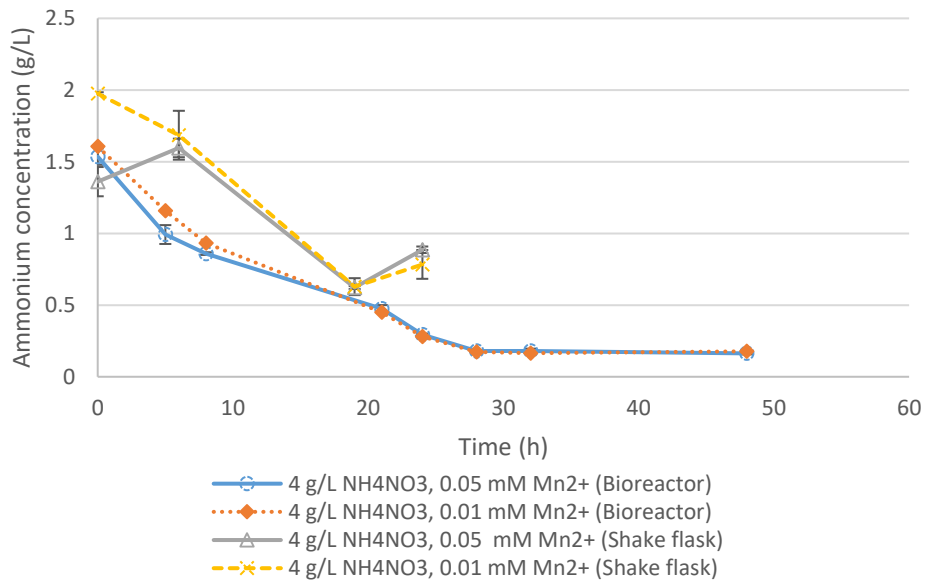


Figure 4-46: Comparison of *B. subtilis* ammonium utilisation in shake flask and batch bioreactor cultures containing 0.01 and 0.05 mM Mn²⁺ and 4 g/L NH₄NO₃

Figure 4-47 shows that Mn²⁺ concentration did not have a significant effect on nitrate utilisation in both shake flask bioreactor cultures as similar trends were observed for 0.01 and 0.05 mM Mn²⁺. Nitrate concentration remained constant during the first 5-6 h in both the shake flask and bioreactor cultures after which nitrate was consumed rapidly until it either ceased due to glucose limitation (shake flask cultures) or was completely consumed (bioreactor cultures). In all cultures nitrate was utilised as an alternative electron acceptor when oxygen became limiting as opposed to its utilisation as a nitrogen source because ammonium, which is the preferred nitrogen source, was in excess.

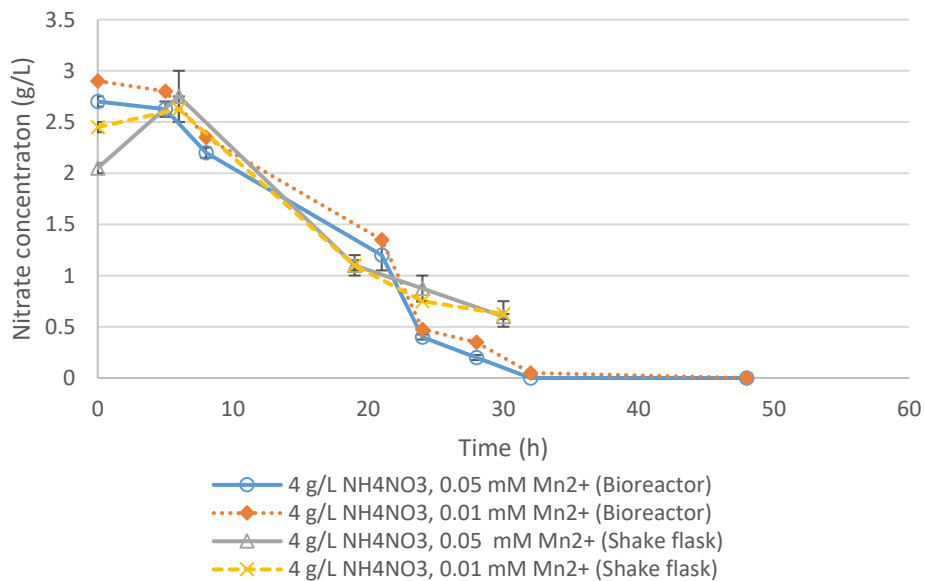


Figure 4-47: Comparison of *B. subtilis* nitrate utilisation in shake flask and batch bioreactor cultures containing 0.01 and 0.05 mM Mn²⁺ and 4 g/L NH₄NO₃

4.4.4 Comparison of lipopeptide production patterns of batch bioreactor cultures and shake flask cultures

Figure 4-48 shows similar trends for the shake flask cultures suggesting that Mn^{2+} did not have a significant effect on surfactin production. The 0.01 and 0.05 mM Mn^{2+} cultures both reached their respective maximum surfactin concentrations of 879 and 937 mg/L at 43 h. A slight difference was observed in the trends for the bioreactor cultures. The 0.01 mM Mn^{2+} bioreactor culture reached a maximum surfactin concentration of 974 mg/L at 32 h after which a decrease a slight decrease in the surfactin concentration was observed between 32 and 48 h. The 0.05 mM Mn^{2+} bioreactor culture achieved a maximum surfactin concentration of 891 mg/L at 48 h. 0.01 mM Mn^{2+} resulted in higher surfactin concentration in the bioreactor cultures which is in contrast with the shake flask cultures where 0.05 mM Mn^{2+} yielded the highest surfactin concentration. Further investigation is required to explain the difference.

In Figure 4-48 it can be seen that surfactin concentration decreased after 43 h, whereas the concentration remained constant in the bioreactor cultures. The decrease was most likely due to pH dropping below 5.0 in the shake flask cultures, where pH was not controlled, causing surfactin to precipitate. The pH in the bioreactor cultures were controlled at 7.0, hence the surfactin remained in the solution.

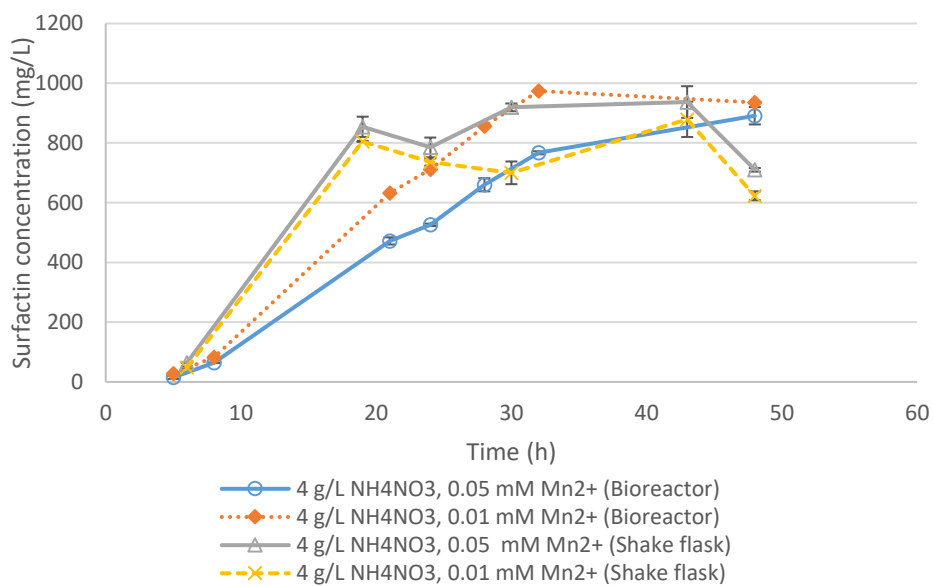


Figure 4-48: Comparison of surfactin production by *B. subtilis* in shake flask and batch bioreactor cultures containing 0.01 and 0.05 mM Mn^{2+} and 4 g/L NH_4NO_3

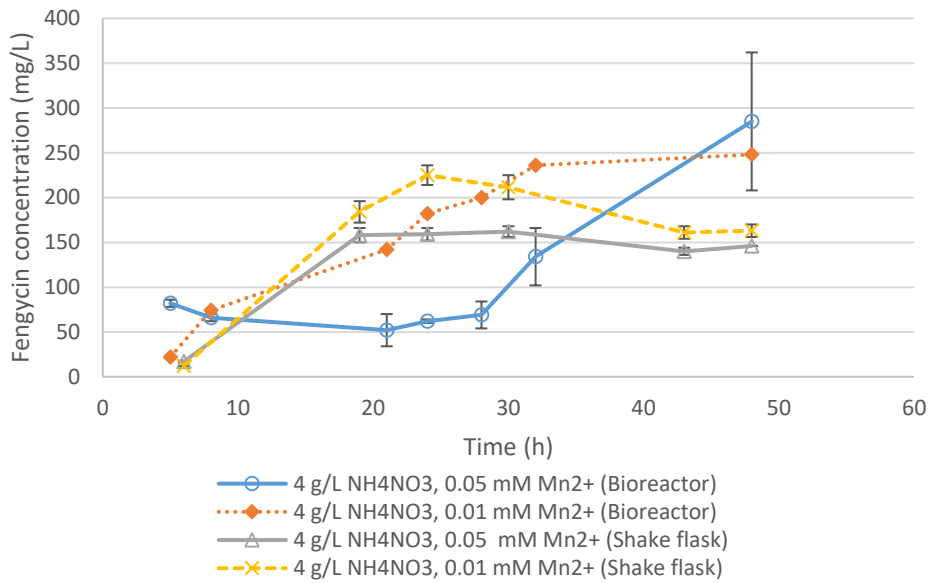


Figure 4-49 shows that Mn²⁺ had a significant effect on fengycin production profiles in both the shake flask and bioreactor cultures. The 0.01 mM Mn²⁺ shake flask culture yielded a maximum fengycin concentration of 158 mg/L after 19 h whilst the 0.05 mM Mn²⁺ shake flask culture achieved a maximum fengycin concentration of 236 mg/L after 24 h. There was a significant difference in the fengycin production profiles of the bioreactor cultures. Fengycin concentration increased at a nearly constant rate between 6 and 32 h for the 0.01 mM Mn²⁺ bioreactor culture whilst the fengycin production only started after 28 h in the 0.05 mM Mn²⁺ bioreactor culture. A maximum fengycin concentration of 236 mg/L was observed for the 0.01 mM Mn²⁺ bioreactor culture after 28 h, whilst the 0.05 mM Mn²⁺ bioreactor culture yielded a maximum fengycin concentration after 48 h. The 0.05 mM Mn²⁺ yielded the highest fengycin concentration in both the shake flask and bioreactor cultures.

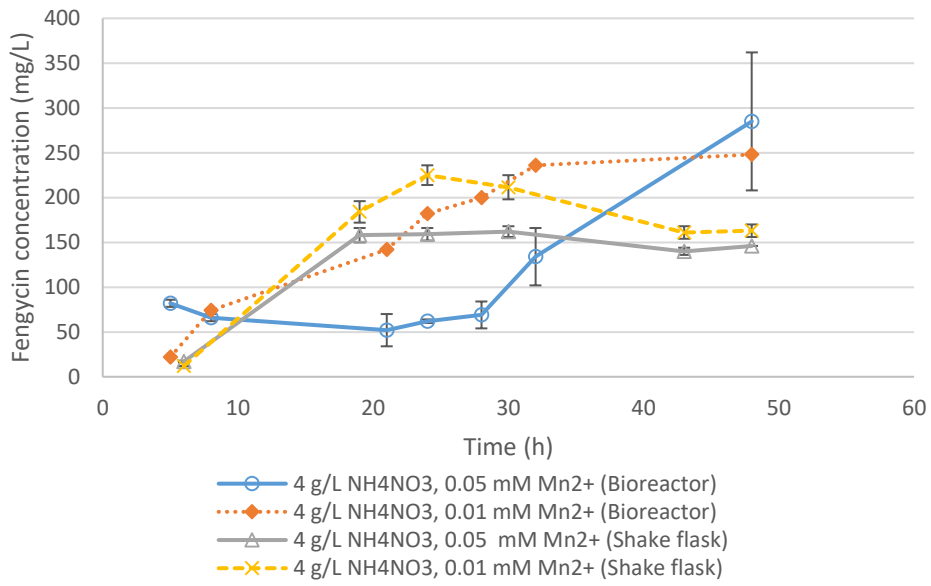


Figure 4-49: Comparison of fengycin production by *B. subtilis* in shake flask and batch bioreactor cultures containing 0.01 and 0.05 mM Mn²⁺ and 4 g/L NH₄NO₃

4.4.5 Comparison of normalised cell and lipopeptide concentrations associated kinetic parameters of batch bioreactor and shake flask cultures

Since this study focused surfactin production by *B. subtilis*, the different kinetic parameters in Table 4-6 were calculated at the time when surfactin concentration reached a maximum. These parameters were normalised relative to their respective maximum values and are presented graphically in Figure 4-50 for ease of comparison.

Table 4-6: Summary of *B. subtilis* growth and lipopeptide related kinetic parameters at maximum surfactin concentration shake flask and bioreactor cultures containing 0.01 and 0.05 mM Mn²⁺ and 4 g/L NH₄NO₃

Kinetic Parameters	4 g/L NH ₄ NO ₃ , 0.05 mM Mn ²⁺ (Bioreactor)	4 g/L NH ₄ NO ₃ , 0.01 mM Mn ²⁺ (Bioreactor)	4 g/L NH ₄ NO ₃ , 0.05 mM Mn ²⁺ (Shake flask)	4 g/L NH ₄ NO ₃ , 0.01 mM Mn ²⁺ (Shake flask)	(Pretorius <i>et al.</i> , 2015)
Time at max surfactin conc. (h)	48	32	19	19	³
μ _{max} (h ⁻¹)	0.39	0.37	0.50	0.57	0.45
CDW (g/L)	7.94	10.58	9.91	10.12	5.150
Y _{x/s} (g/g)	0.19	0.27	0.26	0.25	³
<u>Surfactin</u>					
Surfactin concentration (mg/L)	891	936	854	805	882
Y _{p/s} (g/g)	0.021	0.024	0.022	0.020	³
Y _{p/x} (g/g)	0.113	0.088	0.087	0.080	0.280
Productivity (mg/L/h)	18.56	29.25	44.95	42.37	35.50
<u>Fengycin</u>					
Fengycin concentration (mg/L)	285	248	158	184	35.22 ⁴
Y _{p/s} (g/g)	0.007	0.006	0.004	0.004	³
Y _{p/x} (g/g)	0.036	0.024	0.016	0.018	12.69 ⁵
Productivity (mg/L/h)	5.94	7.75	8.32	9.68	1.47 ⁶
Selectivity (S/F) [g/g]	3.13	3.77	5.41	4.38	3.824

Figure 4-50 compares the effect of Mn²⁺ concentration the growth and lipopeptide related kinetic parameters in shake flask and bioreactor cultures. Mn²⁺ concentration had no significant effect on μ_{max} in both shake flask and bioreactor cultures, however μ_{max} was significantly higher in the shake flask cultures compared to the bioreactor cultures. 0.05 mM Mn²⁺ yielded the highest Y_{x/s} in both shake flask and bioreactor cultures with no significant difference between the shake flask and bioreactor cultures.

³ Data not provided by Pretorius et al., 2015

⁴Unit: mAu·min

⁵ Unit: mAU·min/g cells/L

⁶ Unit: mAU·min/h

0.01 mM Mn^{2+} resulted in a higher surfactin concentration and $Y_{p/s, surfactin}$ in the bioreactor cultures which is in contrast with the shake flask cultures where 0.05 mM Mn^{2+} yielded the highest surfactin concentration and $Y_{p/s, surfactin}$. The reason for the difference requires further investigation. The difference between the surfactin concentrations and $Y_{p/s, surfactin}$ in both shake flask and bioreactor cultures is small suggesting that Mn^{2+} does not have a significant effect on these parameters. 0.05 mM yielded the highest $Y_{p/x, surfactin}$ in both shake flask and bioreactor cultures whereas 0.01 mM yielded the highest surfactin productivity in both bioreactor and shake flask cultures.

0.05 mM Mn^{2+} yielded the highest fengycin concentration and $Y_{p/s, fengycin}$ in both the shake flask and bioreactor cultures, however fengycin concentration and $Y_{p/s, fengycin}$ was significantly higher in the bioreactor cultures compared to the shake flask cultures. 0.05 mM also yielded the highest $Y_{p/x, fengycin}$ in both shake flask and bioreactor cultures, however the difference in $Y_{p/x, fengycin}$ was much smaller in the shake flask cultures. Fengycin productivity, on the other hand, was maximised by 0.01 mM Mn^{2+} in both the bioreactor and shake flask cultures. 0.01 mM Mn^{2+} yielded the highest surfactin selectivity in the bioreactor cultures, which is in contrast with the shake flask cultures where it had the lowest surfactin selectivity.

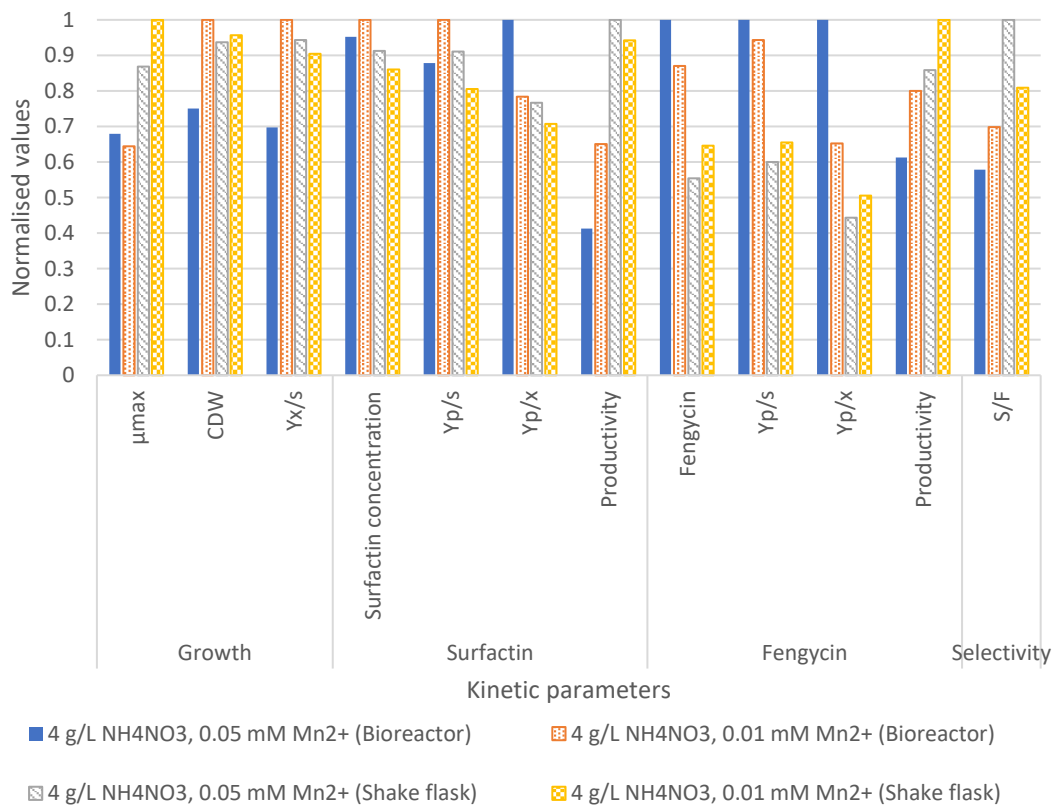


Figure 4-50: Comparison of normalised growth and lipopeptide production kinetics of *B. subtilis* in shake flask and batch bioreactor cultures containing 0.01 and 0.05 mM Mn^{2+} and 4 g/L NH_4NO_3 evaluated at the time of maximum surfactin concentration

4.5 ANTIMICROBIAL ACTIVITY OF LIPOPEPTIDE-CONTAINING CULTURE SUPERNATANT FROM *B. SUBTILIS* AGAINST *MYCOBACTERIUM AURUM*

The cell-free supernatant of a *B. subtilis* culture was tested for antimicrobial activity against *M. aurum*. The supernatant contained 1084 mg/L surfactin and 212 mg/L fengycin. shows that the supernatant did not exhibit any antimicrobial activity against *M. aurum* for four repeat runs. Growth was also observed in the wells containing the cell-free supernatant. Previous studies (Ballot, 2009; Bence, 2009) has shown antimicrobial activity of rhamnolipids from *P. aeruginosa* and surfactin from *B. subtilis* against *M. aurum* respectively using the same method that was used in this study. It is possible that the cell-free supernatant contained spores from *B. subtilis* that was not removed by filtration which explains the growth observed in the wells containing the supernatant. Another possibility is that the method used was not a suitable test for the antimicrobial activity of the supernatant against *M. aurum* thus other methods of testing for antimicrobial activity should be explored, however it goes beyond the scope of this study against *M. aurum*

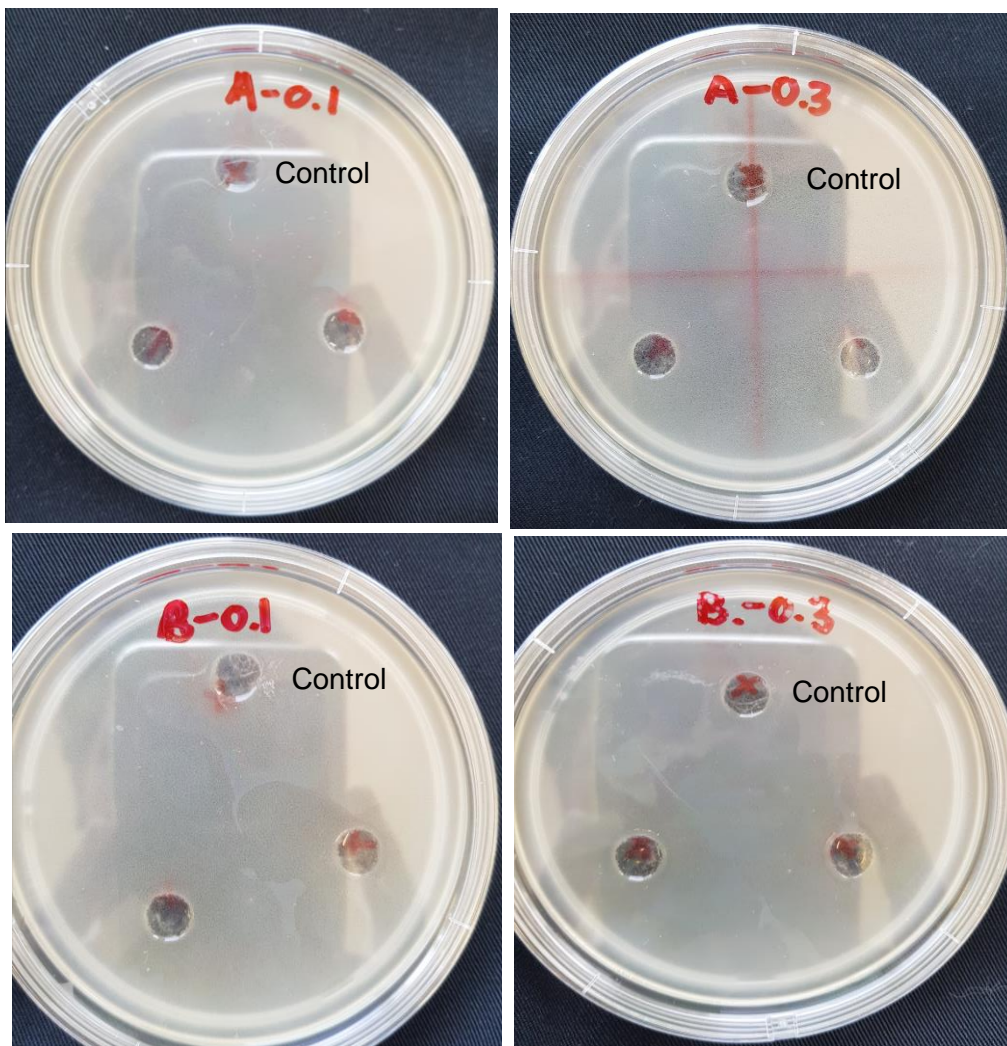


Figure 4-51: *B. subtilis* cell-free supernatant antimicrobial activity against *M. aurum*

Chapter 5

CONCLUSIONS

The overall aim of this study was to investigate the effect of medium composition and process conditions on the growth and lipopeptide production kinetics of *B. subtilis* in batch culture and advise on the conditions that will improve the upstream production of surfactin, for possible use as an antimicrobial agent against *M. tuberculosis*.

Shake flask studies were used to study the effect nitrogen source ratio on the process kinetics by supplying ammonium and nitrate at discrete nitrogen ratios. A rigorous kinetic analysis yielded the optimum nitrogen source ratio for surfactin production by *B. subtilis*. The effect of manganese concentration on the process kinetics were also studied in shake flasks and rigorous kinetic evaluation yielded the optimal manganese concentration for surfactin production. The optimal nitrogen source ratio and manganese concentration from the shake flask studies were used to evaluate the process kinetics under controlled conditions in a batch bioreactor and compared to the process kinetics obtained in the shake flasks. A response surface methodology (CCD) design of shake flask experiments yielded nitrogen source ratio, manganese concentration, and conditions of oxygen availability for maximum surfactin production by *B. subtilis*. Finally, the cell-free supernatant was used to test for antimicrobial activity against *M. aurum*.

The specific conclusions related to hypotheses stated in section 2.1 are discussed below:

- 1) The ratio of nitrogen supplied by ammonium ($\text{NH}_4^+\text{-N}$) and nitrate ($\text{NO}_3^-\text{-N}$) had a significant effect on the process kinetics in terms of growth and lipopeptide production, as well as the selectivity of surfactin relative to the co-produced antifungal lipopeptides (fengycin and iturin) An optimum $\text{NH}_4\text{-N}:\text{NO}_3\text{-N}$ ratio exists which will maximise the process kinetics for surfactin production by *B. subtilis*.**

It was found that if both ammonium and nitrate are present in the culture medium, *B. subtilis* utilises both nitrogen sources simultaneously, however nitrate consumption only started after 6 h, whereas ammonium consumption started immediately after inoculation. The delay in nitrate consumption was due to oxygen being in excess during the first 6 h, after which it became limiting and initiated nitrate consumption as an alternative electron acceptor. This suggests that ammonium is the preferred nitrogen source. The result is not surprising as nitrate first needs to be converted to ammonia to be consumed by *B. subtilis*. Nitrate acts as alternative electron acceptor following oxygen limitation and allows for the growth and lipopeptide production to continue after all of the oxygen has been consumed.

Surfactin production was found to be promoted by oxygen limitation due to the competitive nature of the microorganism. Surfactin has antimicrobial properties, hence surfactin production is promoted as a means for the microorganism to survive when oxygen becomes limiting.

Increasing the fraction of ammonium from 0 to 0.75 increased the maximum CDW from 13.2 to 19.5 g/L suggesting that ammonium plays a vital role in cell growth. The culture containing ammonium as the sole nitrogen had a CDW of 13.4 g/L as a result of oxygen limited growth in the absence of nitrate. Nitrate is thus also important for cell growth as it extends the period of cell growth after oxygen has been depleted resulting in higher cell concentrations being achieved. The effect of $\text{NH}_4\text{-N}:\text{NO}_3\text{-N}$ ratio on μ_{max} was found to be insignificant as increasing the fraction of ammonium from 0 to 0.75 only resulted in a slight increase in μ_{max} from 0.43 - 0.45 h^{-1} .

Nitrate was found to be essential for surfactin production under oxygen limiting conditions as a culture medium devoid of nitrate resulted in low surfactin yields (140 mg/L) as a result of oxygen-limited growth. The presence of nitrate in the culture medium extends the surfactin production period following oxygen limitation allowing higher surfactin concentrations to be achieved. A rapid decrease in surfactin concentration was observed following nitrate depletion which can be attributed to pH dropping below 5.0 which causes surfactin to precipitate from solution. Ammonium, on the other hand, was not essential for surfactin production, however it affected the rate at which surfactin was produced. In the absence of ammonium, surfactin production was slow compared to ammonium containing cultures. This can be attributed to ammonium being a more easily accessible nitrogen source compared to nitrate which first needs to be converted to ammonia for it to be assimilated by the cells.

A $\text{NH}_4\text{-N}:\text{NO}_3\text{-N}$ ratio of 0.5:0.5 was found to be optimal for surfactin production by *B. subtilis*, thus the hypothesis was proved. The $\text{NH}_4\text{-N}:\text{NO}_3\text{-N}$ ratio of 0.5:0.5 yielded the highest surfactin concentration (1084 mg/L), the highest surfactin productivity (36.1 mg/L/h), the second highest specific surfactin production ($Y_{p/x} = 0.078$) as well as the highest surfactin yield on glucose ($Y_{p/x} = 0.031$). The latter also yielded the third highest surfactin selectivity (5.11 g surfactin / g fengycin), which was nearly half of the highest surfactin selectivity of 10.6 g surfactin / g fengycin achieved in the culture with a $\text{NH}_4\text{-N}:\text{NO}_3\text{-N}$ ratio of 0.75:0.25.

- 2) **The concentration of manganese in the growth medium affected the nitrogen metabolism of *B. subtilis* which consequently affected the process kinetics in terms growth and lipopeptide production, as well as the selectivity of surfactin relative to the co-produced antifungal lipopeptides (fengycin and iturin). An optimum manganese concentration exists which will maximise the process kinetics for surfactin production by *B. subtilis*.**

Ammonium consumption was found to be significantly higher when no manganese was present in the culture medium. Glucose limited the growth of all tested manganese concentrations after 19 h. At this point, 88% of the ammonium supplied was consumed by the culture devoid of manganese. The cultures that contained 0.005 - 0.1 mM consumed approximately 66% of the ammonium supplied after 19 h. The higher ammonium consumption in the devoid of manganese is consistent with the findings of Huang *et al.* (2015) who reported a higher ammonium consumption for low manganese concentrations (< 0.005 mM). A metabolic shift takes place from ammonium being the main nitrogen source at concentrations below 0.005 mM manganese to nitrate becoming the main nitrogen source at manganese concentrations above 0.01 mM.

Nitrate consumption was lower for the cultures that had a low manganese concentration (<0.005 mM) than for those with higher manganese concentrations (>0.01 mM). Nitrate consumption increased from 38% for a culture devoid of manganese to 78% in a culture containing 0.01 mM manganese. These findings were consistent with those of Huang *et al.* (2015) who also found nitrate consumption to be lower at manganese concentrations below 0.01 mM. The authors found that increasing the manganese concentration increased nitrate reductase activity which consequently increased nitrate consumption.

Varying the manganese concentration between 0 and 0.1 mM had no significant effect on the maximum cell concentrations as similar cell concentrations were observed for all the tested manganese concentrations. The highest cell concentration (10.27 g/L) was observed in a culture that contained 0.01 mM manganese whilst the lowest cell concentration (9.9 g/L) was observed in the 0.1 mM manganese culture. This is in contrast with the findings of Huang *et al.* (2015) who found that manganese played in significant role in cell growth. The authors reported an 11.4-fold increase in cell concentration when the manganese concentration was increased from 0 to 0.005 mM. Manganese concentration was found to significantly affect μ_{\max} . μ_{\max} increased from 0.48 h⁻¹ in a culture devoid of manganese to a maximum of 0.57 h⁻¹ in a culture containing 0.01 mM manganese.

A 2-fold increase in surfactin concentration was observed when manganese concentration was increased from 0 (496 mg/L) to 0.1 mM (970 mg/L). This was significantly lower than the 6.2-fold increase reported by Huang *et al.* (2015) for the same manganese concentrations. The difference was most likely due to authors using a different growth medium than the one used in this study.

A manganese concentration of 0.1 mM was found to optimal for surfactin production by *B. subtilis*, hence the hypothesis was proved.

3) The nitrogen source ratio (NH₄-N:NO₃-N), manganese concentration, and conditions of oxygen availability that optimises surfactin concentration, specific surfactin yield ($Y_{p/x}$), and surfactin selectivity relative to the co-produced antifungal lipopeptides can be determined.

A response surface methodology design (CCD) of shake flask experiments revealed that NH₄-N:NO₃-N ratio and oxygen availability (relative filling volume) were significant parameters ($\alpha = 0.05$) affecting surfactin concentration, $Y_{p/x}$, and surfactin selectivity, whilst manganese concentration did not have a significant effect on any of the responses. An NH₄-N:NO₃-N ratio of 0.35:0.65, a relative filling volume of 0.5, and a manganese concentration of 0.06 mM was found to be the optimal conditions that maximises the concentration of surfactin produced by *B. subtilis*. The optimal conditions that maximises the specific surfactin yield and surfactin selectivity could not be established because surface plots could not be fitted to data for these responses. This implied that the selected model could not adequately describe the effect of the different variables on $Y_{p/x}$ and surfactin selectivity and that different models should be investigated, or the experimental design should be reviewed in order to determine the conditions that will optimise these parameters. The hypothesis was thus only partially proved as the optimal conditions for specific surfactin yield and surfactin selectivity could not be established.

4) The optimum nitrogen source ratio and manganese concentration from shake flask studies will yield similar kinetics when the experiments are performed under controlled conditions in a batch bioreactor.

An $\text{NH}_4\text{-N}:\text{NO}_3\text{-N}$ ratio of 0.5:0.5 and a manganese concentration of 0.1 mM was found to optimise the surfactin production of *B. subtilis* in shake flasks. The shake flask studies on manganese concentration only showed a small improvement in the surfactin production kinetics when the concentration of manganese was increased from 0.05 to 0.1 mM. It was thus decided to use 0.05 mM manganese and 4 g/L NH_4NO_3 (equivalent to the optimal $\text{NH}_4\text{-N}:\text{NO}_3\text{-N}$ ratio of 0.5:0.5) to evaluate the growth and production kinetics of *B. subtilis* under controlled conditions in an instrumented batch bioreactor and compare it to a shake flask culture with the same $\text{NH}_4\text{-N}:\text{NO}_3\text{-N}$ ratio and manganese concentration.

μ_{max} was significantly higher in the shake flask culture (0.5 h^{-1}) compared to the bioreactor culture (0.39 h^{-1}). Antifoam was added to the bioreactor culture to control the vigorous foaming experienced in batch bioreactor cultures, which may have interfered with the growth and resulted in the lower μ_{max} of the bioreactor culture. Further investigation is required to establish the effect of antifoam addition on growth and lipopeptide production. There was no significant difference in the maximum surfactin concentration achieved in the bioreactor (891 mg/L) and shake flask (919 mg/L) cultures. The bioreactor and shake flask cultures had almost identical specific surfactin yields ($Y_{p/x}$) of 0.113 and 0.111, respectively. There was also no significant difference in the surfactin yield on glucose ($Y_{p/s}$) in the bioreactor (0.021) and shake flask (0.024) cultures. Surfactin productivity was significantly lower in the bioreactor culture (18.56 mg/L/h) than in the shake flask culture (30.63 mg/L/h). Surfactin only reached its maximum concentration after 48 h in the bioreactor culture whilst the maximum surfactin concentration was reached after 30 h in the shake flask culture which explains the lower surfactin productivity recorded for the bioreactor culture. Again, antifoam may have slowed down growth in the bioreactor and consequently resulted in slower surfactin production resulting in the low surfactin productivity in the bioreactor culture.

The hypothesis that optimal conditions from shake flask studies will yield similar kinetics in a controlled batch bioreactor was thus proved since there was no significant difference in all of the process kinetics except for μ_{max} , and surfactin productivity which was ascribed to the possible interference of antifoam with cell growth.

5) *B. subtilis* produces a culture supernatant that exhibits antimicrobial activity against *Mycobacterium aurum*.

A cell-free supernatant that contained 1084 mg/L surfactin and 212 mg/L fengycin was used to test for antimicrobial activity against *M. aurum*. The cell-free supernatant did not exhibit any growth inhibition of *M. aurum*, hence the hypothesis that the cell-free supernatant will exhibit antimicrobial activity against *M. aurum* was disproved. Bacterial growth was observed in the wells that contained the cell-free supernatant which suggested that *B. subtilis* spores could still have been present in the supernatant after filtration. In this case, further processing on the cell-free supernatant may be necessary to observe the antimicrobial activity of surfactin against *M. aurum*. Another explanation could be that the method used was not a suitable for testing the antimicrobial activity of the cell-free supernatant against *M. aurum*. Other methods of antimicrobial testing should be explored in future work.

RECOMMENDATIONS

1) Glucose quantification

This study utilised the colorimetric DNS method to quantify glucose concentration due to the volume of samples generated in shake flask studies. The DNS method allowed for faster analysis at the expense of accuracy. Glucose concentration should be quantified using HPLC instead of the colorimetric DNS method employed in this study to improve the accuracy.

2) Nitrate quantification

Nitrate concentration was quantified using colorimetric test strips as an alternative to ion chromatography which was not available for a large duration of this project. The colorimetric test strips are semi-quantitative and relies on the user's judgement and thus sacrifices the accuracy of the results. Ion chromatography should be used to quantify nitrate concentration.

3) Ammonium quantification

The colorimetric method used to quantify ammonium concentration was adjusted as the reaction involved in the method was found to be temperature sensitive. The test tubes were quenched in ice cold water after the 15-minute reaction time to avoid further reaction when OD measurements were taken. Even though the test tubes were quenched in ice cold water, it did not completely stop the reaction which resulted in large errors between duplicate samples. Alternative methods should be explored to quantify ammonium concentration.

4) Response surface methodology design

Shake flask offers limited control over oxygen availability and since nitrogen source ratio and oxygen availability were found to be significant parameters that affect surfactin production by *B. subtilis* these parameters should be optimised under controlled conditions in a batch bioreactor.

5) Bioreactor experiments

Vigorous foaming was experienced during the batch bioreactor experiments which prompted the addition of antifoam to the culture media. The effect of antifoam addition on growth and surfactin production is not clear and should requires further investigation. Other alternatives such as foam fractionation should also be investigated to deal with foaming *B. subtilis* cultures in batch bioreactors.

Furthermore, it is recommended that once the optimum conditions in batch culture has been defined, other operational strategies such as fed-batch and continuous bioreactor cultures should be explored. Different feed rates should be evaluated in fed-batch cultures to establish an optimum. Continuous cultures could prove useful in further improving process performance by varying a single variable while all other variables are kept constant.

6) Antimicrobial activity

The antimicrobial cell-free supernatant did not show any antimicrobial activity against *M. aurum*. It is suggested that supernatant should undergo further processing such as acid precipitation, solvent extraction and adsorption followed by antimicrobial testing against *M. aurum* after each purification step. Different methods for antimicrobial testing should also be investigated.

7) Amino acid addition

The addition of amino acids to the culture medium should be explored as a way to promote or suppress the production of certain surfactin homologues as certain homologues may have higher antimicrobial activities against different target organisms.

REFERENCES

- Abas, M.R., Kader, A.J.A., Khalil, M.S., Hamid, A.A., Isa, M.H.M., 2013. Production of Surfactin from *Bacillus subtilis* ATCC 21332 by Using Treated Palm Oil Mill Effluent (POME) as fermentation media. *Int. Conf. Food Agric.* 55, 87–93.
- Abdel-Mawgoud, A.M., Aboulwafa, M.M., Hassouna, N.A.H., 2008. Optimization of surfactin production by *Bacillus subtilis* isolate BS5. *Appl. Biochem. Biotechnol.* 150, 305–325. <https://doi.org/10.1007/s12010-008-8155-x>
- Abushady, H.M., Bashandy, A.S., Aziz, N.H., Ibrahim, H.M.M., 2005. Molecular Characterization of *Bacillus subtilis* Surfactin Producing Strain and the Factors Affecting its Production. *Int. J. Agric. Biol.* 7, 337–344.
- Akpa, E., Jacques, P., Wathelet, B., Paquot, M., Fuchs, R., Budzikiewicz, H., Thonart, P., 2001. Influence of culture conditions on lipopeptide production by *Bacillus subtilis*. *Appl. Biochem. Biotechnol.* 91–93, 551–561. <https://doi.org/10.1385/ABAB:91-93:1-9:551>
- Arutchelvi, J.I., Bhaduri, S., Uppara, P.V., Doble, M., 2008. Mannosylerythritol lipids: a review. *J. Ind. Microbiol. Biotechnol.* 35, 1559–1570. <https://doi.org/10.1007/s10295-008-0460-4>
- Atwa, N.A., El-shatoury, E., Elazzazy, A., Abouzeid, M.A., El-diwany, A., 2013. Enhancement of surfactin production by *Bacillus velezensis* NRC-1 strain using a modified bench-top bioreactor 169–174.
- Ballot, F., 2009. Bacterial Production of Antimicrobial Biosurfactants.
- Banat, I.M., Franzetti, A., Gandolfi, I., Bestetti, G., Martinotti, M.G., Fracchia, L., Smyth, T.J., Marchant, R., 2010. Microbial biosurfactants production, applications and future potential. *Appl. Microbiol. Biotechnol.* 87, 427–444. <https://doi.org/10.1007/s00253-010-2589-0>
- Banat, I.M., Makkar, R.S., Cameotra, S.S., 2000. Potential commercial applications of microbial surfactants. *Appl. Microbiol. Biotechnol.* 53, 495–508. <https://doi.org/10.1007/s002530051648>
- Baruzzi, F., Quintieri, L., Morea, M., Caputo, L., 2011. Antimicrobial compounds produced by *Bacillus* spp . and applications in food 1102–1111.
- Bechard, J., Eastwell, K.C., Sholberg, P.L., Mazza, G., Skura, B., 1998. Isolation and Partial Chemical Characterization of an Antimicrobial Peptide Produced by a Strain of *Bacillus subtilis* † 5355–5361.
- Beebe, J.L., Umbreit, W.W., 1971. Extracellular lipid of *Thiobacillus thiooxidans*. *J. Bacteriol.* 108, 612–614.

- Ben Abdallah, D., Frikha-Gargouri, O., Tounsi, S., 2015. *Bacillus amyloliquefaciens* strain 32a as a source of lipopeptides for biocontrol of *Agrobacterium tumefaciens* strains. *J. Appl. Microbiol.* 119, 196–207. <https://doi.org/10.1111/jam.12797>
- Bence, K., 2009. *Bacterial Production of Antimicrobial Biosurfactants*. Stellenbosch University.
- Benincasa, M., Abalos, A., Oliveira, I., Manresa, A., 2004. Chemical structure, surface properties and biological activities of the biosurfactant produced by *Pseudomonas aeruginosa* LBI from soapstock. *Antonie Van Leeuwenhoek* 85, 1–8. <https://doi.org/10.1023/B:ANTO.0000020148.45523.41>
- Besson, F., Michel, G., 1992. Its biosynthesis had been extensively studied (Besson *et al.*, 1990; Hourdou *et al.*, 1989) and it had been found that the *B. subtilis* strain producing iturin also produces another lipopeptide, surfactin, containing a γ -hydroxy fatty acid (Besson *et al.*, 1990, 1013–1018).
- Buchoux, S., Lai-Kee-Him, J., Garnier, M., Tsan, P., Besson, F., Brisson, A., Dufourc, E.J., 2008. Surfactin-triggered small vesicle formation of negatively charged membranes: a novel membrane-lysis mechanism. *Biophys. J.* 95, 3840–9. <https://doi.org/10.1529/biophysj.107.128322>
- Cameotra, S.S., Makkar, R.S., 2004. Recent applications of biosurfactants as biological and immunological molecules. *Curr. Opin. Microbiol.* <https://doi.org/10.1016/j.mib.2004.04.006>
- Carrillo, C., Teruel, J.A., Aranda, F.J., Ortiz, A., 2003. Molecular mechanism of membrane permeabilization by the peptide antibiotic surfactin. *Biochim. Biophys. Acta - Biomembr.* 1611, 91–97. [https://doi.org/10.1016/S0005-2736\(03\)00029-4](https://doi.org/10.1016/S0005-2736(03)00029-4)
- Chen, C.Y., Baker, S.C., Darton, R.C., 2006. Continuous production of biosurfactant with foam fractionation. *J. Chem. Technol. Biotechnol.* <https://doi.org/10.1002/jctb.1624>
- Chen, L., Wang, N., Wang, X., Hu, J., Wang, S., 2010. Characterization of two anti-fungal lipopeptides produced by *Bacillus amyloliquefaciens* SH-B10. *Bioresour. Technol.* <https://doi.org/10.1016/j.biortech.2010.06.054>
- Chenikher, S., Guez, J.S., Coutte, F., Pekpe, M., Jacques, P., Cassar, J.P., 2010. Control of the specific growth rate of *Bacillus subtilis* for the production of biosurfactant lipopeptides in bioreactors with foam overflow. *Process Biochem.* 45, 1800–1807. <https://doi.org/10.1016/j.procbio.2010.06.001>
- Clarke, K.G., 2013. *Bioprocess engineering: an introductory engineering and life science approach*. Woodhead Publishing, UK.
- Clarke, K.G., 2013. Microbial kinetics during batch, continuous and fed-batch processes, in: *Bioprocess Engineering: An Introductory Engineering and Life Sciences Approach*. In Woodhead Publishing Limited, Elsevier, UK, pp. 97–146. <https://doi.org/10.1533/9781782421689.97>

- Clements, L.D., Miller, B.S., Streips, U.N., 2002. Comparative growth analysis of the facultative anaerobes *Bacillus subtilis*, *Bacillus licheniformis*, and *Escherichia coli*. *Syst. Appl. Microbiol.* 25, 284–286. <https://doi.org/10.1078/0723-2020-00108>
- Cooper, D., Macdonald, C., Duff, S., Kosaric, N., 1981. Enhanced Production of Surfactin from *Bacillus subtilis* by Continuous Product Removal and Metal Cation Additions. *Appl. Environ. Microbiol.* 42, 408–412.
- Davis, D.A., Lynch, H.C., Varley, J., 1999. The production of Surfactin in batch culture by *Bacillus subtilis* ATCC 21332 is strongly influenced by the conditions of nitrogen metabolism. *Enzyme Microb. Technol.* 25, 322–329. [https://doi.org/10.1016/S0141-0229\(99\)00048-4](https://doi.org/10.1016/S0141-0229(99)00048-4)
- Deleu, M., Paquot, M., Nylander, T., 2008. Effect of fengycin, a lipopeptide produced by *Bacillus subtilis*, on model biomembranes. *Biophys. J.* 94, 2667–2679. <https://doi.org/10.1529/biophysj.107.114090>
- Desai, J.D., Banat, I.M., 1997. Microbial Production of Surfactants and Their Commercial Potential 61, 47–64.
- Desai, J.D., Banat, I.M., 1997. Microbial production of surfactants and their commercial potential. *Microbiol. Mol. Biol. Rev.* 61, 47–64.
- Desai, J.D., Banat, I.M., 1997. Microbial Production of Surfactants and Their Commercial Potential 61, 47–64.
- du Preez, R., Clarke, K.G., Callanan, L.H., Burton, S.G., 2015. Modelling of immobilised enzyme biocatalytic membrane reactor performance. *J. Mol. Catal. B Enzym.* 119, 48–53. <https://doi.org/10.1016/j.molcatb.2015.05.015>
- Fahim, S., Dimitrov, K., Gancel, F., Vauchel, P., Jacques, P., Nikov, I., 2012. Impact of energy supply and oxygen transfer on selective lipopeptide production by *Bacillus subtilis* BBG21. *Bioresour. Technol.* 126, 1–6. <https://doi.org/10.1016/j.biortech.2012.09.019>
- Fernandes, P.A.V., De Arruda, I.R., Dos Santos, A.F.A.B., De Araújo, A.A., Maior, A.M.S., Ximenes, E.A., 2007. Antimicrobial activity of surfactants produced by *Bacillus subtilis* R14 against multidrug-resistant bacteria. *Brazilian J. Microbiol.* 38, 704–709. <https://doi.org/10.1590/S1517-83822007000400022>
- Glaser, P., Danchin, A., Kunst, F., 1995. Identification and isolation of a gene required for nitrate assimilation and anaerobic growth of *Bacillus subtilis*. *J. ...* 177, 1112–1115.
- Gond, S.K., Bergen, M.S., Torres, M.S., White, J.F., 2015. Endophytic *Bacillus* spp. produce antifungal lipopeptides and induce host defence gene expression in maize. *Microbiol. Res.* 172, 79–87.

<https://doi.org/10.1016/j.micres.2014.11.004>

- Grau, A., Gómez Fernández, J.C., Peypoux, F., Ortiz, A., 1999. A study on the interactions of surfactin with phospholipid vesicles. *Biochim. Biophys. Acta - Biomembr.* 1418, 307–319. [https://doi.org/10.1016/S0005-2736\(99\)00039-5](https://doi.org/10.1016/S0005-2736(99)00039-5)
- Gudiña, E.J., Rangarajan, V., Sen, R., Rodrigues, L.R., 2013. Potential therapeutic applications of biosurfactants. *Trends Pharmacol. Sci.* <https://doi.org/10.1016/j.tips.2013.10.002>
- Guez, J.S., Chenikher, S., Cassar, J.P., Jacques, P., 2007. Setting up and modelling of overflowing fed-batch cultures of *Bacillus subtilis* for the production and continuous removal of lipopeptides. *J. Biotechnol.* <https://doi.org/10.1016/j.jbiotec.2007.05.025>
- Haba, E., Pinazo, A., Jauregui, O., Espuny, M.J., Infante, M.R., Manresa, A., 2003. Physicochemical characterization and antimicrobial properties of rhamnolipids produced by *Pseudomonas aeruginosa* 47T2 NCBIM 40044. *Biotechnol. Bioeng.* 81, 316–322. <https://doi.org/10.1002/bit.10474>
- Heerklotz, H., Wieprecht, T., Seelig, J., 2004. Membrane Perturbation by the Lipopeptide Surfactin and Detergents as Studied by Deuterium NMR. *J. Phys. Chem. B* 108, 4909–4915. <https://doi.org/10.1021/jp0371938>
- Hoffmann, T., Frankenberg, N., Marino, M., Jahn, D., 1998. Ammonification in *Bacillus subtilis* Utilizing Dissimilatory Nitrite Reductase Is Dependent on ResDE. *J. Bacteriol.* 180, 186–189.
- Hommel, R.K., 1990. Formation and physiological role of biosurfactants produced by hydrocarbon-utilizing microorganisms - Biosurfactants in hydrocarbon utilization. *Biodegradation* 1, 107–119. <https://doi.org/10.1007/BF00058830>
- Hoskisson, P.A., Hobbs, G., 2005. Continuous culture - making a comeback? *Microbiology* 151, 3153–3159. <https://doi.org/10.1099/mic.0.27924-0>
- Huang, X., Liu, J., Wang, Y., Liu, J., Lu, L., 2015. The positive effects of Mn²⁺ on nitrogen use and surfactin production by *Bacillus subtilis* ATCC 21332. *Biotechnol. Biotechnol. Equip.* 29, 381–389. <https://doi.org/10.1080/13102818.2015.1006905>
- Jacques, P., Hbid, C., Destain, J., Razafindralambo, H., Paquot, M., De Pauw, E., Thonart, P., 1999. Optimization of Biosurfactant Lipopeptide Production from *Bacillus subtilis* S499 by Plackett-Burman Design. *Appl. Biochem. Biotechnol.* 77, 223–234. <https://doi.org/10.1385/ABAB:77:1-3:223>
- Joshi, S., Yadav, S., Desai, A.J., 2008. Application of response-surface methodology to evaluate the optimum medium components for the enhanced production of lichenysin by *Bacillus licheniformis*

- R2. *Biochem. Eng. J.* 41, 122–127. <https://doi.org/10.1016/j.bej.2008.04.005>
- Kim, H.-S., Yoon, B.-D., Lee, C.-H., Suh, H.-H., Oh, H.-M., Katsuragi, T., 1997. Production and Properties of a Lipopeptide Biosurfactant from *Bacillus subtilis* C9. *J. Ferment. Bioeng.* 84, 41–46.
- Kracht, M., Rokos, H., Özel, M., Kowall, M., Pauli, G., Vater, J., 2009. Antiviral and hemolytic activities of surfactin isoforms and their methyl ester derivatives. *J. Antibiot.* 52, No. 7 613-619. *Lang*, 52, 613–619.
- Lee, J., Lee, S.Y., Park, S., Middelberg, A., 1999. Control of fed-batch fermentations - Lee *et al.* - 1999. *Biotechnol. Adv.* 29–48.
- Lee, S.C., Kim, S.H., Park, I.H., Chung, S.Y., Subhosh Chandra, M., Choi, Y.L., 2010. Isolation, purification, and characterization of novel fengycin S from *Bacillus amyloliquefaciens* LSC04 degrading-crude oil. *Biotechnol. Bioprocess Eng.* 15, 246–253. <https://doi.org/10.1007/s12257-009-0037-8>
- Lin, H.-Y., Rao, Y.K., Wu, W.-S., Tzeng, Y.-M., 2007. Ferrous ion Enhanced Lipopeptide Antibiotic Iturin A Production from *Bacillus amyloliquefaciens* B128. *Int. J. Appl. Sci. Eng.* 5, 123–132.
- Lin, S.-C., Carswell, K.S., Sharma, M.M., Georgiou, G., 1994. Continuous production of the lipopeptide biosurfactant of *Bacillus licheniformis* JF-2. *Appl. Microbiol. Biotechnol.* 41, 281–285. <https://doi.org/10.1007/BF00221219>
- Liu, J.F., Yang, J., Yang, S.Z., Ye, R.Q., Mu, B.Z., 2012. Effects of different amino acids in culture media on surfactin variants produced by *Bacillus subtilis* TD7. *Appl. Biochem. Biotechnol.* 166, 2091–2100. <https://doi.org/10.1007/s12010-012-9636-5>
- Maget-Dana, R., Ptak, M., 1995. Interactions of surfactin with membrane models. *Biophys. J.* 68, 1937–43. [https://doi.org/10.1016/S0006-3495\(95\)80370-X](https://doi.org/10.1016/S0006-3495(95)80370-X)
- Makkar, R.S., Cameotra, S.S., 1997. Biosurfactant production by a thermophilic *Bacillus subtilis* strain. *J. Ind. Microbiol. Biotechnol.* 18, 37–42. <https://doi.org/10.1038/sj.jim.2900349>
- Meena, K., Kanwar, S., 2015. Lipopeptides as the Antifungal and Antibacterial Agents: Applications in Food Safety and Therapeutics. *Biomed Res. Int.*
- Meena, K.R., Kanwar, S.S., 2015a. Lipopeptides as the antifungal and antibacterial agents: Applications in food safety and therapeutics. *Biomed Res. Int.* 2015. <https://doi.org/10.1155/2015/473050>
- Meena, K.R., Kanwar, S.S., 2015b. Lipopeptides as the Antifungal and Antibacterial Agents: Applications in Food Safety and Therapeutics 2015.
- Mukherjee, S., Das, P., Sen, R., 2006. Towards commercial production of microbial surfactants. *Trends*

Biotechnol. 24, 509–515. <https://doi.org/10.1016/j.tibtech.2006.09.005>

Mulligan, C.N., 2009. Recent advances in the environmental applications of biosurfactants. *Curr. Opin. Colloid Interface Sci.* <https://doi.org/10.1016/j.cocis.2009.06.005>

Mulligan, C.N., 2005. Environmental applications for biosurfactants. *Environ. Pollut.* <https://doi.org/10.1016/j.envpol.2004.06.009>

Muthusamy, K., Gopalakrishnan, S., Ravi, T.K., Sivachidambaram, P., 2008. Biosurfactants : Properties , commercial production and application 94.

Nakano, M.M., Dailly, Y.P., Zuber, P., Clark, D.P., 1997. Characterization of anaerobic fermentative growth of *Bacillus subtilis*: Identification of fermentation end products and genes required for growth. *J. Bacteriol.* 179, 6749–6755.

Nakano, M.M., Hulett, F.M., 1997. Adaptation of *Bacillus subtilis* to oxygen limitation. *FEMS Microbiol. Lett.* 157, 1–7. [https://doi.org/10.1016/S0378-1097\(97\)00436-9](https://doi.org/10.1016/S0378-1097(97)00436-9)

Ohno, A., Ano, T., Shoda, M., 1995. Effect of temperature on production of lipopeptide antibiotics, iturin A and surfactin by a dual producer, *Bacillus subtilis* RB14, in solid-state fermentation. *J. Ferment. Bioeng.* 80, 517–519. [https://doi.org/10.1016/0922-338X\(96\)80930-5](https://doi.org/10.1016/0922-338X(96)80930-5)

Okigbo, R.N., Emeka, A.N., 2010. Biological control of rot-inducing fungi of water yam (*Dioscorea alata*) with *Trichoderma harzianum*, *Pseudomonas syringae* and *Pseudomonas chlororaphis*. *J. Stored Prod. Postharvest Res.* 1, 18–23.

Ongena, M., Jacques, P., 2008. *Bacillus* lipopeptides: versatile weapons for plant disease biocontrol. *Trends Microbiol.* 16, 115–125. <https://doi.org/10.1016/j.tim.2007.12.009>

Ongena, M., Jacques, P., Guiro, A., Thonart, P., Toure, Y., 2004. Role of lipopeptides produced by *Bacillus subtilis* GA1 in the reduction of grey mould disease caused by *Botrytis cinerea* on apple 1151–1160. <https://doi.org/10.1111/j.1365-2672.2004.02252.x>

Painter, H.A., 1970. A review of literature on inorganic nitrogen metabolism in microorganisms. *Water Res.* 4, 393–450. [https://doi.org/10.1016/0043-1354\(70\)90051-5](https://doi.org/10.1016/0043-1354(70)90051-5)

Pathak, K. V, 2011. Purification and characterization of antifungal compounds produced by Banyan endophytic *Bacilli*.

Paulová, L., Patáková, P., Brányik, T., 2013. *Advanced Fermentation Processes.* pp. 89–110. <https://doi.org/10.1201/b15426-6>

Pereira, R., 1998. A novel thermostable nitrile hydratase. *Extremophiles* 2.

Peypoux, F., Bonmatin, J.M., Wallach, J., 1999. Recent trends in the biochemistry of surfactin. *Appl.*

Microbiol. Biotechnol. <https://doi.org/10.1007/s002530051432>

- Pretorius, D., 2014. Antimicrobial lipopeptide production by *Bacillus* spp. for post-harvest biocontrol.
- Pretorius, D., van Rooyen, J., Clarke, K.G., 2015. Enhanced production of antifungal lipopeptides by *Bacillus amyloliquefaciens* for biocontrol of postharvest disease. *N. Biotechnol.* 32, 243–252. <https://doi.org/10.1016/j.nbt.2014.12.003>
- Rahman, P.K.S., Gakpe, E., 2008. Production, Characterisation and Application of Biosurfactants-Review. *J. Biotechnol.* 7, 360–370.
- Rangarajan, V., Clarke, K.G., 2015. Process development and intensification for enhanced production of *Bacillus* lipopeptides. *Biotechnol. Genet. Eng. Rev.* 31, 46–68. <https://doi.org/10.1080/02648725.2016.1166335>
- Rangarajan, V., Dhanarajan, G., Sen, R., 2015. Bioprocess design for selective enhancement of fengycin production by a marine isolate *Bacillus megaterium*. *Biochem. Eng. J.* 99, 147–155. <https://doi.org/10.1016/j.bej.2015.03.016>
- Rodrigues, L., Banat, I., Teixeira, J., Oliveira, R., 2006. Biosurfactants: potential applications in medicine. *J. Antimicrob. Chemother.* 57, 609–618.
- Rodrigues, L., van der Mei, H.C., Teixeira, J., Oliveira, R., 2004. Influence of biosurfactants from probiotic bacteria on formation of biofilms on voice prostheses. *Appl. Environ. Microbiol.* 70, 4408–10. <https://doi.org/10.1128/AEM.70.7.4408-4410.2004>
- Rodrigues, L.R., Teixeira, J.A., 2010. Biomedical and therapeutic applications of biosurfactants. *Adv. Exp. Med. Biol.* https://doi.org/10.1007/978-1-4419-5979-9_6
- Rodrigues, L.R., Teixeira, J.A., van der Mei, H.C., Oliveira, R., 2006. Physicochemical and functional characterization of a biosurfactant produced by *Lactococcus lactis* 53. *Colloids Surfaces B Biointerfaces* 49, 79–86. <https://doi.org/10.1016/j.colsurfb.2006.03.003>
- Romero, D., de Vicente, A., Rakotoaly, R.H., Dufour, S.E., Veening, J.-W., Arrebola, E., Cazorla, F.M., Kuipers, O.P., Paquot, M., Pérez-García, A., 2007. The iturin and fengycin families of lipopeptides are key factors in antagonism of *Bacillus subtilis* toward *Podosphaera fusca*. *Mol. Plant. Microbe. Interact.* 20, 430–440. <https://doi.org/10.1094/MPMI-20-4-0430>
- Sabate, D.C., 2009. Inhibition of *Paenibacillus* larvae and *Ascosphaera apis* by *Bacillus subtilis* isolated from honeybee gut and honey samples. *Res. Microbiol.* 160, 193–199. <https://doi.org/10.1016/j.resmic.2009.03.002>
- Salihu, a, Abdulkadir, I., Almustapha, M.N., 2009. An investigation for potential development on

biosurfactants . *Biotechnol. Mol. Biol. Rev.* 3, 111–117.

- Sen, R., Swaminathan, T., 2005. Characterization of concentration and purification parameters and operating conditions for the small-scale recovery of surfactin. *Process Biochem.* 40, 2953–2958. <https://doi.org/10.1016/j.procbio.2005.01.014>
- Sen, R., Swaminathan, T., 1997. Application of response-surface methodology to evaluate the optimum environmental conditions for the enhanced production of surfactin. *Appl. Microbiol. Biotechnol.* 47, 358–363. <https://doi.org/10.1007/s002530050940>
- Seok Oh, J., Kim, B.G., Hyun Park, T., 2002. Importance of specific growth rate for subtilisin expression in fed-batch cultivation of *Bacillus subtilis* spoIIIG mutant, in: *Enzyme and Microbial Technology*. pp. 747–751. [https://doi.org/10.1016/S0141-0229\(02\)00052-2](https://doi.org/10.1016/S0141-0229(02)00052-2)
- Seydlová, G., Svobodová, J., 2008. Review of surfactin chemical properties and the potential biomedical applications. *Open Med.* 3, 123–133. <https://doi.org/10.2478/s11536-008-0002-5>
- Shaligram, N.S., Singhal, R.S., 2010. Surfactin -a review on biosynthesis, fermentation, purification and applications. *Food Technol. Biotechnol.* 48, 119–134.
- Sharma, D., Mandal, S.M., Manhas, R.K., 2014. Purification and characterization of a novel lipopeptide from *Streptomyces amritsarensis* sp. nov. active against methicillin-resistant *Staphylococcus aureus*. *AMB Express* 4, 50. <https://doi.org/10.1186/s13568-014-0050-y>
- Shoeb, E., Akhlaq, F., Badar, U., Akhter, J., Imtiaz, S., 2013. Classification and Industrial Applications of Biosurfactants. *SAVAP Int.* 4, 243–252.
- Singh, P., Cameotra, S.S., 2004. Potential applications of microbial surfactants in biomedical sciences. *Trends Biotechnol.* <https://doi.org/10.1016/j.tibtech.2004.01.010>
- Stein, T., 2005. *Bacillus subtilis* antibiotics: Structures, syntheses and specific functions. *Mol. Microbiol.* 56, 845–857. <https://doi.org/10.1111/j.1365-2958.2005.04587.x>
- Sumi, C.D., Yang, B.W., Yeo, I., Hahm, Y.T., 2015. Antimicrobial peptides of the genus *Bacillus* : a new era for antibiotics 103, 93–103.
- Thonart, P., Razafindralambo, H., Paquot, M., Baniel, A., Popineau, Y., 1996. Foaming properties of surfactin , a lipopeptide biosurfactant from *Bacillus subtilis* Foaming Properties of Surfactin , a Lipopeptide Biosurfactant from *Bacillus subtilis* L-ieu. <https://doi.org/10.1007/BF02523463>
- Todar, K., 2008. *Todar's Online Textbook of Bacteriology*. University of Wisconsin, Madison, Wisconsin.
- Todar, K., 2002. *Todar ' s Online Textbook of Bacteriology*.
- Van Hamme, J.D., Singh, A., Ward, O.P., 2006. Physiological aspects. Part 1 in a series of papers

devoted to surfactants in microbiology and biotechnology. *Biotechnol. Adv.* 24, 604–620. <https://doi.org/10.1016/j.biotechadv.2006.08.001>

Vedaraman, N., Venkatesh, N., 2011. Production of surfactin by *Bacillus subtilis* MTCC 2423 from waste frying oils. *Brazilian J. Chem. Eng.* 28, 175–180. <https://doi.org/10.1590/S0104-66322011000200001>

Vollenbroich, D., Pauli, G., Muhsin, O., 1997. Antimycoplasma properties and application in cell culture of surfactin , a lipopeptide antibiotic from *Bacillus subtilis* . *Antimycoplasma Properties and Application in Cell Culture of Surfactin , a Lipopeptide Antibiotic from Bacillus subtilis* 63, 44–49.

Walsh, C., 2003. *Antibiotics : actions, origins, resistance.* ASM Press.

Wei, Y.H., Chu, I.M., 2002. Mn²⁺ improves surfactin production by *Bacillus subtilis*. *Biotechnol. Lett.* 24, 479–482. <https://doi.org/10.1023/A:1014534021276>

Wei, Y.H., Chu, I.M., 1998. Enhancement of surfactin production in iron-enriched media by *Bacillus subtilis* ATCC 21332. *Enzyme Microb. Technol.* [https://doi.org/10.1016/S0141-0229\(98\)00016-7](https://doi.org/10.1016/S0141-0229(98)00016-7)

Wei, Y.H., Lai, C.C., Chang, J.S., 2007. Using Taguchi experimental design methods to optimize trace element composition for enhanced surfactin production by *Bacillus subtilis* ATCC 21332. *Process Biochem.* 42, 40–45. <https://doi.org/10.1016/j.procbio.2006.07.025>

Wei, Y.H., Wang, L.F., Chang, J.S., 2004. Optimizing iron supplement strategies for enhanced surfactin production with *Bacillus subtilis*. *Biotechnol. Prog.* 20, 979–983. <https://doi.org/10.1021/bp030051a>

Wei, Y.H., Wang, L.F., Chang, J.S., Kung, S.S., 2003. Identification of induced acidification in iron-enriched cultures of *Bacillus subtilis* during biosurfactant fermentation. *J. Biosci. Bioeng.* 96, 174–178. [https://doi.org/10.1016/S1389-1723\(03\)90121-6](https://doi.org/10.1016/S1389-1723(03)90121-6)

White, D., 2000. *The physiology and biochemistry of prokaryotes*, 2nd ed. ed. Oxford University Press, New York.

Willenbacher, J., Rau, J.-T., Rogalla, J., Syldatk, C., Hausmann, R., 2015. Foam-free production of Surfactin via anaerobic fermentation of *Bacillus subtilis* DSM 10(T). *AMB Express* 5, 21. <https://doi.org/10.1186/s13568-015-0107-6>

World Health Organisation, 2016. WHO | Tuberculosis (TB) [WWW Document]. WHO. URL <http://www.who.int/topics/tuberculosis/en/> (accessed 5.19.16).

World Health Organization, 2015. TUBERCULOSIS WHO Global Tuberculosis Report 2015 [WWW Document]. URL http://www.who.int/tb/Global_TB_Facts.pdf (accessed 5.19.16).

Xu, Z., Shao, J., Li, B., Yan, X., Shen, Q., Zhang, R., 2013. Contribution of bacillomycin D in *Bacillus*

amyloliquefaciens SQR9 to antifungal activity and biofilm formation. *Appl. Environ. Microbiol.* 79, 808–815. <https://doi.org/10.1128/AEM.02645-12>

Yakimov, M.M., Timmis, K.N., Wray, V., 1995. Characterization of a New Lipopeptide Surfactant Produced by Thermotolerant and Halotolerant Subsurface *Bacillus licheniformis* BAS50 61, 1706–1713.

Yáñez-Mendizábal, V., Usall, J., Viñas, I., Casals, C., Marín, S., Solsona, C., Teixidó, N., 2011. Potential of a new strain of *Bacillus subtilis* CPA-8 to control the major postharvest diseases of fruit. *Biocontrol Sci. Technol.* 21, 409–426. <https://doi.org/10.1080/09583157.2010.541554>

Yeh, M.S., Wei, Y.H., Chang, J.S., 2006. Bioreactor design for enhanced carrier-assisted surfactin production with *Bacillus subtilis*. *Process Biochem.* 41, 1799–1805. <https://doi.org/10.1016/j.procbio.2006.03.027>

Youssef, N.H., Duncan, K.E., Michael, J., Mcinerney, M.J., 2005. Importance of 3-Hydroxy Fatty Acid Composition of Lipopeptides for Biosurfactant Activity Importance of 3-Hydroxy Fatty Acid Composition of Lipopeptides for Biosurfactant Activity 71, 7690–7695. <https://doi.org/10.1128/AEM.71.12.7690>

Zhang, T., Shi, Z.Q., Hu, L. Bin, Cheng, L.G., Wang, F., 2008. Antifungal compounds from *Bacillus subtilis* B-FS06 inhibiting the growth of *Aspergillus flavus*. *World J. Microbiol. Biotechnol.* 24, 783–788. <https://doi.org/10.1007/s11274-007-9533-1>

Zohora, U.S., Rahman, M.S., Ano, T., 2009. Biofilm formation and lipopeptide antibiotic iturin A production in different peptone media. *J. Environ. Sci.* [https://doi.org/10.1016/S1001-0742\(09\)60029-2](https://doi.org/10.1016/S1001-0742(09)60029-2)

APPENDICES

APPENDIX A: GROWTH, SUBSTRATE UTILISATION AND LIPOPEPTIDE PRODUCTION PATTERNS FOR DIFFERENT MANGANESE CONCENTRATIONS

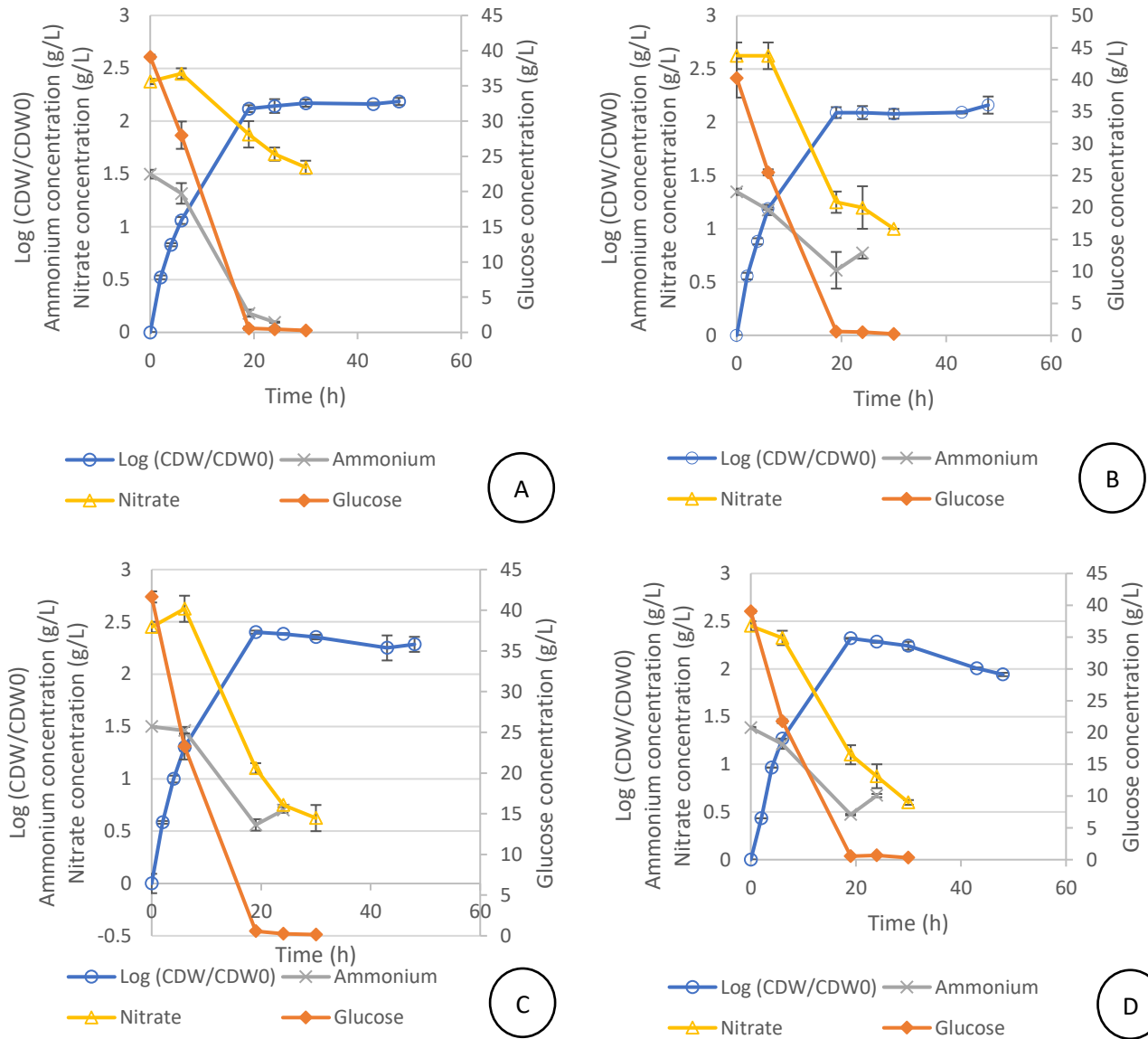


Figure B. 1: Growth and substrate utilisation patterns for different Mn^{2+} concentrations in shake flasks. A – 0 mM; B – 0.005 mM; C – 0.01 mM; D – 0.05 mM.

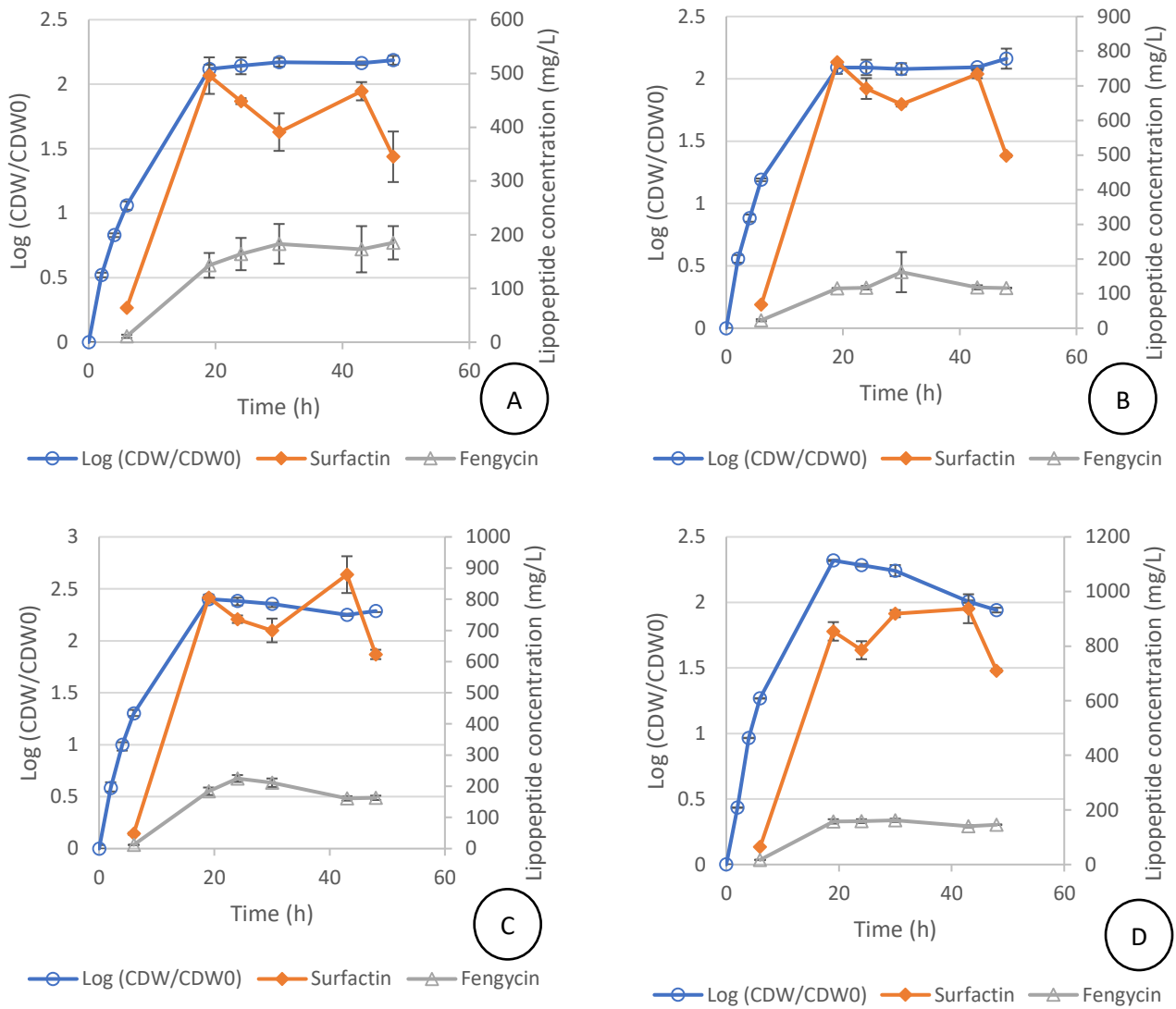


Figure B. 2: Growth and lipopeptide production patterns of *B. subtilis* for different manganese concentrations in shake flasks. A – 0 mM; B – 0.005 mM; C – 0.01 mM; D – 0.05 mM.

APPENDIX B: EQUATIONS AND SAMPLE CALCULATIONS

1. Kinetic parameter equations

The equations used to calculate the different kinetic parameters will be discussed below.

The maximum specific growth rate (μ_{max}) was determined graphically through a semi-log plot of CDW vs. time. μ_{max} was represented by the slope of the linear portion (exponential growth phase) of the $\ln(x)$ vs. t plot according to Equation 1.

Equation 1: Maximum specific growth rate

$$\ln x = \ln x_0 + \mu t$$

The calculations for the yield ($Y_{x/s}$, $Y_{p/s}$ and $Y_{p/x}$) and productivity kinetic parameters were similar; initial CDW, glucose, and lipopeptide concentrations (time 0) and concentrations at a certain sample time after (time i) were used. The time where surfactin concentration reached a maximum was used as time i in the calculation of all the kinetic parameters.

Equation 2: Cell yield per gram substrate

$$Y_{x/s} = \frac{x_i - x_0}{s_0 - s_i}$$

Equation 3: Lipopeptide yield per gram substrate

$$Y_{p/s} = \frac{p_i - p_0}{s_0 - s_i}$$

Equation 4: Specific lipopeptide production

$$Y_{p/x} = \frac{p_i - p_0}{x_i - x_0}$$

Equation 5: Productivity

$$Productivity = \frac{p_i - p_0}{t_i - t_0}$$

2. Nitrogen source ratio calculation

The nitrogen source experiments were based on a total nitrogen concentration equivalent to that present in 4 g/L NH_4NO_3 .

Nitrogen content of 4 g/L NH_4NO_3

$$Total\ N = 4 \frac{g}{L} NH_4NO_3 \times \frac{2 \times MW_N}{MW_{NH_4NO_3}} = \frac{2(14.0067)}{80.052} = 1.4 \frac{g}{L} N$$

The nitrogen source ratios represented the fraction of nitrogen supplied by ammonium to the fraction of nitrogen supplied by nitrate ($\text{NH}_4\text{-N}:\text{NO}_3\text{-N}$). Ammonium and nitrate were supplied in form of the salts, NH_4Cl and NaNO_3 , respectively. The calculation to determine the required concentrations of NH_4Cl and NaNO_3 for a given nitrogen source ratio is illustrated below by using $\text{NH}_4\text{-N}:\text{NO}_3\text{-N} = 0.75:0.25$ as an example:

Determining NH_4Cl and NaNO_3 concentration

$$[\text{NH}_4] = \text{fraction } \text{NH}_4 - \text{N} \times [\text{N}] \times \frac{MW_{\text{NH}_4}}{MW_{\text{N}}} = 0.75 \times 1.4 \frac{\text{g}}{\text{L}} \text{N} \times \frac{18.04 \frac{\text{g}}{\text{mol}} \text{NH}_4}{14 \frac{\text{g}}{\text{mol}} \text{N}} = 1.353 \frac{\text{g}}{\text{L}} \text{NH}_4$$

$$[\text{NH}_4\text{Cl}] = [\text{NH}_4] \times \frac{MW_{\text{NH}_4\text{Cl}}}{MW_{\text{NH}_4}} = 1.353 \frac{\text{g}}{\text{L}} \text{NH}_4 \times \frac{53.491 \frac{\text{g}}{\text{mol}} \text{NH}_4\text{NO}_3}{18.04 \frac{\text{g}}{\text{mol}} \text{NH}_4} = 4.01 \frac{\text{g}}{\text{L}} \text{NH}_4\text{Cl}$$

$$[\text{NO}_3] = \text{fraction } \text{NO}_3 - \text{N} \times [\text{N}] \times \frac{MW_{\text{NO}_3}}{MW_{\text{N}}} = 0.25 \times 1.4 \frac{\text{g}}{\text{L}} \text{N} \times \frac{62 \frac{\text{g}}{\text{mol}} \text{NO}_3}{14 \frac{\text{g}}{\text{mol}} \text{N}} = 1.55 \frac{\text{g}}{\text{L}} \text{NO}_3$$

$$[\text{NaNO}_3] = [\text{NO}_3] \times \frac{MW_{\text{NaNO}_3}}{MW_{\text{NO}_3}} = 1.55 \frac{\text{g}}{\text{L}} \text{NO}_3 \times \frac{53.491 \frac{\text{g}}{\text{mol}} \text{NaNO}_3}{18.04 \frac{\text{g}}{\text{mol}} \text{NO}_3} = 4.6 \frac{\text{g}}{\text{L}} \text{NaNO}_3$$

APPENDIX C: HPLC CHROMATOGRAMS

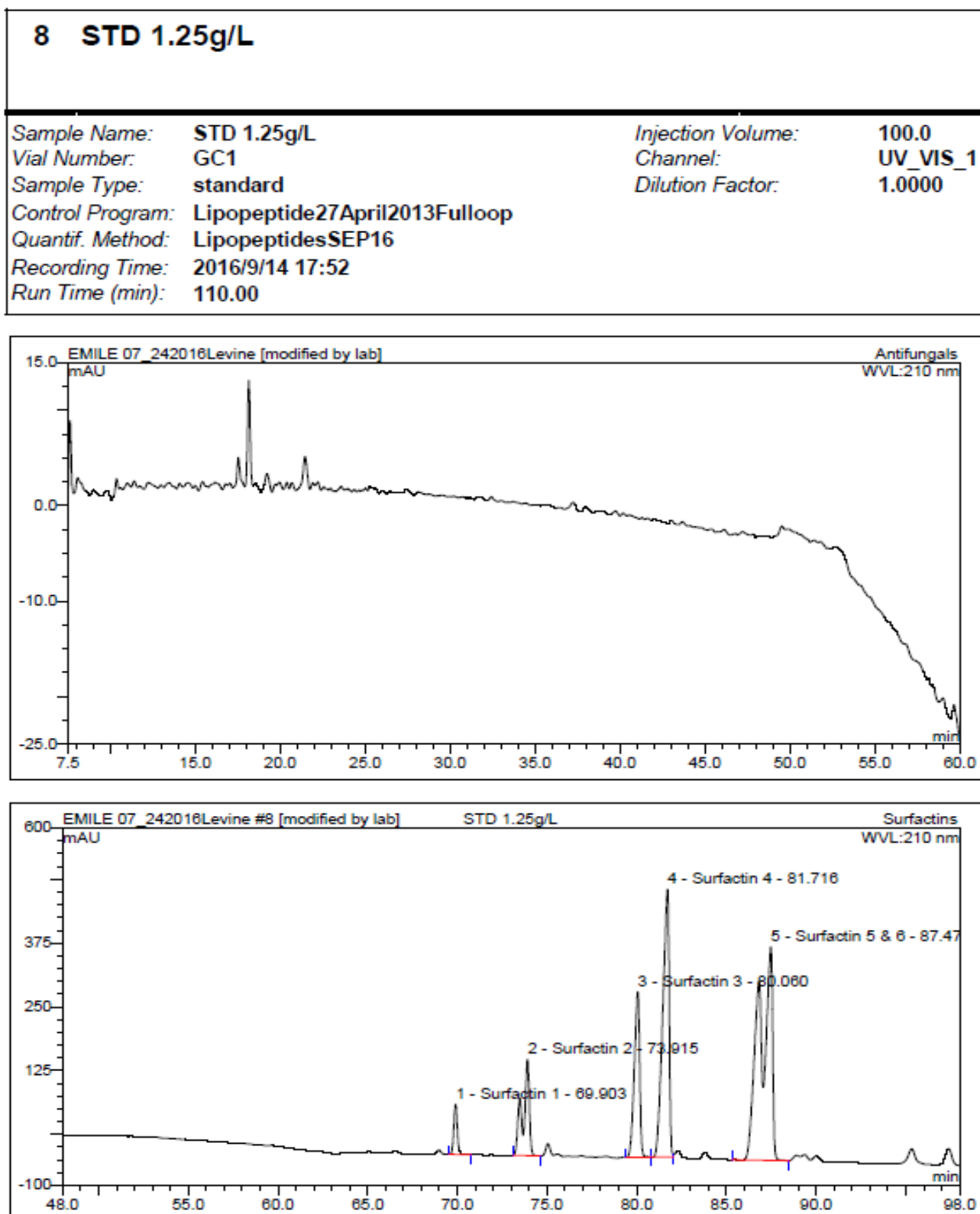


Figure C. 1: Example of surfactin chromatogram

4 F500			
Sample Name:	F500	Injection Volume:	100.0
Vial Number:	RA4	Channel:	UV_VIS_1
Sample Type:	standard	Dilution Factor:	1.0000
Control Program:	Lipopeptide27April2013Fullloop		
Quantif. Method:	LipopeptidesSEP16		
Recording Time:	2016/7/8 17:24		
Run Time (min):	110.00		

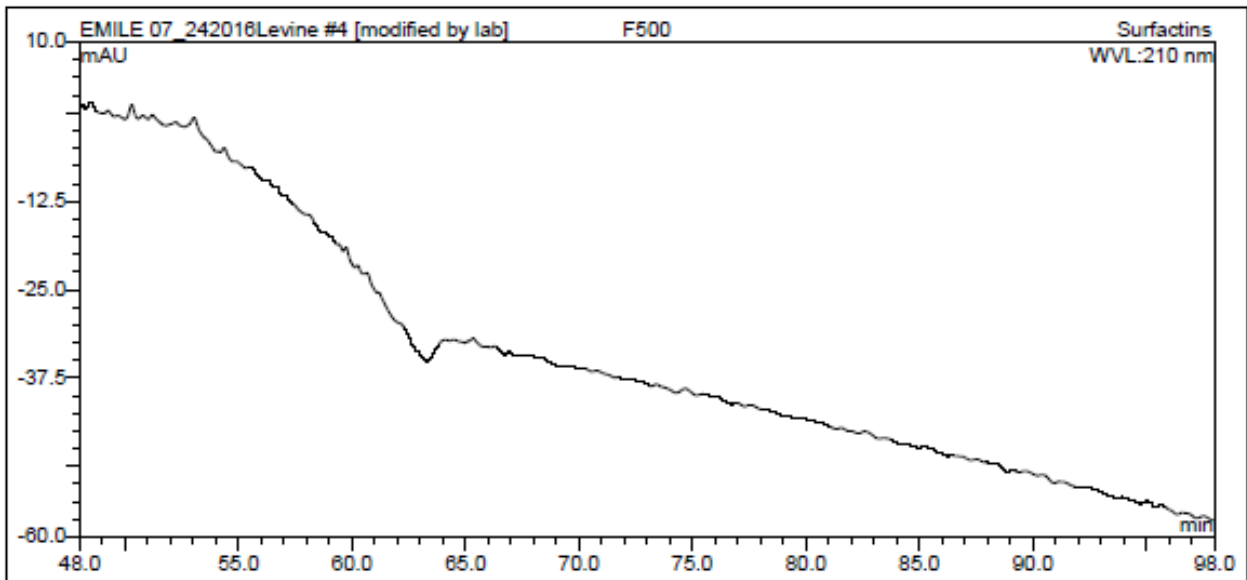
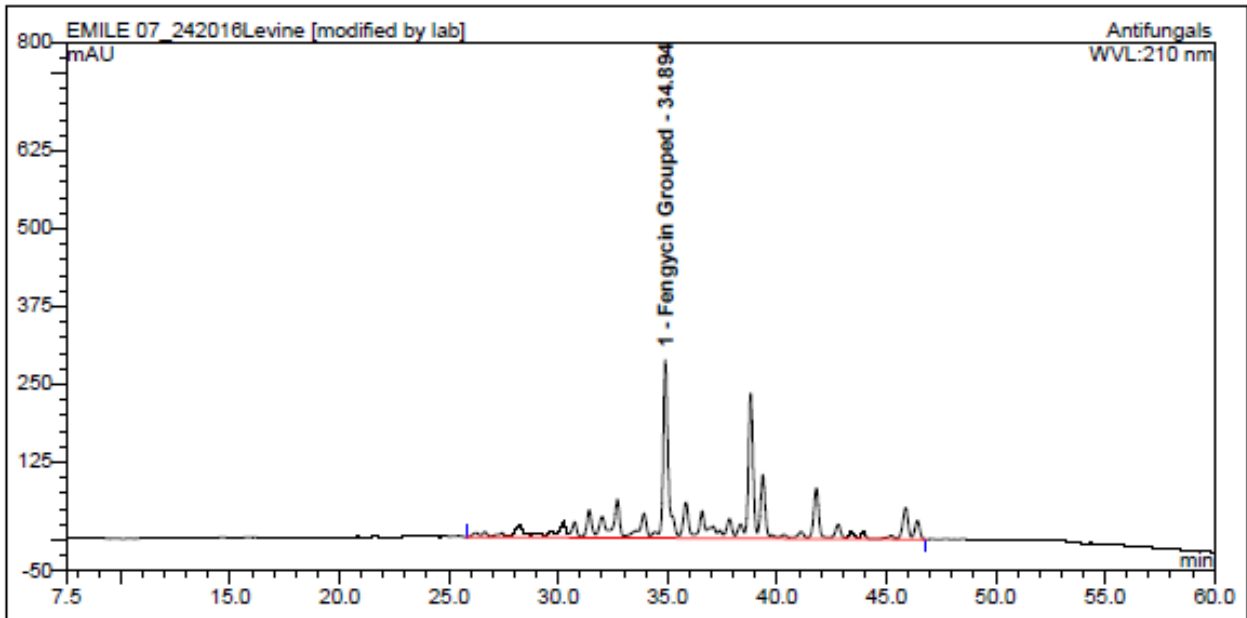


Figure C. 2: Example of fengycin chromatogram